Wissenschaftszentrum Weihenstephan für Ernährung, Landnutzung und Umwelt

Model extensions to capture multiple forest ecosystem services in future scenarios on landscape scale

Werner Franz Wolfgang Poschenrieder

Vollständiger Abdruck der von der Fakultät
Wissenschaftszentrum Weihenstephan für Ernährung, Landnutzung und Umwelt
der Technischen Universität München zur Erlangung des akademischen Grades
eines Doktors der Naturwissenschaften
genehmigten Dissertation.

Vorsitzende/-r: Prof. Dr. Michael Suda

Prüfende/-r der Dissertation:

1. Prof. Dr. Hans Pretzsch

2. Prof. Dr. Anja Rammig

Die Dissertation wurde am 21.08.2018 bei der Technischen Universität München eingereicht und durch die Fakultät Wissenschaftszentrum Weihenstephan für Ernährung, Landnutzung und Umwelt am 29.01.2019 angenommen.

Index

1 Acknowledgements

First and foremost, I would like to sincerely express my gratitude to my advisor Prof. Dr. Hans Pretzsch for providing me with his scientific expertise, his continuous support and the instructive and innovative challenges that he presented me with. Also, I wish to thank him for his confidence and his encouragement. Special thanks go to Dr. Peter Biber, to my mentor Dr. Rüdiger Grote at Karlsruhe Institute of Technology (IMK-IFU) and to my colleague Dr. Andreas Rais who supported me with their valuable knowledge and many inspiring discussions.

Particular thanks also go to Enno Uhl who contributed his profound knowledge of experimental plots and regeneration as well as administrative support, to Gerhard Schütze for his excellent expertise in the evaluation of core-boring data and to Matthias Ulbricht for the thorough sampling and measuring of core-boring probes. My sincere thanks go to Prof. Dr. Arthur Gessler who coordinated and together with Dr. Rüdiger Grote initiated the project that my first publication was part of. Furthermore, I would like to express my gratitude to Prof. Dr. Thomas Seifert for critical discussions about the concept of the second publication. Furthermore, I wish to thank Ralf Moshammer who provided his valuable knowledge about inventory data to the third publication. Thanks to all my colleagues at the Chair of Forest Growth and Yield Science for inspiring scientific discussions and cordial colleagueship.

Thanks also go to the German Science Foundation / Deutsche Forschungsgemeinschaft (DFG) for funding the first publication within the Project “Modelling beech-dominated deciduous forest development based on competitive mechanisms of water and nitrogen partitioning” under contract number GE 1090/9-1.

I also thank the Bavarian State Ministry for Nutrition, Agriculture and Forestry for making the second publication possible through permanent support of the project W07 “Long-term experimental plots for forest growth and yield research” and funding of the project X36 ”Relationship between spacing and wood quality of Douglas-fir in Bavaria“.

Furthermore, I also wish to express my gratitude to the Bayerische Staatsforsten AÖR, Regensburg (BaySF) for providing valuable data from their regular inventories to the third publication. Thanks are also due to the Thünen Institut Eberswalde for supplying national forest inventory data. In particular, I would like to thank Thomas Riedel (Thünen Institut) for consultancy in biomass computation and biomass extraction from the public database. Thanks are also due to the European Union for partial funding of that study through (1) project

ALTERFOR within the Horizon 2020 research and innovation programme under grant agreement No 676754 and of (2) project ClusterWIS within the European Regional Development fund under grant agreement EFRE-0800038 (EFRE.NRW 2014-2020).

2 Abstract

While forest management originally focused on growth and yield, it now has to provide a wide range of additional ecosystem services (ES). The forest manager, moreover, has to maintain resilience towards an interannual and intraannual variability of weather that is yet unknown. Accordingly, there is an increasing demand for simulation studies that support forestry stakeholders in decision making. While such scenarios originally focus on the scale level of the forest management unit, recent simulation studies consider the scale level of the whole landscape. Such a study has to (1) cover multiple ES provided by forests of complex structure and management, (2) take into account a future change of climate and weather variability linked to an increase of CO_2, (3) consider the long-term influence of management on the hydrological system, and (4) account for at least one rotation period. A large variety of models today cover forest growth and structure development. Most model types, however, consider a narrow range of scale levels and objectives only. They neglect processes outside their main scope or represent them simplistically. On the contrary, studies on landscape scale level need to consider multiple effects of competing management options under a large variety of environmental conditions.

Therefore, the study at hand contributes three optionally interconnected components to a wider conceptual modelling framework. For this purpose, a growth model component has been developed which combines carbon allocation with individual tree growth and thus competition. In contrast to non-physiological individual tree models that first component enables considering the sensitivity of the forest to environmental change in atmosphere and soil. The second component is a wood quality module that describes the individual board strength. It aims at facilitating the economical evaluation of simulated forest growth. As a pivotal component within scenarios that cover generational change, the third component estimates the initial state of the regeneration process.

The first development combines a well-established physiological model to an individual tree module. It applies a mass conservative linkage that maintains consistence between both components. The second development embeds the envisaged wood quality module into a specifically developed simple forest growth model in order to identify key properties within both parts. The third development estimates the biomass of regeneration trees from stand structure and site based on inventory data. All components may extend existing models. Moreover, they may be used in connection to represent key processes of ecosystem service provision within representative landscape subareas. To that end, they might be embedded into a yet conceptual framework for complementing more parsimonious models that represent

overarching landscape processes. Experimental data and yet established theory enable further extension of each component. Their synthesis may support forest management in maintaining multifunctionality as well as resilience under environmental change of yet unknown extent and direction.

3 Introduction

3.1 Development of forest growth models

Following a severe wood shortage in the 18th century (Radkau 1983), the utilization of German forests began to follow the concept of sustainability after a long period of intensive exploitation (v. Carlowitz 1732). In order to maintain the overall stock of forest estates, modern forestry required reliable tools for predicting the long-term development of stands.

The earliest predictive models in forestry were experience-based tables that showed the development of tree dimensions and numbers over time (e.g. Hartig 1795). Within the course of the 19th century the system of experimental plots was established that ever since supports the prediction of stand growth based on controlled management conditions. In the first half of the 20th century, forest scientists (e.g. Gehrhardt 1909) derived parameterized biometric equations for the stock of pure stands from experimental plot data that were able to provide continuous values for all management related variables. For practical use, however, they still published the resulting time series of stand development in tables. In a next step, Wiedemann (1942) considered the possibility of managing stands with several tree species, adding a further degree of freedom to management. However, given the large variability of possible forest structures and site conditions that approach, although it still focused on stands of a simple even-aged structure, was not practicable. Nevertheless, the aim to predict the growth of heterogeneous stands defined a pioneering benchmark. Starting in the 1960s, computers enabled the comprehensive statistical evaluation of data and the parameterization of growth curves. They enabled calculation of yield tables from a large amount of data. These novel computer-based tables could differentiate between a large variety of management options, such as thinning and planting density (e.g. Curtis 1982). A further line of model evolution aimed at the simulation of stand development based on both an explicit description of stand dynamics and an initial state. It represents the state of a stand by the tree number frequency per size class and comprises three basically different approaches (Pretzsch et al. 2007): (1) differential equation models, (2) distribution prediction models and (3) stochastic evolution models (preceding paragraph section mostly based on Pretzsch et al. 2007). Differential equation models describe the rate of biomass change on a per stand layer basis as balance of tree biomass influx and efflux by a discrete-time approximation of the corresponding differential equation system (Pretzsch 2009, p. 445). Distribution prediction models represent the stand by a probability density function of tree size. They describe stand development as change of the function parameters over time (Pretzsch 2009, p. 446). Stochastic evolution models (Suzuki 1971, 1983, Sloboda 1976) also

aim at describing the evolution of the stem size frequency distribution based on its initial characteristics (Pretzsch et al. 2007). However, that type of model considers individual trees. Growth per tree is represented by a stochastic differential equation that comprises a deterministic term (drift) and a stochastic one (Sloboda 1988). The deterministic share of growth is obtained from the first derivative of the drift, i.e. the change of growth over time that may be related to increasing competition. It is considered as identical for all trees and uses uniform growth parameters for all. The individual deviation from average growth within the drift term, thus, exclusively depends on both the initial tree size and the initial size-related growth. Within the model's deterministic part, these initial conditions suffice to determine the progressive shift of the tree size distribution at given growth parameters. However, the assumption that the growth rate of all trees changes identically over time implies homogeneity of structure and species within a stand being considered. Furthermore, that type of model requires calibration of growth curves specific both to site conditions and management. Still, an important innovation introduced by the stochastic evolution model is the second term that describes an unpredictable alteration of growth through neglected and unknown influences like weather extremes and disturbances.

Matrix models for forestry (e.g. Usher 1979, 1981) originate from general matrix models for population dynamics (Lewis 1942, Leslie 1945). Their theory has been summarized by Liang and Picard (2013). Such models represent the state of forest, by at least one matrix. The matrice's columns (resp. rows) correspond to a specific property and each column (resp. row) corresponds to a specific discrete property value. Thus, each matrix cell refers to a set of discrete properties, e.g. a species and a diameter class. The cell's coefficient is the amount of forest with corresponding properties, e.g. the number of all individuals that share the cell's species and diameter class. Matrix models work on discrete time steps. Within each step and per each cell they calculate the amount of forest that is gained or lost, e.g. the number of individuals that have grown into the cell's diameter class vs. the number that has died or grown into a superordinate class. The definition of properties and coefficients depends on the type of matrix model. For example, EFISCEN (Sallnäs 1990; Schelhaas et al. 2007) represents the forest area per cell where each cell corresponds to volume per ha, species composition and further states. Matrix models calculate losses from cells and transitions among cells based on transition probabilities, that may take into account climate, stand density and stochastic events. These models have widely been applied to serve the objectives of finding a general optimum of management strategies (e.g. Tahvonen et al. 2010, Roessiger et al. 2016) and estimating the impact of climatic change and related disturbances on large scales (Dolstra 2002, Meyer 2005).

However, matrix models emphasize the principle of theoretical parsimony. They rather support fundamental analyses and large-scale studies than ecosystem service studies on landscape scale.

Growth and yield oriented individual tree models that are based on the records of long term plot observation have been developed since the 1970s. They have often been considered as empirical as they refrain from a description of tree-internal processes. However, they apply growth curves that are basically reflecting the balance of catabolism and anabolism (Bertalanffy 1957, Richards 1959, Zhao-gang and Feng-ri 2003). These curves are restricted by the size and density of competing neighbors and modified by a random component. The growth equations and probability distribution functions of growth and yield oriented individual tree models are calibrated based on long-term records of individual tree dimensions. Observation based models, as the group will be denoted in the following, thus further break down tree size distribution into individual tree sizes. They have become regularly applied tools of forest management within a broad range of conditions, including site, forest structure and management system. Some prominent examples are SILVA (Pretzsch et al. 2002) MONTE (Palahí et al. 2004), FVS (Crookston and Dixon 2005), and Heureka (Wikström et al. 2011).

Against the background of ecosystems research, a further model type has been presented by Botkin et al. (1972) with JABOWA. That type is called gap model (reviewed by Bugmann 2001). Its original objective is to model long-term succession as the outcome of growth and competition. Therefore, common gap models represent the stand as a large collection of idealized patches. In the early gap model concept, each tree fully covers the patch it resides on with its two-dimensional ground-parallel crown. Initially, numerous small trees of arbitrarily defined size are randomly distributed across each patch. Each tree is supposed to grow as determined by site conditions and competition with all other trees inside the patch boundary. In a final state, only one tree fully covers the patch it resides on with its crown, reflecting the outcome of a competition process that is driven by site-species relations as well as a random component. The death of this final tree opens a patch-spanning gap with improved light conditions. That drop of competition pressure promotes growth of small trees, starting a new cycle of succession. Gap models originally do not aim at the precision of short term stock prediction but put strong emphasis on competition and survival within long-ranging stand development. Therefore, they often explain growth by a straightforward but physiologically reasoned theory. Within their original scope, thus, gap models rather serve to determine potentially suitable tree species than to predict merchantable timber production.

Physiologically-based models may be considered as an elaboration of growth principles already hinted at in the basic theory of gap models. They specifically aim on the interacting effects of simultaneously changing environmental boundary conditions. To that end, physiological models represent the coupling of various driving forces (light, temperature, nutrient availability) on the level of the plant organ (e.g. TREEDYN, Bossel 1996). On the one hand, their design strives for generalist equations. Such equations serve to represent growth and structure development under a wide range of weather conditions, including markedly novel weather. On the other hand, a typical physiological model describes growth as a result of interconnected processes within soil and canopy. These processes are driven by conditions at the stand's system boundary. Therefore, the theory of such a model, beyond the influence of weather, takes into account the effect of soil fertility, air pollution, and CO_2 concentration. Physiological models, hence, are particularly suitable to represent environmental change effects but often are restricted to a homogeneous stand structure. Nevertheless, a particular group of physiologically-based models also aims at the cohort or even the individual tree level. That way, it combines a high responsiveness with a flexible consideration of stand structure. For example, an individual-based physiological model can be used to explore the impact of weather variability on growth in dependence on stand and canopy structure (Rötzer 2013).

Landscape models, within the study at hand, are models that consider the interaction among landscape units. To that end they consider processes like seed dispersal or spread of fire (Luo et al. 2014). A prominent example for a forest landscape model is the LANDIS model (He et al. 2004). As a different type of landscape model, GraS (Siehoff et al. 2011) considers forest as one among various other vegetation types. That model uses a high resolution. It works on a regular quadrangle grid of laterally interacting small area tiles (e.g. 100 m^2). Tree growth within that model is simplistic and based on yield tables. With particular focus on forest dynamics, however, Hudjetz et al. (2014) further developed GraS to WoodS (Hudjetz et al. 2014) using algorithms from gap models for describing individual tree growth.

Climate impact research on global scale level spawned the development of global vegetation models. Such models consider an adequately limited number of vegetation types including types of forest, e.g. boreal coniferous forest. An early representative of that group is the phytogeographical model of Box (1981). Later versions were developed particularly for climate impact research such as the related but refined model BIOME (Prentice et al. 1992) which could be run with output from global climate models (GCM). Dynamic global vegetation models (DGVM) are dynamic models that have been developed within the same scope in order to assess

transient changes of the vegetation cover (reviewed by Cramer 2002). They typically describe changing pools of carbon, water, and to a part also of nutrients, i.e. nitrogen. Therefore, they consider the exchange of heat and radiation, and of matter, typically carbon and water. Prominent examples are LPJ (Sitch et al. 2003) and HYBRID (Friend et al. 1997). DGVM have been directly coupled to GCMs in order to represent feedback responses (e.g. Giorgetta et al. 2013). They typically consider a homogeneous vegetation cover that is characterized by plant functional types rather than species (e.g. in LPJ, Sitch et al. 2003). Some represent stand structure and species composition at higher detail such as ORCHIDEE-CAN (Naudts et al. 2015). DGVMs have rarely been applied in research studies on landscape scale level, where they did not consider any lateral exchange but were used to provide estimates of the potential natural vegetation (e.g. MC1 by Yospin et al. 2015, Rogers et al. 2011). For that purpose, they do consider a relatively small grid size (e.g. Peaucelle et al. 2017). The general objective of that model group, however, are studies from continental to global scale.

Each of the model types considered adheres to a specific field of application. That application context determines (1) each model type's scale level, (2) the set of system components it covers, (3) the depth to which it explains processes, and (4) the boundary conditions it takes into account. The smaller the scale addressed by the model, e.g. forest management unit vs. continent, the higher is the expectation on the precision of the model result. Accordingly, the more realistic has to be the model theory and the more precise have to be the model's input data. Model properties that promote precision, such as spatial explicitness and depth of process explanation, are not necessarily linked to each other. For example, an imaginary model may represent forest growth on the continental level by an accordingly fast algorithm that considers vegetation just as a homogeneous layer of a particular plant functional type. Still, that model might use a physiological algorithm driven by climate variables to explain growth. Conversely, on the enterprise scale, another imaginary model may use a spatially explicit representation of individual tree competition and management and consider various species. Although that management oriented model is spatially much more explicit, it may apply a growth algorithm that is purely empirical.

A further pivotal determinant of model design is the time period covered by potential simulation scenarios. Since rotation periods are typically long and forests react slowly to interventions and disturbances, forest analysis typically considers decades to centuries. Therefore, scenarios often take into account novel boundary conditions that might be relevant within such a long time range. Such a scenario may imply a climate of unprecedented characteristics. It, moreover,

might either be considered as transient (e.g. Prentice et al. 1993) or as intransient, assuming the formation of a stable equilibrium (e.g. Claussen 1994). Simulation of future scenarios also requires considering the interannual and intraannual variability of weather. For example, it has to capture the strong effect of individual years marked by extreme summer drought (Zang et al. 2014).

3.2 Models for landscape-scale ecosystem service studies

3.2.1 Observation based individual tree models

Facilitation as well as competition among neighboring trees have gained considerable attention in present research on forest dynamics (e.g. Fichtner et al. 2018). That development is strongly driven by modelling demands that origin from the active conversion of homogeneous stands to structured, multi-species forest in some European countries. A part of that development is due to a requirement for increased resilience (e.g. Cavers and Cottrell 2015). Mixed forests exploit resources differently from monocultures. They may have a notably higher individual tree growth as well as maximum stand density (e.g. Pretzsch 2016, Pretzsch and Biber 2016, Thurm and Pretzsch 2016). Since forest structure, mixture composition, and thus response capacity can be very different in forests with the same density or average dimensions, individual tree models are ideal for simulating the development of structured and mixed forests. Prominent members of that model group are observation based individual tree models (e.g. Pretzsch et al. 2002). These stand models directly derive growth and dimensions of individual trees from observed relationships to their environment. Typically, they calculate stem height growth and diameter growth per time step. Based on the new diameter and height, crown dimensions are derived. The resulting idealized crown shape and often that of other trees within the stand being considered, are affecting the tree's stem growth within the next time step. Observation-based individual tree models are used in forest management planning from stand to enterprise level over several decades, up to a rotation period. These practice-oriented models aim at the control of stock, yield and structure of the mature stand.

One important group of observation based models originates from the Stand Prognosis Model by Wykoff et al. (1982). That model group directly estimates growth of each individual tree from the tree's dimensions as well as from site properties. For example, the Stand Prognosis Model describes individual tree diameter growth per time step with an empirical function. That function uses the individual tree diameter and indicators of crown vitality, site and stand-level competition as predictors. Therefore, the function's parameters were calibrated to observed data

of tree growth and the function's predictors using regression analysis. The specific growth algorithm of that group, the direct estimation approach (Pretzsch 2009, p. 453) refrains from calculating competition based on explicit tree positions. Instead, it represents growth presuming average competition on a per tree size basis. That competition average, still, may refer to a confined range around the tree being considered. Prominent models of the group are BwinPro (Nagel et al. 2006), FVS (Crookston and Dixon 2005), Heureka (Elfving 2010, Wikström et al. 2011) and PROGNAUS (Sterba and Monserud 1997).

Another group of models considers the explicit position per tree for calculating the tree's growth. That group comprises models such as MOSES (Hasenauer et al. 2006, Thurnher et al. 2017), MOTTI (Hynynen et al. 2002, 2005), SILVA (Pretzsch et al. 2002) and SYBILA (Fabrika and Ďurský 2005). Models of that group are based on a potential growth to time relation that is specific to site and species, but general with respect to structure. To that end, its representatives approximate the potential tree size over tree age by a high quantile of size over age. In order to describe that relation, they often use the integral of a differential growth equation (e.g. Chapman-Richards in Pretzsch et al. 2002) and calculate the equation's parameters from site conditions (e.g. Kahn 1994). These models reduce the growth potential per tree and time step by a competition factor that is based on attributes of dominance. That approach, denoted as potential modifier method (Pretzsch 2009, p. 454), often predicts potential growth starting at each time step from a biological age that is obtained from the potential growth function via tree size (often height). This algorithm implies that the growth potential at a given point in time was exclusively determined by developmental state and not by history (Monserud 1975). In that respect it thus conforms to the state-space concept in forest modelling as explained by García (1994).

Observation based individual tree models originally focused on growth and yield under observed climate conditions. More recently, however, they have been applied within landscape studies of ecosystem service provisioning under various future scenarios of management and climate (Biber et al. 2015). The time step of the model type typically covers several years (e.g. five, Pretzsch et al. 2002). It corresponds to the one used by management planning that traditionally extrapolates from periodic evaluation of inventory data. The spatial unit considered by observation based models is usually the stand, often represented by a number of inventory plots (Pommerening 2000) that share identical preconditions of growth and management.

Both types of observation based models consider competition, either as a growth predictor or as a modifier of potential growth. If competitive pressure exerted on a tree is assumed to be

independent of its horizontal position, a corresponding competition indicator may be calculated on a per stand basis (e.g. Wensel and Koehler 1985). However, models that are applied to a stand structure of horizontal heterogeneity (e.g. variable mixture within same size class, species clusters, irregular shelterwood) need to take into account nearest neighbor competition and, therefore, individual tree position (e.g. Pretzsch et al. 2002, Hasenauer 2006). The potential modifier method facilitates the representation of nearest neighbor competition as dependent on site, species and tree arrangement, because it separates competition from the set of growth predictors. Thus, models which apply that method are particularly responsive to the stand-intrinsic spatial pattern of thinning. Accordingly, they may represent structure and stock development also for highly heterogeneous forests that emerge from structural conversion. Forests of that kind constitute an important future forest type in many Central European regions (Bolte et al. 2009). Keeping in mind the relevance of the other approaches, this work will therefore focus on the model type that applies both potential growth and a distance dependent modifier. That model type will be denoted as potential modifier model hereinafter (e.g. SILVA, Pretzsch et al. 2002). The development of such models strives to maintain applicability to various site conditions, including those affected by climate change. To that end, dose-response functions have been derived in order to dynamically calculate a potential modifier based on various climatic variables and soil properties (Kahn 1994).

3.2.2 Gap models

Gap models, reviewed by Bugmann (2001), originally aim to predict the development of species composition on a regional scale as it develops over centuries. To that end, they most often presume an equilibrium climate. The common gap model considers a representative virtual stand of independent patches and models a long-term secondary succession that starts from a presumed seed bank on bare ground. This structural development typically proceeds until a stable state of species composition is achieved. The context in which gap models have been applied since the 1990s are often scenarios of novel climate that may develop due to global change (Bugmann et al. 1997, Fontes et al. 2010). The patch size of a gap model is originally 100 to 1000 m², in order to represent the area influenced by a large tree. The time step of gap models is one year or less.

Gap model design originally used a simplistic physiological explanation of growth. This was based on the multiplication of growth factors that were calculated from weather and soil conditions on the one hand, and competition pressure on the other (JABOWA, Botkin et al. 1972). Given the high relevance of competition for the long-term development of stands, more

recent models derive these factors from more ecophysiological theory (e.g. 4c, Bugmann et al. 1997, FORMIX, Huth et al. 1998). Therefore, these models require a sub-annual to even sub-daily time step.

While gap models originally describe neighbor competition based on a highly simplistic tree crown, more recent ones use a three-dimensional crown shape that is at least realistic in diameter and length. The majority of these gap models, in order to spare computational time, still calculate light competition from the horizontal average of light transmission per patch. In contrast, the model SORTIE (Pacala et al. 1996), although it originates from common gap models, calculates light extinction from the explicit arrangement of neighboring trees. Owing to computational efficiency demands, however, growth in that model is based on a straightforward theory: SORTIE represents diameter growth per tree and time step from site-related growth per unit diameter at high vs. zero light, and the tree-related proportion of light being received. Other modern gap models, e.g. PICUS (Seidl et al. 2005) and FORMIND (Fischer et al. 2016) retain the patch based description of neighbor competition. For representing light competition, both neglect the explicit position of trees inside a patch being considered. However, they take into account the dominance related competition among trees through light extinction as determined by the average of canopy leaf area per patch and unit of height. Due to the efficiency of the patch-based approach, both PICUS and FORMIND are able to describe growth based on more advanced physiological theory.

As the original focus of gap models is on the long-term change of species composition and structure, they are particularly feasible to describe processes of disturbance and regeneration. Accordingly, their field of application has extended towards forest dynamics within particular landscape types, such as the ecotone between the montane and subalpine Pyrenees (Ameztegui et al. 2015). Gap models have also supported studies on ecosystem service provision within particular landscapes (e.g. Wehrli et al. 2003, 2006). Some have been extended for studying effects of management within a rotation period. Seidl et al. (2005), moreover, couple the gap model PICUS with a simplified physiological production model in order to increase the sensitivity of the gap model to environmental changes. Bose et al. (2015) and Yasuda et al. (2013) study possible effects of thinning patterns within the typical time range of a rotation period. Accordingly, they have put emphasis on an individual based stand representation at the cost of physiological realism.

3.2.3 Physiological models

Physiological models were originally designed to represent the average growth of trees within homogeneously structured forest (for reviews see Agren et al. 1991, Mäkelä et al. 2000, Le Roux et al. 2001, Landsberg 2003). Such models disaggregate the stand and tree perception into interacting modules which consider tree internal processes down to the subcellular level. The concept of physiological models is to use general equations that describe sub-processes of growth in order to explain tree biomass changes and matter exchange. Presuming an adequately complete theory, they enable extrapolation of tree responses to environmental changes beyond the range that has yet been observed. The range of such changes is not restricted to unprecedented weather of novel variability but also includes other boundary conditions, such as the exposure to different ozone and CO_2 concentrations. Physiologically-based models describe carbon-, nitrogen-, and water balances that depend on the conditions at the leaf and root surface and, hence, on the micrometeorological fluxes within the forest canopy (Jarvis and Mc. Naughton 1986, Whitehead 1998) as well as on the soil-intrinsic conditions. Therefore, physiological models generally also include an estimate of light, temperature, and water distribution which is often based on physical processes such as radiation extinction, reflectance and absorption. That way, they may use weather records or climate scenario data given above canopy in order to obtain the according driving force variables at leaf area and soil surface. Besides temperature and radiation transfer, an accurate notion about the availability of water is particularly important. Therefore, the water balance includes interception, transpiration and ground evaporation processes and considers the belowground water storage and distribution as dependent on soil properties. However, a lateral exchange between adjacent forest patches or access to the ground water table is generally not considered.

While physiological models originally work on monthly (e.g. Landsberg and Waring 1997) down to daily time steps (e.g. Kirschbaum 1999, 2000), more recent representatives of that group calculate at least some processes in a temporal resolution of less than one day (e.g. Grant et al. 2007, Grote et al. 2011). That investment into computational expense is required as the models' depth of process explanation is related to interdependences on a small time scale. The early physiological model TREEDYN 3 (Bossel 1996) presumed a single-species even aged stand. That model simulated one single tree as a stand representative. In contrast, the also physiologically-based model BALANCE is a distance-dependent individual tree model that uses explicit tree positions (Grote and Pretzsch 2002). As the application of such a model is limited by computational effort, several more recent developments consider a number of

competing cohorts. These cohorts are groups of trees or ground vegetation. Typically, each cohort is represented by a single individual (Grote et al. 2011, Deckmyn et al. 2008). Cohorts may occupy and also share different canopy or soil layers of variable extension.

Scientific work on physiological models has also approached the prediction of wood quality as a result of carbon balance and allocation (e.g. Mäkelä and Mäkinen, 2003). A very detailed example is an extension developed for the ANAFORE cohort model which applies the pipe model theory (Shinozaki et al. 1964, Deckmyn et al. 2006). Such models may calculate year ring internal properties such as latewood biomass and sapwood extension at high spatial resolution (Deckmyn et al. 2008, 2009).

3.2.4 Landscape models

A typical landscape model such as LANDIS (He et al. 2004) runs on the regional scale. It represents succession based on presence or absence of species-age cohorts at a grain of 10 to 500 m, and operates with a 10-year time step. LANDIS notably takes into account the effect of disturbances (i.e. fire) on vegetation dynamics based on fuel accumulation and fire probability. A variant of this model, LANDIS PRO (Wang et al. 2013), also accounts for competition between tree cohorts. It therefore uses a more detailed cohort definition than the original LANDIS model that is based on tree number per species and an age dependent DBH. This structure enables LANDIS PRO to quantify stand-scale resource competition based on the Stand Density Index SDI (Reineke 1933). Fire spread in many regions is a major source of disturbance and seed dispersal is an essential process of fire resilience. Thus, models of the LANDIS type typically represent both processes based on properties of neighboring grid cells, realizing horizontal exchange. Schumacher et al. (2004) further developed LANDIS to LandClim. They added a quantitative description of biomass growth that models individual tree development on a 10-year time step based on a potential modifier method.

Some models in this group are designed for more detailed calculations and therefore concentrate on relatively small landscapes. For example, the Woodland Succession Model (WoodS, Hudjetz et al. 2014) predicts succession as a result of expansion, disturbance and competition. It uses a species-specific mean growth rate from yield tables in order to calculate tree height growth from a modified Bertallanffy equation. WoodS is applied for areas of a few thousand ha and over a time range of 50 to 100 years. To that end, it discretizes the target area by a fine grain quadrangle grid of up to 10 m × 10 m tiles. WoodS notably takes into account the spread of herbaceous species.

At even higher spatial resolution of 1 m² tiles, Rammig et al. (2006) modeled the establishment of forest stands after heavy blowdown inside a total area of several hectares. They describe seedling dispersal, germination, seedling survival and growth as dependent on herb layer properties based on cellular automata rules. Although the model works on a scale far below that of a typical landscape model, it also takes into account horizontal interactions of grid tiles, represented by spatial correlation and clustering. Similar to typical landscape models, it uses a simplistic representation of individual tree growth in order to spare computational time.

3.3 Innovation requirements

Each model type takes into account specific processes and target variables that are all highly relevant if the impact of climate change on forest ecosystem services is considered. As summarized in the following, there is considerable requirement for new modules that together link key processes of competition, disturbance and regeneration with forest growth and development.

3.3.1 Sensitivity to thinning

The horizontal and vertical location of thinning and harvest interventions decides on which individuals are released from competition and to what extent. Depending on the spatial intervention pattern, particular species, e.g. shadow tolerant ones, may be fostered or a particular size-class composition achieved. That process is crucial where forestry puts emphasis on forest conversion. Therefore, some prominent observation based individual tree models consider position, size and competition per individual tree (Pretzsch et al. 2002). Some gap models that have been applied to study effects of different management systems (e.g. Pacala 1996) also describe competition on a per-tree basis at the cost of physiological detail. Others still consider competition as horizontally homogeneous within each patch but take into account the vertical gradient of transmission calculated from realistic individual tree crown shapes. (e.g. FORMIND, Fischer et al. 2016). Each of these modelling approaches follows the overall objective to represent stand structure details at high spatial resolution while maintaining acceptable computation speed. Such stand models address managers on the level of the forest management unit and political decision makers on the landscape scale level. In order to be computationally efficient, they generally settle for a shallow depth of process explanation.

3.3.2 Sensitivity to environmental change

Future scenarios of environmental change require forest simulation models that represent the combined effect of weather, CO_2, and air pollution. Against that background, the coupling between light competition and competition for soil resources, i.e. nutrients and water is an important process of stand development (Pretzsch and Biber 2010). It results in a relevant shift of competitive advantage towards smaller trees if site quality decreases and vice-versa (size-symmetric vs. asymmetric competition, Schwinning and Weiner 1998, Wichmann 2001, 2002). Under conditions of aggravated drought, CO_2 increase and atmospheric pollution, the competitive advantage gained through height dominance might thus differ from the one currently observed. That change may affect the applicability of parameters defining competition within observation based models. One well-reasoned approach to implement size-symmetric vs. asymmetric competition within the potential modifier approach (see section 3.2.1) is modifying competition based on the dynamically calculated site index (Pretzsch and Biber 2010). Modelling the combined impact of extreme drought and atmospheric pollution on forest development, still, might require describing key processes that underlie the additional influence of species, mixture and structure (e.g. Pretzsch et al. 2013, Pretzsch et al. 2016, Rais et al. 2014a). Therefore, physiological models try to explain the carbon allocation process directly from environmental influences that are modified by stand structural properties. They can thus serve to study the effect of stand structure on competition under scenarios of novel weather variability. Long-term studies may hence benefit from linking physiologically-based models with others that describe species-specific and structure-dependent individual tree growth. Physiologically-based individual tree models (Grote and Pretzsch 2002), however, are slow. A hybrid model for application on landscape scale level, in contrast, has to be fast in order to consider numerous stand types and climate scenarios.

3.3.3 Regeneration

Regeneration has been particularly important within long-term succession studies using gap models. However, against the background of forest conversion and climatic resilience (Kölling 2007, Ende et al. 2010, Cavers and Cottrell 2015), there is now general demand for representing establishment and growth of saplings. Given the rise of forestal labor cost since the 1920s (Macgregor 1947), natural regeneration in particular has become increasingly interesting for forest management. Recent work, therefore, has embedded regeneration modules into management-oriented observation-based models (e.g. Biber and Herling 2002, Herling 2004,

Millington et al. 2013). That development may generally benefit from gap models that provide a valuable pool of comprehensive regeneration theory. However, long-term succession modelling usually starts on bare ground and retrieves its initial regeneration state from spin-up runs (e.g. Didion et al. 2009). Practical model application and scenario studies on landscape scale level, in contrast, consider a shorter time period. Within that scope, spin up-runs might notably extend the computational effort per simulation scenario. Moreover, while understory stock and species composition are decisive for stand structure development throughout a rotation period, they are difficult to evaluate. Thus, obtaining the initial state of regeneration from realistic relations to stand structure and site may notably benefit regeneration modelling (Schweiger and Sterba 1997, Tremer et al. 2005).

3.3.4 Linkage to landscape processes

Management decisions on species composition and structure as well as forest fertilization may affect the water balance and water quality of a landscape being considered. For example, thinning intensity and tree species selection influence groundwater recharge (Sutmöller and Meesenburg 2012) and the quality of rivers and lakes (Gundersen et al. 2006; Weis et al. 2001). Mediated by the flow of ground and surface water, the local effects of stand management disseminate into the landscape. That way, planting, thinning, harvesting, and fertilization influence the landscape's available water amount and quality both in the short-term and in the long run. Forest management on landscape scale level may also aim at explicitly controlling processes of lateral exchange. Within regions of notable fire risk, such a process is fire spread. Another regional process, seed dispersal, may be important for establishing forest resilience, both towards fire and windthrow. Model development, therefore, needs to capture the combined effects of management on the landscape scale. Representing these effects comprehensively with a physiologically based individual tree model would be computationally expensive. Moreover, a physiological model is sensitive to numerous parameters that could not be obtained at adequate precision within a heterogeneous landscape. Therefore, consideration of landscape processes is typically linked to a diminished depth of process explanation and stand structure representation (e.g. Tietjen and Huth 2006). A possible solution to this dilemma would be to apply a model that combines the specific advantages of observation based models (individual trees), physiological models (profound explanation of processes), and gap models (regeneration) within representative subareas. Such a hybrid approach would use a dynamic regeneration module to provide an interface to landscape processes such as seed dispersal (e.g. Luo et al. 2014) and at the same time could represent the understory fuel load realistically.

3.3.5 Wood quality development

Within a given scenario of forest development, the quality distribution of harvested wood determines the economic return achieved. That distribution depends on management options like planting density, thinning regime, and rotation period (e.g. Schütz et al. 2015, Tahvonen et al. 2013). The assortment structure of wood available for long-term usages such as building and furniture is highly important for determining the long-term substitution effect of forest management on the atmospheric CO_2 balance (Oliver et al. 2014, Skog and Nicholson 1998). The wood quality distribution thus, determines the scenario-specific effect of management on economic productivity on the one hand, and on the atmospheric CO_2 balance on the other. Thus, it may be crucial for representing the tradeoff between acceptable incomes in forestry, reduction of atmospheric CO_2, and further ecosystem services like biodiversity (Oliver et al. 2014). Accordingly, Mäkelä et al. (2010) recommend implementing wood quality simulation into models for long-term silvicultural planning.

A particularly important trait of wood quality is yield per strength grade. Wood strength modelling might simply consider the outer properties per log. That approach, however, cannot represent the density and knottiness of boards obtained from a particular log. In order to estimate the bending strength per individual board based on a sawing simulation (Todoroki and Rönnqvist 2001), models need to derive the log's inner structure from its growth history. Deckmyn et al. (2008) use a physiological cohort model that simulates the allocation of carbon to conductive pipes, fibers, parenchyma, and bark in order to simulate the development of wood tissue composition on a daily time step. The benefit of such a detailed approach, however, is limited by the precision of parameters that are expensive to obtain (Deckmyn 2009). An alternative approach derives the ring width and the log-intrinsic arrangement of branches from the annual stem and branch growth of an observation-based model. A prominent example for that method is SYLVER (Mitchell 1988) which describes the effect of crown interference on branch and knot positioning in particular detail. The growth component of SYLVER is the individual tree model TASS. That non-physiological growth model calculates crown growth based on branch growth. Based on the resulting quantity of foliage it computes the annual stem growth. TASS provides hence very detailed algorithms for crown competition and crown shape that enable an accordingly precise representation of the crown-intrinsic and hence stem-intrinsic branch architecture (Mitchell 1975). In contrast, common observation based individual tree models calculate an idealized convex crown hull from the dimensions of the stem. Nevertheless,

it may be assumed that they may infer a simplistic branch architecture from that crown shape and thereby retain their high computational efficiency.

4 Objectives

Forest simulation studies at landscape scale level may serve to estimate the effect of various possible management pathways on ecosystem service provision (e.g. Egnell et al. 2011). Such studies, on the one hand need to consider the direct influence of future climate. On the other hand, they have to take into account risk mitigation measures and silvicultural interventions that represent socio-economic boundary conditions, such as wood demand and recreational criteria (Biber et al. 2015). The coupling of different modelling approaches might thus be required in order to represent the important processes regarding a particular research question within selected subareas. To that end, the thesis at hand presents various model components that are embedded in a conceptual framework with an individual tree model at the core. Emphasis is put on the objective that the computational efficiency of a potential modifier approach is retained (Figure 1).

Growth allometry and nearest-neighbor competition are particularly elaborate in observation based individual tree models that apply the potential modifier method. To allow for weather sensitivity and possible coupling to a hydrological component, the thesis at hand firstly suggests a new hybrid model concept. That concept combines the individual tree growth allometry of the observation-based model SILVA (Figure 1, module S) with the cohort-related carbon and water balance calculations of the physiological model MoBiLE-PSIM (Figure 1, module M). Secondly, the thesis suggests a wood quality module (Figure 1, module Q) that can be coupled with a SILVA-based individual tree allometry module (Figure 1, module S). That module simulates yield per timber grade and thus supports the estimation and valuation of wood supply. Based on the simplistic crown perception of the individual tree module (Figure 1, module S), the wood quality component computes virtual stem structure and finally performs virtual sawing and individual board grading. The thesis at hand assumes that an existing dynamic regeneration module is part of the conceptual framework (Figure 1, module R). It is based on previous work of Biber and Herling (2002) and Herling (2004), and might be linked to the individual tree allometry module. In order to complement that dynamic regeneration module, the thesis thirdly suggests a statistical regeneration module (Figure 1, module I). That module provides initial values of regeneration that cannot be obtained from inventory data. To that end, it derives regeneration stock from mature stand properties and site conditions. Modules M, S, and R, where no physiological module is required, may be straightforwardly replaced by the complete SILVA model.

To achieve the outlined objectives, the thesis at hand has used the following methodology. The first objective has been met by merging the core theory of SILVA (Figure 1, module S) which is the individual tree growth allometry of stem and crown with MoBiLE (Figure 1, module M), a weather-sensitive cohort model based on physiological processes (Grote et al. 2011). That way, it incorporates species-specific and competition-induced individual tree growth dynamics, and at the same time provides responsiveness towards yet unobserved changes of environmental conditions. For the second objective, the prototype of a wood quality module has been newly implemented (Figure 1, module Q). It has been embedded into a specifically designed potential modifier individual tree model in order to identify pivotal properties for board strength simulation both in model and module. Finally, a novel statistical regeneration module has been developed addressing the third objective (Figure 1, module I). This inventory-based module enables a plausible initialization of the modelled regeneration process. Thus, it is an essential prerequisite for the representation of dynamic regeneration (Figure 1, module R) within an individual tree allometry module (Figure 1, module S). The specific model developments that have been implemented to support each of these objectives are presented in the following section.

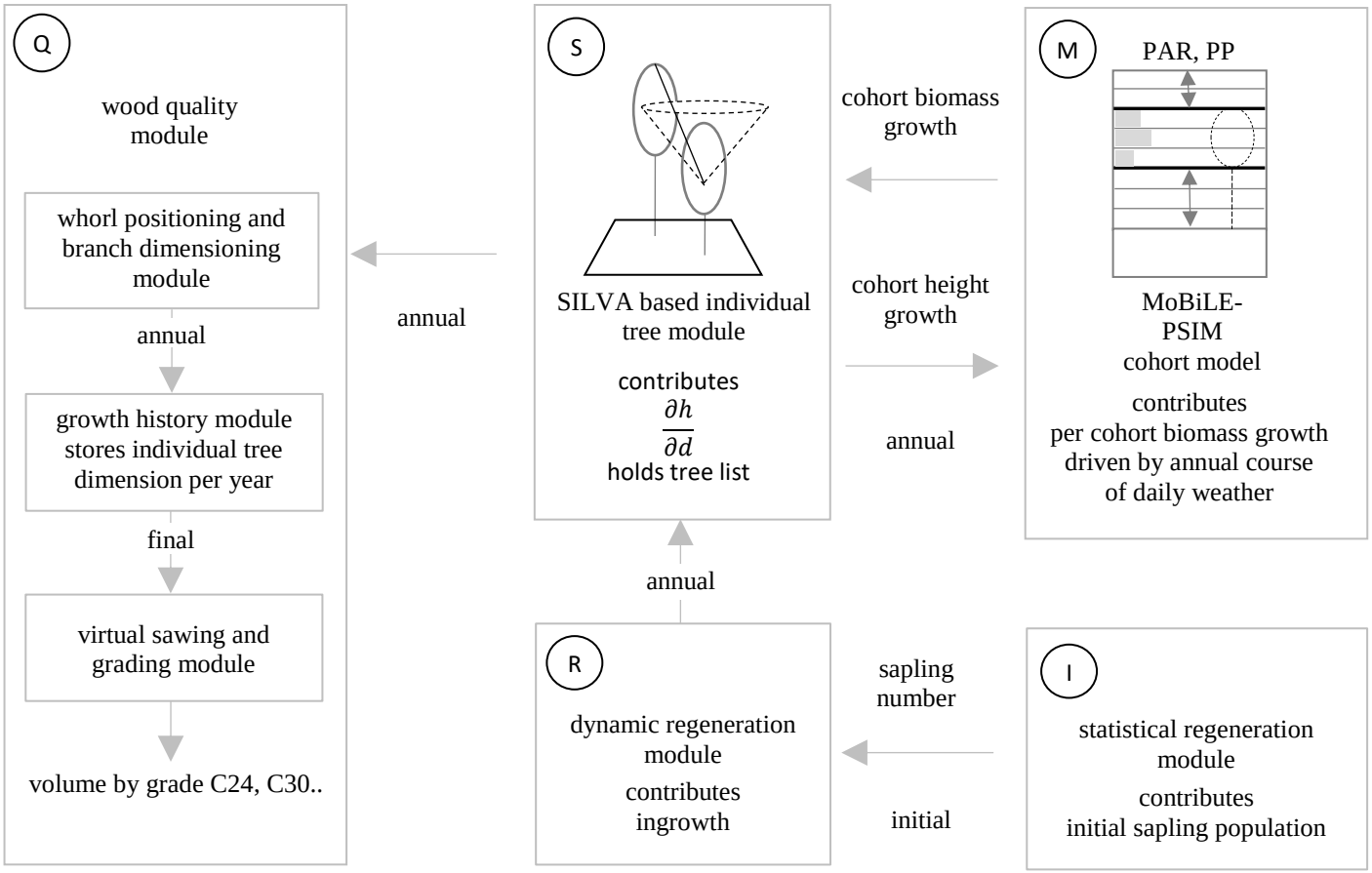

Figure 1. Conceptual modelling framework that combines the allometry description of a SILVA-type individual tree module (S) with the per cohort biomass prediction of the physiological cohort model MoBiLE-PSIM (M); individual tree module S provides individual tree stem size data to a wood quality module for logging, sawing and strength grading on board level (Q); module S also includes a dynamic regeneration module (R) that receives its initial regeneration biomass based on overstory properties from a statistical model (I); symbol *h* is tree height, *d* is diameter; C24, C30 .. refer to strength classes in accordance to CEN (2009); PAR is photosynthetically active radiation and PP is precipitation.

5 Publications

The following section outlines the methods and the results per each publication that contributed to the thesis at hand. To that end, the section confines itself to concise explanations. It exclusively considers the results that are most relevant for the thesis objectives. Therefore, it is intentionally succinct in description of data properties and detail of result. Each abstract is slightly modified at its beginning to comply with the objective of that thesis. For a profound evaluation, the reader may kindly refer to the peer-reviewed publications appended to that work.

5.1 Short contents

Within the first publication -

Extending a physiological forest growth model by an observation-based tree competition module improves spatial representation of diameter growth -

Poschenrieder et al. (2013) develop and test a mass conservative bidirectional coupling between MoBiLE and SILVA. That coupling translates cohort-related subdaily carbon allocation and biomass growth to annual height and diameter growth of individual trees at the end of each simulated year. Based on the resulting tree dimensions, it redefines the top and bottom limits of each cohort. These limits define the starting condition of the ensuing year. The hybrid model that results from the coupling is weather sensitive. It is evaluated based on experimental plot data.

Within the second publication -

Modelling sawn timber volume and strength development at the individual tree level – essential model features by the example of Douglas fir -

Poschenrieder et al. (2016) provide a model architecture for the simulation of board strength over a rotation period by an observation based management model. The core module of that architecture translates crown shape, branch arrangement and annual growth into the inner structure of the stem. A serially connected module based on that structure calculates the bending strength per individual board. The model architecture is evaluated based on experimental plot data from previous work.

Within the third publication -

An inventory-based regeneration biomass model to initialize landscape scale simulation scenarios -

Poschenrieder et al. (2018) present a statistical model that infers regeneration stock from overstory and site characteristics. That model is based on inventory plot data. It uses regeneration biomass as a predicted variable, as biomass closely depends on the stand intrinsic resistances to radiation, heat, and water. In order to represent the influence of local disturbances the modelling approach works on a stand-intrinsic scale and includes a stochastic component. The approach is evaluated based on spatially dense plot data from the Bavarian state forest inventory.

5.2 Author's contribution

5.2.1 Contribution to Poschenrieder et al. (2013)

I sampled the trees, oversaw core-boring and verification of year ring data and statistically evaluated the data. I developed the theory of model coupling, designed, programmed and tested the individual tree module for MoBiLE. I wrote the major part of the manuscript before first submission and restructured and rewrote most of it within a major revision.

5.2.2 Contribution to Poschenrieder et al. (2016)

My co-author Andreas Rais and I formed the complete model theory through close cooperation. As my individual contribution, I designed the dominance and distance dependent parts of competition and the theory of early growth reconstruction. Within that scope, I introduced the random effect of growth and calibrated it based on stem disc and experimental plot data. Furthermore, I formed the theory to translate branch architecture and crown shape into the inner stem structure. I designed the whole model architecture. Finally, I conceptualized and carried out the statistical analysis to evaluate the model. I wrote the publication and elaborated improvement suggestions of my co-authors.

5.2.3 Contribution to Poschenrieder et al. (2018)

I conceptualized the model, the data preparation, the model calibration, the model evaluation, and the article's structure. I lead through all practical work of modelling and data handling. I wrote the major part of the publication and elaborated the contributions of my co-authors.

5.3 First publication (short version)

Poschenrieder et al. (2013) was published in European Journal of Forest Research with title

Extending a physiological forest growth model by an observation-based tree competition module improves spatial representation of diameter growth.

5.3.1 Abstract

Future scenarios of forest development need to consider a changing interannual and intraannual variability of weather. Therefore, they have to consider within-year feedbacks between growth and environmental conditions. To meet this challenge, models are needed which support and complement the widely-used observation-based decision systems in forest management and consulting. Physiological models in particular provide the fundamental prerequisites to reflect the impact of various simultaneously changing environmental conditions. However, a physiological representation at the individual tree level is computationally very expensive and sensitive to uncertain initializations. We thus propose an approach that combines a modern representative of the physiological cohort model type, MoBiLE-PSIM, with the individual tree competition concept of a distance dependent empirical growth simulator, represented by SILVA. The resulting hybrid provides a key feature for the consideration of forest management in long-term simulations at high computational efficiency. That extended model was evaluated with growth-diameter distributions obtained from core-boring at two beech (*Fagus sylvatica* L.) forest sites in Southwest Germany that differ in exposure and soil conditions. The mean bias of annual stand scale growth from 2001 to 2007 decreased from -0.59 to -0.41 mm at one evaluation plot and from -0.55 to -0.24 mm at the other when the competition module was coupled in. Inclusion of the SILVA based individual tree module into MoBiLE-PSIM improved the size dependent representation of competition and growth on five year and even annual time scale. This was particularly the case where the spatial distribution of dominant trees was clustered.

Arthur Gessler and Rüdiger Grote initiated the project. Werner Poschenrieder sampled the trees, oversaw core-boring and verification of year ring data, statistically evaluated the data and designed and tested the individual tree module for MoBiLE. Werner Poschenrieder and Rüdiger Grote wrote the manuscript. Hans Pretzsch finally reviewed the manuscript and contributed to it.

5.3.2 Short introduction and methods

The first publication extends the ecophysiological cohort model MoBiLE-PSIM (short MoBiLE) with an individual tree growth interpolation that is based on the potential modifier method of SILVA (Pretzsch et al. 2002) but is set up in order to satisfy the simulated cohort volume increase. Inside the extended version of MoBiLE (MoBiLE-ST) both MoBiLE and the interpolation plug-in are coupled in both directions on the annual timescale: the controlling variable provided by MoBilE is the cohort volume growth, and the ones returned back are the new dimensions of the cohort representative tree (Figure 2) that redefine the extension of the cohort. The algorithm that scales down cohort biomass and volume growth to the individual tree level applies a calculation of tree volume and tree growth based on SILVA that precedes the actual calculation of height and diameter growth. The key step of the downscaling algorithm is to correct both SILVA-based growth of height and diameter of each individual tree by the factor *f* shown in Equation 1:

(1) $$f = \frac{\sqrt[3]{\omega} - 1}{\sqrt[3]{\omega^*} - 1} \quad \text{where} \quad \omega = \frac{v_1}{v_0} \quad \text{and} \quad \omega^* = \frac{v_1^*}{v_0^*}.$$

Variables v_0* and v_1* are individual tree volumes at the start and end of year respectively that are calculated from the timber-wood taper function of SILVA. The volume at the end of year v_1* results from dimension growth calculated by the potential modifier method. Tree volumes v_0 and v_1 are calculated from the cohort volumes at start and end of year that are passed to the module and the share respectively of v_0* and v_1* within the cohort. Intuitively explained, the expression approximately is the ratio of a relative volume and dimension change resulting from the physiological part of the hybrid model to one that corresponds to the SILVA growth curves. The original publication gives an in-depth explanation of the approach.

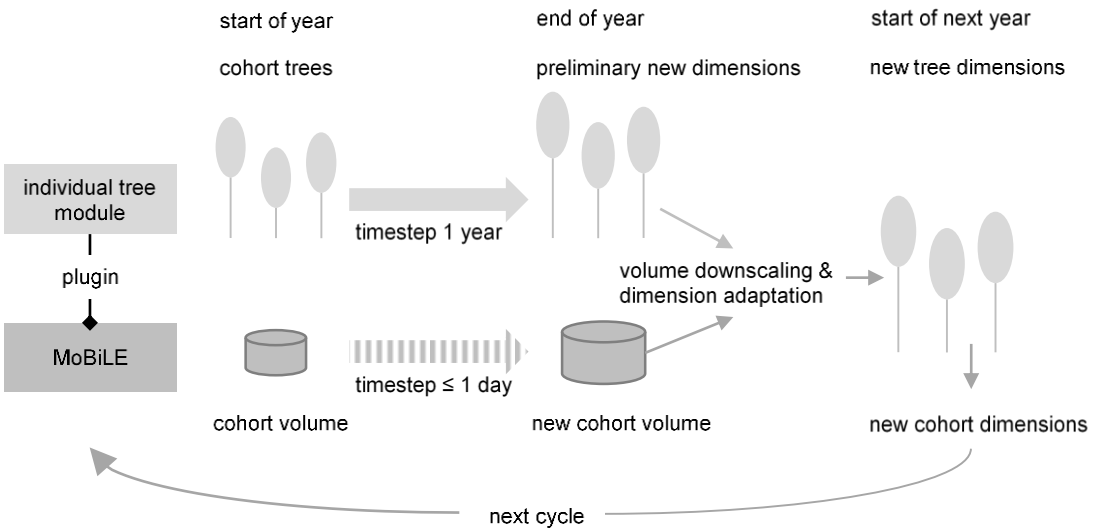

Figure 2. Interaction of MoBiLE and the individual tree module simplified; the individual tree module (top) works on a time step of one year and contributes growth allometry; the physiological model (bottom) works on a time step of less than one day and contributes biomass growth based on carbon allocation; both contributions (right) yield an update of the individual tree dimensions within a mass conservative algorithm; the updated tree dimensions form new cohort dimensions at the start of the next simulated year.

Our model evaluation took advantage of extensive data from two sloped areas near Tuttlingen in south-west Germany (slope 25°, elevation 800 m a.s.l) that have repeatedly been investigated for forestry and ecophysiological purposes (e.g. Geßler et al. 2001; Holst et al. 2010). They are situated within a region of shallow soils on porous limestone where growth depressions due to drought have repeatedly affected stand development in the past (Maaten 2011).

One slope is facing towards SW direction (defined as SW-slope), while the aspect of the second slope is NE (NE-slope). The horizontal distance between both sites is about 800 m. Both hillsides are covered with 80 to 90-year-old single-layer, beech-dominated (> 90 %) forest stands.

Two control plots of previous work were selected for evaluation, NE-C (68 m x 77 m at horizontal projection) and SW-C (71 m x 70 m) which had not been thinned after setup of the experimental site in early 1999. Mean stand properties based on a forest inventory in Winter 1998/99 are given in Table 1 (height and diameter have been taken from Hauser 2003, and the number of trees per ha at horizontal projection have been calculated based on the tree lists reported within the scope of that work).

Table 1. Growth and yield related key properties of the two experimental plots considered (Figure 3); the name per property is given by column Plot property; the property's value is given per plot, i.e. NE-C vs. SW-C.

Plot property		NE-C	SW-C
Mean basal area stem	height (m)	26.5	21.1
	diameter at 1.3 m (cm)	25.6	21.5
Diameter 95% range of variation (cm)		10 to 39	11 to 32
Number of trees per ha		516	658

The pattern of stem base position and DBH at NE-C is rather irregular whereas at SW-C it has a clear concentration of larger trees at the center of the downhill side (Figure 3). The species distribution within each of the two plots included 94% beech and minor contribution of other hardwood. All trees were thus considered as beech in the simulations and following analysis.

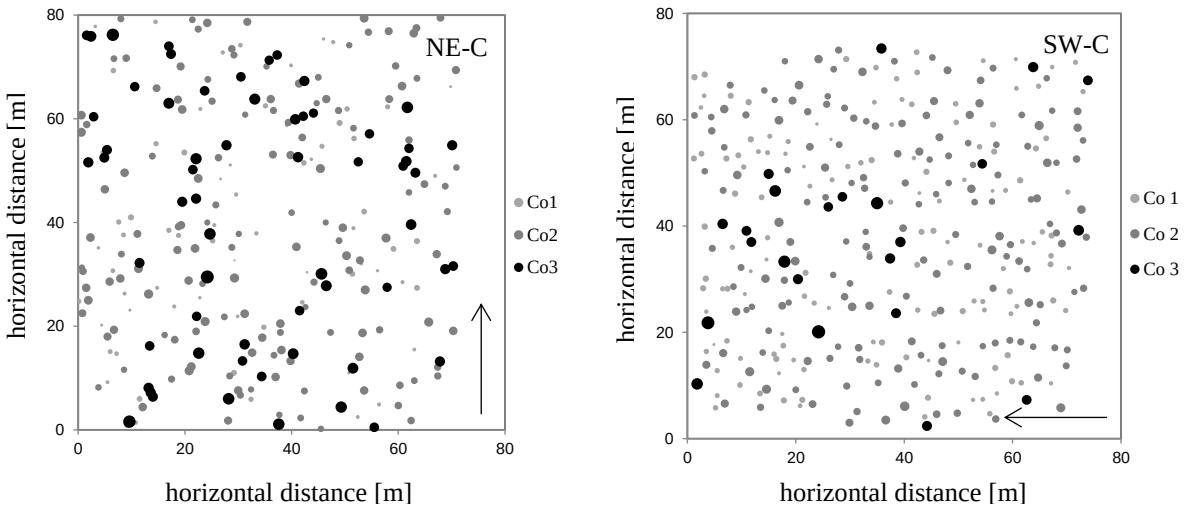

Figure 3. Stem base positions within plots NE-C and SW-C, differentiated by diameter interval (in cm, end diameter excluded) 0 to 20, 20 to 30, 30 to ∞, designated by Co1, Co2 and Co3 respectively; arrows designate the direct down-slope direction; key properties of both plots are compared by Table 1.

The study used DBH and position that had been taken in winter 1998/99 (Hauser 2003) and borer probes taken in early spring 2011. Based on the age corrected DBH distribution of 1999 and on the observed frequency of DBH within intervals of 10 cm, we selected a stratified tree sample within each plot in March 2011 (n=27 at NE-C, n=26 at SW-C) and obtained two stem wood cores from each sample tree. Tree height, height to crown base and crown diameter were computed by the growth simulator SILVA (Pretzsch et al. 2002), based on the individual tree lists and the mean basal area stem height.

Soil profile data for model initialization were taken from Holst et al. (2010). Weather data had been collected from 2001 to 2007 on a tower of approximately 1.5 times stand height within each of the sites. They have been published in Holst et al. (2004, 2010) as well as in Holst and Mayer (2005). Detailed descriptions of the instrumentation can be found in Mayer et al. (2002).

Simulation spanned the time range from start of 2001 to end of 2007. A pre-run of three years preceded each simulation run to provide a plausible internal state of variables that cannot directly be initialized, such as e.g. pool specific nitrogen concentrations within the soil. Such variables typically stabilize to realistic values within three simulated years. The stabilizing run was based on repetition of the weather of 2002 that had average characteristics.

This digest version of the study has its focus on the evaluation of MoBiLE-ST versus the original version of MoBiLE. Within that scope it presents a selection of the most relevant results. One part of the corresponding evaluations considers the 5-year diameter growth (2001 to 2005) per individual tree over the tree's diameter (2001). The linkage of that relation to tree size class within each plot is one of the crucial evaluation criteria applied. It reflects the capability of MoBiLE-ST to represent the dependence of carbon allocation on (1) tree size on the one hand and (2) aboveground vs. belowground resource competition on the other (Schwinning and Weiner 1998, Wichmann 2002, Pretzsch and Biber 2010). A further evaluation part considered results on the annual time scale from 2001 to 2007. From that part the digest presents the comparison of both model versions by the mean bias of the mean basal area stem DBH growth over the time range being considered.

5.3.3 Results and discussion

The distribution of measured DBH growth from 2001 to 2005 over DBH at both plots (Figure 4) is equivalent to growth as dependent on tree size class. It is a particularly important evaluation criterion of the hybrid approach. Diameter growth predicted through linear regression lies within a confidence band that notably widens at both the estimated 2.5% and 97.5% quantile limits of DBH, due to the restricted number of data available. However, the evaluation indicates that the trend of growth over size depends on the site, i.e. NE vs. SW.

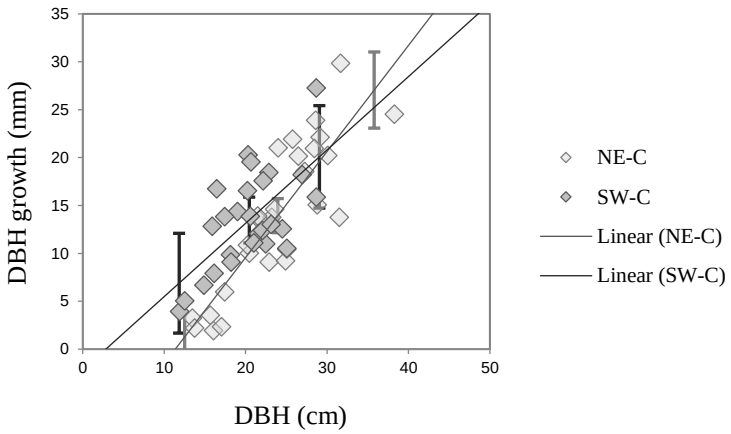

Figure 4. General sample data properties: diameter growth from 2001 to 2005 for each sample tree as differentiated by plot (Table 1, Figure 3); the confidence band of the regression line is indicated by error bars at mean DBH, at the estimated 2.5% quantile limit, and at the 97.5% quantile limit of DBH.

Generally, site quality is somewhat better at plot NE-C that has a larger basal area than the slightly older plot SW-C. SW-C is more homogeneous in tree size, and growth at this site is more equally distributed among trees than at NE-C. This finding is consistent with the theory of symmetric versus asymmetric competition that postulates a smaller competitive advantage of large trees for light competition on a less favorable site (Schwinning and Weiner 1998; Weiner 1990; Wichmann 2001, 2002; Pretzsch and Biber 2010; Pretzsch and Dieler 2011). As represented by both per plot samples, NE-C and SW-C cover a range of tree classes from suppressed to dominant trees.

The similarity of measured and simulated individual tree DBH growth over DBH from 2001 to 2005 depends on the trial plot (Figure 5). The confidence band of the simulated data regression does not exceed a growth span of about 1 mm at five-year growth within the range of DBH variability given. Hence the reliability of the comparisons shown in Figure 5 is largely governed by the sample data confidence bands that may be taken from Figure 4. MoBiLE-ST shows a more realistic distribution of diameter growth among the three cohorts than MoBiLE that

overestimates growth in the lowest cohort as compared to the others. Within the two topmost cohorts MoBiLE-ST shows a better estimation than MoBiLE alone that also underestimates there. In the lowest cohort, MoBiLE-ST underestimates and MoBiLE overestimates or estimates accurately (SW-C).

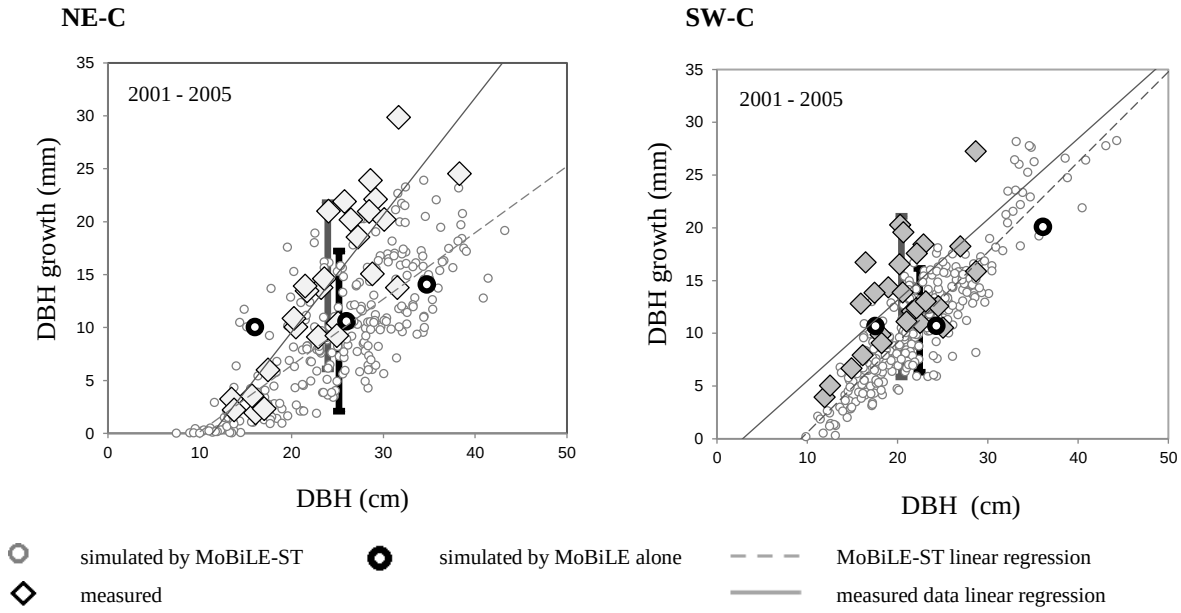

Figure 5. Comparison of simulated and measured tree growth in the time range 2001 to 2005; simulated data were based on the hybrid model MoBiLE-ST and on the original cohort model MoBiLE; each of three cohorts was defined by the initial DBH range of all trees therein; the cohort intervals (in cm, end diameter excl.) where at 0 to 20, 20 to 30, 30 to ∞; range of growth variation is indicated by bars (simulated black).

At plot NE-C, the bias of modelled mean basal area stem DBH growth over the 7-year timescale of 2001–2007 that is given as mean bias in mm was -0.59 with MoBiLE alone and -0.41 with MoBiLE-ST. At SW-C, that bias strongly changed from -0.55 to -0.24 when MoBiLE-ST was used (confidence interval about ±0.8).

The gap in improvement achieved by use of MoBiLE-ST between sites NE-C and SW-C might be due to the differences in stand structure between both sites: at NE-C the topmost cohort is populated by more than 100 well established dominant trees. Possibly, there is more investment into diameter and less into height within the dominant layer than it is predicted by the model at that site. Trees are in a clearly dominant position and thus from a functional point of view might invest into leaf area and hence diameter rather than into height. In contrast, at SW-C only about 40 dominant trees are established in the largest cohort. These biggest trees are concentrated within a circle of radius 20 m near the border of the plot. Here the notable improvement of

diameter growth within the upper two cohorts in MoBiLE-ST might be due to clustering of the most dominant group and hence lowered individual tree competition on the middle cohort.

MoBiLE-ST as the main objective of its design represented a close to nature distribution of diameter growth over DBH. Whatsoever, it generally underestimated diameter increase yet: one possible cause could be a deviation in the allometry of dominant trees at NE-C. Another likely reason is that volume growth both in MoBiLE-ST and MoBiLE is not sensitive to structural heterogeneity, as the physiological main model still perceives a cohort as horizontally homogeneous. Hence, improvements of diameter growth shown by MoBiLE-ST as compared to MoBiLE are exclusively due to a better description of allometry yet. Thus, one possible approach of further model optimization might be to correct the assumptions about canopy density in the light transmission of MoBiLE based on structural aspects like clustering.

5.4 Second publication (short version)

Poschenrieder et al. (2016) was published in Silva Fennica with title

Modelling sawn timber volume and strength development at the individual tree level – essential model features by the example of Douglas fir.

5.4.1 Abstract

Wood production is a major ecosystem service. It competes with other services and constraining conditions, such as nutrient feedback. Simulation scenarios, therefore, require an economical evaluation of the wood assortment produced. Typical wood quality models, however, work on a high level of detail. In contrast, scenarios that comprise processes of disturbance, land use and nutrient feedback consider scale levels up to that of the landscape. They need to confine themselves to an adequate level of explanation and accurateness, in order to retain computational efficiency. Studies that compare the effect of various management options such as planting density on the volume of sawn timber, firewood, industrial wood and residual wood may benefit from prediction of timber strength. To that end, they require an algorithm that is compatible to the lean crown perception of the observation based individual tree model but captures the relevant processes.

We designed a streamlined timber growth and quality model that aims at the effect of stand management on the efficiency of wood resource use. Applying the R based module toolbox to experimental plots of Douglas fir (*Pseudotsuga menziesii* (Mirb.) Franco) we analysed essential model features for reflecting the influence of planting density on board strength. The current version realistically predicted a significant increase of center board bending strength at tree age 40 with initial stand density. Model performance gained clear advantage from
a) parameterization of height to diameter allometry as dependent on planting density
b) consideration of cambial age and cross-sectional knot area in board strength computation.
Crown shape was less decisive. The model produced a significant effect of planting density even after a whole rotation period of 70 years as well as a realistic spectrum of board bending strength.

Hans Pretzsch and Jan-Willem G. van de Kuilen initiated the project. Werner Poschenrieder designed the model architecture. Andreas Rais contributed the data. Werner Poschenrieder and Andreas Rais together developed the model theory. Werner Poschenrieder designed the evaluation and wrote the manuscript. Andreas Rais reviewed the manuscript and contributed to

it. Hans Pretzsch and Jan-Willem G. van de Kuilen oversaw model development. Hans Pretzsch reviewed the manuscript and contributed to it.

5.4.2 Short introduction and methods

Within the second publication, Poschenrieder et al. (2016) designed a model toolbox for simulation of individual tree growth, logging, sawing, and strength grading on the individual board level. They evaluated modelled board strength from simulation runs starting at stand age 20 and ranging to age 40. Within that scope, they considered two stands of Douglas fir (*Pseudotsuga menziesii*, (Mirb.) Franco), one in a moist and fertile situation (Heigenbrücken, N49°59'20.2", E9°22'50.6", denoted as site Favorable in the study) and the other in one that is marked by shallow soil and rather dry and poor conditions (Ansbach, N49°13'24.0", E10°33'38.2", denoted as site Dry). Each site provided plots of planting density 1000 ha^{-1}, 2000 ha^{-1} and 4000 ha^{-1}. Both sites are subject to systematic long-term observation backed by regular data collection and permanent data maintenance. The individual tree inventory on all plots had started in 1989 at age 19 (setup inventory) and had been repeated on a five-year time step. Particular focus of the study was on the evaluation of board strength as related to planting density. The original study, furthermore, considers the effect of the initial stand density on the board strength distribution from a simulation run up to a stand age of 70 years.

The growth modules of the model toolbox apply a straightforward distance dependent version of the potential modifier method (Pretzsch 2009, p 454). They aim at simulated growth that is sufficiently plausible for development and test of the pivotal model capabilities, i.e. stem structure construction and board strength computation. As the potential modifier in general is not capable to explain the whole variation of growth, growth prediction in a common manner samples a growth fraction from a Gaussian residual distribution. It then adds that simulated residual to the yet modified growth value after competition has been taken into account. Within the center focus of model development were construction of year rings from annual growth, translation of crown shape to branch architecture (Figure 6), construction of the stem intrinsic structure of rings and knots (Figure 7) and finally simulated logging, sawing and board strength grading.

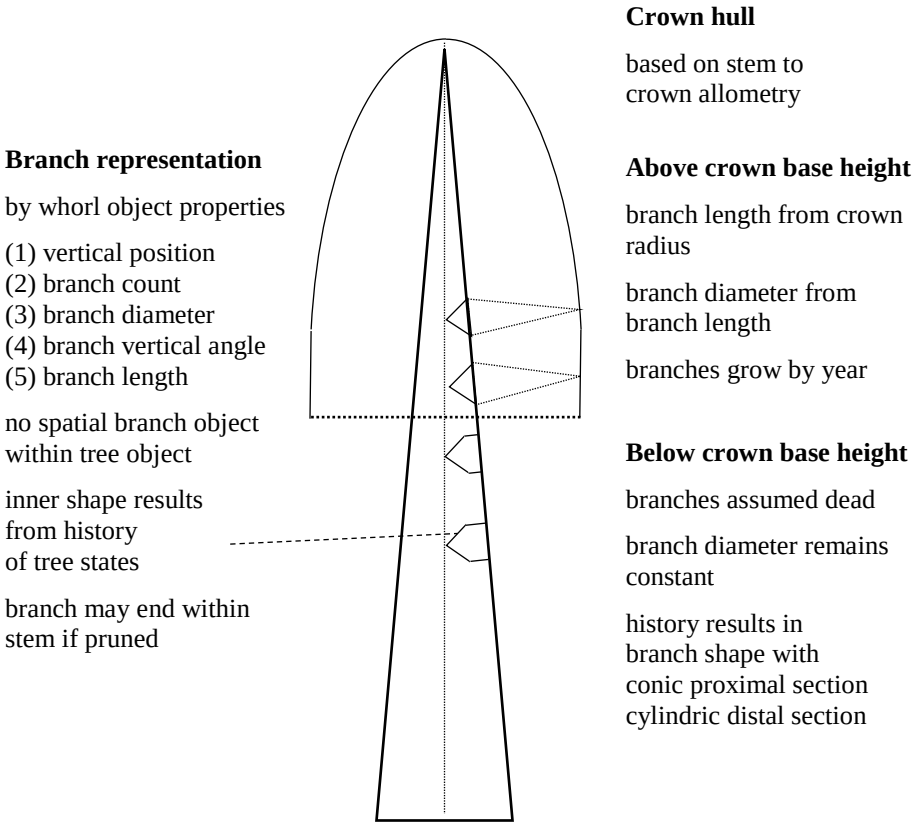

Figure 6. Principle of branch growth reconstruction and prediction; to maintain clearness of the figure, branches below crown base are presented as pruned.

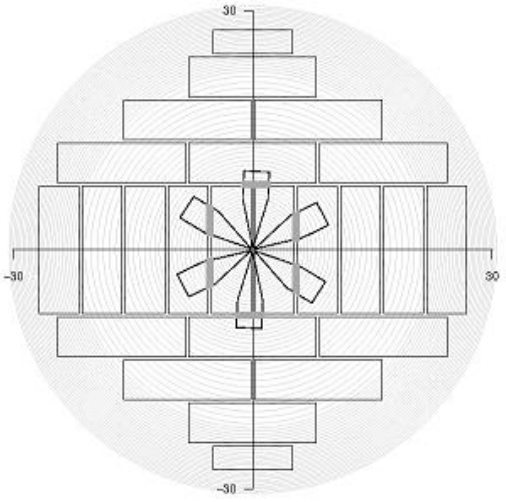

Intersection of geometries

board pattern associated to log object

each registered branch in log selected

origin of radial branch angle set to random value

branch replicated by count-1 at equal radial angular distance

each board intersected with each traversing branch and intersection points registered

each board intersected with traversing annual rings

Figure 7. Inner structure of boards resulting from application of a sawing pattern to simulated branches and annual rings from a stem 60 cm in diameter.

Predicted growth is driven by diameter increase on an annual time step as dependent on individual tree size and position. It starts at the earliest state of the stand that had been recorded on the individual tree level and is initialized with a list of tree positions and tree diameters. Previous growth is reconstructed on annual time step from the first inventory of the tree individual as well as from the distribution of annual growth over time from collective year ring data. It covers the early phase of stand development when structure has not been recorded by inventory of individual trees. Tree height is calculated from DBH based on a stand height curve (Michailoff 1943). Height curve parameters were calibrated by the diameter of the quadratic mean diameter stem (Dq) as an indicator of biological age. The model applies the crown shape equations of SILVA (Pretzsch et al. 2002) to calculate the crown hull dimensions and translates them into branch length and branch diameter on a per year basis (Figure 8). Each whorl is straightforwardly presumed to comprise six branches that are radially aligned at equal angular distance (60°).

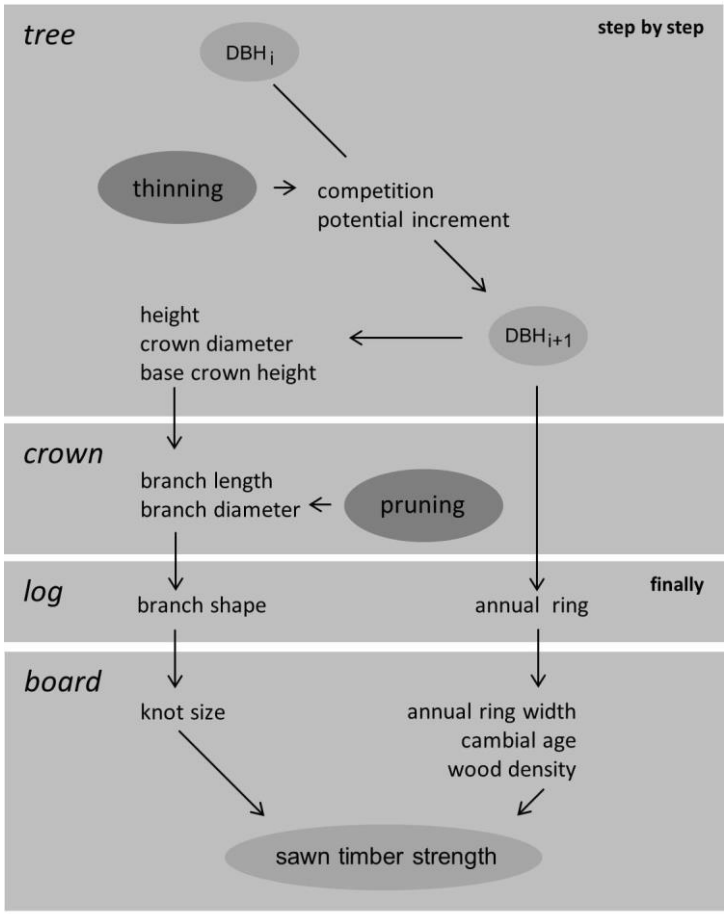

Figure 8. Simulation of individual tree growth, finalized by logging and sawing; tree and crown components are computed within each time step; thinning and pruning are optional and occasional.

At the end of each simulated year, the model stores the state of the stand on a per tree basis comprising crown and stem dimensions of each tree. Finally, it takes a user defined sample of all felled trees. From each it constructs timber logs (top diameter 20 cm), industrial wood logs (not used in this work) and residual wood (not used in this work) using top diameter definitions and the taper function of Paine and Boyer (1996). Based on the vertical position of each timber log and the history of the tree that it refers to, the model constructs the set of annual rings at log median position. It then intersects the resulting year ring pattern both with (1) the branch projections from the log internal whorl of biggest branch diameter and (2) a log diameter dependent sawing template. While the horizontal angle between neighboring branches within a whorl is fixed to 60°, the rotational position of each whorl is set by random sampling from an equal distribution between 0° and 360° when the inner structure of the log is constructed. The vertical angle of each branch to the stem axis was set close to 90° within the part of the stem that is sawn to timber logs.

The original work evaluates a more refined model version versus a more simplistic one to identify essential model features. This digest is focused on the refined model. That model version uses parameters of the height to diameter allometry that are specific for the planting density of the simulated stand. The calculation of board strength within that version uses cambial age to distinguish between juvenile and mature timber. Moreover, it is based on two criteria for knot impact of the biggest branch in board, i.e. (1) the ratio of knot to board cross-sectional area (total knot area ratio, tKAR) of British Standard BS 4978 (2007) and (2) the DEK value from German standard DIN 4074-1 (2012) that is defined as the largest ratio among all knots of the minimal surface knot diameter to the side width of the board on which the knot is visible. The first calculation step on board level computes wood density based on Auty et al. (2014) as defined by Equation 2:

$$\rho = a_{10} \times e^{\frac{-a_{11}}{\mathcal{A}}} + a_{12} + a_{13} \times \mathcal{W}, \quad (2)$$

where $\mathcal{A}$ is the mean cambial age and $\mathcal{W}$ is mean ring width of the board. The parameter set a_{10} to a_{13} are parameters.

Based on wood density, the final step calculates board strength (Equation 3):

(3) $$s = a_{20} + a_{21} \times \rho + a_{22} \times \mathcal{E} + a_{23} \times \mathcal{A} + a_{24} \times \mathcal{K},$$

where $\mathcal{E}$, $\mathcal{A}$, $\mathcal{K}$ are DEK, mean cambial age and tKAR and a_{20} to a_{24} are parameters.

Parameterization, simulation and evaluation used stem disk, board strength and board structure data from previous work within the experimental plots of this study (Rais et al. 2014b). Stem disk data from the site of higher and more general growth potential (Favorable) were preferred for parameterization, as the sample from the dryer site was still investigated for representation of dominant trees (sampling restricted to non-future crop trees). For the main focus of the analysis that is presented here, exclusively growth parameters of site Favorable were used based on 60 individuals that had been felled in winter 2011 to sample stem disks and detailed data of crown size, branch length and diameter. That tree sample provided (1) year ring data for the calibration of potential growth and (2) individual tree dimensions for fitting the parameters of competition and residual distribution. Computation of board strength from internal board structure was parameterized including the tree samples from both sites. Measured strength had been taken from 998 center boards and 936 side boards. Details are given in Rais et al. (2014b).

The main focus of this work was on the quality of board strength prediction. The according evaluation used measured board bending strength data that had been obtained from a Microtec GoldenEye 706 multiscanner quality sensor within the doctorate thesis of Rais (2015). The measured boards originated from a sample of non-future crop trees of DBH > 25 cm that had been taken in winter 2010/2011, i.e. a rough average of 27 (14 to 50) per each site and planting density (1000, 2000, 4000 ha^{-1}). Accordingly, simulations ran from an age of 19 at setup inventory (referred to as an age of 20 for convenience) to an age of 40 (2010). Simulation thinned plots exactly as it had been recorded within the long-term observation database on the individual tree level. Simulated stand growth ended with a clearcut but exclusively non future crop trees were selected to comply with the sample from the experimental plots. The subsequent sawing simulation took a random subsample of the felled trees that exclusively comprised trees of DBH > 25 cm in accordance to the field sample, i.e. a rough average of 77 (50 to 112) per site and planting density (1000, 2000, 4000 ha^{-1}). To evaluate the quality of prognosis we compared the simulated board strength distribution to the measured one on a per planting density basis. At the site of parameterization (Heigenbrücken, site Favorable) the evaluation

considered simulated board strength from measured board structure data as well as simulated strength from simulated structure. More straightforwardly, evaluation at site Ansbach (site Dry) focused on simulated board strength from simulated board structure. The resulting probability distributions of strength were compared (1) visually through box plots, (2) by confidence interval of estimated median (3) the post-hoc Tukey HSD test (Miller 1981) based on the results of a preceding analysis of variance (Chambers et al. 1992).

5.4.3 Results and discussion

The parameterization of the height to diameter allometry as dependent on planting density was decisive for the predictive quality of the whole model. It lead to both a realistic crown shift and realistic branch diameters. Simulation of wood strength by an observation based individual tree model may therefore require to take into account the site-specific density of young stands and its long-term effect on tree allometry. Within the wood quality module, a further key property was the consideration of cambial age and cross sectional knot area in board strength computation. Both results are presented and discussed in-depth within the original study.

At the site of parameterization (Favorable), board strength measured on the real board sample significantly increased with initial planting density (Figure 9 A). The model reproduced the effect if it used the knot and year ring data of the sampled boards (Figure 9 B) and, moreover, if it used the structure data of simulated boards (Figure 9 C). The results indicate that the model represents the internal structural properties of stem and board that it takes into account yet. However, there is considerable potential in further refinement of the structure to strength translation that lead to a markedly similar and underestimated data spread when it was both applied to real and simulated boards. Variability as currently predicted by the model was low if compared to the measured data. Hence, at the current state of development it is recommendable (1) to discuss the sensitivity of scenario evaluations to an estimated bias of variability, or (2) to parameterize a random generator for residual deviation and to add its result to strength on the individual board level.

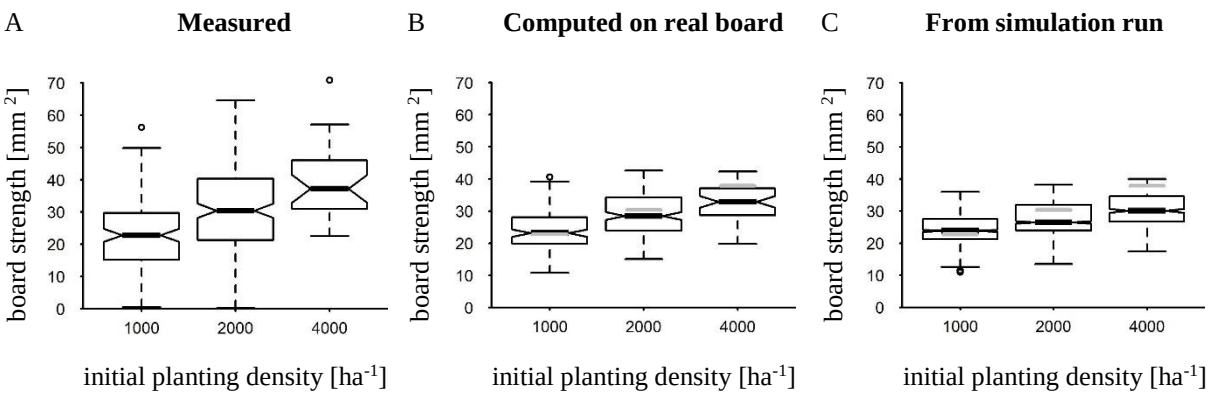

Figure 9. Board strength at parameterization site by planting density after 40 years as measured (A), as computed based on sample board structure (B) and as simulated by the current version (C); the boxplot notches correspond to the 95% confidence interval of the median; grey horizontal lines mark the median of measured data in diagrams of simulated result distributions.

The lower real growth potential and a resulting higher cambial age of sample boards at site Ansbach (dry) were a likely determinant of a relatively high measured board strength at planting density 2000 ha^{-1} (Figure 10 A). It likely resulted in an underestimated strength from simulation at intermediate planting density (Figure 10 B) and overemphasis of the linearity within the strength to density relation. As potential growth data at the dryer site were still to be verified, the effect has yet to be proven. However, it is plausible and would likely be met by the site-specific calibration of potential growth that is common to potential modifier individual tree models.

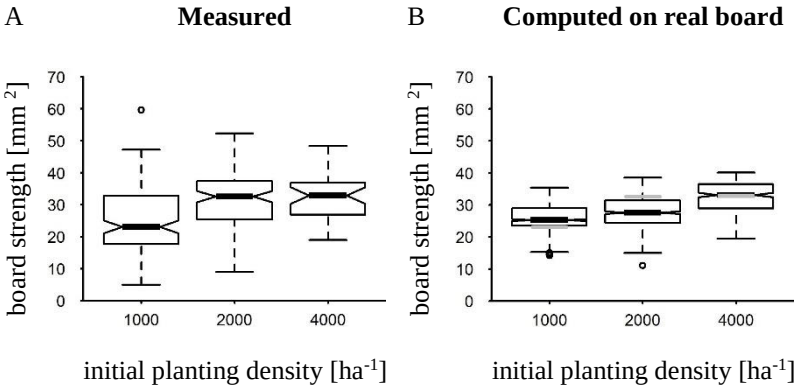

Figure 10. Board strength by planting density at site Dry after 40 years as measured and as simulated by the current version. Grey lines mark the median of measured data; the boxplot notches correspond to the 95% confidence interval (CI) of the median; grey horizontal lines mark the median of measured data in diagrams of simulated result distributions.

5.5 Third publication (short version)

Poschenrieder et al. (2018) has been published in Forests with title

An inventory-based regeneration biomass model to initialize landscape scale simulation scenarios.

5.5.1 Abstract

Ingrowth and generational change are key processes of forest development. In order to represent the regeneration process up to the time horizon of forest management on landscape level, simulation scenarios require an initial regeneration stock specific to the characteristics of each simulated stand. Forest inventories, however, are sparse with regard to regeneration. Moreover, statistical regeneration models are rare. We introduce an inventory-based statistical model type that (1) quantifies regeneration biomass as a fundamental regeneration attribute and (2) uses the overstory's quadratic mean diameter (Dq) together with several other structure attributes and the Site Index as predictors. We form two such models from plots dominated by European beech (Fagus sylvatica L.), one from national forest inventory data and the other from spatially denser federal state forest inventory data. We evaluate the first one for capturing the predictors specific to the larger scale level and the latter one to infer the degree of landscape discretization above which the model bias becomes critical due to yet unquantified determinants of regeneration. The most relevant predictors were Dq, stand density, and maximum height (significance level $p < 0.0001$). If plot data sets for evaluation differed by the forest management unit in addition to the average diameter, the bias range among them increased from 0.1-fold of predicted biomass to 0.3-fold.

Hans Pretzsch initiated the project. Werner Poschenrieder conceptualized the model, the data preparation, the model calibration, the model evaluation and the article's structure. Werner Poschenrieder lead through all practical work of modelling and data handling and wrote the paper. Peter Biber gave specialist advice in statistical modelling and evaluation. Peter Biber reviewed the paper and contributed to all sections through editing. Hans Pretzsch supervised and reviewed the study and gave profound expert advice in regeneration dynamics.

5.5.2 Short introduction and methods

Within the third publication, Poschenrieder et al. (2018) designed a statistical model that aims at predicting regeneration stock from overstory characteristics and site. The overall objective of that work is the initialization of modelled forest stands within dynamic simulation scenarios on landscape scale level. Such virtual stands result from grouping of inventory plot data by their overstory attributes. That stratification approach aims to provide a statistically stable representation of each stand type within a landscape considered. It is a well-established method for representing the overstory, where stand inventory data are missing (Jonsson et al. 1993, Pott and Fabrika 2002). However, stratification might not yield a realistic spatial pattern of regeneration trees (DBH < 7 cm) within each modelled representative stand. That limitation is due to the sparse alignment of plots within many inventories (e.g. Canadian Forest Inventory Committee 2008; Polley 2014) and to the high stand intrinsic variability of regeneration. Moreover, remote sensing that can often not detect the understory increasingly supports terrestrial inventories (Kayitakire et al. 2006, Abdullahi et al. 2016, 2017). To some part, remote detection of stand structure attributes might even replace expensive terrestrial inventory methods in future. Therefore, landscape scale simulation scenarios will benefit from a statistical regeneration model that provides a realistic pattern of regeneration stock to each virtual stand. Such a statistical model has to overcome the challenge that, on the one hand, overstory structure strongly influences regeneration and, on the other, may vary on a small spatial scale in horizontal direction (Lutze et al. 2004, Hunziker and Brang 2005, Gravel et al. 2008). Accordingly, as the relation between regeneration stock and the model's predictors is not necessarily linear, such a model has to obtain its predictors on the scale of small stand subsectors. That restriction of the spatial scale aims to avoid bias due to predictor averaging over the whole virtual stand. Still, a statistical regeneration model, due to unknown disturbance history, cannot precisely predict within small scale stand subsectors. Notwithstanding, it can estimate the statistical distribution of regeneration stock per each small-scale area considered. In order to represent that local distribution, we first and foremost consider regeneration stock as a scalar variable, i.e. regeneration biomass. Biomass is a fundamental outcome of both the stand-intrinsic driving forces and the resistances to them (Landsberg and Waring 1997). Our modelling concept accordingly comprises a statistical regeneration biomass model. That model is the particular objective of the original study (Poschenrieder et al. 2018). It estimates regeneration biomass per each small scale subunit within a virtual stand considered. A further model part, yet to be published, then generates a realistic tree profile per species based on that

estimated biomass and the overstory's species composition. The regeneration biomass model, in order to initialize a virtual stand, first considers each of numerous small-scale sectors therein. These sectors correspond to the typical tiles of regeneration models and gap models. Such tiles are gaplessly aligned within a quadratic grid pattern and have an edge length of 2.5 to 20 meters within the regeneration module of SILVA (Pretzsch et al. 2002) and modern gap models (Seidl et al. 2005, Fischer et al. 2016). Within each tile, the model first applies a deterministic component in order to estimate mean regeneration biomass. That predicted biomass constitutes the primary approximation to the tile intrinsic biomass distribution. The model then applies a stochastic component in order to account for the stochastic effects on regeneration biomass within the tile being considered. Based on the predicted value, that second model component estimates parameters of a tile intrinsic probability distribution. That distribution is one of a relative residual, i.e. the ratio between observed and predicted value. Thus, in order to obtain one value per tile, the model samples exactly one random value from the local distribution of relative residuals. Then it multiplies that overstory-related random deviation with the value obtained from the deterministic model part. Finally, the virtual stand's pattern of the regeneration biomass results from all its modelled per-tile values.

Within the model type being considered, the deterministic module aims to predict the distribution's expectancy value. As a complement, the stochastic part serves to estimate the variation around that predicted average. We designed two closely related versions of such a model. One model version applies data from the German national forest inventory (NFI, Polley 2014), in order to identify important predictors of regeneration biomass within the large spatial scope of the German state territory (36 million ha with 11 million ha of forest). The other version serves to evaluate the modelling approach of that study: based on that model version we estimate the degree of stratum differentiation, beyond which a model of that type produces a critical bias of the per-stratum average. In order to parameterize and test the second model version, thus, we apply the spatially much denser Bavarian state forest inventory data (BSFI, Neufanger et al. 2012). At the current state of model development, our study focuses on plots dominated by European beech (Fagus sylvatica L.) within the overstory. European beech is by far the most important broadleaved species in Central Europe. As it is shade tolerant, it occurs along a broad range of stand structures and sites. Moreover, it primarily regenerates through natural seed dispersion.

Model tiles and inventory plots for regeneration are of similar size. Hence, both, the NFI and the BSFI based model version use plot-scale predictors derived from the inventory data. These

predictors represent attributes of structure and site. The complete predictor set, as reasoned in detail within the original publication, comprises (1) the Stand Density Index *SDI* (to represent density), (2) the Species Profile Index *SPI* (Pretzsch 2009, pp. 281 ff, heterogeneity of size class and species), (3) the Height Diameter Characteristic *HD* (a size-related height-diameter ratio), (4) the maximum height *Hmax* (the plot's developmental state), (5) the Site Index *SI* (site index as computed by SILVA, Pretzsch et al. 2002), and (6) *Dq* (the quadratic mean diameter). The study used 7 784 plots of the NFI and 11 954 plots of the BSFI. Of the BSFI plots, 6 073 had been spared from model calibration for model evaluation.

At the current stage of development, we aimed to restrict the presumptions for the deterministic module to a minimum. Accordingly, to predict regeneration biomass per ha *B*, we used a generalized additive mixed model (GAMM) for both the NFI based model (Equation 4a) and the BSFI based one (Equation 4b):

(4a) $$B_{ij} = \beta_0 + \beta_1 \cdot SDI_{ij} + \beta_2 \cdot SPI_{ij} + \beta_3 \cdot HD_{ij} + \beta_4 \cdot Hmax_{ij} + \beta_5 \cdot SI_{ij} + s(Dq_{ij}) + r_{ij}.$$

(4b) $$B_{ijk} = \beta_0 + \beta_1 \cdot SDI_{ijk} + \beta_2 \cdot SPI_{ijk} + \beta_3 \cdot HD_{ijk} + \beta_4 \cdot Hmax_{ijk} + \beta_5 \cdot SI_{ijk} + s(Dq_{ijk}) + r_{ijk}.$$

The fixed effects in this model are the Stand Density Index *SDI*, the Species Profile Index *SPI*, the Height Diameter Characteristic *HD*, the stand maturity indicator *Hmax*, the Site Index *SI*, and the quadratic diameter *Dq*. Except for *Dq*, all fixed effects in the model are linear (i.e. they are multiplied by one of the regression parameters β_1, …, β_5). In contrast, the effect of *Dq* is modeled with a nonlinear spline-based smoother (Wood 2017) which is indicated by the symbol *s(Dq)*. It accounts for a hypothesized nonlinear relation between *Dq* and regeneration stock due to a likely minimum of light transmission between the phase of adolescence and intense harvest. The indexes i, j, and k account for nesting of inventory plots into groups. Such nesting may induce autocorrelation into the data and is accounted for by the mixed models. The nesting levels depend on the design of the inventory and differ between Equation 4a and 4b.

The stochastic component is explained in detail within Poschenrieder et al. (2018). It is based on a gamma probability density function and describes the distribution of relative residuals around the predicted regeneration biomass. As that distribution is heteroscedastic, the stochastic component calculates the distribution's parameters from the regeneration biomass value predicted by Equation 4a resp. 4b.

Evaluation of the deterministic module used the Akaike Information Criterion (AIC, Akaike 1985) in order to assess the importance of each individual predictor variable within Equation 4a and Equation 4b. Details are given within the original study. The AIC is a criterion of relative

model quality. A smaller AIC indicates a better tradeoff between goodness of fit and model parsimony.

A further part of the evaluation applied the BSFI based model to strata formed from inventory plots of the BSFI. That evaluation part considered the model precision as related to the degree of stratum differentiation. To that end, it formed strata on two discretization levels. On the lower one of both levels, strata were exclusively based on their diameter class as defined within the original study. On the more detailed level, they also differed by the forest management unit. For that stratum related evaluation, the BSFI based model was not applied to each tile of a virtual stand formed per each stratum, but directly to each of the stratum's plots. Two evaluation criteria were computed per-stratum. One criterion was the stratum's average regeneration biomass. The other was the cumulative frequency of that average. That frequency served to indicate, whether the stratum had a realistic probability of an above-average vs. below average regeneration biomass. Thus, the cumulative frequency serves as an indicator, whether the method may generate a realistic abundance of clustered vs. sparse regeneration stock within a virtual stand considered. Each criterion was computed from the modelled as well as, for comparison, from the observed per-plot values. In order to corroborate our per stratum evaluation, we stabilized the value of each evaluation criterion through bootstrapping (Efron 1979) with 100 replicates per stratum.

5.5.3 Results and discussion

Most fixed effects of the deterministic model part, i.e. *Dq*, *Hmax*, Stand Density Index *SDI*, Species Profile Index *SPI*, and Height-Diameter Characteristic *HD* had significant influence on regeneration biomass within both models. The remainder predictor, Site Index *SI*, was exclusively relevant for the NFI based model. Thus, the deterministic part of the NFI based model with minimum AIC (see section 5.5.2, AIC values presented in the original study) was Equation 4a, while the corresponding part of the BSFI model with smallest AIC was a version of Equation 4b without Site Index *SI*.

The typical biomass-trend associated to each fixed effect indicates an outstanding relevance of *Dq*, *Hmax* and *SDI* (NFI: Figure 11 a to f, BSFI: Figure 12 a to e). Within both the NFI and the BSFI based model, the fitted nonlinear effect of *Dq* revealed a strong influence of that predictor on regeneration biomass. That relation had a marked minimum of 3 t ha^{-1} at a *Dq* of 30 cm vs. a value of 5 t ha^{-1} at *Dq* values larger than 40 cm (Figure 11 a, Figure 12 a).

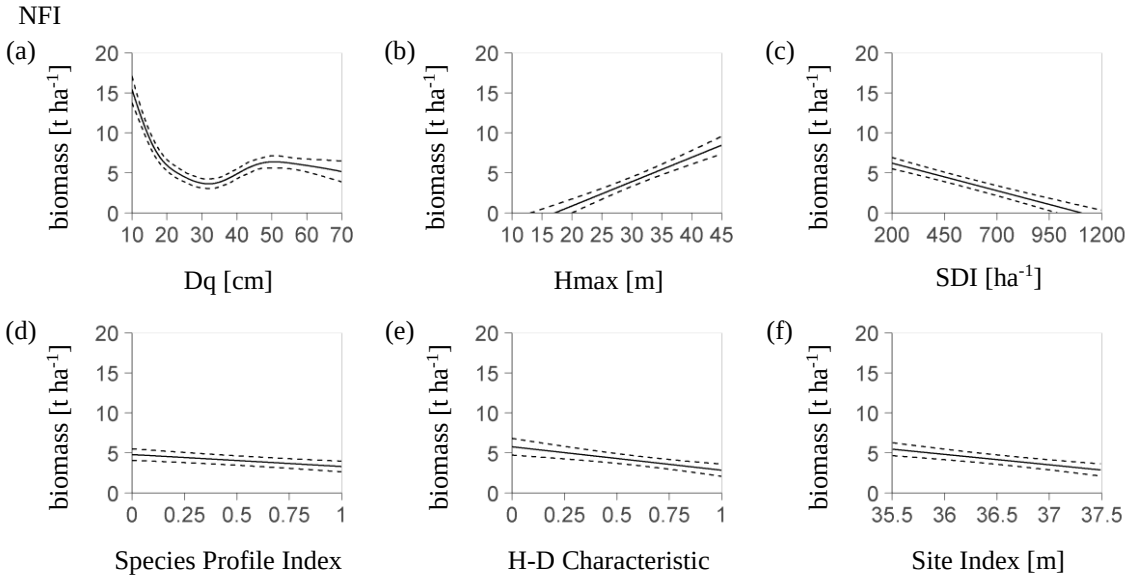

Figure 11. Profiles of regeneration biomass as predicted by the deterministic model part based on the NFI (German National Forest Inventory, Equation 4a). Each profile is presented over one predictor with, at the same time, the remainder predictors at their mean value (abbreviation H-D: Height-Diameter); profiles ordered by the relevance of the referring predictor based on the AIC criterion (a to f, see section 2.4); dotted lines refer to the confidence interval; each predictor shown within its 95% interval; the stochastic part (Figure 3 a, b) covers the residual distribution. (profiles based on 7 823 NFI plots used for model calibration).

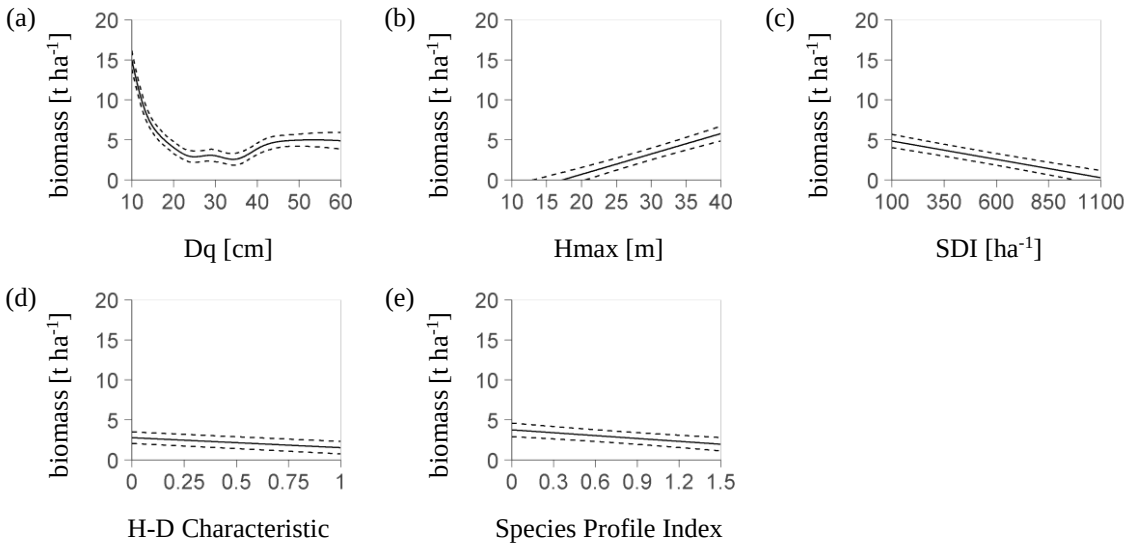

Figure 12. Profiles of regeneration biomass as predicted by the deterministic model part based on the BSFI (Bavarian State Forest Inventory, Equation 4b). Each profile is presented over one predictor with, at the same time, the remainder predictors at their mean value (abbreviation H-D: Height-Diameter); profiles ordered by the relevance of the referring predictor based on the AIC criterion (a to e, see section 2.4); dotted lines refer to the confidence interval; each predictor shown within its 95% interval; the stochastic part (Figure 3 c, d) covers the residual distribution (profiles based on 5 881 BSFI plots used for model calibration).

In both models, the most important predictor was *Dq*, followed by *Hmax* and Stand Density Index *SDI*. However, the NFI based model and the BSFI based model differed in the importance of their remainder common predictors: Species Profile Index *SPI* was more relevant than Height-Diameter Characteristic *HD* in the NFI based model.

Kolo et al. (2017) present a model of regeneration probability based on German national forest inventory data. They underpin the high relevance of *Dq* and report an increase of probability with that predictor. However, they point to the converse trend within previous work. The study at hand demonstrated that both tendencies exist and depend on stand maturity.

Furthermore, the results section of the original publication considers the stochastic model part. In particular, it successfully evaluates the gamma probability distribution as an approximation to the observed distribution of relative residuals. Furthermore, it quantifies the dependence of the distribution's parameters on the regeneration biomass value predicted by the deterministic part. Previous work (Foster and Reiners 1986, Asner et al. 2013) reports a distribution of canopy gap size that resembles a falling exponential function. It underpins that the gamma density distribution function is a suitable approximation to the regeneration biomass distribution at given overstory structure attributes.

The following stratum-related evaluation of the BSFI based model considers the model bias as dependent on the level of stratum differentiation, i.e. on the degree of landscape discretization. Within the study's concise version at hand, that section exclusively evaluates the average biomass per stratum. The basic stratification that only used the criterion of diameter class formed a set of seven strata. Among these strata, the ratio of measured to modelled regeneration biomass had a mean of one-fold (Figure 13 a). It ranged from 0.8 to 1.2-fold. Among three diameter classes, given by the ranges 30±5 cm, 40±5 cm, 50±5 cm that represent 71% of all 11 954 BSFI plots used, the bias range was markedly smaller, i.e. at 0.8 to 1.0-fold.

Stratification resulted in a notably smaller plot number per stratum, if it was based on the forest management unit in addition to the diameter class. Then, exclusively strata of diameter classes 30±5 cm, 40±5 cm, 50±5 cm provided the minimum sample size postulated by the study at hand (140 plots). Hence, the following analysis will focus on that group of strata. The range of bias between measured and predicted per-stratum mean biomass among these strata was notably higher than the typical one among such strata that were based on the diameter class only. Their bias range was at 0.6 to 1.2-fold vs. 0.8 to 1.0-fold. The bias had a mean of 0.9-fold (Figure 13 b vs. a). Thus, there was an additional bias of predicted stratum biomass within ± 0.2-fold, if the strata formation used the forest management unit as a further criterion. That additional data

spread was due to the scatter of the observed per-stratum values around their diameter-class average (± 0.15-fold).

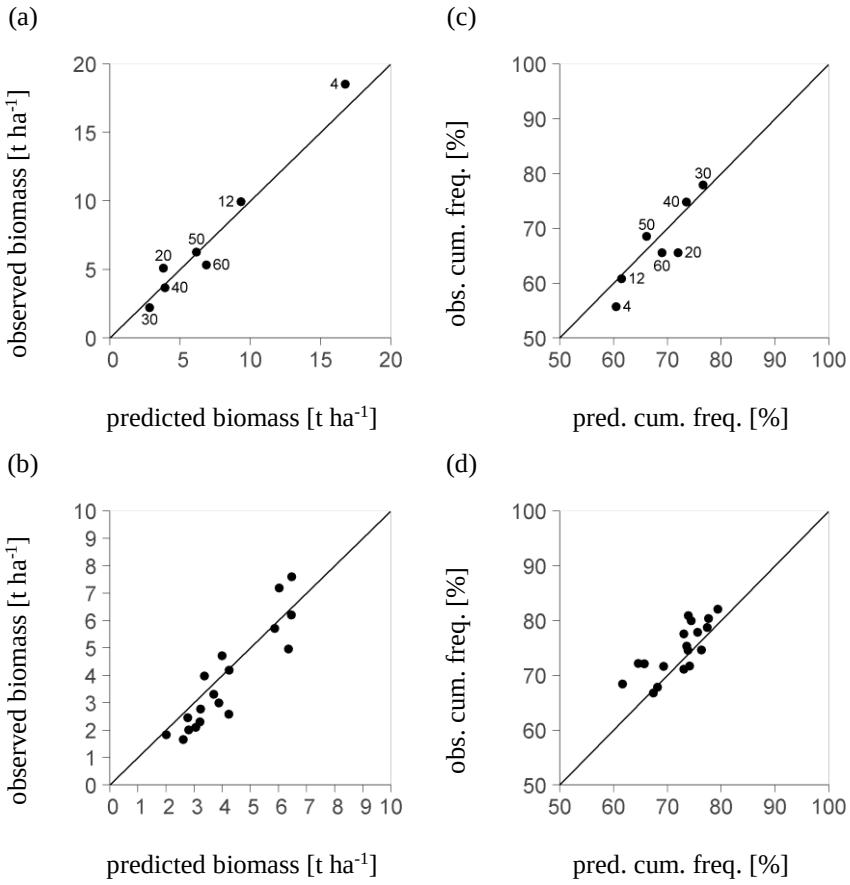

Figure 13. Diagrams a, b: Mean of measured regeneration biomass over mean of predicted regeneration biomass per stratum obtained from the BSFI (Bavarian State Forest Inventory); (a) if strata have been formed based on the diameter class; (b) if strata have both been formed based on diameter class and Forest Management Unit: the higher data spread on that scale level points to an as yet stochastic factor to be captured; in diagram a the numbers 4 to 60 denote diameter classes [cm] of 4±4, 12±3, 20±5, 30±5, 40±5, 50±5 and 55 to 80; in diagram b due to the sample size required per stratum the data focus on diameter classes 30, 40, 50 (71% of all 11 954 BSFI plots); diagrams c, d show the according result of the cumulative frequency (cum. freq.) of mean biomass; the cumulative frequency serves to indicate the quality of the modelled distribution characteristics (all based on 6 073 inventory plots spared from model calibration for evaluation).

Thus, there was a notable stochastic effect on the forest management unit-level that reduced the precision of the model, if strata were formed by both diameter class and forest management unit. That additional bias was certainly due to processes that, on the one hand, vary among strata with size of a forest management unit but, on the other, have no equivalents in the model as fixed effects. Kupferschmid et al. (2015) point out that browsing intensity considerably varies among Swiss federal states (Kanton), many of which have a total area of about 150 000 ha. That area size corresponds to the average size of the total landscape around a typical German state forest management unit. Browsing in general has been reported to be a severe inhibitor of regeneration (Ammer 1996, Motta 1996, Boulanger et al. 2009). Kolo et al. (2017) accordingly

assume that browsing is a major cause of leeway within their prediction of regeneration probability.

6 Discussion

6.1 Publications' contribution to landscape scale studies

Starting from its second meeting in Helsinki, The Ministerial Conference on the Protection of Forests in Europe has increasingly confirmed that, beyond wood production, forests provide a wide range of services to the human society, such as regulation, protection and recreation (MCPFE 1993). Biber et al. (2015) accordingly investigated the sensitivity of forest ecosystem services to management by scenario simulation within 20 European case study areas. Based on a service classification by Borges et al. (2014), their study reveals that, overall, both market services and non-market services are rated approximately equal to the provision of market wood products. Moreover, Biber et al. (2015) point out that these most relevant forest ecosystem services markedly depend on forest management decisions. Typical case study areas for such management evaluation often have an area between 20 000 and 100 000 ha (Biber et al. 2015). Their extent corresponds to the minimum size of a geographical unit that is within the scope of forest political decision makers and supporting experts. For revealing the possible effect of management decisions taken by that group, simulation scenarios have to consider the underlying key processes both on stand scale and landscape scale level. Management scenarios that consider the time horizon of planning on landscape level have to take into account environmental change. Therefore, they require embedding of detailed stand-scale models into more parsimonious models that however represent crucial interactions within the landscape such as fire spread and seed dispersal.

The original focus of observation based models that apply the potential modifier method is the mutual influence of structure, thinning, harvest and growth up to a time horizon that is typical for forest management planning. Their predictive capability has been corroborated through routinely application under current climate conditions. If that observed intraannual weather course may be assumed to persist over the time range of simulation, a theory of growth and competition that is based on an external description of the individual tree is the most efficient one. Moreover, as models like SILVA have been parameterized along a large climatic gradient, they may be expected to be also applicable under moderate conditions of climate change. SILVA in particular applies dose-response functions to calculate its growth potential. Thus, to a certain extent it is sensitive to coincident changes of climate and the concentrations of CO_2 and NO_x (Kahn 1994). However, if potential modifier models were to be realistically sensitive even to the most extreme scenarios of future climate, they would have to capture growth as determined by yet unobserved weather variability. An imaginary approach for implementing

weather sensitivity into an observation based model might strive to relate tree growth to tree size and average weather on a seasonal time step. Such a state-space approach (García 1994), however, would certainly be limited by the large number of state-weather combinations to be recorded and the small scale of growth measurement per season.

Future scenarios of stand growth and structure have to consider possible extremes of weather, like a frequency of summer drought that is far outside the range observed (Sheffield 2008, Qian et al. 2014). One approach to extend the observation based model within that scope could be a straightforward realization of the signal transfer concept (Luxmoore 2002, Henning and Burk 2004, Matala et al. 2006). That method applies the results of physiological models in order to modify growth potential and maximum capacity for biomass per site. Signal transfer, however, requires recalibration of the observation based model as dependent on the climate scenario to be applied. Accordingly, Mäkelä (2003) recommends the construction of model hybrids (e.g. Weiskittel et al. 2010). Such hybrids link the stand-based or cohort-based net carbon assimilation of a physiological model with the individual tree allometric development.

The thesis at hand has developed prototypes that serve as a basis of further refinement and integration into modelling frameworks. Extension of the physiological model MoBiLE-PSIM by an individual tree module taken from SILVA within the first publication (Poschenrieder et al. 2013) improved the spatial representation of competition and growth. This was notably the case where the spatial distribution of dominant trees was clustered and the consideration of individual tree competition, hence, was particularly important. The major improvement achieved through the bidirectional and mass conservative coupling between a physiological cohort model and an individual tree module is the sensitivity of a physiological growth description to spatially explicit thinning. Such a thinning regime selects individual trees by horizontal position and size class. Position dependent thinning within a model is pivotal for representing the influence of management on horizontal species and crown clustering within a stand. Such clustering, as it determines the spatial pattern of canopy coverage, constitutes a fundamental metric for biodiversity of animals (Gao et al. 2015) and plants (Gao et al. 2014). It might also take influence on risk of fire and windthrow through the spatial arrangement of less inflammable species (Frejaville et al. 2013) and mechanical influence on the wind field (Byrne and Mitchell 2013).

The wood quality module described within the second publication (Poschenrieder et al. 2016) provides model extensions for dynamic stem structure simulation and board strength prognosis. These optional extensions may even be coupled to the most abstract individual tree

representation with a branchless crown of convex hull shape. The wood quality module realistically predicted the shift of center board bending strength between stands of minimum and maximum initial planting density. That notable realism, on the one hand, was due to the explanation of bending strength by cambial age and knot area ratio. On the other, it was linked to improvement of the individual tree model, particularly to reconstruction of early growth and dependence of allometry on early stand density. Accordingly, the study contributes to individual tree modelling by a wood quality module and additional algorithms that reconstruct the effect of sapling density on the crown allometry and stem structure of larger trees. That reconstruction is important, as a typical individual tree model does not represent each young tree by explicit stem and crown dimensions. The wood quality module enables simulation of individual board strength as determined by stand management decisions. It contributes to the evaluation of management options with respect to financial output and carbon sequestration (Geng et al. 2017).

One might object that in reality there would be no incentive for private forest owners to provide high quality sawn timber with a long residence time of carbon, even if scenarios would recommend to do so. This is likely true, as long as the price of timber is based on roundwood quality. Recent technological research, however, aims at the non-destructive prediction of timber quality at the level of the standing tree or of the individual log based on acoustic tools (Wagner et al. 2003, Amishev and Murphy 2008a, Amishev and Murphy 2008b, Rais et al. 2014b). Such a prediction method might allow to grade on a per tree level basis in countries where timber is regularly sold as standing trees. Such grading is already common in France and Poland. Hence, it is possible that future criteria of timber pricing will be more closely related to the strength of sawn timber. Accordingly, forest management might control the strength of resulting sawn timber through active stand structure development (Rais et al. 2014b).

A module for sawing and strength grading may support the estimation of nutrient feedback to the forest system through the stem top section that most often remains within the stand but also might be utilized. Paré and Thiffault (2016), within a review study, underpinned the relevance of that feedback process as well as the requirement to represent its biogeochemical components. Such decomposition processes, in turn, are within the overall scope of the physiological model component used by Poschenrieder et al. (2013).

The statistical regeneration model introduced by the third publication (Poschenrieder et al. 2018) significantly relates regeneration biomass to indicators of structure and site. Within large subunits of forest landscape classified by dominating species and average diameter, such a

model represents regeneration stock at an acceptable precision. For initializing dynamic management scenarios on the landscape scale level, thus, the approach is yet promising. Due to its generalist target variable, such a statistical model may initialize a wide spectrum of dynamic simulation models. Individual tree models are notably within that scope, as regeneration biomass is a fundamental predictor of tree number if the vertical profile of biomass per species within the stand's regeneration layer has been estimated. Characteristics of that profile, such as the regeneration trees' maximum height and the biomass share by species, likely correlate with overstory properties. In order to support dynamic simulations, the statistical model may either provide the starting condition of a scenario or update the regeneration layer after several steps of dynamic simulation. Moreover, it may support the initial state of regeneration if that starting condition is based on spin-up runs, as in Didion et al. (2009).

6.2 Perspectives

Hybrid of individual tree module and ecophysiological model (Figure 1, S and M)

The hybrid model MoBiLE-ST (Poschenrieder et al. 2013) links a SILVA based individual tree component to a physiological cohort model (modules S and M in Figure 1). Therefore, it maintains individual tree competition across cohort boundaries. The hybrid captures the influence of nearest neighbor competition and the effect of stand structure on the weight, by which each individual tree contributes to the total biomass growth of its cohort. Future development of the hybrid model will enhance the model's ability to describe the influence of species interaction and species separation on stand growth. Another developmental objective aims to represent the effect of horizontal gaps and clusters within dominant cohorts on subordinate ones.

In order to meet the first objective, future research on the individual tree module has to evaluate and possibly to improve the stem and crown allometries that determine the species-specific extent of canopy occupation (Pretzsch and Rais 2016). That occupation results from competition, facilitation (Pretzsch and Biber 2016) and crown extension. Theory validation and formation will likely consider the influence of mixture on the height-diameter ratio (Thurm and Pretzsch 2016) as well as on the shape of the crown (Bayer et al. 2013). A realistic model of the spatial canopy structure is highly important in order to provide the amount of leaf area per canopy layer and species to the physiological cohort model. Notably within stands that are marked by horizontal clustering of species and by large gaps within dominant cohorts, the physiological and purely cohort related part of the hybrid model might therefore also require

extension. Such additional theory captures the effect of a horizontally inhomogeneous light transmission on the growth of subordinate cohorts. As MoBiLE-PSIM computes growth on a per cohort basis, an approach that delineates cohorts also by vertically inserted tiers is a likely candidate. That vertical delineation might be based on criteria of light transmission, such as tree size class, density and species.

Still, the next steps of development will consider each cohort as horizontally homogeneous within the physiological part of MoBiLE-ST. One future task might be the refinement of competition-related crown allometry within the individual tree module. Within that scope, a fundamental research question is, whether the module can represent the species-related occupation of the canopy space adequately precise, to guarantee a realistic light transmission within the physiological model. A conceivable test concept uses typical crown shape data from experimental plots as retrieved by terrestrial laser scanning, e.g. from Bayer et al. (2013). Within a stand being considered, these surveyed crown shapes provide a leaf density profile per cohort, in order to define the starting condition of an annual simulation run. A further reference run is based on idealized crown shapes from the same stand, obtained from the individual tree module. Per-layer transmission and biomass allocation within both runs are then compared in order to evaluate the drift related to the module's crown shape abstraction. Future modelling of crown dynamics might include the effect of competition and mixture on crown base height and crown shape through self-pruning. That effect has been approximated within an experimental branch of SILVA based on algorithms of Arney (1972) as modified by Biber and Seifert (Biber P, Seifert T pers. comm.).

Interconnected sets of stand structure and weather data are particularly valuable for future model development. Such sets are available from the experimental site used by Poschenrieder et al. (2013). Moreover, weather, air biochemistry, growth, and individual tree position might be obtained from ICP Level II stations (Ferretti et al. 2010). Promising data sets of stand structure, weather, ozone level and growth have resulted from the Kranzberg Forest Experiment (Fabian et al. 2006). These data might provide a data base for more advanced development within the physiological model part.

Wood quality module (Figure 1, Q)

The species-specific response of crown structure, stem taper, and tree size to management interventions is highly relevant also within the scope of wood quality modelling (Pretzsch and Rais 2016). Thus, one important direction of development will take into account further tree species within the wood quality module (Q in Figure 1). That module prototype was

implemented within a potential modifier simulation model by Poschenrieder et al. (2016). Its future extension will primarily focus on European beech that holds the main share of broadleaf species in Germany (BMEL 2015). Therefore, as part of an ongoing project at the Chair of Forest Growth and Yield Science, the species-specific properties of stem structure and branch architecture that are relevant for timber strength of beech will be identified. Subsequently, algorithms that relate these properties to crown and stand structure will be implemented within the modules for stem construction and wood strength computation (Rais A pers. comm.). At a later stage, the modules for stem and branch growth recording, stem and log structure construction, sawing and board strength computation might be ported for optional embedding into various growth models. One possible target of that transfer is the individual tree module of the hybrid model MoBiLE-ST.

The isotropic crown model of SILVA will most likely be retained for computing nearest neighbor competition. Accordingly, that straightforward shape representation will still be applied in future versions of the individual tree module. However, if models focus on the timber strength of a species with high crown plasticity such as beech (Pretzsch and Rais 2016), they might, in parallel to the straightforward crown model, require a more precise description of competition related crown shape and asymmetry. Piboule et al. (2005), by the example of a broadleaf mixed forest, present an algorithm that aims to reconstruct radially asymmetric, i.e. anisotropic crown shapes at a given point in time. That stepwise approximation on a per height layer basis, denoted as Overlap Minimization, aims to suffice a target crown volume. To that end, it considers crown isotropism as positively related to tree dominance. Overlap Minimization starts from an isotropic crown representation that has a circular cross section and is defined by crown base height and maximum crown radius. Therefore, the approach might be coupled to the refined crown base height estimation based on Arney (1972) that is part of a SILVA experimental branch. Measured branch position data from terrestrial laser scanning (Bayer et al. 2013) may provide a precise validation reference. A resulting anisotropic crown model might provide the initial state of the stand, while a complementing model of crown shyness (Goudie et al. 2009) might represent the dynamics of the crown shape within the course of simulation. A particular focus of growth model extension for wood quality and timber strength of beech will be on the representation of branch architecture. While the simplistic assumption of branch diameter as being exclusively related to crown radius was adequately precise for a prototypic Douglas fir model (Poschenrieder et al. 2016), wood quality modelling of European beech requires a more explicit representation of branch architecture. Branch growth of beech may either follow a monopodial pattern with short shoots or a pseudo-

sympodial one of long shoots that exploit gaps (Peters 1997, p 90, Letort et al. 2008). Possibly as a result of pseudo-sympodial growth, beech branches often have a large diameter that may be close to the one of the stem. Laser scanning inventory as applied by Bayer et al. (2013) may thus provide data to identify various types of branching and their probability of occurrence. Based on branching pattern statistics, each virtual tree within a scenario stand might initially obtain one branching pattern sampled from a realistic set. The branch diameters within that pattern might then be adapted to correspond to the initial crown shape. Therefore, the lowest branch might be assumed to originate at the base of the crown. First order branches straightforwardly might be considered as unbranched. Their base diameters as in Poschenrieder et al. (2016) might be determined by branch length as computed from both the vertical angle of the branch and the crown hull. The base diameter computation likely has to include a random component and needs to be constrained by a typical range based on the main axis diameter and the pipe-model theory (Shinozaki et al. 1964). Data on various stands with highly differentiated mixture and structure both for calibration and validation are provided by the project W07 "Long-term experimental plots for forest growth and yield research", funded by the Bavarian State Ministry for Nutrition, Agriculture and Forestry.

Dynamic regeneration module (Figure 1, R)

Ingrowth and its control through forest management is among the most relevant determinants of forest structure. In order to improve the applicability of the hybrid model within scenarios of structure conversion, a dynamic regeneration module (R in Figure 1) might be embedded into the individual tree module (S in Figure 1). The statistical regeneration model (I) might then initialize and support such a dynamic module. For the same purpose, it has yet been implemented into SILVA. Model coupling might also link the physiological cohort model to the dynamic regeneration module in order to capture the interactive influence that both light competition by the mature stand and belowground competition (Petter et al. 2014) exert on the regeneration process. Therefore, that coupling would likely aim to maintain identity of mass between the regeneration layers of the physiological model and the corresponding layers of the dynamic regeneration module.

Statistical regeneration module (Figure 1, I)

Rammig and Fahse (2009) underpin the relevance of horizontal correlations within the regeneration process using sensitivity analysis with a cellular automata model (Rammig et al. 2006, see section 3.2.4). Their study revealed that spatial correlation among planar tiles of 1 m² may result in clustering of favorable vs. less favorable microsite conditions for regeneration. If

that effect is taken into account, the resulting ingrowth is spatially concentrated. Hence, competition among the ingrown trees is strong as compared to the lower competition pressure within a spatially homogeneous tree arrangement. Vice versa, neglecting microsite correlation may lead to notable overestimation of stand growth. As microsite conditions to a certain part are governed by overstory properties, such as canopy openness, a realistic spatial pattern of the canopy structure may thus be important for realistically initializing regeneration within a simulated stand. Moreover, the statistical model introduced by Poschenrieder et al. (2018) might also benefit from a realistic arrangement of microsite clusters that do not depend on the canopy structure. Such clusters, for example, might result from fallen logs that may inhibit or, if decaying, foster nurse-log regeneration.

Damage of sapling shoots by grazing animals is common. It has a significant impact on regeneration (Ammer 1996, Price et al. 2001, Didion et al. 2009). Therefore, further development of the statistical regeneration model presented by Poschenrieder et al. (2018) will aim to include browsing as an additional predictor. To that end, the percentage of saplings marked by a browsed terminal shoot (Eiberle 1986) would be a practice oriented indicator. It may be readily obtained from forest practitioners within a region considered. As summarized by Rüegg and Nigg (2003), that indicator is directly related to the abundance of sapling dieback (Eiberle 1989, Rüegg 1999). Future research that aims to derive an indicator of browsing might also take into account that the relation between browsing intensity and sapling mortality may depend on site conditions. That dependence is presented by Kupferschmid et al. (2015) based on various research within the montane region.

As soon as the statistical regeneration model is parameterized for tree species that are notably promoted through planting, the predicted regeneration biomass will include both the fraction that is due to natural regeneration and the one that results from underplanting. Planting, on the one hand, may influence sapling abundance through the share of palatable vs. less palatable (Duncan et al. 2001) species. On the other hand, it may foster such species that are more effective in resource acquisition than the ones present within the mature stand. Moreover, as a spatially explicit measure, planting may aim at optimizing light supply. Thus, it is likely to influence the total biomass of the sapling fraction even in the absence of browsing. While for beech dominated forest one may assume, that regeneration is first and foremost established through seeding by mature trees, a further predictor that quantifies underplanting might generally contribute to the precision of the model. Therefore, further research might aim to derive and test an indicator of planting activity.

Future development of the statistical regeneration model will take into account additional species within the overstory. Concomitantly, research will consider the share of regeneration biomass on a per species basis. That share, on the one hand, certainly depends on the overstory's density and the species composition of the mature stand fraction. On the other hand, it may strongly be influenced by browsing intensity as well as species-specific sensitivity to browsing (Clasen et al. 2015). That species-related sensitivity is crucial. It may even lead to loss of the admixed species (Clasen et al. 2011). Therefore, future extension of the statistical model might include an estimation of species-specific shares within regeneration that takes into account an indicator of browsing intensity.

As browsing is a major concern of forest management, a wide data base exists to report browsing incidence (e.g. Hothorn and Müller 2010, Kupferschmid et al. 2015). Stock oriented inventories, like German NFI and Bavarian State Forest inventory, provide a valuable basis for the estimation of regeneration biomass. They also include quantifiers of browsing that might be complemented with data from browsing-oriented inventories, such as the Bavarian Forestral Survey on the Situation of Forest Regeneration (Hothorn and Müller 2010, StMELF 2015). That regeneration survey represents browsing by the percentage of saplings with browsed terminal shoot per each of 750 game management districts.

Implementation of the conceptual modelling framework (Figure 1)

The model prototypes from the thesis at hand might be further developed and coupled to fully implement the conceptual modelling framework outlined by Figure 1. However, any of them may also be linked standalone to existing models. Correspondingly, the results of Poschenrieder et al. (2018) have been implemented within SILVA to provide the starting condition to its regeneration module. A primary realization of the conceptual framework likely would comprise MoBiLE-ST, the hybrid of MoBiLE and the SILVA-based individual tree module (modules S and M in Figure 1). Optionally, it might include the dynamic regeneration module of SILVA (module R) and the statistical module for its initialization (module I). Further development might, in a first step, aim to apply MoBiLE-ST within studies on landscape scale. The hybrid might be used to back scenario results of SILVA and to compute levels of groundwater recharge related to representative stand structure types. Development at a later stage might implement the wood quality model concept both within MoBiLE-ST and SILVA, in order to study the effect of future climate scenarios and management on timber strength. Within that scope, a relevant process might be the influence of climate on wood density (Filipescu et al. 2014).

In Germany, plot inventory data are the most relevant data source for model test and application against the background of landscape-related ecosystem service studies (e.g. ALTERFOR, Fraunhofer-Gesellschaft 2017). Within German state forest, as depending on the federal state, the grid width of such inventories may be as small as 200 m (Bavaria). In some federal states, moreover, plot-based inventories are complemented by stand level inventories, such as the DSW2 in Brandenburg (Thünen-Institut 2017b). Within private forest, however, due to the high relevance of data privacy there, the prominent source of inventory data are federal state plot inventories of 2 km grid width or the German NFI of often 4 km grid width (four inventory plots per each grid point at 150 m distance). Landscape scale studies will certainly benefit from data and further support by private forest owners. Accordingly, modern scenario studies that strive to involve a broad range of stakeholders intentionally address that group (Fraunhofer-Gesellschaft 2017). Simulation scenarios, in return, provide valuable insights into the impact that future climate and economy may take on the forestry sector in general.

7 Conclusions

The conceptual modelling framework being considered may represent the effect of management on a modern spectrum of ecosystem services. Prominent examples are timber and bioenergy production, CO_2 sequestration and indicators of recreational value. Due to its physiological component, the modelling concept takes into account, that individual tree competitiveness is sensitive to the intraannual and interannual variability of weather. That model quality is crucial, as future weather variability may often exceed the range limits of climatological observation. Based on its individual tree component and its regeneration module, the yet conceptual model being envisaged may represent spatially explicit methods of thinning and planting that aim to control generational change. Furthermore, that model concept enables linkage to seed dispersal from landscape models and to landscape-related evaluations of average water balance and quality. Its primary objective is supporting of ecosystem service studies on landscape scale level. The components developed by the thesis at hand yet implement key features of the concept. Thus, they may readily support landscape-related studies. Moreover, they may extend the capabilities of the observation-based simulation model as a tool for the forest management unit that is challenged to support a widening portfolio of ecosystem services today.

8 References

Abdullahi S, Kugler F, Pretzsch H (2016) Prediction of stem volume in complex temperate forest stands using TanDEM-X SAR data. Remote Sensing of Environment 174:197-211. doi: 10.1016/j.rse.2015.12.012

Abdullahi S, Schardt M, Pretzsch H (2017) An unsupervised two-stage clustering approach for forest structure classification based on X-band InSAR data. A case study in complex temperate forest stands. Intern. Journal of Applied Earth Observation and Geoinformation 57:36-48. doi: 10.1016/j.jag.2016.12.010

Agren GI, McMurtrie RE, Parton WJ, Pastor J, Shugart HH (1991) State-of-the-Art of Models of Production-Decomposition Linkages in Conifer and Grassland Ecosystems. Ecol. Appl. 1(2):118–138. doi:10.2307/1941806

Aherne J, Posch M, Forsius M, et al (2012) Impacts of forest biomass removal on soil nutrient status under climate change: A catchment-based modelling study for Finland. Biogeochemistry 107:471–488. doi: 10.1007/s10533-010-9569-4

Akaike H (1985). Prediction and Entropy. In: Atkinson AC, Fienberg SE (ed) A Celebration of Statistics. Springer New York, New York, NY, USA, 1985. pp 1–24.

Ameztegui A, Coll L, Messier C (2015) Modelling the effect of climate-induced changes in recruitment and juvenile growth on mixed-forest dynamics: The case of montane–subalpine Pyrenean ecotones. Ecol Modell 313:84–93.
doi: 10.1016/j.ecolmodel.2015.06.029

Amishev D, Murphy GE (2008a) Preharvest veneer quality evaluation of Douglas-fir stands using time-of-flight acoustic technique. Wood Fiber Sci 40:587–598.

Amishev D, Murphy GE (2008b) In-forest assessment of veneer grade Douglas-fir logs based on acoustic measurement of wood stiffness. For Prod J 58:42–47.

Ammer C (1996) Impact of ungulates on structure and dynamics of natural regeneration of mixed mountain forests in the Bavarian Alps. For Ecol Manage 88:43–53. doi: 10.1016/S0378-1127(96)03808-X

Arney JD (1972) Computer simulation of Douglas fir tree and stand growth. PhD Thesis. Oregon State University, Corvallis, OR, USA.

Asner GP, Kellner JR, Kennedy-Bowdoin T, Knapp DE, Anderson C, Martin RE (2013) Forest Canopy Gap Distributions in the Southern Peruvian Amazon. PLoS One 8 (4). doi: 10.1371/journal.pone.0060875

Auty D, Achim A, Macdonald E, Cameron AD, Gardiner BA (2014) Models for predicting wood density variation in Scots pine. Forestry 87(3):449–458.
doi:10.1093/forestry/cpu005

Baldwin VC, Burkhart HE, Westfall JA, Peterson KD (2001) Linking growth and yield and process models to estimate impact of environmental changes on growth of loblolly pine. For Sci 47:77–82.

Bayer D, Seifert S, Pretzsch H (2013) Structural crown properties of Norway spruce (Picea abies [L.] Karst.) and European beech (Fagus sylvatica [L.]) in mixed versus pure stands revealed by terrestrial laser scanning. Trees 27:1035–1047. doi: 10.1007/s00468-013-0854-4

Bertalanffy L von (1957) Quantitative laws in metabolism and growth. The Quarterly Review of Biology 86:75–96. doi: 10.1086/659883

Biber P, Herling H (2002) Modellierung der Verjüngungsdynamik als Bestandteil von einzelbaumorientierten Waldwachstumsmodellen. Jahrestagung der Sektion Ertragskunde im Deutschen Verband Forstlicher Forschungsanstalten in Schwarzburg. Tagungsbericht: 194-216 [Modelling regeneration dynamics within distance dependent individual tree forest growth simulators. Annual proceedings of the yield science section within the German association of forest research institutions.]

Biber P, Borges JG, Moshammer R, Barreiro S, Botequim B, Brodrechtová Y, Brukas V, Chirici G, Cordero-Debets R, Corrigan E, Eriksson LO, Favero M, Galev E, Garcia-Gonzalo J, Hengeveld G, Kavaliauskas M, Marchetti M, Marques S, Mozgeris G, Navrátil R, Nieuwenhuis M, Orazio C, Paligorov I, Pettenella D, Sedmák R, Smreček R, Stanislovaitis A, Tomé M, Trubins R, Tuček J, Vizzarri M, Wallin, I, Pretzsch H, Sallnäs O (2015) How Sensitive Are Ecosystem Services in European Forest Landscapes to Silvicultural Treatment? Forests 6(5):1666-1695. doi:10.3390/f6051666.

BMEL (2015) The Forests in Germany. Selected Results of the Third National Forest Inventory. Federal Minstry of Food and Agriculture, Berlin, Germany. https://www.bundeswaldinventur.de/fileadmin/SITE_MASTER/content/Dokumente/Downloads/BMEL_The_Forests_in_Germany.pdf [Cited 10 January 2017]

Bolte A, Ammer C, Löf M, Madsen P, Nabuurs G-J, Schall P, Spathelf P, Rock J (2009) Adaptive forest management in central Europe: Climate change impacts, strategies and integrative concept. Scand J For Res 24(6):473–482. doi:10.1080/02827580903418224

Bose AK, Harvey BD, Coates KD, et al (2015) Modelling stand development after partial harvesting in boreal mixedwoods of eastern Canada. Ecol Modell 300:123–136. doi: 10.1016/j.ecolmodel.2015.01.002

Bossel H (1996) TREEDYN3 forest simulation model. Ecological Modelling, 90(3):187–227. doi:10.1016/0304-3800(95)00139-5

Botkin DB, Janak JF,Wallis JR (1972) Some ecological consequences of a computer model of forest growth. Journal of Ecology 60:849–872.

Boulanger V, Baltzinger C, Saïd S, et al (2009) Ranking temperate woody species along a gradient of browsing by deer. For Ecol Manage 258:1397–1406. doi: 10.1016/j.foreco.2009.06.055

Box EO (1981) Macroclimate and Plant Forms: an Introduction to Predictive Modeling in Phytogeography, Dr W Junk Publishers, The Hague.

Bugmann H (2001) A review of forest gap models. Clim. Change 51:259–305.

Bugmann H, Grote R, Lasch P, Lindner M, Suckow F (1997) A new forest gap model to study the effects of environmental change on forest structure and functioning. Impacts of Global Change on Tree Physiology and Forest Ecosystems: proceedings of the international conference on impacts of global change on tree physiology and forest ecosystems, November 1996, Wageningen, Netherlands 51:255–261.

Byrne KE, Mitchell SJ (2013) Testing of WindFIRM/ForestGALES_BC: A hybrid-mechanistic model for predicting windthrow in partially harvested stands. Forestry 86(2):185–199. Oxford University Press. doi:10.1093/forestry/cps077.

Canadian Forest Inventory Committee (2008) Canada's National Forest Inventory ground sampling guidelines: Specifications for ongoing measurement . Natural Resources Canada, Canadian Forest Service, Pacific Forestry Centre, Victoria, BC, Canada.

Carlowitz von HC (1732) Sylvicultura Oeconomica. Hausswirthliche Nachricht und Naturmäßige Anweisung zur Wilden Baum-Zucht. Reprint der zweiten Auflage von 1732. In: Bendix B (ed) Forstliche Klassiker. Kessel, Germany. ISBN: 978-3-941300-19-4 [nature compliant directive for tree fostering].

Cavers S, Cottrell JE (2015) The basis of resilience in forest tree species and its use in adaptive forest management in Britain. Forestry 88:13–26.
doi: 10.1093/forestry/cpu02710.1093/forestry/cpu027.

CEN (2009) EN 338:2009, structural timber—strength classes, European Committee for Standardization, Brussels.

Chambers JM, Freeny A, Heiberger,RM (1992) Analysis of variance; designed experiments. Statistical Models in S, Chapter 5. In: Chambers JM, Hastie TJ (ed) Wadsworth & Brooks/Cole, Pacific Grove, California, 1992.

Clasen C, Griess VC, Knoke T (2011) Financial consequences of losing admixed tree species: A new approach to value increased financial risks by ungulate browsing. For Policy Econ 13:503–511. doi: 10.1016/j.forpol.2011.05.005

Clasen C, Heurich M, Glaesener L, et al (2015) What factors affect the survival of tree saplings under browsing, and how can a loss of admixed tree species be forecast? Ecol Modell 305:1–9. doi: 10.1016/j.ecolmodel.2015.03.002

Claussen M (1994) Coupling global biome models with climate models. Climate Research 4:203–221.

Cramer W (2002). Biome Models - The Earth System: biological and ecological dimensions of global environmental change. Encyclopedia of Global Environmental Change 2:166–171.

Cramer W, Bondeau A, Woodward FI, Prentice IC, Betts R, Brovkin V, Cox PM, Fischer V, Foley JA, Friend AD, Kucharik C, Lomas MR, Ramankutty N, Sitch S, Smith B, White A, Young-Molling C (2001) Global response of terrestrial ecosystem structure and function to CO_2 and climate change: results from six dynamic global vegetation models. Global Change Biology 7:357-373.

Crookston NL, Dixon GE (2005) The forest vegetation simulator: A review of its structure, content, and applications. Comput. Electron. Agric. 49(1):60–80. doi:10.1016/j.compag.2005.02.003

Curtis RO, Clendenen GW, Reukema DC, De Mars DJ (1982) Yield tables for managed stands of coast Douglas-fir. General Technical Report PNW-135. Portland, OR: USDA, Forest and Range Experimental Station.

Dantas de Paula M, Groeneveld J, Huth A (2015) Tropical forest degradation and recovery in fragmented landscapes — Simulating changes in tree community, forest hydrology and carbon balance. Global Ecology and Conservation 3:664–677. doi:10.1016/j.gecco.2015.03.004

Deckmyn G, Evans SP, Randle TJ (2006) Refined pipe theory for mechanistic modeling of wood development. Tree Physiol. 26:703–717.

Deckmyn G, Verbeeck H, Op de Beeck M, Vansteenkiste D, Steppe K, Ceulemans R (2008) ANAFORE: A stand-scale process-based forest model that includes wood tissue development and labile carbon storage in trees. Ecological Modelling 215(4):345–368. doi:10.1016/j.ecolmodel.2008.04.007

Deckmyn G, Mali B, Kraigher H, Trorelli N, Op de Beeck M, Ceulemans R (2009) Using the process-based stand model ANAFORE including Bayesian optimisation to predict wood quality and quantity and their uncertainty in Slovenian beech. Silva Fennica 43:523-534. doi:10.14214/sf.204

Didion M, Kupferschmid AD, Bugmann H (2009) Long-term effects of ungulate browsing on forest composition and structure. For Ecol Manage 258:44–55. doi: 10.1016/j.foreco.2009.06.006

Dieler J, Pretzsch H (2013) Morphological plasticity of European beech (Fagus sylvatica L.) in pure and mixed-species stands. For Ecol Manage 295:97–108. doi: 10.1016/j.foreco.2012.12.049

Dolstra F (2002) Simulating growth and development of the German forest: a large-scale scenario study incorporating the impact of natural disturbances and climate change. Afstudeerverslag, Wageningen University, Environmental Sciences. 29 pp.

Duncan AJ, Hartley SE, Thurlow M, Young S, Staines BW, (2001) Clonal variation in monoterpene concentrations in Sitka spruce (Picea sitchensis) saplings and its effect on their susceptibility to browsing damage by red deer (Cervus elaphus). For Ecol Manage 148:259–269.

Efron B (1979) Bootstrap Methods: Another Look at the Jackknife. Ann. Stat. 7(1):1–26. doi:10.1214/aos/1176344552

Egnell G, Laudon H, Rosvall O (2011) Perspectives on the Potential Contribution of Swedish Forests to Renewable Energy Targets in Europe. Forests 2:578–589. doi: 10.3390/f2020578

Eiberle K (1986) Zur Kontrolle des Wildverbisses – einige Daten über den erforderlichen Stichprobenumfang. Schweiz. Jagdztg. 14, 8:32–37. [Control of browsing – some data to represent the required sample size.]

Eiberle K (1989) Über den Einfluss des Wildverbisses auf die Mortalität von jungen Waldbäumen in der oberen Montanstufe. Schweiz. Z. Forstwes. 140 (12):1031–1042. [On the influence of browsing on mortality of young forest trees within the upper montane region.]

Elfving B (2010). Growth modelling in the Heureka system. Swedish University of Agricultural Sciences, Faculty of Forestry.

http://heurekaslu.org/wiki/Heureka_prognossystem_(Elfving_rapportutkast).pdf. [Cited 04 December 2016]

Ende HP, Jenssen M, Englert H, Gasche R, Klenke R, Aenis T, Anders K (2010) Thesen zum klimaplastischen Wald. In: Aenis, T, Ende HP, Foos E, Nagel UJ (eds) Klimaplastische Wälder im nordostdeutschen Tiefland. Leitfaden zur Bildung für eine nachhaltige Entwicklung (Abschnitt 2.2). Humboldt-Universität zu Berlin, Landwirtschaftlich-Gärtnerische Fakultät, pp 11-15. [Theses regarding climate resilient forest: Climate resilient forests in the North-East German Lowlands.]

Fabian P, Häberle K-H, Heerdt C, Pretzsch H, Werner H, Wipfler P (2006) Kranzberg Forest Experiment: Plot characterization and free-air ozone fumigation. In: Wieser G (ed) Proc. CASIROZ UN/ECE Workshop "Critical levels of ozone", Obergurgl/Austria, Nov. 15-19, 2005: 10-15. http:// www.casiroz.de [cited 14 January 2017]

Fabrika M, Ďurský J (2005) Algorithms and software solution of thinning models for SIBYLA growth simulator. Journal of Forest Science, 51(10):431-445.

Fahrmeir L, Kneib T, Lang S, Marx B (2013) Extensions of the Classical Linaer Model. In: Fahrmeir L, Kneib T, Lang S (eds) Regression. Springer Berlin, Heidelberg. pp 177–267. doi: 10.1007/978-3-642-34333-9

Ferretti M, Fischer R, Mues V, Granke O, Lorenz M, (2010) Basic design principles for the ICP Forests Monitoring Networks. Manual Part II. In: Manual on methods and criteria for harmonized sampling, assessment, monitoring and analysis of the effects of air pollution on forests. UNECE ICP Forests Programme Co-ordinating Centre, Hamburg, Germany. 22 pp. ISBN: 978-3-926301-03-1.

Fichtner A. Härdtle W, Bruelheide H, Kunz M, Li Y. Von Oheimb G (2018) Neighbourhood interactions drive overyielding in mixed-species tree communities. Nature Communications, 9(1). doi:10.1038/s41467-018-03529-w

Filipescu CN, Lowell EC, Koppenaal R, Mitchell AK (2014) Modeling regional and climatic variation of wood density and ring width in intensively managed Douglas-fir. Can J For Res. doi: 10.1139/cjfr-2013-0275

Fischer R, Bohn F, Dantas de Paula M, Dislich C, Groeneveld J, Gutiérrez AG, Kazmierczak M, Knapp N, Lehmann S, Paulick S, Pütz S, Rödig E, Taubert F, Köhler P, Huth A (2016) Lessons learned from applying a forest gap model to understand ecosystem and carbon

dynamics of complex tropical forests. Ecological Modelling 326:124–133. doi:10.1016/j.ecolmodel.2015.11.018

Fontes L, Bontemps JD, Bugmann H, et al (2010) Models for supporting forest management in a changing environment. For. Syst. 19:8–29.

Forsyth DM, Wilson DJ, Easdale TA, et al (2015) Century-scale effects of invasive deer and rodents on the dynamics of forests growing on soils of contrasting fertility. Ecol Monogr 85:157–180. doi: 10.1890/14-0389.1

Foster JR, Reiners WA (1986) Size Distribution and Expansion of Canopy Gaps in a Northern Appalachian Spruce-Fir Forest. Vegetatio 68 (2):109–114.

Fraunhofer-Gesellschaft (2017) ALTERFOR in a nutshell. https://www.alterfor-project.eu/key-facts.html. [cited 29 January 2017]]

Frejaville T, Curt T, Carcaillet C (2013) Bark flammability as a fire-response trait for subalpine trees. Front Plant Sci 4(November):1–8. doi:10.3389/fpls.2013.00466

Friend AD, Stevens AK, Knox RG, Cannell MGR (1997) A process-based, terrestrial biosphere model of ecosystem dynamics (Hybrid v3.0). Ecol Modell 95:249–287. doi: 10.1016/S0304-3800(96)00034-8

Gao T, Hedblom M, Emilsson T, Nielsen AB (2014) The role of forest stand structure as biodiversity indicator. For Ecol Manage 330:82–93. Elsevier. doi:10.1016/J.FORECO.2014.07.007.

Gao T, Nielsen AB, Hedblom M (2015) Reviewing the strength of evidence of biodiversity indicators for forest ecosystems in Europe. Ecol Indic 57:420–434. Elsevier. doi:10.1016/J.ECOLIND.2015.05.028.

García O (1994) The state-space approach in growth modelling. Can J For Res 24:1894–1903. doi: 10.1139/x94-244

Gehrhardt E (1909) Über Bestandes-Wachstumsgesetze und ihre Anwendung zur Aufstellung von Ertragstafeln. Allgemeine Forst- und Jagdzeitung 85:117–128.

Geng A, Yang H, Chen J, Hong Y (2017) Review of carbon storage function of harvested wood products and the potential of wood substitution in greenhouse gas mitigation. For Policy Econ 85:192–200. Elsevier. doi: 10.1016/j.forpol.2017.08.007

Gerten D, Schaphoff S, Haberlandt U, et al (2004) Terrestrial vegetation and water balance—hydrological evaluation of a dynamic global vegetation model. J Hydrol 286:249–270. doi: 10.1016/j.jhydrol.2003.09.029

Geßler A, Schrempp S, Matzarakis A, Mayer H, Rennenberg H (2001) Radiation modifies the effect of water availability on the carbon isotope composition of beech (Fagus sylvatica). New Phytol 150:653-664.

Giorgetta MA, Jungclaus J, Reick CH, Legutke S, Bader J, Böttinger M, Brovkin V, Crueger T, Esch M, Fieg K, Glushak K, Gayler V, Haak H, Hollweg H-D, Ilyina, T, Kinne S, Kornblueh L, Matei D, Mauritsen T, Mikolajewicz U, Mueller W, Notz D, Pithan F, Raddatz T, Rast S, Redler R, Roeckner E, Schmidt H, Schnur R, Segschneider J, Six KD, Stockhause M, Timmreck C, Wegner J, Widmann H, Wieners K-H, Claussen M, Marotzke J, and Stevens B (2013) Climate and carbon cycle changes from 1850 to 2100 in MPI-ESM simulations for the Coupled Model Intercomparison Project phase 5. J Adv Model Earth Syst 5(3):572–597. doi: 10.1002/jame.20038

Grant RF, Black TA, Humphreys ER, Morgenstern K (2007) Changes in net ecosystem productivity with forest age following clearcutting of a coastal Douglas-fir forest: testing a mathematical model with eddy covariance measurements along a forest chronosequence. Tree Physiol. 27(1):115–131. doi:10.1093/treephys/27.1.115

Gravel D, Beaudet M, Messier C (2008) Partitioning the factors of spatial variation in regeneration density of shade-tolerant tree species. Ecology 89(10):2879–2888. Ecological Society of America. doi:10.1890/07-1596.1.

Grote R, Pretzsch H (2002) A Model for Individual Tree Development Based on Physiological Processes. Plant Biology 4(2):167–180. doi:10.1055/s-2002-25743

Grote R, Korhonen J, Mammarella I (2011) Challenges for evaluating process-based models of gas exchange at forest sites with fetches of various species. For Syst 20(3):389–406.

Goudie JW, Polsson KR, Ott PK (2009) An empirical model of crown shyness for lodgepole pine (Pinus contorta var. latifolia [Engl.] Critch.) in British Columbia. Forest Ecology and Management 257(1):321–331. doi:10.1016/j.foreco.2008.09.005

Gundersen P, Schmidt IK, Raulund-Rasmussen K (2006) Leaching of nitrate from temperate forests - effects of air pollution and forest management. Environ. Rev. 14:1-57. doi:10.1139/a05-015

Hartig GL (1795) Anweisung zu Taxation der Forsten oder zur Bestimmung des Holzertrages der Wälder. Heyer Verlag, Gießen, Germany.

Hasenauer H, Kindermann G, Steinmetz P (2006) The tree growth model MOSES 3.0. In: Hasenauer H (ed) Sustainable forest management. Springer, Berlin, pp 64–70.

Hauser S (2003) Dynamik hochaufgelöster radialer Schaftveränderungen und des Dickenwachstums bei Buchen (Fagus sylvatica L.) der Schwäbischen Alb unter dem Einfluss von Witterung und Bewirtschaftung. Freiburg i. Brsg., Albert-Ludwigs-Universität, Freiburg i. Brsg, Germany. 212 pp.

He HS, Li W, Sturtevant BR, Yang J, Shang BZ, Gustafson EJ, Mladenoff DJ (2004) LANDIS 4.0 Users Guide. School of Natural Resources, University of Missouri-Columbia, Columbia, 1–91. http://www.nrs.fs.fed.us/pubs/gtr/gtr_nc263.pdf [cited 08 December 2016]

Henning JG, Burk TE (2004) Improving growth and yield estimates with a process model derived growth index. Can J For Res 34:1274–1282. doi: 10.1139/x04-021

Herling H (2004) Rekonstruktion von Verjüngung auf Grundlage von Forstinventurdaten. Jahrestagung der Sektion Ertragskunde im Deutschen Verband Forstlicher Versuchsanstalten. Tagungsbericht. pp 129-145. [Reconstruction of regeneration based on forest inventory data. Annual proceedings of the yield science section within the German association of forest research institutions.]

Holst T, Mayer H (2005) Radiation components of beech stands in Southwest Germany. Meteorol Zeitschrift 14:107-115

Holst J, Grote R, Offermann C, et al (2010) Water fluxes within beech stands in complex terrain. Int J Biometeorol 54:23–36. doi: 10.1007/s00484-009-0248-x

Holst T, Hauser S, Kirchgäßner A, Matzarakis A, Mayer H, Schindler D (2004) Measuring and modelling plant area index in beech stands. Int J Biometeorol 48:192-201

Hothorn T, Müller J (2010) Large-scale reduction of ungulate browsing by managed sport hunting. For Ecol Manage 260:1416–1423. doi: 10.1016/j.foreco.2010.07.019

Hudjetz S, Lennartz G, Krämer K, Roß-Nickoll M, Gergs A, Preuss TG (2014) Modeling Wood Encroachment in Abandoned Grasslands in the Eifel National Park – Model Description and Testing. PLoS One 9:e113827. doi: 10.1371/journal.pone.0113827

Hunziker U, Brang P (2005) Microsite patterns of conifer seedling establishment and growth in a mixed stand in the southern Alps. For Ecol Manage 210:67–79. doi: 10.1016/j.foreco.2005.02.019

Huth A, Ditzer T, Bossel H (1998) The rain forest growth model FORMIX3: model description and analysis of forest growth and logging scenarios for the Deramakot Forest Reserve (Malaysia). Erich Goltze, Göttingen.

Hynynen J, Ojansuu R, Hökkä H, et al (2002) Models for predicting stand development in MELA System. Finnish Forest Research Institute Research Papers 835(3): 116pp.

Hynynen J, Ahtikoski A, Siitonen J, Sievänen R, Liski J (2005) Applying the MOTTI simulator to analyse the effects of alternative management schedules on timber and non-timber production. For Ecol Manage 207(1–2 SPEC. ISS.): 5–18. doi:10.1016/j.foreco.2004.10.015

Jarvis PG, McNaughton KG (1986). Stomatal Control of Transpiration: Scaling Up from Leaf to Region. pp 1–49. doi:10.1016/S0065-2504(08)60119-1

Jonsson B, Jacobsson J, Kallur H (1993) The Forest Management Planning Package Theory and Application. Stud. For. Suec. 189:1–56. ISBN 91 -576-4698-8

Kahn M (1994): Modellierung der Höhenentwicklung ausgewählter Baumarten in Abhängigkeit vom Standort. Thesis. Forstwissenschaftliche Fakultät, Universität München. [Modelling height development of selected tree species as dependent on site.]

Kändler G, Bösch B (2013) Überprüfung und Neukonzeption einer Biomassefunktion. Abschlussbericht 2b, Forstliche Versuchs- und Forschungsanstalt Baden-Württemberg, Abt. Biometrie und Informatik Wonnhaldestraße 4, 79100 Freiburg, Germany. [Test and redesign of a biomass function. Final Report 2b, forest experiment and research institution of the federal state of Baden-Württemberg, Germany.]

Kayitakire F, Hamel C, Defourny P (2006) Retrieving forest structure variables based on image texture analysis and IKONOS-2 imagery. Remote Sensing of Environment 102(3 4): 390-401. doi: 10.1016/j.rse.2006.02.022.

Kirschbaum MUF (1999) CenW, a forest growth model with linked carbon, energy, nutrient and water cycles. Ecological Modelling 118(1):17–59. doi:10.1016/S0304-3800(99)00020-4

Kirschbaum MUF (2000) CenW: A generic forest growth model. New Zeal J For 45:15–19.

Kölling C (2007) Klimahüllen von 27 Waldbaumarten. AFZ-Der Wald, 62:1242–1245. [Climate envelopes of 27 forest tree species.]

Kolo H, Ankerst D, Knoke T (2017) Predicting Natural Forest Regeneration: A Statistical Model Based on Inventory Data. Eur. J. For. Res, 136 (5–6):923–938. doi:10.1007/s10342-017-1080-1

Kozlowski, T.T. (2002). Physiological ecology of natural regeneration of harvested and disturbed forest stands: implications for forest management. Forest Ecology and Management 158(1-3):195–221. doi:10.1016/S0378-1127(00)00712-X

Kupferschmid AD, Heiri C, Huber M, Fehr M, Frei M, Gmür P, Imesch M, Zinggeler J, Brang P, Clivaz JC, Odermatt O (2015) Einfluss wildlebender Huftiere auf die Waldverjüngung: ein Überblick für die Schweiz. Schweizerische Zeitschrift Für Forstwesen 166(6):420–431. doi: 10.3188/szf.2015.0420 [Influence of wild ungulates on the forest regeneration in Switzerland.]

Landsberg JJ, Waring RH (1997) A generalised model of forest productivity using simplified concepts ofradiation-use efficiency , carbon balance and partltlonlng. For Ecol Manage 95(3):209–228. doi:10.1016/S0378-1127(97)00026-1

Landsberg, J. 2003. Physiology in forest models: history and the future. For. Biometry Model. Inf. Sci. 1(July): 49–63.

Le Roux X, Lacointe A, Escobar-Gutierrez A, Le Dizes S (2001) Carbon-based models of individual tree growth: A critical appraisal. Ann. For. Sci. 58:469-506. doi:10.1051/forest:2001140

Leslie PH (1945) On the use of matrices in certain population mathematics. Biometrika 33(3):183-212.

Levy PE, Friend AD, White A, Cannell MGR (2004) The Influence of Land Use Change On Global-Scale Fluxes of Carbon from Terrestrial Ecosystems. Climatic Change 67(2–3):185–209. doi:10.1007/s10584-004-2849-z

Lewis EG (1942) On the generation and growth of a population. Sankhya 6(1):93-96.

Liang J, Picard N (2013).Matrix Model of Forest Dynamics: An Overview and Outlook. Forest Science 3(59):359–378. doi:10.5849/forsci.11-123

Lutze M, Ades P, Campbell R (2004) Spatial distribution of regeneration in mixed-species forests of Victoria. Aust. For. 67(3):172–183. doi:10.1080/00049158.2004.10674931.

Luo X, He HS, Liang Y, Wang WJ, Wu Z, Fraser JS (2014). Spatial simulation of the effect of fire and harvest on aboveground tree biomass in boreal forests of Northeast China. Landscape Ecology, 29(7), 1187–1200. https://doi.org/10.1007/s10980-014-0051-x

Luxmoore RJ, Hargrove WW, Lynn Tharp M, Mac Post W, Berry MW, Minser KS, Cropper, Wendell P Jr, Johnson DW, Zeide B, Amateis RL, Burkhart HE, Baldwin VC Jr, Peterson KD (2002) Addressing multi-use issues in sustainable forest management with signal-transfer modeling. For Ecol Manage 165:295–304. doi:10.1016/S0378-1127(01)00631-4

Maaten E (2011) Climate sensitivity of radial growth in European beech (Fagus sylvatica L.) at different aspects in southwestern Germany. Trees 26:777-788.

Macgregor JJ (1947) Labour costs in English forestry since 1824. Forestry 20(1):30–43. doi:10.1093/Forestry/20.1.30.

Mäkelä A (2003) Process-based modelling of tree and stand growth: towards a hierarchical treatment of multiscale processes. Canadian Journal of Forest Research 33(3):398–409. doi:10.1139/x02-130

Mäkelä A, Mäkinen H (2003) Generating 3D sawlogs with a process-based growth model. For Ecol Manage 184:337–354. doi: 10.1016/S0378-1127(03)00152-X

Mäkelä, A., Grace, J., Deckmyn, G., Kantola, A., & Kint, V. (2010). Simulating wood quality in forest management models. Forest Systems, 19, 48–68.

Mäkelä A, Landsberg J, Ek AR, Burk TE, Ter-Mikaelian M, Ågren GI, Oliver CD, Puttonen P (2000) Process-based models for forest ecosystem management: current state of the art and challenges for practical implementation. Tree Physiol 20:289–298. doi: 10.1093/treephys/20.5-6.289

Matala J, Hynynen J, Miina J, et al (2003) Comparison of a physiological model and a statistical model for prediction of growth and yield in boreal forests. Ecol Modell 161:95–116. doi: 10.1016/S0304-3800(02)00297-1

Matala J, Ojansuu R, Peltola H, et al (2006) Modelling the response of tree growth to temperature and CO2 elevation as related to the fertility and current temperature sum of a site. Ecol Modell 199:39–52. doi: 10.1016/j.ecolmodel.2006.06.009

Mayer H, Holst T, Schindler D (2002) Microclimate within Beech Stands - Part I: Photosynthetically Active Radiation. Forstwissenschaftliches Cent 121:301–321. doi: 10.1046/j.1439-0337.2002.02038.x

Meyer J (2005) Fire effects on forest resource development in the French Mediterranean region - projections with a large-scale forest scenario model. Technical Report 16. European Forest Institute, Joensuu Finland. 86 pp.

Michailoff I (1943) Zahlenmäßiges Verfahren für die Ausführung der Bestandeshöhenkurven. Forstw. Cbl. u. Thar. Jahrb. 6:273-279. [Numerical algorithm for the implementation of stand height curves]

Miller RG (1981) Simultaneous Statistical Inference. Springer New York, New York, NY. doi: 10.1007/978-1-4613-8122-8

Millington JDA, Walters MB, Matonis MS, Liu J (2013) Filling the gap: A compositional gap regeneration model for managed northern hardwood forests. Ecol Modell 253:17–27. doi: 10.1016/j.ecolmodel.2012.12.033

Millington JDA, Walters MB, Matonis MS, Laurent EJ, Hall KR, Liu J (2011) Combined long-term effects of variable tree regeneration and timber management on forest songbirds and timber production. For Ecol Manage 262:718–729. doi: 10.1016/j.foreco.2011.05.002

Mitchell KJJ (1975) Dynamics and simulated yield of Douglas-fir. Forest Science 17(4):1–39.

Mitchell KJJ (1988) SYLVER: modelling the impact of silviculture on yield, lumber value, and economic return. Forestry Chronicle 64(2):127–131.

Monserud RA (1975) Methology for simulating Wisconsin northern hardwood stand dynamics. PhD Thesis. University of Wisconsin-Madison, Madison, WI, USA.

Motta R (1996) Impact of wild ungulates on forest regeneration and tree composition of mountain forests in the Western Italian Alps. For. Ecol. Manage. 88(1–2):93–98. doi:10.1016/S0378-1127(96)03814-5

Nagel J, Duda H, Hansen J (2006) Forest Simulator BWINPro7. Forst u. Holz 61:427-429.

Naudts K, Ryder J, McGrath MJ, Otto J, Chen Y, Valade A, Bellasen V, Berhongaray G, Bönisch G, Campioli M, Ghattas J, De Groote T, Haverd V, Kattge J, MacBean N, Maignan F, Merilä P, Penuelas J, Peylin P, Pinty B, Pretzsch H, Schulze ED, Solyga D, Vuichard N, Yan Y, Luyssaert S (2015) A vertically discretised canopy description for ORCHIDEE (SVN r2290) and the modifications to the energy, water and carbon fluxes. Geosci Model Dev 8:2035–2065. doi: 10.5194/gmd-8-2035-2015

Neufanger M, Faltl W, Schelhaas C (2012) Anleitung zur Durchführung von Betriebsinventuren in den Bayerischen Staatsforsten. FE AA 010 Durchführung von Betriebsinventuren. Bayerische Staatsforsten AöR, Munich, Germany. 52 pp. [Survey instructions for forest enterprise inventories in the Bavarian State Forest. Bavarian State Forestry, Munich, Germany. 52 pp.]

Oliver CD, Nassar NT, Lippke BR, McCarter JB (2014). Carbon, Fossil Fuel, and Biodiversity Mitigation With Wood and Forests. J Sustain For 33(3):248–275. doi:10.1080/10549811.2013.839386

Pacala SW, Canham CD, Saponara J, Silander JAJ, Kobe RK, Ribbens E (1996) Forest models defined by field measurements: II. Estimation, error analysis and dynamics. Ecol Monogr 66:1–43. doi:10.2307/2963479

Paine O, Boyer E (1996) A whole individual tree growth model for Norway spruce. In: Workshop IUFRO S5, 1996: 01-04-Topic 1. INRA-Nancy, Nancy, France 1996.

Palahí M, Pukkala T, Trasobares A (2004) Presentación del sistema de planificación forestal MONTE. Revista Montes 4º Trimestre 2004, Nº 78. [Presentation of the forest planning system monte.]

Pardos M, Montero G, Cañellas I, Ruiz del Castillo J (2005) Ecophysiology of natural regeneration of forest stands in Spain. For Syst 14:434–445.

Paré D, Thiffault E (2016) Nutrient Budgets in Forests Under Increased Biomass Harvesting Scenarios. Curr For Reports 2(1):81–91. Springer International Publishing. doi: 10.1007/s40725-016-0030-3

Peaucelle M, Bellassen V, Ciais P, Peñuelas J, Viovy N (2017) A new approach to optimal discretization of plant functional types in a process-based ecosystem model with forest management: a case study for temperate conifers. Glob Ecol Biogeogr 26(4):486–499. doi:10.1111/geb.12557

Peters J, Baets B De, Verhoest NEC, et al (2007) Random forests as a tool for ecohydrological distribution modelling. Ecol Modell 207:304–318. doi: 10.1016/j.ecolmodel.2007.05.011

Petter Axelsson E, Lundmark T, Högberg P, Nordin A (2014) Belowground competition directs spatial patterns of seedling growth in boreal pine forests in fennoscandia. Forests 5:2106–2121. doi: 10.3390/f5092106

Piboule A, Collet C, Frochot H, Dhôte J (2005) Reconstructing crown shape from stem diameter and tree position to supply light models. I. Algorithms and comparison of light simulations. Annals of Forest Science 62:645–657. doi: 10.1051/forest:2005071

Polley H (2014) Survey instructions for the 3rd National Forest Inventory (2011-2012) 2nd revised version, May 2011 with 4. Corrigendum (21.03.2014). Federal Ministry of Food, Agriculture and Consumer Protection (BMELV), Referat 535, Bonn, Germany.

Pommerening A (2000) Methoden zur Reproduktion und Fortschreibung einzelner konzentrischer Probekreise von Betriebs- und Landeswaldinventuren. Forstarchiv 71(5):190-199. [Methods for replication and forward projection of concentric inventory circles of forest enterprise and federal state inventories].

Poschenrieder W, Biber P, Pretzsch H (2018) An Inventory-Based Regeneration Biomass Model to Initialize Landscape Scale Simulation Scenarios. Forests 9(4). doi: 10.3390/f9040212

Poschenrieder W, Grote R, Pretzsch H (2013) Extending a physiological forest growth model by an observation-based tree competition module improves spatial representation of diameter growth. Eur J For Res 132:943–958. doi: 10.1007/s10342-013-0730-1

Poschenrieder W, Rais A, van de Kuilen J-WG, Pretzsch H (2016) Modelling sawn timber volume and strength development at the individual tree level – essential model features by the example of Douglas fir. Silva Fenn 50:1–25. doi: 10.14214/sf.1393

Polley H (2014) Survey instructions for the 3rd National Forest Inventory (2011-2012) 2nd revised version, May 2011 with 4. Corrigendum (21.03.2014). Fed. Minist. Food, Agric. Consum. Prot. Bundesministerium für Ernährung, Landwirtschaft und Verbraucherschutz Ref. 535, Bonn, Germany.

Pott M, Fabrika M (2002) An Information System for the Evaluation and Spatial Analysis of Forest Inventory Data. Forstwissenschaftliches Cent. 121 (Suppl 1):80–88.

Prentice IC, Sykes MT, Cramer W (1993) A simulation model for the transient effects of climate change on forest landscapes. Ecological Modelling 65(1-2):51–70. doi: 10.1016/0304-3800(93)90126-D

Prentice IC, Cramer W, Harrison SP, Leemans R, Monserud RA, Solomon, AM (1992) A Global Biome Model Based on Plant Physiology and Dominance, Soil Properties and Climate. J. Biogeogr. 19:117–134.

Pretzsch H (2009) Forest Dynamics, Growth and Yield. Springer Verlag Berlin 2009. 664 pp. ISBN 978-3-540-88306-7

Pretzsch H (2016) Ertragstafel-Korrekturfaktoren für Umwelt- und Mischungseffekte. AFZ-Der Wald 14:47–50. [Yield table correction factors that take into account effects of site and mixture.]

Pretzsch H, Biber P (2010) Size-symmetric versus size-asymmetric competition and growth partitioning among trees in forest stands along an ecological gradient in central Europe. Canadian Journal of Forest Research 40(2):370–384. http://doi.org/10.1139/X09-195

Pretzsch H, Biber P (2016) Tree species mixing can increase maximum stand density 1. Canadian Journal of Forest Research (ii). doi:10.1139/cjfr-2015-0413

Pretzsch H, Dieler J (2011) The dependency of the size-growth relationship of Norway spruce (Picea abies [L.] Karst.) and European beech (Fagus sylvatica [L.]) in forest stands on long- term site conditions, drought events, and ozone stress. Trees 25:355–364.

Pretzsch H, Rais A (2016) Wood quality in complex forests versus even-aged monocultures: review and perspectives. Wood Sci Technol 50:1–36. doi: 10.1007/s00226-016-0827-z

Pretzsch H, Biber P, Ďurský J (2002) The single tree-based stand simulator SILVA: construction, application and evaluation. For Ecol Manage 162:3–21. doi: 10.1016/S0378-1127(02)00047-6

Pretzsch H, Biber P, Uhl E, Dauber E (2015) Long-term stand dynamics of managed spruce–fir–beech mountain forests in Central Europe: structure, productivity and regeneration success. Forestry 88:407–428. doi: 10.1093/forestry/cpv013

Pretzsch H, Grote R, Reineking B, Rötzer T, Seifert S (2007) Models for Forest Ecosystem Management: A European Perspective. Ann Bot 101:1065–1087. doi: 10.1093/aob/mcm246

Pretzsch H, del Rio M, Schütze G, Ammer Ch, Annighöfer P, Avdagic A, Barbeito I, Bielak K, Brazaitis G, Coll L, Drössler L, Fabrika M, Forrester DI, Kurylyak V, Löf M, Lombardi F, Matovic B, Mohren F, Motta R, den Ouden J, Pach M, Ponette Q, Skzyszewski J, Sramek V, Sterba H, Svoboda M, Verheyen K, Zlatanov T, Bravo-Oviedo A (2016) Mixing of Scots pine (Pinus sylvestris L.) and European beech (Fagus sylvatica L.) enhances structural heterogeneity, And the effect increases with water availability. For Ecol Manage 373:149–166. doi: 10.1016/j.foreco.2016.04.043

Pretzsch H, Schütze G, Uhl E (2013) Resistance of European tree species to drought stress in mixed versus pure forests: Evidence of stress release by inter-specific facilitation. Plant Biol 15:483–495. doi: 10.1111/j.1438-8677.2012.00670.x

Pretzsch H, Block J, Dieler J, Gauer J, Göttlein A, Moshammer R, Schuck J, Weis W, Wunn U (2014) Nährstoffentzüge durch die Holz- und Biomassenutzung in Wäldern. Teil 1: Schätzfunktionen für Biomasse und Nährelemente und ihre Anwendung in Szenariorechnungen. Allgemeine Forst- Und Jagdzeitung 185(11–12):261–285. [Nutrient removal due to wood and biomass utilization in forests.]

Price DT, Zimmermann NE, van der Meer PJ, Lexer MJ, Leadley P, Jorritsma ITM, Schaber J, Clark DF, Lasch P, Mc Nulty S, WU J, Smith B (2001) Regeneration in Gap Models : Priority Issues for Studying Forest Responses To Climate Change. Clim Change 51:475–508. doi: 10.1023/A:1012579107129

Qian C, Yu J-Y, Chen G (2014) Decadal summer drought frequency in China: the increasing influence of the Atlantic Multi-decadal Oscillation. Environ Res Lett 9:124004. doi: 10.1088/1748-9326/9/12/124004

Radkau, J (1983) Holzverknappung und Krisenbewußtsein im 18. Jahrhundert. Geschichte und Gesellschaft 9:513-543. [Wood shortage and crisis awareness in the 18th century.]

Rais A (2015) Growth and wood quality of Douglas-fir. Doctoral Thesis. Technische Universität München, Munich, Germany. 122 pp.

Rais A, van de Kuilen JW, Pretzsch H (2014a) Growth reaction patterns of tree height, diameter, and volume of Douglas-fir (Pseudotsuga menziesii [Mirb.] Franco) under acute drought stress in Southern Germany. Eur J For Res 1043–1056. doi: 10.1007/s10342-014-0821-7

Rais A, Poschenrieder W, Pretzsch H, van de Kuilen J-WG (2014b) Influence of initial plant density on sawn timber properties for Douglas-fir (Pseudotsuga menziesii (Mirb.) Franco). Ann For Sci 71:617–626. doi: 10.1007/s13595-014-0362-8

Rammig A, Fahse L, Bugmann H, Bebi P (2006) Forest regeneration after disturbance: A modelling study for the Swiss Alps. For Ecol Manage 222:123–136. doi: 10.1016/j.foreco.2005.10.042

Rammig A, Fahse L (2009) Simulating forest succession after blowdown events: The crucial role of space for a realistic management. Ecol Modell 220(24):3555–3564. doi: 10.1016/j.ecolmodel.2009.06.040

Reineke LH (1933) Perfecting a stand-density index for even-aged forests. J. Agric. Res. 46(7):627–638.

Richards FJ (1959) A flexible growth function for empirical use. J. Exp. Botany, 10(2):290-300.

Röhling S, Dunger K, Kändler G, et al (2016) Comparison of calculation methods for estimating annual carbon stock change in German forests under forest management in the German greenhouse gas inventory. Carbon Balance Manag 11:12. doi: 10.1186/s13021-016-0053-x

Roessiger J, Ficko A, Clasen C, Griess VC, Knoke T (2016) Variability in growth of trees in uneven-aged stands displays the need for optimizing diversified harvest diameters. Eur J For Res 135(2): 283–295. doi:10.1007/s10342-015-0935-6.

Rötzer T (2013) Mixing Patterns of Tree Species and their Effects on Resource Allocation and Growth in Forest Stands. Nov Acta Leopoldina NF 254:239–254.

Rogers BM, Neilson RP, Drapek R, et al (2011) Impacts of climate change on fire regimes and carbon stocks of the U.S. Pacific Northwest. J Geophys Res 116:G03037. doi: 10.1029/2011JG001695

Rüegg D (1999) Erhebungen über die Verjüngung in Gebirgswäldern und den Einfluss von freilebenden Paarhufern als Grundlage für die forstliche und jagdliche Planung. PhD Thesis. ETH Zürich. Beih Schweiz Z Forstwes (88):182 pp. [Surverys of regeneration in mountain forests and influence of free-living unglulates as a basis for planning in forestry and hunting.]

Rüegg D, Nigg H (2003) Mehrstufige Verjüngungskontrollen und Grenzwerte für die Verbissintensität. Schweiz Z Forstwes 154:314–321. [Multi stage browsing surveys and limits of browsing intensity.]

Sallnäs O (1990) A matrix model of the Swedish forest. Studia Forestalia Suecica 183. 23pp. ISBN 91-576-4174-9

Schelhaas MJ, Eggers J, Lindner M, Nabuurs GJ, Päivinen R, Schuck A, Verkerk PJ, Werf DC v.d., Zudin S (2007) Model documentation for the European Forest Information Scenario model (EFISCEN 3.1.3). Alterra report 1559 and EFI technical report 26. Alterra and European Forest Institute, Wageningen and Joensuu, 118 pp.

Schütz JP, Ammann PL, Zingg A (2015) Optimising the yield of Douglas-fir with an appropriate thinning regime. Eur J For Res 134(3):469–480. doi: 10.1007/s10342-015-0865-3

Schumacher S, Bugmann H (2006) The relative importance of climatic effects, wildfires and management for future forest landscape dynamics in the Swiss Alps. Glob Chang Biol 12:1435–1450. doi: 10.1111/j.1365-2486.2006.01188.x

Schumacher S, Bugmann H, Mladenoff DJ (2004) Improving the formulation of tree growth and succession in a spatially explicit landscape model. Ecol Modell 180:175–194. doi: 10.1016/j.ecolmodel.2003.12.055

Schweiger J, Sterba H (1997) A model describing natural regeneration recruitment of Norway spruce (Picea abies (L.) Karst.) in Austria. In: Forest Ecology and Management. pp 107–118

Schwinning S, Weiner J (1998) Mechanisms determining the degree of size asymmetry in competition among plants. Oecologia 113:447–455.

Seidl R, Lexer MJ, Jager D, Honninger K (2005) Evaluating the accuracy and generality of a hybrid patch model. Tree Physiol 25:939–951. doi: 10.1093/treephys/25.7.939

Sheffield J, Wood EF (2008) Projected changes in drought occurrence under future global warming from multi-model, multi-scenario, IPCC AR4 simulations. Climate Dynamics 31.1:79–105.

Shinozaki K, Yoda K, Hozumi K, Kira T (1964) A quantitative analysis of plant form – the pipe model theory. ii. further evidence of the theory and its application in forest ecology. Jpn. J. Ecol. 14:133–139.

Siehoff S, Lennartz G, Heilburg IC, Roß-Nickoll M, Ratte HT, et al. (2011) Process-based modeling of grassland dynamics built on ecological indicator values for land use. Ecological Modelling 222:3854–3868. doi: 10.1016/j.ecolmodel.2011.10.003

Sitch S, Smith B, Prentice IC, et al (2003) Evaluation of ecosystem dynamics, plant geography and terrestrial carbon cycling in the LPJ dynamic global vegetation model. Glob Chang Biol 9:161–185. doi: 10.1046/j.1365-2486.2003.00569.x

Skog KE, Nicholson GA (1998) Carbon Cycling Through Wood Products: The Role of Wood and Paper Products in Carbon Sequestration. For Prod J 48(7–8):75–83.

Sloboda B (1976) Mathematische und stochastische Modelle zur Beschreibung der Statik und Dynamik von Bäumen und Beständen – insbesondere das bestandesspezifische Wachstum als stochastischer Prozess. Habil, Univ Freiburg. 310 pp. [Mathematical and stochastic models to describe the statics and dynamics of trees and stands – with particular focus on stand specific growth as a stochastic process.]

Sloboda B (1988) Representation and projection of diameter distribution in regarding change of rank in indicative experimental plots. In: Sloboda B (ed) BiometrischeModelle und Simulationstechniken bei Prozessen in forstlicher Forschung und Praxis. Schr Forstl Fak Univ G¨ottingen und der Niedersächs Forstl Versuchsanst 90:6–21.

Sterba H, Monserud RA (1997) Applicability of the forest stand growth simulator prognaus for the Austrian part of the Bohemian Massif. Ecol Modell 98:23–34. doi: 10.1016/S0304-3800(96)01934-5

Sutmöller J, Meesenburg H (2012) Auswirkungen forstlicher Maßnahmen auf den Wasserhaushalt. In: Nordwestdeutsche Forstliche Versuchsanstalt (ed) SILVAQUA–Auswirkungen forstlicher Bewirtschaftungsmaßnahmen auf den Zustand von Gewässern in bewaldeten Einzugsgebieten am Beispiel der Oker im Nordharz. Beiträge aus der Nordwestdeutschen Forstlichen Versuchsanstalt.
http://webdoc.sub.gwdg.de/univerlag/2013/NWFVA9_SILVAQUA.pdf [cited 08 June 2018] [Effects of silvicultural interventions on water balance in forested watersheds by the example of the Oker in Northern Harz. Contributions of the Northwest German Forest Research Institute.]

Suzuki T (1971) Forest transition as a stochastic process. Mitteilungen der Forstlichen Bundesversuchsanstalt (FBVA) Wien 91:69–86.

Suzuki T (1983) Übergang des Waldbestandes als ein stochastischer Prozess. Schriften aus der Forstlichen Fakultät der Universität Göttingen und der Niedersächsischen Forstlichen Versuchsanstalt 74:23–58. Sauerländer's Verlag, Frankfurt am Main, Germany. [Forest transition as a stochastic process.]

StMELF (2015) Anweisung für die Erstellung der Forstlichen Gutachten zur Situation der Waldverjüngung 2015. Bayerisches Staatsministerium für Ernährung, Landwirtschaft und Forsten, Munich, Germany. [Forestral survey on the situation of forest regeneration 2015. Bavarian State Ministry for Food, Agriculture and Forestry.]

Tahvonen O, Pukkala T, Laiho O, et al (2010) Optimal management of uneven-aged Norway spruce stands. For Ecol Manage 260:106–115. doi: 10.1016/j.foreco.2010.04.006

Tahvonen O, Pihlainen S, Niinimäki S (2013) On the economics of optimal timber production in boreal Scots pine stands. Can J For Res 43(8):719–730. doi: 10.1139/cjfr-2012-0494

Thünen-Institut (2017a) Landeswaldinventur Brandenburg (2013). https://bwi.info/inhalt1.aspx?Text=Landeswaldinventur+Brandenburg%2c+2013&

prRolle=public&prInv=LWIBB2013&prKapitel=0. [cited 29 January 2017]

Thünen-Institut (2017b) Der Datenspeicher Wald - das naturale Informationssystem der Landesförster! http://www.dsw2.de/dswueberblick.html. [cited 29 January 2017]

Thurm EA, Pretzsch H (2016) Improved productivity and modified tree morphology of mixed versus pure stands of European beech (Fagus sylvatica) and Douglas-fir (Pseudotsuga menziesii) with increasing precipitation and age. Ann For Sci 1–15. doi: 10.1007/s13595-016-0588-8

Thurnher C, Klopf M, Hasenauer H (2017) MOSES – A tree growth simulator for modelling stand response in Central Europe. Ecol Modell 352:58–76. Elsevier B.V. doi:10.1016/j.ecolmodel.2017.01.013

Tietjen B, Huth A (2006) Modelling dynamics of managed tropical rainforests—An aggregated approach. Ecol Modell 199:421–432. doi: 10.1016/j.ecolmodel.2005.11.045

Todoroki C, Rönnqvist M (2001) Log sawing optimisation directed by market demands. New Zeal J For 45:29–33.

Tremer N, Schmidt M, Hansen J (2005) Estimating the structure of natural regeneration based on inventory data. Allg Forst und Jagdzeitung 176:1–13.

Usher, MB (1979). Markovian approaches to ecological succession. J. Anim. Ecol. 48(2):413-426.

Usher MB (1981) Modelling ecological succession, with particular reference to Markovian models. In: Poissonet P, Romane F, Austin MA, et al. (eds) Vegetation dynamics in grasslans, healthlands and mediterranean ligneous formations: Symposium of the Working Groups for Succession research on permanent plots, and Data-processing in

phytosociology of the International Society for Vegetation Science, held at Montpellier, France, September 1980. Springer Netherlands, Dordrecht, pp 11–18.

Yospin GI, Bridgham SD, Neilson RP, et al (2015) A new model to simulate climate-change impacts on forest succession for local land management. Ecol Appl 25:226–242. doi: 10.1890/13-0906.1

Wagner FG, Gorman TM,Wu SY (2003) Assessment of intensive stress- wave scanning of Douglas-fir trees for predicting lumberMOE. For Prod J 53:36–39

Wang WJ, He HS, Spetich M a., et al (2013) A large-scale forest landscape model incorporating multi-scale processes and utilizing forest inventory data. Ecosphere 4:art106. doi: 10.1890/ES13-00040.1

Wehrli A, Schönenberger W, Brang P (2003) Long-term development of protection forests: combining models of forest dynamics with models of natural hazards. ETFRN news 38:20-25.

Wehrli A, Weisberg PJ, Schö0nenberger W, et al (2006) Improving the establishment submodel of a forest patch model to assess the long-term protective effect of mountain forests. Eur J For Res 126:131–145. doi: 10.1007/s10342-006-0142-6

Weiner J (1990) Asymmetric competition in plant populations. Trends Ecol Evol 5:360–364. doi: 10.1016/0169-5347(90)90095-U

Weis W, Huber C, Göttlein A (2001) Regeneration of mature Norway spruce stands: early effects of selective cutting and clear cutting on seepage water quality and soil fertility. The Scientific World 10:493-499. doi:10.1100/tsw.2001.327

Weiskittel AR, Maguire DA, Monserud RA, Johnson GP (2010) A hybrid model for intensively managed Douglas-fir plantations in the Pacific Northwest, USA. Eur J For Res 129:325–338. doi: 10.1007/s10342-009-0339-6

Wensel LC, Koehler JR (1985) A tree growth projection system for Northern California coniferous forests.

Whitehead D (1998). Regulation of stomatal conductance and transpiration in forest canopies. Tree Physiology 18(8_9):633–644.

Wichmann L (2001) Annual Variations in Competition Symmetry in Even-aged Sitka Spruce. Ann Bot 88:145–151. doi: 10.1006/anbo.2001.1445

Wichmann L (2002) Modelling the effects of competition between individual trees in forest stands. PhD Thesis. Unit of Forestry, Royal Veterinary University, Copenhagen, Denmark.

Wiedemann E (1942) Der gleichaltrige Fichten-Buchen-Mischbestand. Mitteilungen aus Forstwirtschaft und Forstwissenschaft 13(1). [The even-aged spruce and beech mixed forest stand.]

Wikström P, Edenius L, Elfving B, Eriksson LO, Lämås T, Sonesson J, Öhman K, Wallerman J, Waller C, Klintebäck F (2011) The Heureka Forestry Decision Support System: An Overview. Math Comput For Nat Sci 3:87–94.

Wood SN (2017) Generalized Additive Models: An Introduction with R (2nd edition), Chapman and Hall/CRC Press. Publisher: Taylor Francis Inc, United States 2017. 476 pp. ISBN 978-1-49-872833-1

Wykoff WR, Crookston NL, Stage AR (1982) User's Guide to the stand prognosis model. General Technical Report INT-133. Ogden, UT: US Forest Service.

Yasuda A, Yoshida T, Miya H, Harvey BD (2013) An alternative management regime of selection cutting for sustaining stand structure of mixed forests of northern Japan: a simulation study. J For Res 18:398–406. doi: 10.1007/s10310-012-0362-1

Zang C, Hartl-Meier C, Dittmar C, et al (2014) Patterns of drought tolerance in major European temperate forest trees: climatic drivers and levels of variability. Glob Chang Biol 20:3767–3779. doi: 10.1111/gcb.1263

Zhao-gang L, Feng-ri L (2003) The generalized Chapman-Richards function and applications to tree and stand growth. J For Res 14:19–26. doi: 10.1007/BF02856757

9 Appendix A: Contribution to further publications (not part of thesis)

9.1 Contribution to Rais et al. (2014b)

I reviewed the manuscript and I contributed to introduction and discussion.

9.2 Contribution to Hentschel et al. (2016)

I oversaw core boring and measuring of year ring data from cores and stem disks. I performed growth analysis. I contributed to the writing of the manuscript.

9.3 Contribution to Grote et al. (2016)

I prepared the outline of the review, wrote a first version of the introduction and collected most of the references.

9.4 Contribution to Rais et al. (preparing re-submission)

I was responsible for the development of the wood quality simulation model. I reviewed the study and contributed to its text.

9.5 Contribution to Schwaiger et al. (accepted)

I took part in designing the approach and in conceptualizing the study. I modified the physiological BALANCE model for extensive simulation within a cloud system. I reviewed the study and edited parts of it. In particular, I edited the discussion section.

9.6 Contribution to Nordström et al. (submitted)

I contributed to the discussion section within the scope of the ALTERFOR project.

9.7 Contribution to Toraño Caicoya et al. (2018)

I supported the algorithm development and the simulation.

9.8 References of Appendix A

Grote R, Gessler A, Hommel R, Poschenrieder W, Priesack E (2016) Importance of tree height and social position for drought-related stress on tree growth and mortality. Trees - Struct Funct. doi: 10.1007/s00468-016-1446-x

Hentschel R, Hommel R, Poschenrieder W, Grote R, Holst J, Biernath C, Gessler A, Priesack E (2016) Stomatal conductance and intrinsic water use efficiency in the drought year 2003: a case study of European beech. Trees 30:153–174. doi: 10.1007/s00468-015-1284-2

Nordström EM, Nieuwenhuis M, Başkent EZ, Biber P, Black K, Borges JG, Bugalho MN, Corradini G, Corrigan E, Eriksson LO, Felton A, Forsell N, Hengeveld G, Hoogstra-Klein M, Korosuo A, Lindbladh M, Lodin Lundholm A, Marto M, Masiero M, Mozgeris G, Pettenella D, Poschenrieder W, Sedmak R, Tucek J, Zoccatelli D (under major revision) Forest decision support systems for analysis of ecosystem services provisioning at landscape scale under global climate and market change scenarios. European Journal of Forest Research.

Rais A, Poschenrieder W, Pretzsch H, van de Kuilen J-WG (2014) Influence of initial plant density on sawn timber properties for Douglas-fir (Pseudotsuga menziesii (Mirb.) Franco). Ann For Sci 71:617–626. doi: 10.1007/s13595-014-0362-8

Rais A, Poschenrieder W, van de Kuilen J-W G, Pretzsch H (preparing re-submission) Quantifying volume and quality of Douglas-fir sawn timber, as determined by stand density, based on a distance-dependent individual tree model

Schwaiger F, Poschenrieder W, Rötzer T, Biber P, Pretzsch H (2018). Groundwater recharge algorithm for forest management models. Ecological Modelling.

Toraño Caicoya A, Biber P, Poschenrieder W, Schwaiger F, Pretzsch H (2018) Forestry projections for species diversity-oriented management: an example from Central Europe. Ecological Processes, 7(1):1-23. doi: 10.1186/s13717-018-0135-7

10 Appendix B: Journal data

10.1 Journals of publications within the thesis (Table B1)

Table B1. Journal data of the publications that were part of the thesis.

Name	Website
European Journal of Forest Research	www.springer.com
Silva Fennica	www.silvafennica.fi
Forests	www.mdpi.com

10.2 Journals of publications not part of the thesis (Table B2)

Table B2. Journal data of the publications that were not part of the thesis.

Name	Website
Annals of Forest Science	www.springer.com
Trees	www.springer.com

11 Appendix C: Original publications of the thesis

Eur J Forest Res (2013) 132:943–958
DOI 10.1007/s10342-013-0730-1

ORIGINAL PAPER

Extending a physiological forest growth model by an observation-based tree competition module improves spatial representation of diameter growth

Werner Poschenrieder · Rüdiger Grote · Hans Pretzsch

Received: 30 October 2012 / Revised: 7 June 2013 / Accepted: 9 August 2013 / Published online: 22 August 2013

Abstract One of the pivotal objectives in forestry research is to estimate the response of silvicultural target variables to climate change scenarios at high temporal resolution in order to consider within-year feedbacks between growth and environmental conditions. To meet this challenge, models are needed which support and complement the widely used observation-based decision systems in forest management and consulting. Physiological models in particular provide the fundamental prerequisites to reflect the impact of various simultaneously changing environmental conditions. However, a physiological representation at the individual tree level is computationally very expensive and sensitive to uncertain initializations. We thus propose an approach that combines a modern representative of the physiological cohort model type, MoBiLE-PSIM, with the individual tree competition concept of a distance-dependent empirical growth simulator (SILVA). The resulting hybrid provides a key feature for the consideration of forest management in long-term simulations at high computational efficiency. The extended model was evaluated with growth-diameter distributions obtained from core-boring at two beech (*Fagus sylvatica L.*) forest sites in south-west Germany that differ in exposure and soil conditions. The mean bias of annual stand-scale growth from 2001 to 2007 decreased from −0.59 to −0.41 mm at one evaluation plot and from −0.55 to −0.24 mm at the other when the competition module was coupled in. Inclusion of the SILVA-based individual tree module into MoBiLE-PSIM improved the size-dependent representation of competition and growth on five-year and even annual timescale. This was particularly the case where the spatial distribution of dominant trees was clustered.

Keywords Cohort model · Physiological model · Individual tree growth · European beech · MoBiLE · SILVA

Communicated by A. Weiskittel.

Electronic supplementary material The online version of this article (doi:10.1007/s10342-013-0730-1) contains supplementary material, which is available to authorized users.

W. Poschenrieder · H. Pretzsch
Chair of Forest Yield Science, Technische Universität München, Hans-Carl-von-Carlowitz-Platz 2, 85354 Freising, Germany

R. Grote (✉)
Institute for Meteorology and Climate Research (IMK-IFU), Karlsruhe Institute of Technology (KIT), Kreuzeckbahnstr. 19, 82467 Garmisch-Partenkirchen, Germany
e-mail: Ruediger.Grote@kit.edu

Introduction

Simulation models play an increasingly important role as supporting instruments for the decision maker in his task to provide multifunctional sustainability (Muys et al. 2010). The most common type of model in practice is the observation-based individual tree management model (Pretzsch et al. 2008). It is based on the long-term monitoring of experimental sites and provides for a reliable estimation of future stock, growth, yield or even structure and diversity under the environmental conditions of observation. Real forest systems of today are exposed to climatic change (Saxe et al. 2002; Boisvenue and Running 2006) in combination with an increase in soil nitrogen and atmospheric CO_2 accompanied by prevalent atmospheric intoxication (Ollinger et al. 2002) at least in the strongly industrialized part of the world. Additionally, the inter-annual and intra-

annual variability of weather will be different in future. As a further source of uncertainty, all environmental factors are interacting via plant internal processes (Löw et al. 2006; Matyssek et al. 2006), and their synergetic impact is strongly influenced by the changing inter-annual variation of weather (Kubiske et al. 2006). Hence, the observed relation between integrated climate variables and growth (Porte' and Bartelink 2002) is likely to change. Thus, there is a demand for models that reflect the influence of various climatic driving forces and chemical boundary conditions in yet unobserved combination.

As a basic prerequisite, they must take into account all physiological processes which are individually affected by environmental impacts and all relevant positive and negative feedbacks among them (Landsberg 2003). On a higher level of causality, this is also true for long-term effects of structural changes in the vicinity of a tree, e.g. from an increase in light supply to a decrease in leaf area index (e.g. Portsmuth and Niinemets 2007). Structure and structural development must also be considered on the stand level (e.g. Langvall and Löfvenius 2002) to estimate how the impact of long-term changes might be mitigated or best capitalized (Goreaud et al. 2006). In individual tree, physiological models such as BALANCE (Grote and Pretzsch 2002; Rötzer et al. 2005) modellers have merged available theory about the underlying processes of growth into mechanistic aggregates of soil and vegetation modules that take into account individual tree position, dimension and vertical crown stratification. In contrast to the typical process model which is mechanistic and detailed for processes that are relevant to a selected focus (as reviewed by Mäkelä et al. 2000), such as carbon fixation, the ecopyhsiological individual tree model is designed to estimate the distribution of tree dimensional growth with a very high generality. It provides a high spatial differentiation of processes and runs in subdaily to daily time steps, and it is very sensitive to uncertainties in individual initialization (Fontes et al. 2010), costly in parameterization and comparatively slow. To reduce complexity while preserving a high degree of mechanistic description, Grote et al. (2011b) have represented stand structure in MoBiLE-PSIM as an ensemble of spatially interacting single species cohorts, where each cohort consists of trees that are identical in dimension and are ordered on a regular grid. Presuming this approximation, competition may be covered by exclusively simulating one representative tree per cohort, and computational efficiency is increased by an order of magnitude.

One central criterion of individual tree model evaluation is to meet the interannual variability of the growth to size distribution: following an increasingly well-confirmed theory (Schwinning and Weiner 1998; Weiner 1990; Wichmann 2001, 2002; Pretzsch and Biber 2010; Pretzsch and Dieler 2011), a concentration of growth on either larger or smaller trees reflects the coupling of aboveground and belowground competition. If belowground resource supply is not limiting, tree dominance is characterized by shading (asymmetric competition) and the regression line between diameter growth and diameter has a steep slope and an intersect with the DBH axis at the right side of the origin. With decreasing soil resource availability, the slope inclines around some point near the centre of the distribution towards the horizontal. A cohort model which accounts for size-specific resource limitations could principally reflect this response, but the relationship between growth and diameter would only be represented by one single point per cohort. Hence, the distributional width has to be recreated with a semi-empirical individual tree algorithm, if the simplicity which is gained by the cohort approach is to be preserved.

Within the scope of this article, we present the extension of the ecophysiological cohort model MoBiLE-PSIM (short MoBiLE) by an individual tree growth interpolation that is based on the semi-empirical competition algorithm used in the growth simulator SILVA (Pretzsch et al. 2002) but is set up in order to satisfy the simulated cohort volume increase. Both MoBiLE and the interpolation plug-in are coupled in both directions on the annual timescale: the controlling variable provided by MoBilE is the cohort volume growth, and the ones returned back are the new dimensions of the cohort representative tree. Our method is innovative as compared to earlier approaches of model coupling (Baldwin et al. 2001; Milner et al. 2003; Henning and Burk 2004) because it combines many of their different benefits, (a) extends them by most recent physiological concepts, (b) implies a bidirectional control between individual growth and stand development on a timescale of one year, which is also sensitive to management actions and (c) uses a mass conservative algorithm to calculate individual tree dimensional growth from cohort total stem biomass increase: the approach is related to the work of Weiskittel et al. (2010), Kirschbaum (1999) and Korol et al. (1996) in that it aims to scale the biomass increment simulated by a stand-level physiological model down to the individual tree level. However, it is different in that it uses an individual tree growth prediction by a distance-dependent empirical model as the weighting criterion.

Within the context of European forestry, one important application of our hybrid model will be sensitivity assessment of European beech (*Fagus sylvatica L.*) to future environmental conditions: beech is supposed to be very competitive under a wide range of conditions (Bolte et al. 2007, 2010) but has been replaced by spruce and other coniferous species that are thought to be less adapted to expected environmental conditions in many regions (Koca et al. 2006; Bolte et al. 2010). As comprehensively

explained by Brumme and Khanna (2009), its increased cultivation in central Europe is heavily advocated to preserve and enhance biodiversity in a changing climate and to provide long-term sustainability of forests and the productivity of forest stands. In this situation, some concern has been expressed about the relatively small knowledge base about the response of European beech to drought conditions (Jump et al. 2006; Geßler et al. 2007; Friedrichs et al. 2009). Our model evaluation takes advantage of extensive data from two areas in south-west Germany that have repeatedly been investigated for forestry and ecophysiological purposes (e.g. Geßler et al. 2001; Holst et al. 2010). They are situated within a region of shallow soils on porous limestone where growth depressions due to drought have repeatedly affected stand development in the past (Maaten 2011).

Materials and methods

Site description

The experimental sites are located in south-western Germany near Tuttlingen, about 100 km east of the city of Freiburg (47°59′N, 8°45′E) at about 800 m a.s.l. They have repeatedly been described elsewhere in more detail (e.g. Geßler et al. 2001; Mayer et al. 2002). One slope is facing towards SW direction (defined as SW slope), while the aspect of the second slope is NE (NE slope). The horizontal distance between both sites (control plots) is about 800 m. Both hillsides are covered with 80–90-year-old single-layer, beech-dominated (>90 %) forest stands. A summary of general site properties and stand characteristics is presented in Table 1, and the situation is shown in Fig. 1 (taken from Holst et al. 2004a, b, 2010; Paul 2003; photosynthetically active radiation PAR from Mayer et al. 2002).

According to the site description by Geßler et al. (2005), soil profiles are characterized as Rendzic Leptosols derived from limestone (Weißjura beta and gamma series). On both slopes, the soil profiles are shallow, averaging less than 50 cm depth of topsoil before becoming dominated by parent rock interspersed with pockets of organic matter and mineral soil. The soil profile on the SW slope is particularly rocky, containing more than 40 % (volumetric basis) rocks and stones (>63 mm diameter) in the top 20 cm of the soil, rising to 80 % below 50 cm depth. The soil on the NE slope contains 15 % rocks and stones in the uppermost 20 cm of the soil and about 30 % below 50 cm depth.

Two control plots NE-C (68 m × 77 m at horizontal projection) and SW-C (71 m × 70 m) were selected for evaluation, which had not been thinned after setup of the experimental site in early 1999. Mean stand properties based on a forest inventory in Winter 1998/99 are given in Table 2 (height and diameter have been taken from Hauser (2003), and the number of trees per ha at horizontal projection has been calculated based on the tree lists).

Although the stand at site NE is about 10 years younger, its mean basal area stem is higher and has a larger diameter. Even if NE-C has a wider range of variation in DBH than SW-C, both plots have a bell-shaped DBH distribution that indicates an even-aged structure. Number of trees by DBH (diameter at breast height) interval and height over

Table 1 Experimental site properties (numbers in italics are estimates based on soil type)

Site property	NE			SW		
Elevation (m a.s.l.)	820			760		
Slope (degree)	23			25		
Annual mean temperature, 2001–2007 (°C)	7.4			7.5		
Annual average precipitation, 2001–2007 (mm)	906			1,064		
PAR at 1.3-fold stand height in 2001 (μmol m^{-2} s^{-1})	243			245		
Soil type	Silty clay loam			Silty clay loam		
Humus type	Mull			Mull		
Litter height (mm)	90			80		
Specific soil parameters in depth of (cm):	**10**	**30**	**50**	**10**	**30**	**50**
Depth of the soil profile (mm)	190	160	200	190	160	100
Stone fraction (0–1)	0.21	0.20	0.30	0.52	0.35	0.35
Soil bulk density (kg dm^{-3})	0.74	*1.73*	*1.85*	0.59	*1.73*	*1.85*
Clay content (0–1)	*0.45*	*0.49*	*0.49*	*0.46*	*0.49*	*0.49*
Water holding capacity (mm m^{-1})	500	500	500	500	500	500
Water content at wilting point (mm m^{-1})	270	75	270	170	75	270

The bold values indicate on the one hand the information about the soil depth investigated, on the other hand they also representthe heading for the depth-specific information in the following rows

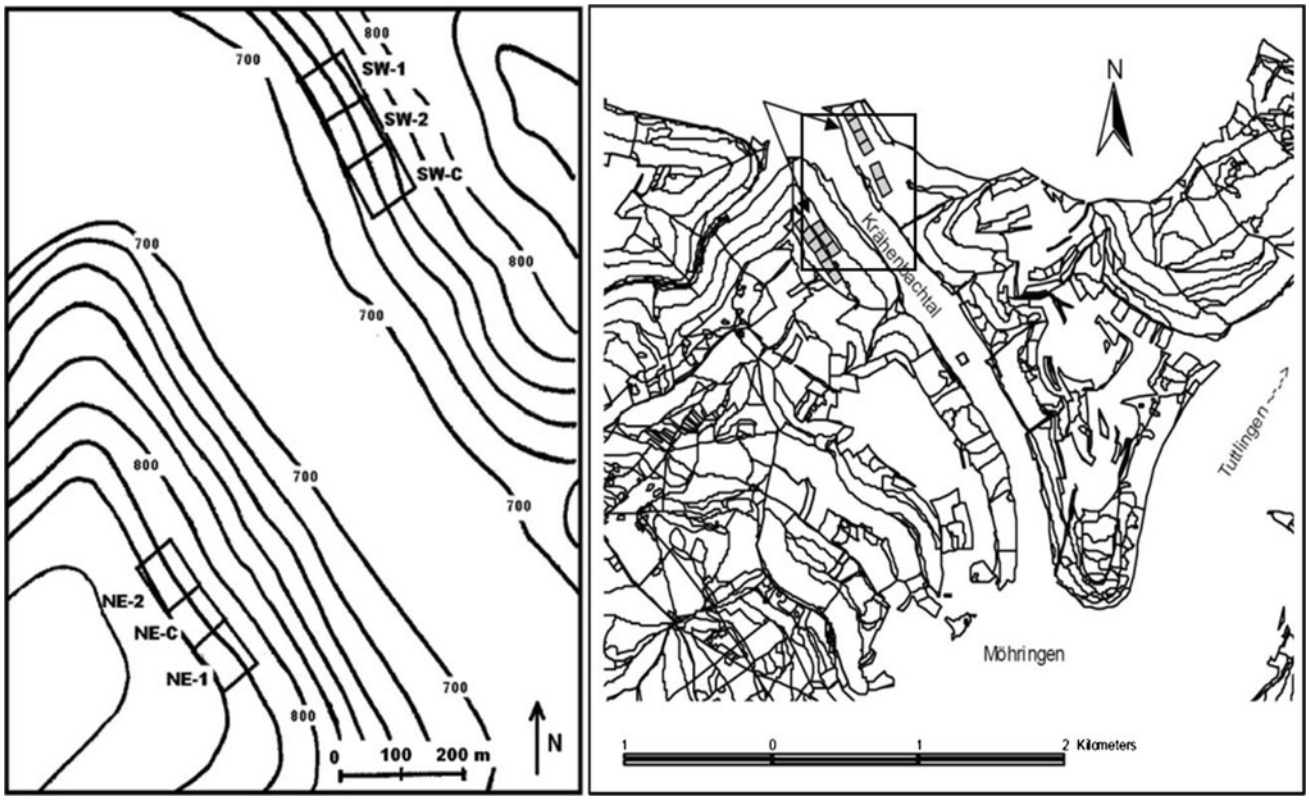

Fig. 1 Position of the two experimental sites and three trials at each location. Only control trials (SW-C and NE-C) are used in this investigation, and other trials represent different thinning intensities. (Figures reproduced from Holst et al. 2004a; Paul 2003)

Table 2 Growth- and yield-related key properties by plot

Plot property	NE-C	SW-C
Mean basal area stem		
Height (m)	26.5	21.1
Diameter at 1.3 m (cm)	25.6	21.5
Diameter 95 % range of variation (cm)	10–39	11–32
Number of trees per ha	516	658

DBH as determined from a stand height curve by the growth simulator SILVA (Pretzsch et al. 2002) are shown in Fig. 2a, b. Figure 3 is a map of stem base position and DBH: at NE-C, it has a rather irregular pattern, whereas at SW-C it shows a clear concentration of larger trees at the centre of the downhill side. The species distribution within each of the two plots included 94 % beech and minor contribution of other hardwood. All trees were thus considered as beech in the simulations and following analysis.

Measurements

Individual tree data within our study were DBH and position that had been taken in winter 1998/99 (Hauser 2003) and borer probes taken in early spring 2011. Based on the age-corrected DBH distribution of 1999 and on the observed frequency of DBH within intervals of 10 cm, a stratified sample of each plot was taken in March 2011 ($n = 27$ at NE-C, $n = 26$ at SW-C, Fig. 2c). From each sample tree, two stemwood cores were taken at breast height with an angular distance of 90° from each other, and one of the cores was taken on the uphill side. At NE-C, both cores of 23 trees were used for evaluation while in the remaining four cases, only one core per tree could be used due to damage of the second probe. At SW-C, all probes were suitable for analyses. Tree height, height to crown base and crown diameter were computed by the growth simulator SILVA (Pretzsch et al. 2002), based on the individual tree lists and the mean basal area stem height.

Model description

The physiological part of the hybrid model is represented by the modelling framework MoBiLE (Modular Biosphere simuLation Environment; Grote et al. 2009; Holst et al. 2010) in a configuration that uses the physiologically based vegetation module PSIM (Physiological SImulation Model, Grote 2007; Grote et al. 2009) and a newly implemented version of the biogeochemical module DNDC (DeNitrification–DeComposition, Li et al. 1992) along with modules that describe micro-environmental conditions within the

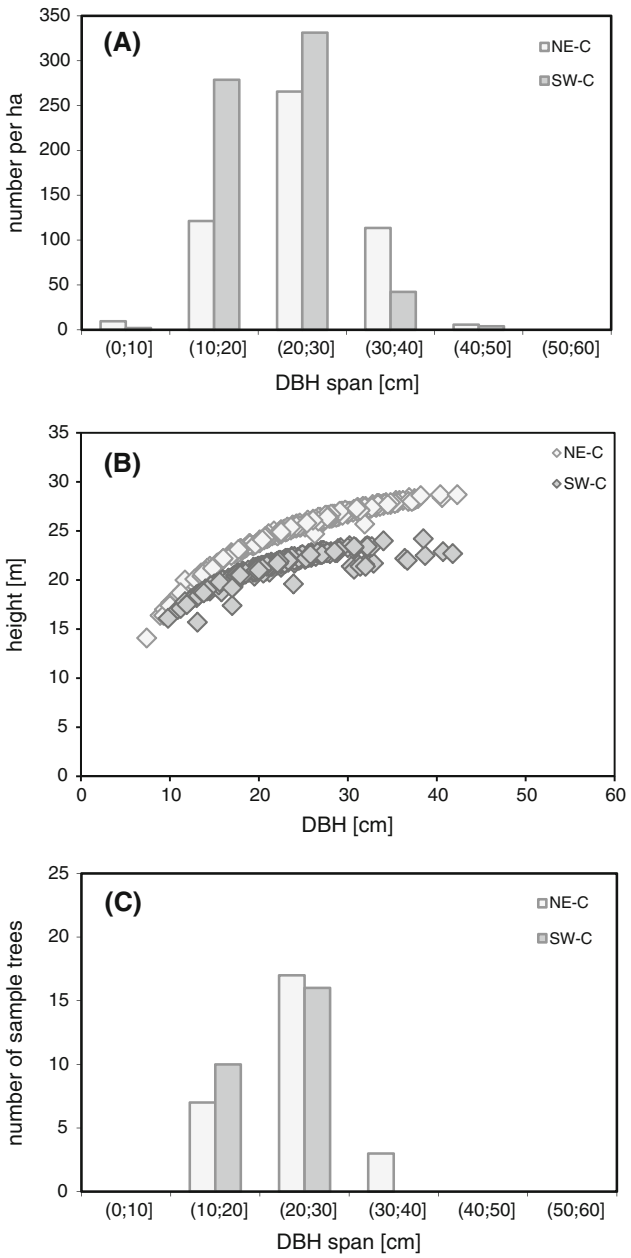

Fig. 2 Stand structure indicated as **a** number of trees per ha by DBH interval and **b** height by DBH, as compared to **c** frequency distribution by coring subsample, given as the number of trees used for subsampling

biosphere (e.g. light distribution, soil temperature development and water availability). It is represented by the left part of Fig. 4 and commonly named MoBiLE-PSIM (short MoBiLE).

MoBiLE runs in a subdaily (hourly) time step with respect to the photosynthetic equations and in a daily time step for other processes. Photosynthesis is computed according to Farquhar et al. (1980) with modifications suggested by Ball et al. (1987). The PSIM module simulates uptake, loss and allocation of C and N within the plant as determined by sink strength (Grote 1998; Grote et al. 2011a) that is based on allometric rules. It runs on a daily time step. PSIM considers the ecosystem to be consisting of 'vegetation types' or 'cohorts' of distinct species, vertical dimension and ground coverage. Each cohort is represented by its average tree characterized by diameter, height, height at crown base and stem number: a separate vegetation structure module converts the carbon gain of the cohort given by PSIM to the corresponding total stem volume increase at annual time step. It then uses a taper function to convert the average stem volume increase to the dimension growth of the representative tree as described in Grote et al. (2011a, b). The new representative tree dimensions define the new structural features that influence leaf distribution and thus radiation regime and competition within the canopy in the following year.

If a detailed tree list is used as input, the average cohort tree at simulation start is calculated from this list, using tree height and crown base height as selection criteria for a cohort. All trees within a cohort are thus considered equal and are assumed to be arranged in a homogeneous pattern that also might allow for a certain amount of gaps, provided the ground coverage—as calculated from diameter and crown diameter ratio—is below 100 % (see Grote et al. 2011a for further information). Stem volume and consequent biomasses are calculated from species-specific taper functions and allometric relationships.

PSIM differentiates canopy and soil into a number of vertical layers with a thickness of about 50 cm aboveground and—depending on initialization—10–50 cm belowground. The environmental conditions experienced by a cohort in MoBiLE are defined by the resources available within the above- and belowground layers that it occupies according to its height, height at crown base and rooting depth. Foliage area and fine root biomass are explicitly distributed in vertical direction at the spatial resolution of the layering. Several cohorts may occupy the same layer. Hence, a tree cohort affects its own environment and that of other cohorts by shading and uptake (nitrogen, water) on the level of canopy and soil layers. On the stand level, it may thus exert aboveground competition on other cohorts that concentrate their foliage in canopy layers further down. Belowground, the competition strength of a cohort depends on the presence of fine roots in a particular soil layer and the species-specific uptake capacity. As maximum rooting depth for mature beech trees is considered to be approximately 3 m in the model, all cohorts are assumed to have access to the whole soil profile. Despite the differentiation into cohorts and the consideration of a certain gap fraction, all processes are simulated as 'one-dimensional', and thus, the emerging forest is still horizontally homogeneous—implicitly assuming a uniform distribution of trees within a cohort.

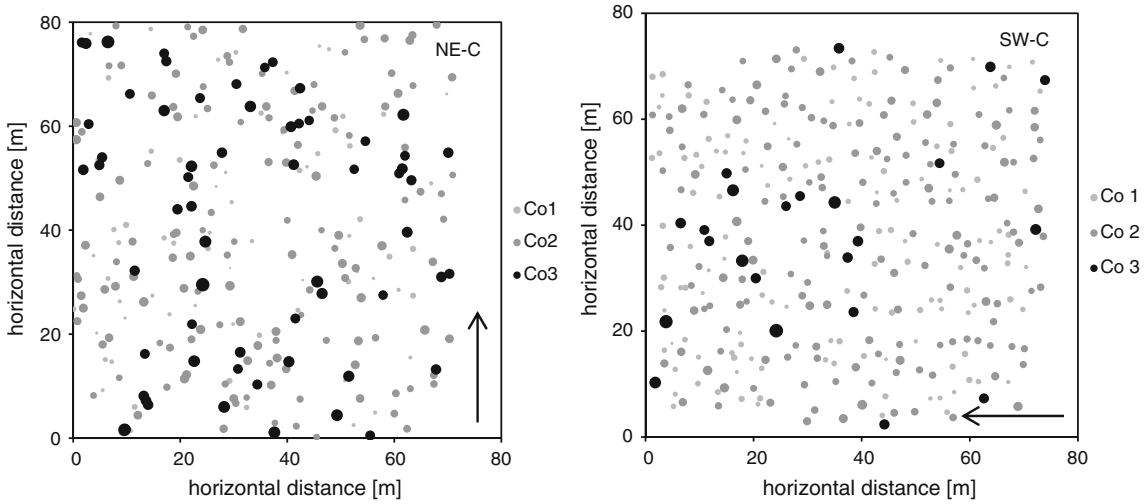

Fig. 3 Stem base positions at site NE-C and SW-C, differentiated by diameter interval (in cm, end diameter excluded) 0–20, 20–30, 30–∞, designated by Co1, Co2 and Co3, respectively; arrows designate the direct down-slope direction

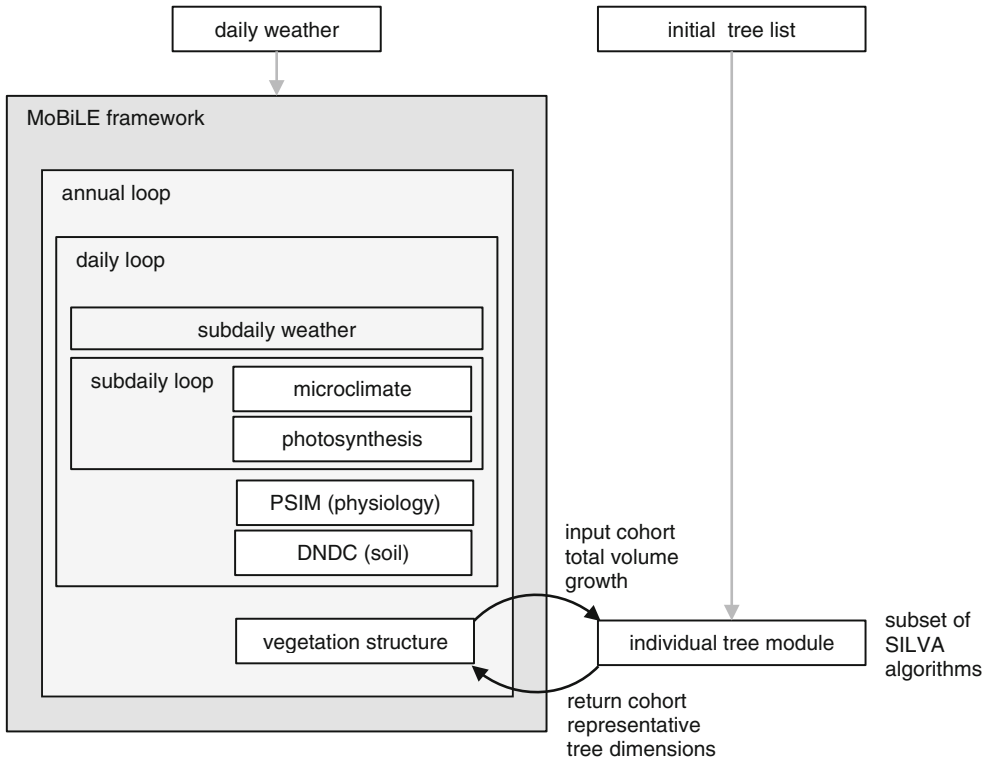

Fig. 4 Integration of the individual tree module into the MoBiLE framework as configured and extended within the scope of this study; the MoBiLE framework part is distinguished from the modules by a grey background

MoBiLE uses a ground basal area weighting to aggregate the cohort representative tree dimensions to the stand level.

The ability of the model to simulate the micro-meteorological conditions and the water balance at the selected sites has been evaluated in an earlier publication (Holst et al. 2010). Species-specific parameters to describe physiological processes, i.e. carbon exchange and biomass allocation, have been determined from literature sources and were evaluated using beech trials at other investigation sites (Grote et al. 2011a). The setup of a cohort simulation and an application for a mixed stand dominated by Scots pine have been presented in Grote et al. (2011b).

To complement MoBiLE with a fast individual tree component, an additional module was embedded into the framework that is based on potential dimension growth and competition equations taken from the individual tree model

SILVA (Pretzsch et al. 2002). SILVA describes stand development at a level of detail of individual trees and their aboveground dimensions. The model has no physiological or micrometeorological theory of anabolism, catabolism or transport. SILVA models potential growth of an individual tree using the Chapman–Richards equation for height and diameter growth (Richards 1959). The prevailing process within a cohort tree's actual growth is competition, as expressed in the following highly simplified form:

$$g = \mathcal{P} \cdot c \tag{1}$$

where g is actual growth and $\mathcal{P}$ is the site-specific potential growth for both height and diameter increment. Variable c is the competition-related reduction term that is different for height and diameter growth. It depends on a tree's dimension in relation to the dimension and position of each competing neighbour tree. Hence, total stand density determines each individual tree's growth indirectly via the local density, arrangement and geometry of its competing neighbours: a competitor takes influence only if its tree top reaches into a solid angle (about 60°) that opens towards the sky with vertex inside the central tree's crown and position coaxial to the crown vertical axis. The exact value of the virtual cone's angle as well as its position is species specific. If a neighbour reaches into the cone, it exerts competition on the tree depending on the angle between crown base and neighbour tree top, the crown cross-sectional areas and a species-specific light transmission coefficient of the competitor. Furthermore, the resulting competition factor depends on the horizontal distance between the central tree's stem and the centre of gravity of competition. Plot edge effects are corrected by linear expansion based on earlier work of Martin et al. (1977).

Potential growth parameters in SILVA are based on the long-term observation of a high number of plots ranging from northern Germany to Switzerland. They reflect growth as dependent on stand-scale soil and climate conditions. The competition factor equations for height and diameter growth use parameters which are exclusively dependent on species (for more details see Pretzsch et al. 2002). SILVA uses a time step of five years, because its growth curves do not represent the interannual variability of weather, and a higher temporal resolution would not add quality to the simulation result: the curves of potential growth are sigmoid (height) or unimodal (diameter). Potential height at time t is defined as:

$$h_t = A\left(1 - e^{-kt}\right)^p \tag{2}$$

As SILVA is kept independent of stand age, t is computed from height at the beginning of a simulation interval via the inverse of Eq. 2. In the original model implementation, A, k and p are internal variables that are not given as parameters but calculated from site conditions and species-specific unimodal dose–response functions.

For potential diameter growth, the independent variable is diameter d itself that represents biological age. Diameter increase (δ_d) is

$$\delta_d = \alpha\kappa\varphi\left(1 - e^{-\kappa d}\right)^{\varphi} e^{-\kappa d} \tag{3}$$

where α, κ and φ are of the same mathematical meaning as A, k and p in Eq. 2 but of distinct value and species-specific. Furthermore to get the actual value of potential growth, the basal area growth that results from Eq. 3 is modified by a climate and nutrient-dependent factor that is named *ESto* in Pretzsch et al. (2002).

MoBiLE was modified in such way that the vegetation structure module delegates the cohort's representative tree dimension growth to the individual tree module (Fig. 4): the individual tree component offers an interface that takes the cohort volume both at start and end of year and returns the resulting new cohort representative tree dimensions. Therefore, the individual tree component uses an intermediate step that scales down the annual total volume growth of a cohort to an individual volume and dimensional increase in each individual tree (Fig. 5). An individual tree list has to be provided to the individual tree

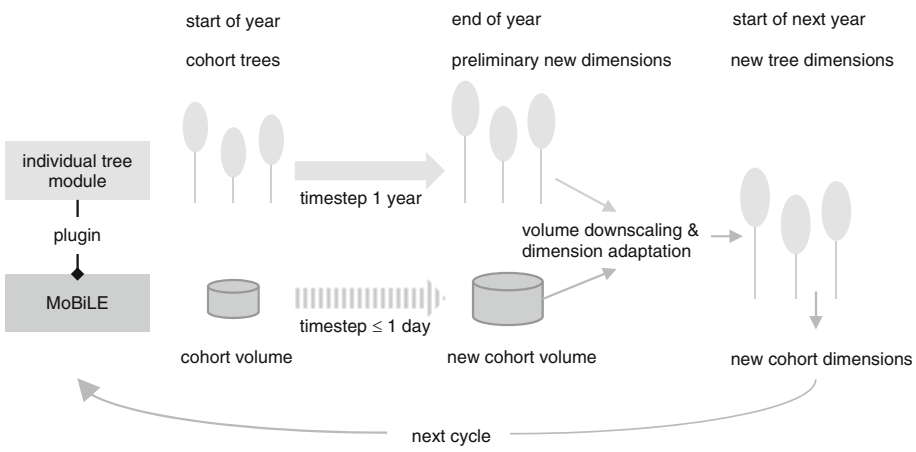

Fig. 5 Interaction of MoBiLE and the individual tree module simplified

module at simulation start to define starting dimensions for each tree in the stand. The key step of the downscaling algorithm is to compute height and diameter growth of each individual tree at annual time step based on Eqs. 1, 2 and 3 and correct it by the factor shown in Eq. 4 (details are given in the online supplement).

$$f = \frac{\sqrt[3]{\omega} - 1}{\sqrt[3]{\omega^*} - 1} \quad \text{where} \quad \omega = \frac{v_1}{v_0} \quad \text{and} \quad \omega^* = \frac{v_1^*}{v_0^*} \qquad (4)$$

Variables v_0^* and v_1^* are individual tree volumes at the start and end of year, respectively: they are calculated from the timber-wood taper function of SILVA. The volume at the end of year v_1^* results from dimension growth based on Eqs. 1, 2 and 3. Tree volumes v_0 and v_1 are calculated from the cohort volumes at start and end of year that are passed to the module and the share respectively of v_0^* and v_1^* within the cohort. Intuitively spoken, the expression approximately is the ratio of a dimension change that is in accordance with the physiological part of the hybrid model and one that corresponds to the SILVA growth curves.

To explain the whole concept in a nutshell, the sole task of the physiological part is to calculate the annual carbon gain and volume growth of the cohort representative tree but not the change of its dimensions. The key role of the individual tree module on the other hand is to provide the relative growth of height and diameter on a per tree basis via potential dimensional growth and competition. Based on the absolute cohort volume growth given by the physiological main model, the module uses the allometry to calculate the absolute height and diameter growth of each individual tree and the resulting new dimensions of the cohort representative. Both components are coupled within a feedback loop on annual timescale that keeps cohort layering and growth processes on one hand and individual tree stem- and crown dimensions on the other hand consistent with each other and prevents the module -states from drifting apart.

Simulation setup and parameters

Simulation runs with MoBiLE were conducted with the individual tree version (named MoBilE-ST in the following) and with the original version (MoBiLE alone). Tree initial diameters were available from measurements which had been taken in winter 1998/99 (Hauser 2003) and reflect the situation immediately after a thinning that had been applied before the definition of control plots. Initial height and crown dimensions were computed by SILVA. Three cohorts that were based on the diameter intervals (in cm, end diameter excluded) 0–20, 20–30, 30–∞ were defined on each site. As MoBiLE is generally designed to require sparse configuration, the individual tree module does not calculate the growth curve parameters A, k and p in Eq. 2 and the basal area growth modifier *Esto* via dose–response functions and additional site description. Instead, A, k, p and *Esto* are directly given: within the scope of this study, their values refer to an average growth potential for southern Germany, following the idea, that the sole responsibility of the individual tree module is to control the relation of height to diameter growth and that it hence is sensitive to stand structure but robust with respect to site. A synopsis of the important parameters is given in Table 3.

Weather data had been collected from 2001 to 2007 on a tower of approximately 1.5 times stand height within each of the sites and have been published in Holst et al. (2004a, 2010) as well as in Holst and Mayer (2005). Detailed descriptions of the instrumentation can be found in Mayer et al. (2002). The time interval of simulation was started from 2001 to end of 2007. A pre-run of 3 years preceded each simulation run to provide a plausible internal state of variables that cannot directly be initialized such as pool-specific nitrogen concentrations within the soil: they result from boundary conditions such as the total nitrogen concentration per layer and usually stabilize to realistic values within three simulated years. The stabilizing run was based on repetition of the weather of 2002.

Five-year plot level results of MoBilE-ST and MoBiLE alone at NE-C and SW-C (2001–2005) were also compared with the ones of the stand-alone SILVA model. The observation-based model was initialized with the same tree lists and parameterized with the average of the same weather records.

The diameter growth to diameter distribution on the individual tree level as simulated by MoBiLE-ST was compared to the one that resulted from coring differentiated by plot, either as total growth of 2001–2005 or in selected years. As the tree diameters of the sample in the years of comparison were not directly measured, they were reconstructed from the tree ring analysis. Regressions between growth and DBH were done with the ordinary least squares algorithm (OLS), and prediction intervals were calculated from the residual variance.

Table 3 Growth curve parameters

Parameter	Value	Equation
A	54	Height growth (Chapman–Richards, Eq. 2): $h_t = A\left(1 - e^{-kt}\right)^p$
k	0.011	
p	1.11	
α	1,327.8481	Diameter growth (Chapman–Richards 1st derivative, Eq. 3): $\delta_d = \alpha\kappa\varphi\left(1 - e^{-\kappa d}\right)^{\varphi} e^{-\kappa d}$
κ	0.016363272	
φ	0.775173759	

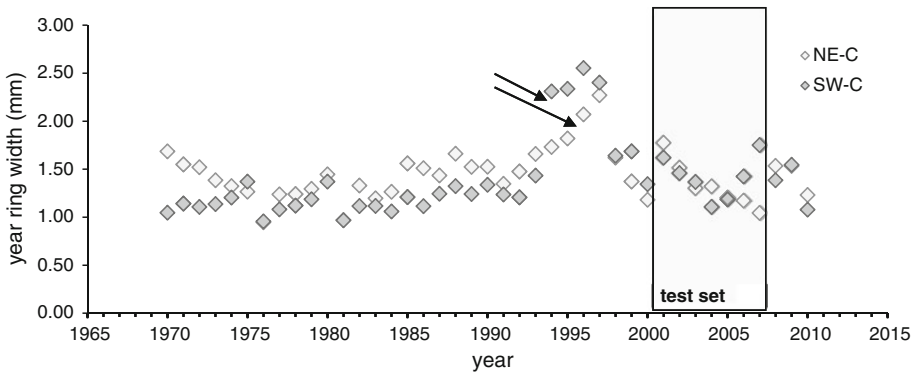

Fig. 6 General sample data properties: Mean year ring width by coring subsample of plot NE-C and plot SW-C. Ring widths directly after thinning are indicated by arrows. The measurements between 2001 and 2007 (test-set) served for further data analyses. Confidence interval of ring width is about ±0.25 mm

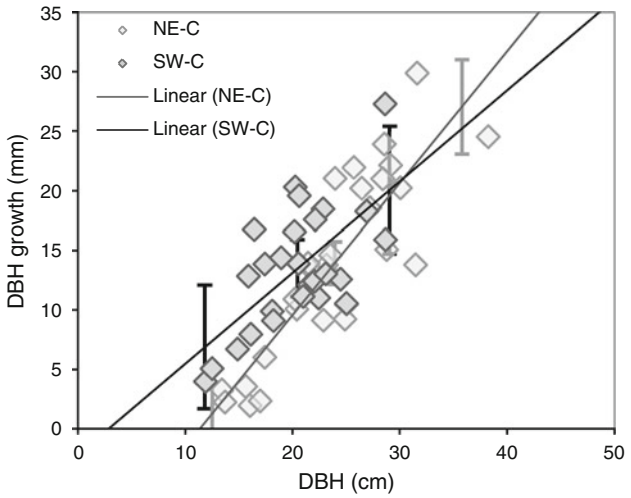

Fig. 7 General sample data properties: Diameter growth from 2001 to 2005 for each sample tree differentiated by site; the confidence band of the regression line is indicated by *error bars* ($R^2 = 0.74$ at NE-C, $R^2 = 0.43$ at SW-C)

Results

Figures 6 and 7 show general properties of the sample data to give an impression of the plausibility and reliability of the dataset that was used for evaluation. In Fig. 6, the mean year ring width overtime from coring differentiated into plot NE-C and SW-C is presented. It shows a sharp decline in 1976, which was a year of severe drought. Growth peaks starting in 1994 at SW-C and 1996 at NE-C coincide with the last thinning before experimental site setup in 1999 (Hauser 2003). Within the time period of the simulation from 2001 to 2007, the year ring width displays a growth variation also typical for the period 1970–1994. From 2001 to 2005, NE-C and SW-C show a similar growth response with no particular incident in the dry year 2003. Figure 7 presents the distribution of DBH growth from 2001 to 2005 over DBH at both plots. It is equivalent to growth as dependent on tree size class and is one important evaluation criterion of the hybrid approach. The confidence band of diameter growth that is predicted by regression is indicated by error bars at mean DBH, at the estimated 2.5 %—quantile limit, and at 97.5 %—quantile limit of DBH. The data spread shows a usual variation of residuals at the individual tree level with $R^2 = 0.74$ at NE-C and $R^2 = 0.43$ at SW-C.

Figure 8 shows variability of tree growth as well as mean basal area stem growth of the coring subsample as compared to simulation results from MoBiLE without single-tree interpolation module (MoBiLE), MoBiLE with interpolation module (MoBiLE-ST) and SILVA from 2001 to 2005 differentiated by NE-C and SW-C. Error bars indicate confidence intervals of variability and growth here. MoBiLE alone underestimates measured growth in that five-year period from 2001 to 2005. It underestimates stand-scale variability at NE-C and overestimates it at SW-C. MoBiLE-ST shows slight improvement with respect to mean basal area stem growth at NE-C and more realistic variability, which is somewhat underestimated at the site. At SW-C, the results are very close to measurement when the interpolation module is used. SILVA is close to the coring sample at NE-C, but at SW-C it overestimates local five-year growth and variability.

On the annual timescale (Fig. 9), the improvement of stand-level growth 2001–2007 that comes along with the use of the individual tree module is moderate at plot NE-C as well but remarkable at site SW-C. SILVA which is purely climate driven yields no additional information at that timescale. At plot NE-C, the deviation of mean over the 7 year timescale of 2001–2007 that is given as mean bias in mm was −0.59 with MoBiLE alone and −0.41 with MoBiLE-ST. At SW-C, the deviation strongly changed from −0.55 to −0.24 when MoBiLE-ST was used (confidence interval about ±0.8). As an indicator of quality on the annual timescale, the mean absolute bias decreased from 0.26 to 0.21 at NE-C and from 0.23 to 0.13 at SW-C when MoBiLE was used with the individual tree module (confidence interval about ±0.25).

Figure 10 shows measured and simulated individual tree DBH growth over DBH from 2001 to 2005 as well as in the

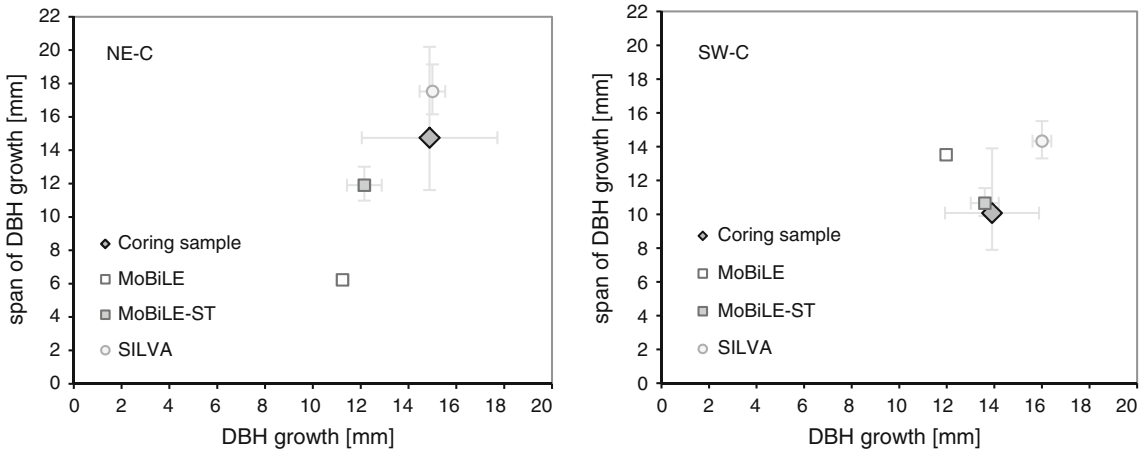

Fig. 8 Individual tree DBH growth 2001–2005 shown as plot level span of DBH growth over the mean basal area stem DBH growth at NE-C (*left*) and SW-C (*right*) differentiated by coring subsample, MoBiLE without interpolation module (MoBiLE), MoBiLE with interpolation module (MoBiLE-ST) and SILVA (*error bars* are confidence intervals here)

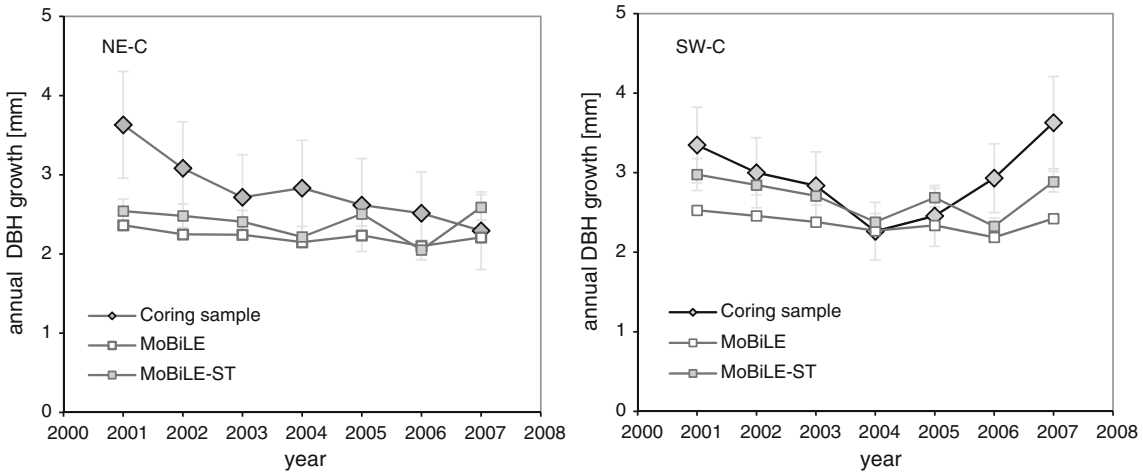

Fig. 9 Simulated and measured mean basal area stem DBH growth on plot NE-C and plot SW-C on annual timescale differentiated by MoBiLE without interpolation module (MoBiLE) and MoBiLE with interpolation module (MoBiLE-ST); confidence intervals are indicated by *error bars*

selected years 2001 and 2005 differentiated by trial plot: within the five-year range, the two individual years are marked by growth to size distributions and regressions of MoBiLE-ST that correspond to a large and a small stand-scale bias of growth, respectively, and limit the span of slope and data spread of the years with deviations lying in between. Cohort representative tree growth from MoBiLE alone is shown by one individual point per interval within the five-year growth to size distributions of NE-C and SW-C.

The confidence band of the simulated data regression does not exceed a growth span of about 1 mm at 5-year growth within the range of DBH variability given. Hence, the reliability of the comparisons shown in Fig. 10 is largely governed by the sample data confidence bands that may be taken from Fig. 7. The regression lines reflect a stronger underestimation of diameter growth by MoBiLE-ST on the individual tree level as compared to stand-level aggregated growth in Figs. 8 and 9. MoBiLE-ST shows a more realistic distribution of diameter growth among the three cohorts than MoBiLE that overestimates growth in the lowest cohort as compared to the others. Within the two topmost cohorts, MoBiLE-ST shows a better estimation than MoBiLE alone that also underestimates there. In the lowest cohort, MoBiLE-ST underestimates and MoBiLE overestimates or estimates accurately (SW-C).

To give an impression how the model represents the distributional width of growth at the centre of the DBH distribution, the 95 % prediction interval of growth at mean DBH is presented by error bars on the regression lines of simulation and measurement. The spread of individual tree diameter growth at site NE-C is met by the simulation results. In accordance with the measured distributional

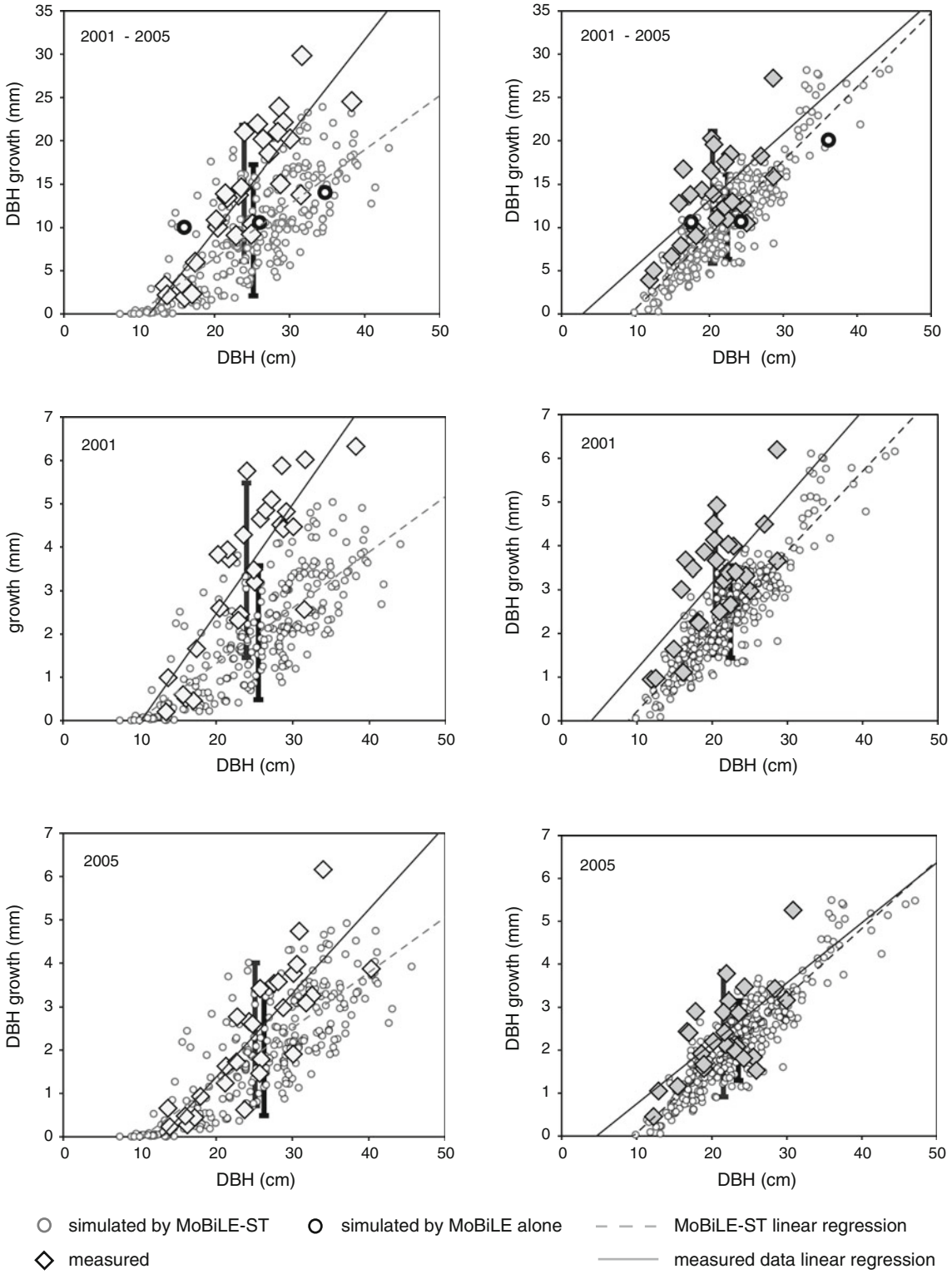

Fig. 10 Comparison of simulated and measured tree growth in the time range 2001–2005 (*above*), in 2001 (*middle*) and in 2005 (*bottom*); cohort intervals (in cm, end diameter excl.) at 0–20, 20–30, 30–∞; range of growth variation is indicated by *bars* (simulated black)

width of diameters, simulated growth at SW-C is more narrow than at NE-C, albeit the absolute values are still underestimated.

Discussion

Generally, site quality is somewhat better at plot NE-C that has a larger basal area than the slightly older plot SW-C. Consistently, SW-C is more homogeneous in tree size and growth at this site is more equally distributed among trees. The year-to-year changes of average year ring width at both sites from 1970 to 2010 are often quite similar, including the significant drop in the very dry year 1976. In the mid of the 1990s, there are remarkable growth peaks at both sites. Interestingly, the SW-C plot showed inferior diameter growth than NE-C until this period but is growing similarly good or even better after this event. One plausible explanation for that shift is a mitigation of competition due to the last thinning before setup of the test sites in 1999. Another likely candidate to explain the observed change is that beech is relatively sensitive to drought (e.g. Friedrichs et al. 2009; Scharnweber et al. 2011) and precipitation might have increased at site SW: in contrast to the former statement about the sites that no significant differences appear across the valley (Geßler et al. 2001), measured precipitation at site SW-C from 2001 to 2007 was higher than at NE-C (1,027 compared to 865 mm annual average).

During the simulation period, the driest year was 2003 that has been shown to decrease carbon assimilation in Europe in general (Ciais et al. 2005) and for beech in particular (Charru et al. 2010). However, no growth depression in that year became obvious from the average year ring width of both plots. Similar results had been reported from other beech stands in Germany and the Netherlands (Mund et al. 2010; van der Werf et al. 2007), which were attributed to favourable growth conditions in early spring or after drought. It should also be noted that 2002 was the wettest year in the simulation period so that soil water storages were well filled.

Stand-scale results from all models were compared as growth over a five-year time period (the basic time step of SILVA), and simulations with MoBiLE-ST were compared to those of the original MoBiLE cohort model on an annual basis. During the time period from 2001 to 2005, simulations with SILVA correctly estimated average diameter growth at NE-C and overestimated it at SW-C, while the original MoBiLE version underestimated growth in both cases. With MoBiLE-ST, the results at NE-C were slightly better, and at SW-C, the representation of measured DBH growth considerably improved as compared to the original model.

On the individual tree level, MoBiLE-ST shows a more realistic relation between five-year diameter growth and tree diameter than MoBiLE alone, if the commonly used linear regression is applied to the result. It represents diameter growth in the two dominant cohorts better, albeit it underestimates growth in the lowest cohort. Both model versions would be more similar in total stand growth, if the cohorts were simply weighted by tree number. Even if the better representation of total stand growth by MoBiLE-ST notably at SW-C implies emphasis of dominant trees in averaging, it is also based on a more realistic diameter growth within the two upper cohorts and a better reflection of the size to growth relationship within the stand.

The gap in improvement between sites NE-C and SW-C might reflect the differences in stand structure between both sites: at NE-C, the topmost cohort is populated by more than 100 well-established dominant trees. Possibly, there is more investment into diameter and less into height within the dominant layer than it is predicted by the model, as trees are in a clearly dominant position and thus from a functional point of view might invest into leaf area and hence diameter rather than into height. In contrast, at SW-C, only about 40 dominant trees are established in the largest cohort, and these are concentrated within a circle of radius 20 m near the border of the plot. Here, the notable improvement of diameter growth within the upper two cohorts in MoBiLE-ST might be due to clustering of the most dominant group and hence lowered individual tree competition on the middle cohort.

In 2005 which is a year of good concordance between simulated and measured diameter growth on both sites, MoBiLE-ST accordingly showed a realistic slope and intercept of the diameter growth to diameter regression on the individual tree level. Whatsoever, it generally underestimated diameter increase as yet: one possible cause could be a deviation in the allometry of dominant trees at NE-C. Another is that volume growth both in MoBiLE-ST and MoBiLE is not sensitive to structural heterogeneity, as the physiological main model still perceives a cohort as horizontally homogeneous. Hence, improvements of diameter growth shown by MoBiLE-ST as compared to MoBiLE are exclusively due to a better description of allometry as yet, and one possible approach of further model optimization might be to correct the assumptions about canopy density in the light transmission of MoBiLE based on structural aspects like clustering.

At NE-C, the distributional width of simulated diameter growth at mean diameter was similar to the one of measured growth in the individual years 2001 and 2005 as well as over the time range 2001–2005. At site SW-C, the data spread of simulated growth was more narrow in accordance with the more homogeneous stand structure. However, it was smaller than the measured one in all cases which indicates that MoBiLE-ST could not capture the whole variability. On the other hand, the variation of year ring

width might have been artificially increased due to general measurement uncertainties, particularly related to diffuse porous wood. However, simulated residual variability of annual growth did not exceed the one of the coring sample in any of the cases.

One of the key challenges for the physiological model is the age dependence of parameters and processes, e.g. with respect to water supply, stomatal conductance and assimilation (Magnani et al. 2008; Delzon et al. 2004) that is relevant in particular for simulations of uneven-aged stands or over rotations. Therefore, one of the major tasks of future research and development is the investigation of the tree size dependence of water stress and the according further refinement of the physiological model part. The focus of this study is on the dependence of allometry on biological age and competition that is delegated to an observation-based module. As a matter of model simplicity, the approach as yet implies that allometry at a given stand structure was site independent within a large ecoregion. A further step of development might be to add dose–response functions of growth potential taken from SILVA and to extend the model preferences by site information: To increase the site dependence of height growth to diameter growth on one hand could improve the results on the short time range that have been presented in this study. On the other hand, although the physiological main model and the individual tree component are coupled in a feedback loop to prevent from module drift, a higher spatial resolution of allometry might be beneficial to mitigate a possible bias between modelled and real individual tree dimension over a rotation. The approach used so far aims to save costs of model maintenance and parameterization. As the dose–response functions of SILVA were parameterized on the stand-scale level, the investment into a more stand-related allometry might pay off.

Our results indicate that the average stand development indeed depends on individual tree size distribution and that the incorporation of individual tree competition into MoBiLE improves the representation of environmental influences in long-term simulations of forest development. The added value of the hybrid model in comparison with the SILVA growth simulator is the consideration of inter-annual variability: MoBiLE-ST is not necessarily more accurate in the prediction of growth considering current climate conditions, but it is sensitive to a change in the inter-annual as well as intra-annual weather regime and hence adds understanding about the long-term effect of a changing climate on competition and structural dynamics. The coupling of an individual tree module into MoBiLE follows a well-justified demand for hybrid models that combine physiological responses with observation-based stand structure development (Mäkelä et al. 2000). Earlier coupling approaches used either a unidirectional linkage between physiological- and observation-based module (Henning and Burk 2004) or bidirectional linkages with large (several years) time steps before considering structural feedbacks (Milner et al. 2003). Also, dimensional change was eventually not consistently related to biomass growth (Baldwin et al. 2001). Weiskittel et al. (2010), Kirschbaum (1999) and Korol et al. (1996) have addressed the issue of mass conservative stand NPP distribution by a weight that was related to the estimated proportion of light acquired by a tree's crown. Dimension growth was calculated via allometric equations from the individual tree volume. As underlined by Watt and Kirschbaum (2011), allometry is not only age dependent but also related to site factors that are at least to a part related to competition, such as stand density. Hence, our approach within the same interpolation step (1) pre-estimates individual tree growth with a distance-dependent observation-based model to provide competition-dependent allometry as well as to scale down cohort volume growth to an individual tree volume change and then (2) corrects the pre-estimated individual tree dimension growth to suffice the individual tree relative volume increase. It aims to minimize the investment into site-specific calibration and to achieve generality with respect to species composition and age class. The specific advantage of the presented coupling is a clear division of tasks between physiological carbon allocation and observation-based allometry: on one hand, the physiological main model is highly sensitive to environmental variability but would be expensive to parameterize and slow on the individual tree level. Therefore, it uses the concept of a cohort model. On the other hand, the observation-based individual tree module is more straightforward and much faster in simulating individual tree growth. It is less sensitive to site conditions. Hence, it exclusively centres upon the ratio of growth in height and diameter, i.e. allometry. The approach combines the major advantages of both model types. Furthermore, it all in one (1) utilizes a mass conservative algorithm to convert stand carbon allocation to individual tree dimensional change, (2) has a bidirectional coupling of cohort mass and volume growth on one hand and of individual tree allometry on the other at the annual timescale, (3) implies a feedback loop to prevent cohort carbon allocation and individual tree dimensional change from drifting apart and (4) utilizes a fast allometry algorithm from a tried and tested observation-based model to extend a physiological model.

Similar to what we propose here, Kimmins et al. (1999) addressed hybridization with the FORCAST model by predefining the time course of stem size distribution at simulation start. The rates of growth of all trees are computed relative to the median tree. Our approach, however, extends this concept, in that it includes the distribution of tree dimension as an intrinsic variable that dynamically

evolves from the initial size and position of the stand's trees, the growth of the stand cohorts and the competition within the stand. Therefore, the approach is well suited to address some interesting questions in the future. For example, whether management can mitigate increasing drought stress by reducing the competition on water (Kohler et al. 2010), or to what degree the relation between aboveground and belowground competition processes might change under changing environmental conditions (Pretzsch and Biber 2010; Pretzsch and Dieler 2011).

Conclusion

Inclusion of an individual tree module (taken from SILVA) into a physiological model (MoBiLE-PSIM) improved the spatial representation of competition and growth on 5 year and even annual timescale. This is particularly the case where the spatial distribution of dominant trees is clustered. Still, there might be room for model improvement in a more detailed relation between crown dominance and development of the height to diameter ratio. In a year where the accuracy of stand growth simulation is high, also mean growth at given tree size is well represented. The competition module might require further improvement in reproducing the distributional width in structurally homogeneous stands. Further investigations would be needed to assert that the model reflects the relation between tree dominance and competitive advantage also in years of extremely low soil resource supply.

Acknowledgments Funding of this work by the German Science Foundation/Deutsche Forschungsgemeinschaft (DFG) within the Project 'Modelling beech-dominated deciduous forest development based on competitive mechanisms of water and nitrogen partitioning' under contract number GE 1090/9-1 is greatly acknowledged. Furthermore, we thank Matthias Ulbricht and Gerhard Schütze for their thorough sampling of tree cores and careful measurement of growth rings, without which this investigation would not have been possible.

References

Baldwin VC Jr, Burkhart HE, Westfall JA, Peterson KD (2001) Linking growth and yield and process models to estimate impact of environmental changes on growth of loblolly pine. Forest Sci 47:77–82

Ball JT, Woodrow IE, Berry JA (1987) A model predicting stomatal conductance and its contribution to the control of photosynthesis under different environmental conditions. In: Biggins J (ed) Progress in photosynthesis research. Martinus-Nijhoff Publishers, Dordrecht, pp 221–224

Boisvenue C, Running SW (2006) Impacts of climate change on natural forest productivity—evidence since the middle of the 20th century. Global Change Biol 12:862–882

Bolte A, Czajkowski T, Kompa T (2007) The north-eastern distribution range of European beech—a review. Forestry 80:413–429

Bolte A, Hilbrig L, Grundmann B, Kampf F, Brunet J, Roloff A (2010) Climate change impacts on stand structure and competitive interactions in a southern Swedish spruce-beech forest. Eur J Forest Res 129:261–276

Brumme R, Khanna PK (2009) Stand, soil and nutrient factors determining the functioning and management of beech forest ecosystems: a synopsis. In: Brumme R, Khanna PK (eds) Functioning and management of european beech ecosystems. Springer, Berlin-Heidelberg, pp 459–491

Charru M, Seynave I, Morneau F, Bontemps JD (2010) Recent changes in forest productivity: an analysis of national forest inventory data for common beech (*Fagus sylvatica* L.) in north-eastern France. For Ecol Manage 260:864–874

Ciais Ph, Reichstein M, Viovy N, Granier A, Ogee J, Allard V, Aubinet M, Buchmann N, Bernhofer C, Carrara A, Chevallier F, De Noblet N, Friend AD, Friedlingstein P, Grünwald T, Heinesch B, Keronen P, Knohl A, Krinner G, Loustau D, Manca G, Matteucci G, Miglietta F, Ourcival JM, Papale D, Pilegaard K, Rambal S, Seufert G, Soussana JF, Sanz MJ, Schulze ED, Vesala T, Valentini R (2005) Europe-wide reduction in primary productivity caused by the heat and drought in 2003. Nature 437:529–533

Delzon S, Sartore M, Burlett R, Dewar R, Loustau D (2004) Hydraulic responses to height growth in maritime pine trees. Plant Cell Environ 27(9):1077–1087

Farquhar GD, Von Caemmerer S, Berry JA (1980) A biochemical model of photosynthetic CO_2 assimilation in leaves of C_3 species. Planta 149:78–90

Fontes L, Bontemps J-D, Bugmann H, Van Oijen M, Gracia C, Kramer K, Lindner M, Rötzer T, Skovsgaard JP (2010) Models for supporting forest management in a changing environment. For Syst 19:8–29

Friedrichs D, Trouet V, Büntgen U, Frank D, Esper J, Neuwirth B, Löffler J (2009) Species-specific climate sensitivity of tree growth in Central-West Germany. Trees 23:729–739

Geßler A, Schrempp S, Matzarakis A, Mayer H, Rennenberg H (2001) Radiation modifies the effect of water availability on the carbon isotope composition of beech (*Fagus sylvatica*). New Phytol 150:653–664

Geßler A, Jung K, Gasche R, Papen H, Heidenfelder A, Börner E, Metzler B, Augustin S, Hildebrand E, Rennenberg H (2005) Climate and forest management influence nitrogen balance of European beech forests: microbial N transformations and inorganic N net uptake capacity of mycorrhizal roots. Eur J For Res 124:95–111

Geßler A, Keitel C, Kreuzwieser J, Matyssek R, Seiler W, Rennenberg H (2007) Potential risks for European beech (*Fagus sylvatica* L.) in a changing climate. Trees 21:1–11

Goreaud F, Alvarez I, Courbaud B, de Coligny F (2006) Long-term influence of the spatial structure of an initial state on the dynamics of a forest growth model: a simulation study using the Capsis platform. Simulation 82:475–495

Grote R (1998) Integrating dynamic morphological properties into forest growth modeling. II. Allocation and mortality. For Ecol Manage 111:193–210

Grote R (2007) Sensitivity of volatile monoterpene emission to changes in canopy structure—a model based exercise with a process-based emission model. New Phytol 173:550–561

Grote R, Pretzsch H (2002) A model for individual tree development based on physiological processes. Plant Biol (Stutt) 4:167–180

Grote R, Lehmann E, Brümmer C, Brüggemann N, Szarzynski J, Kunstmann H (2009) Modelling and observation of biosphere-atmosphere interactions in natural savannah in Burkina Faso, West Africa. Phys Chem Earth 34:251–260

Grote R, Kiese R, Grünwald T, Ourcival J-M, Granier A (2011a) Modelling forest carbon balances considering tree mortality and removal. Agric For Meteorol 151:179–190

Grote R, Korhonen J, Mammarella I (2011b) Challenges for evaluating process-based models of gas exchange at forest sites with fetches of various species. For Syst 20(3):389–406

Hauser S (2003) Dynamik hochaufgelöster radialer Schaftveränderungen und des Dickenwachstums bei Buchen (*Fagus sylvatica* L.) der Schwäbischen Alb unter dem Einfluss von Witterung und Bewirtschaftung. Freiburg i. Brsg., Albert-Ludwigs-Universität Freiburg i. Brsg. pp 212

Henning JG, Burk TE (2004) Improving growth and yield estimates with a process model derived growth index. Can J For Res 34:1274–1282

Holst T, Mayer H (2005) Radiation components of beech stands in Southwest Germany. Meteorol Zeitschrift 14:107–115

Holst T, Hauser S, Kirchgäßner A, Matzarakis A, Mayer H, Schindler D (2004a) Measuring and modelling plant area index in beech stands. Int J Biometeorol 48:192–201

Holst T, Mayer H, Schindler D (2004b) Microclimate within beech stands—part II: thermal conditions. Eur J Forest Res 123:13–28

Holst J, Grote R, Offermann C, Ferrio JP, Gessler A, Mayer H, Rennenberg H (2010) Water fluxes within beech stands in complex terrain. Int J Biometeorol 54:23–36

Jump AS, Hunt JM, Peñuelas J (2006) Rapid climate change-related growth decline at the southern range edge of *Fagus sylvatica*. Global Change Biol 12:2163–2174

Kimmins JP, Mailly D, Seely B (1999) Modelling forest ecosystem net primary production: the hybrid simulation approach used in FORECAST. Ecol Modell 122:195–224

Kirschbaum MUF (1999) CenW, a forest growth model with linked carbon, energy, nutrient and water cycles. Ecol Modell 118:17–59

Koca D, Smith B, Sykes MT (2006) Modelling regional climate change effects on potential natural ecosystems in Sweden. Clim Chang 78:381–406

Kohler M, Sohn J, Nägele G, Bauhus J (2010) Can drought tolerance of Norway spruce (*Picea abies* (L.) *Karst*.) be increased through thinning? Eur J For Res 129:1109–1118

Korol RL, Milner KS, Running SW (1996) Testing a mechanistic model for predicting stand and tree growth. For Sci 42:139–153

Kubiske ME, Quinn VS, Heilman WE, McDonald EP, Marquardt PE, Teclaw RM, Friend AL, Karnosky DF (2006) Interannual climatic variation mediates elevated CO_2 and O_3 effects on forest growth. Global Chang Biol 12:1054–1068

Landsberg J (2003) Physiology in forest models: history and the future. FBMIS 1:49–63

Langvall O, Löfvenius MO (2002) Effect of shelterwood density on nocturnal near-ground temperature, frost injury risk and budburst date of Norway spruce. For Ecol Manage 168:149–161

Li C, Frolking S, Frolking TA (1992) A model of nitrous oxide evolution from soil driven by rainfall events: 1. Model structure and sensitivity. J Geophys Res 97:9759–9776

Löw M, Herbinger K, Nunn AJ, Häberle K-H, Leuchner M, Heerdt C, Werner H, Wipfler P, Pretzsch H, Tausz M, Matyssek R (2006) Extraordinary drought of 2003 overrules ozone impact on adult beech trees (*Fagus sylvatica*). Trees 20:539–548

Maaten E (2011) Climate sensitivity of radial growth in European beech (*Fagus sylvatica* L.) at different aspects in southwestern Germany. Trees 26:777–788

Magnani F, Bensada A, Cinnirella S, Ripullone F, Borghetti M (2008) Hydraulic limitations and water-use efficiency in *Pinus pinaster* along a chronosequence. Can J For Res 38(1):73–81

Mäkelä A, Landsberg J, Ek AR, Burk TE, Ter-Mikaelian M, Ågren GI, Oliver CD, Puttonen P (2000) Process-based models for forest ecosystem management: current state of the art and challenges for practical implementation. Tree Physiol 20:289–298

Martin GL, Ek AR, Monserud RA (1977) Control of plot edge bias in forest stand growth simulation models. Can J For Res 7(1):100–105

Matyssek R, Le Thiec D, Löw M, Dizengremel P, Nunn AJ, Häberle KH (2006) Interactions between drought and O_3 stress in forest trees. Plant biol 8:11–17

Mayer H, Holst T, Schindler D (2002) Microclimate within beech stands—part I: photosynthetically active radiation. Forstw Cbl 121:301–321

Milner KS, Coble DW, McMahan AJ, Smith EL (2003) FVSBGC: a hybrid of the physiological model STAND-BGC and the forest vegetation simulator. Can J For Res 33:476–479

Mund M, Kutsch WL, Wirth C, Kahl T, Knohl A, Skomarkova MV, Schulze E-D (2010) The influence of climate and fructification on the inter-annual variability of stem growth and net primary productivity in an old-growth, mixed beech forest. Tree Physiol 30(6):689–704

Muys B, Hynynen J, Palahí M, Lexer MJ, Fabrika M, Pretzsch H, Gillet F, Briceño E, Nabuurs G-J, Kint V (2010) Simulation tools for decision support to adaptive forest management in Europe. For Syst 19:86–99

Ollinger SV, Aber JD, Reich PB, Freuder RJ (2002) Interactive effects of nitrogen deposition, tropospheric ozone, elevated CO_2 and land use history on the carbon dynamics of northern hardwood forests. Global Chang Biol 8:545–562

Paul T (2003) Die Vegetation in Kalkbuchenwäldern in Abhängigkeit von Standort und forstlicher Nutzung. Albert-Ludwigs-Universität, Freiburg in Breisgau 257 pp

Porte′ A, Bartelink HH (2002) Modelling mixed forest growth: a review of models for forest management. Ecol Modell 150:141–188

Portsmuth A, Niinemets Ü (2007) Structural and physiological plasticity in response to light and nutrients in five temperate deciduous woody species of contrasting shade tolerance. Funct Ecol 21:61–77

Pretzsch H, Biber P (2010) Size-symmetric versus size-asymmetric competition and growth partitioning among trees in forest stands along an ecological gradient in central Europe. Can J For Res 40:370–384

Pretzsch H, Dieler J (2011) The dependency of the size-growth relationship of Norway spruce (*Picea abies* [L.] Karst.) and European beech (*Fagus sylvatica* [L.]) in forest stands on long-term site conditions, drought events, and ozone stress. Trees 25:355–364

Pretzsch H, Biber P, Dursky J (2002) The single tree-based stand simulator SILVA: construction, application and evaluation. For Ecol Manage 162:3–21

Pretzsch H, Grote R, Reineking B, Rötzer T, Seifert S (2008) Models for forest ecosystem management: a European perspective. Ann Bot 101:1065–1087

Richards FJ (1959) A flexible growth function for empirical use. J Exp Bot 10:290–300

Rötzer T, Grote R, Pretzsch H (2005) Effects of environmental changes on the vitality of forest stands. Eur J For Res 124:349–362

Saxe H, Cannell MGR, Johnsen O, Ryan MG, Vourlitis G (2002) Tree and forest functioning in response to global warming. New Phytol 149:369–399

Scharnweber T, Manthey M, Criegee C, Bauwe A, Schröder C, Wilmking M (2011) Drought matters—declining precipitation influences growth of *Fagus sylvatica* L. and *Quercus robur* L. in north-eastern Germany. For Ecol Manage 262:947–961

Schwinning S, Weiner J (1998) Mechanisms determining the degree of size asymmetry in competition among plants. Oecologia 113:447–455

van der Werf GW, Sass-Klaassen UGW, Mohren GMJ (2007) The impact of the 2003 summer drought on the intra-annual growth pattern of beech (*Fagus sylvatica* L.) and oak (*Quercus robur* L.) on a dry site in the Netherlands. Dendrochronologia 25:103–112

Watt MS, Kirschbaum MUF (2011) Moving beyond simple linear allometric relationships between tree height and diameter. Ecol Modell 222:3910–3916

Weiner J (1990) Asymmetric competition in plant populations. Trends Ecol Evol 5:360–364

Weiskittel A, Maguire D, Monserud R, Johnson G (2010) A hybrid model for intensively managed Douglas-fir plantations in the Pacific Northwest, USA. Eur J For Res 129:325–338

Wichmann L (2001) Annual variations in competition symmetry in even-aged Sitka spruce. Ann Bot 88:145–151

Wichmann L (2002) Modelling the effects of competition between individual trees in forest stands. Royal Veterinary and Agricultural University, Copenhagen

Online supplement to:

Extending a physiological forest growth model by an observation-based tree competition module improves spatial representation of diameter growth

The subject of this work is the extension of the physiological cohort model MoBiLE-PSIM (Grote et al. 2009) with an observation based module that provides individual tree potential growth, competition and allometry taken from SILVA (Pretzsch et al. 2002), and scales down the cohort volume growth to the individual tree level. On annual time step the module first computes preliminary tree volumes at the start (v_0^*) and at the end (v_1^*) of the current year (Figure A1, step 1) based on the timber-wood taper function of SILVA. Next, the total cohort volumes at start and end of year that are passed to the module by the physiological main part of the hybrid model are refined to the individual tree level via the shares of v_0^* and v_1^* within the cohort (resulting in v_0 and v_1, Figure A1, step 2). Hence each individual tree can be assigned a preliminary relative volume increase that is consistent with potential growth and competition of the individual tree module (result of Figure A1, step 1) and a relative volume increase that is consistent with the physiological main model (result of Figure A1, step 2). The next step is to correct the preliminary dimension increases to values that are consistent with the total cohort volume increase from carbon allocation using the correction factor defined by Eq.1 of the basic publication

$$f = \frac{\sqrt[3]{\omega}-1}{\sqrt[3]{\omega^*}-1} \quad \text{where } \omega = \frac{v_1}{v_0} \text{ and } \omega^* = \frac{v_1^*}{v_0^*}. \qquad \text{Eq.1}$$

The preliminary dimension change of each cohort tree is multiplied by the tree specific correction factor to get an updated cohort tree list of the following year: It has a total volume that is consistent with the carbon allocation of the cohort. The new dimensions of the average cohort tree are then formed from the updated individual trees.

Equations A1) to A8) give a detailed explication of the new downscaling algorithm in MoBiLE. For convenience, we use a matrix notation to explain operations across groups of trees, such as the full stand or a cohort of trees. One boundary condition of particular importance is stand structure U as dependent on time t

$$U_t = \begin{pmatrix} h_{t1} \cdots h_{tm} \\ d_{t1} \ldots d_{tm} \\ b_{t1} \ldots b_{tm} \\ r_{t1} \ldots r_{tm} \\ x_1 \ldots x_m \\ y_1 \ldots y_m \end{pmatrix}. \qquad \text{Eq.A1}$$

Each column corresponds to exactly one tree of index j from $\{1,..,m\}$ at time t where m is the total number of trees within the stand. Variables b_{tj}, r_{tj}, x_j and y_j are height to the crown base, crown diameter, x coordinate and y coordinate of tree j. They are essential to capture competition at time t (C_t)

$$C_t = \begin{pmatrix} \gamma_{t1} \cdots \gamma_{tm} \\ \delta_{t1} \ldots \delta_{tm} \end{pmatrix} \qquad \text{Eq.A2}$$

where γ_{tj} and δ_{tj} are the reduction factors of potential height and diameter growth.

The structure of a cohort at time t with n trees is defined here as a submatrix of U_t (S_t)

$$S_t = \begin{pmatrix} h_{t1} \cdots h_{tn} \\ d_{t1} \ldots d_{tn} \end{pmatrix} \quad \text{Eq.A3}$$

where each column refers to exactly one cohort tree i of index $1,..,n$ and corresponds to its dimension vector at time t ($\vec{D}_t$, tree index omitted)

$$\vec{D}_t = \begin{pmatrix} h_t \\ d_t \end{pmatrix}. \quad \text{Eq.A4}$$

Cohorts may intersect spatially in height and ground position but are completely discrete from each other with respect to their trees. Any stand tree is part of exactly one cohort. The adherence of a stand tree to a cohort is independent of time at the current state of development.

When PSIM has finished a year, all cohorts are updated: The structure of the cohort at the beginning of year (t_0) is mapped to the structure at the end of year (t_1) (for convenience we denote t_0 as 0 and t_1 as 1 where time is the index in the following)

$$S_0, V_0, V_1 \rightarrow S_1 \quad \text{Eq.A5}$$

where S_0 is the cohort structure at t_0, V_0 and V_1 are the cohort volumes at t_0 and t_1 and S_1 is the cohort structure at t_1. V_0 and V_1 are both provided by PSIM and are boundary conditions to the interpolation.

An essential step of the algorithm is the formation of the tree dimension change matrix, i.e. cohort growth at time t (G_t)

$$G_t = \begin{pmatrix} \Delta h_{t1} \cdots \Delta h_{tn} \\ \Delta d_{t1} \ldots \Delta d_{tn} \end{pmatrix}. \quad \text{Eq.A5.1}$$

Growth at time t_0 (G_0) is added to S_0 to form S_1

$$S_1 = S_0 + G_0. \quad \text{Eq.A5.2}$$

In a first approximation, a preliminary value of G_0 is computed, named G_0^* which is marked with an asterisk, as all preliminary results will be within the scope of this article. The precursor of G_0^* is potential growth G_0'

$$G_0' = \begin{pmatrix} \Delta h'_{01} \cdots \Delta h'_{0n} \\ \Delta d'_{01} \ldots \Delta d'_{0n} \end{pmatrix}. \quad \text{Eq.A5.3}$$

Computation of G_0'

$$S_0, \ \vec{\varphi} \ \rightarrow G_0' \quad \text{Eq.A5.4}$$

implies the use of the growth curves for height and diameter which have been taken from SILVA. Vector $\vec{\varphi}$ defines parameters of the curve equations.

G_0^* results from G_0' and from E_0, which is a subset of the competition matrix C_0 that exclusively includes the cohort trees

$$G_0', E_0 \rightarrow G_0^* \qquad \text{Eq.A5.5}$$

where potential growth and corresponding reduction factor are multiplied. The preliminary growth G_0^* is added to the cohort structure at t_0 to get a preliminary structure at t_1

$$S_1^* = S_0 + G_0^*. \qquad \text{Eq.A5.6}$$

The decisive refinement of G_0^* to G_0 is based on the comparison of the preliminary individual tree volume change to a tree volume change that is consistent with the cohort volume change which results from PSIM. The step is explained in the following.

Using stem volume equations taken from SILVA a timber volume of each tree at t_0 and t_1 is computed

$$S_0,\ \vec{\tau} \rightarrow \vec{V}_0^* \qquad \text{Eq.A5.7}$$

$$S_1^*,\ \vec{\tau} \rightarrow \vec{V}_1^* \qquad \text{Eq.A5.8}$$

where $\vec{\tau}$ comprises the species specific timber volume parameters. $\vec{V}_0^*$ and $\vec{V}_1^*$ are the resulting vectors of individual tree volume at t_0 and t_1 respectively. $\vec{V}_0^*$ is marked as preliminary as well

as $\vec{V}_1^*$, because the sum of all its tree volumes may deviate from the corresponding cohort volume that results from PSIM.

In the following steps, v_{i0}^* and v_{i1}^* are the volume of any tree i within $\vec{V}_0^*$ and $\vec{V}_1^*$ respectively. The relative share r_i in the cohort's timber volume of each tree i at t_0 and t_1 is computed as

$$r_i = \frac{v_i^*}{\sum_{j=1}^{n} v_j^*} \quad \text{where} \quad i \in \{1,..,n\}. \qquad \text{Eq.A5.9}$$

The resulting volume share vectors $\vec{R}_0$ and $\vec{R}_1$, are used to calculate absolute tree volumes which now comply with the PSIM cohort volume at t_0 and t_1:

$$\vec{V}_0 = \vec{R}_0 \cdot V_0 \qquad \text{Eq.A5.10}$$

$$\vec{V}_1 = \vec{R}_1 \cdot V_1. \qquad \text{Eq.A5.11}$$

V_0, V_1 are the PSIM volumes referring to t_0 and t_1, which had already been introduced at the beginning of this part. Calculation of $\vec{R}_1$ may involve a correction if preliminary volume change is much higher than PSIM volume change, which is explained at the end.

The final step of the interpolation is to correct the dimension change of each cohort tree i, so that all tree dimensions within the cohort at t_1 become consistent with $\vec{V}_1$ and the sum of all stem volumes is identical to V_1: Each column of $G_0{}^*$ corresponds to a false dimension change vector $\vec{\Delta}_i^*$ (time index omitted for convenience)

$$\vec{\Delta}_i^* = \begin{pmatrix} \Delta h_i^* \\ \Delta d_i^* \end{pmatrix}. \qquad \text{Eq.A5.12}$$

A correction factor f is multiplied to $\vec{\Delta}_i^*$ which depends on volume change of the specific tree i:

$$f = \frac{\sqrt[3]{\omega}-1}{\sqrt[3]{\omega^*}-1} \quad \text{where} \quad \omega = \frac{v_1}{v_0} \quad \text{and} \quad \omega^* = \frac{v_1^*}{v_0^*}. \qquad \text{Eq.A5.13}$$

The tree index has been dropped here. Variables v_0, v_1, $v_0{}^*$ and $v_1{}^*$ are the volume of tree i within $\vec{V}_0$, $\vec{V}_1$, $\vec{V}_0^*$ and $\vec{V}_1^*$ respectively.

Factor f may be considered as a tree specific slope correction to the curves of height and diameter. Details to the derivation of f are given at the end. Cohort growth G then is received as follows (time index omitted again):

$$G = \left(\vec{\Delta}_1 \cdots \vec{\Delta}_n\right) = \left(f_1 \vec{\Delta}_1^* \cdots f_n \vec{\Delta}_n^*\right). \qquad \text{Eq.A6}$$

The new cohort structure at t_1 is formed by

$$S_1 = S_0 + G_0. \quad \text{Eq.A7}$$

Finally, matrix S_1 is mapped to the new dimensions of the cohort mean tree

$$S_1 \rightarrow \vec{D}_1. \quad \text{Eq.A8}$$

The elements height and diameter within $\vec{D}_1$ are calculated as mean values of the corresponding row in S_1. These updated dimensions are calculated for each cohort within the stand. They are returned to the MoBiLE framework and define the new structural boundary conditions that influence leaf distribution and thus radiation regime within the canopy for the next simulation time step.

Correction implicit in Eq.A5.11:

The correction takes into account that the relative volume share at t_1 which corresponds to the volume given by PSIM may remarkably deviate from the one after preliminary growth. It is applied to the volume share of the individual tree:

(i) $r_1 = r_0 + (r_1^* - r_0) \cdot s$ where $0 \leq s \leq 1$.

Variables r_1 and r_0 are the volume shares within $\vec{V}_1$ and $\vec{V}_0$ respectively and r^*_1 is the preliminary individual tree volume share. The slope s of the correction implies comparison of

the relative cohort volume increase which is named θ here at PSIM growth and θ^* at preliminary growth

(ii) $s = \frac{\theta - 1}{\theta^* - 1}$.

The volume increase is defined as relative change, because the cohort volume that is given by PSIM and the one computed by interpolation are unequally defined:

(iii) $\theta = \frac{V_1}{V_0}$. $\theta^* = \frac{V_1^*}{V_0^*}$.

V^* and $V_0{}^*$ are the cohort volumes at preliminary growth at t_1 and t_0 respectively.

Derivation of Eq.A5.13:

The slope of a dimension growth curve, as shown for diameter d here, is approximately

(i) $m = \frac{\Delta d}{\Delta t} = \frac{d_1 - d_0}{\Delta t} = \frac{\delta d_0 - d_0}{\Delta t} = \frac{d_0(\delta - 1)}{\Delta t}$

where δ is relative increase and defined as

(ii) $\delta = \frac{d_1}{d_0}$.

In the following, μ^* and μ are the value of m resulting from preliminary growth G^* and from corrected growth respectively. Factor f is defined as a correction to μ^*

(iii) $f = \frac{\mu}{\mu^*} = \frac{\delta - 1}{\delta^* - 1}$.

Variable δ^* is relative increase at preliminary growth. The diameter at start of year has been assumed to be identical in numerator and denominator of (iii) and cancelled.

Next δ is expressed as dependent on change in volume. The approach is

(iv) $v_1 = d_1^2 \cdot h_1 \cdot k = d_1^3 \cdot \rho_1 \cdot k$, where $\rho_1 = \frac{d_1}{h_1}$

and k implies all factors of volume calculation.

With (ii) in (iv):

(v) $v_1 = \delta^3 \cdot d_0^3 \cdot D \cdot \rho_0 \cdot k = \delta^3 \cdot v_0 \cdot D;$

(vi) $\delta = \sqrt[3]{\frac{v_1}{v_0 D}}$, where $D = \frac{\rho_1}{\rho_0}$.

With analogous definitions the relative increase at preliminary growth is

(vii) $\delta^* = \sqrt[3]{\frac{v_1^*}{v_0^* D^*}}$.

The correction factor for height is

(viii) $g = \frac{\gamma - 1}{\gamma^* - 1}$.

The height at beginning of year has been assumed to be identical in numerator and denominator of (viii) and cancelled.

Relative increase for h, named γ resolves to a similar expression as the definition of δ

(ix) $\gamma = \sqrt[3]{\frac{v_0 D^2}{v_1}}$.

At preliminary growth the increase is

(x) $\gamma^* = \sqrt[3]{\frac{v_0^* D^{*2}}{v_1^*}}$.

The postulate, that the correction factor be equal for both, diameter and height,

(xi) $f = g$;

is equivalent to

(xii) $\frac{\delta - 1}{\delta^* - 1} = \frac{\gamma - 1}{\gamma^* - 1}$

and is true for $D = D^* = 1$.

Thus Eq.A5.13) i.e. Eq.1 of the basic publication is based on the assumption, that with sufficient approximation (1) the change of the height to diameter ratio at corrected growth is identical to the change at preliminary growth and both are equal to 1, i.e. that the error in assuming h to d as constant over one year in (vi, vii, ix, x) may be neglected, and (2) that at the beginning of the year the individual tree volume that results from the biomass given by PSIM is consistent with the tree dimensions within the corresponding individual tree list (implicit in iii and viii).

References

Grote R, Lehmann E, Brümmer C, Brüggemann N, Szarzynski J, Kunstmann H (2009) Modelling and observation of biosphere-atmosphere interactions in natural savannah in Burkina Faso, West Africa. Phys Chem Earth 34:251-260

Pretzsch H, Biber P, Dursky J (2002) The single tree-based stand simulator SILVA: construction, application and evaluation. For Ecol Manage 162:3-21

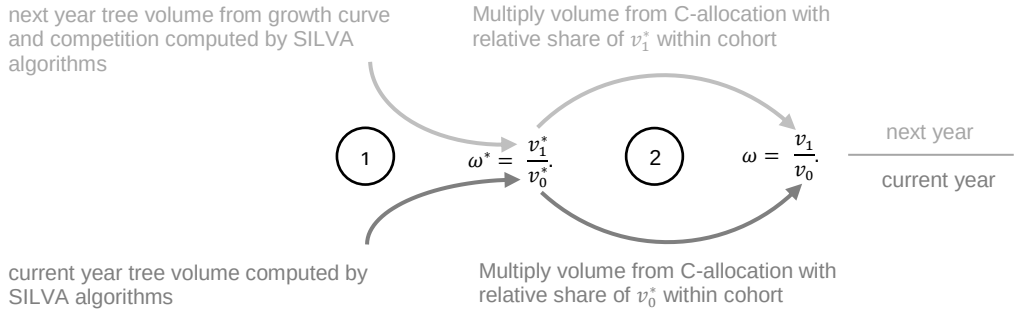

correction factor for individual tree dimension $f = \frac{\sqrt[3]{\omega} - 1}{\sqrt[3]{\omega^*} - 1}$

Figure A1 Computation of the individual tree dimension correction factor from the individual tree volume v of current (v_0) and next year (v_1).

Betreff:
Re: Reprint paper and present it in appendix of phD thesis
Von:
Chat Support - Digital Customer Service <chatsupport@springernature.com>
Datum:
14.01.2017 05:01
An:
werner.poschenrieder@lrz.tum.de

Dear Werner Poschenrieder,

According to our colleague you may reprint the paper and use it for is PhD thesis.
The authors retain the copyright of the paper according to the OA mandate.

==

Kind Regards,
Feedback Support
Springer Nature
Digital Customer Service
chatsupport@springer.com

Springer Nature is one of the world’s leading global research, educational and professional publishers, created in May 2015 through the combination of Nature Publishing Group,
Palgrave Macmillan, Macmillan Education and Springer Science+Business Media.

Springer Customer Service Center GmbH, Tiergartenstrasse 15-17, 69121 Heidelberg, Germany
Registered Office: Heidelberg / Amtsgericht Mannheim, HRB 336546
Managing Directors: Derk Haank, Martin Mos, Dr. Ulrich Vest
==

On Fri, 23 Dec, 2016 at 1:56 AM , Chat Support - Digital Customer Service <chatsupport@springernature.com> wrote:
Dear Werner Poschenrieder,

Thank you for contacting us.

Please be informed that we have forwarded this concern to our responsible colleagues for further assistance and we'll get back to you as soon as we receive their response.

==

Kind Regards,
Feedback Support
Springer Nature

Digital Customer Service
chatsupport@springer.com

Springer Nature is one of the world's leading global research, educational and professional publishers, created in May 2015 through the combination of Nature Publishing Group,
Palgrave Macmillan, Macmillan Education and Springer Science+Business Media.

Springer Customer Service Center GmbH, Tiergartenstrasse 15-17, 69121 Heidelberg, Germany
Registered Office: Heidelberg / Amtsgericht Mannheim, HRB 336546
Managing Directors: Derk Haank, Martin Mos, Dr. Ulrich Vest
==

On Wed, 21 Dec at 4:18 AM , Werner Poschenrieder <werner.poschenrieder@lrz.tum.de> wrote:
Dear Sirs,

the paper
Poschenrieder, W., Grote, R., & Pretzsch, H. (2013). Extending a physiological forest growth model by an observation-based tree competition module improves spatial representation of diameter growth. European Journal of Forest Research, 132(5–6), 943–958. http://doi.org/10.1007/s10342-013-0730-1

is Open Access at your journal. Does that include permission to reprint the paper and attach it to my phD thesis?

Kind regards
Werner Poschenrieder

5829

Silva Fennica vol. 50 no. 1 article id 1393
Category: research article

SILVA FENNICA

www.silvafennica.fi
ISSN-L 0037-5330 | ISSN 2242-4075 (Online)
The Finnish Society of Forest Science
Natural Resources Institute Finland

Werner Poschenrieder [1], Andreas Rais [1,2], Jan-Willem G. van de Kuilen [2] and Hans Pretzsch [1]

Modelling sawn timber volume and strength development at the individual tree level – essential model features by the example of Douglas fir

Poschenrieder W., Rais A., van de Kuilen J.-W.G., Pretzsch H. (2016). Modelling sawn timber volume and strength development at the individual tree level – essential model features by the example of Douglas fir. Silva Fennica vol. 50 no. 1 article id 1393. 25 p.

Highlights

- An individual tree timber growth and quality model toolbox was designed.
- It realistically predicts an increase of bending strength with planting density.
- Prediction was shown to be based on consideration of essential intrinsic variables.
- Height-diameter-allometry depending on planting density was effective.
- Consideration of cambial age and knot area ratio was crucial.

Abstract

We designed a streamlined timber growth and quality model that aims at the effect of stand management on the efficiency of wood resource use. Applying the R based module toolbox to experimental plots of Douglas fir (*Pseudotsuga menziesii* [Mirb.] Franco) we analysed essential model features for reflecting the influence of planting density on board strength. The current version realistically predicted a significant increase of centre board bending strength at tree age 40 with initial stand density. Model performance gained clear advantage from a) parameterisation of height to diameter allometry as dependent on planting density b) consideration of cambial age and cross-sectional knot area in board strength computation. Crown shape was less decisive. The model produced a significant effect of planting density even after a whole rotation period of 70 years as well as a realistic spectrum of board bending strength.

Keywords wood quality modelling; stem structure; sawing; grading; sensitivity test; R statistical environment
Addresses [1] Technische Universität München, Chair of Forest Growth and Yield Science, Hans Carl von Carlowitz Platz 2, 85354 Freising, Germany; [2] Technische Universität München, Holzforschung München, Winzererstrasse 45, 80797 Munich, Germany
E-mail werner.poschenrieder@lrz.tum.de
Received 20 May 2015 **Revised** 9 November 2015 **Accepted** 11 November 2015
Available at http://dx.doi.org/10.14214/sf.1393

1 Introduction

The earliest tools for the prediction of wood and timber yield were observation based tables for single species stands that exclusively focused on volume growth. In the course of the 1960s and 1970s they were replaced by empirical models of stand development that were implemented in computer programs to calculate printed yield tables. During the same period simulators of stand growth were developed to follow new requirements such as the prediction of volume growth in mixed forest stands. On the one hand, model evolution lead to observation based individual tree simulators to capture the effect of local competition in heterogeneous stands. On the other hand, it resulted in physiological process models that often assume a simplified representation of stand structure e.g. as a single vegetation layer or an ensemble of interacting cohort layers (Pretzsch et al. 2008). To describe the effect of a changing weather regime on stand dynamics, structure and yield, also hybrids of both types were constructed (Mäkelä et al. 2000; Weiskittel et al. 2010). They model carbon assimilation mechanistically and describe its allocation within the stand based on individual tree competition (ibid).

An additional challenge to modelling arose from timber quality management, covering the whole production chain from stand treatment to sawing. Wood quality models aim to predict the properties of timber based on measured forest inventory data or assumptions of stand development in response to scenarios of management or future climate. Following the references in Mäkelä et al. (2010), their main development phase began in the late 1980s with the SYLVER growth and sawing simulation system (Mitchell 1988). As also presented by Mäkelä et al. (2010), a spectrum of models and modules since has evolved that covers all main types of growth algorithms and may imply a high level of stem shape and structure detail description (Houllier et al. 1995; Hann et al. 1997; Di Lucca 1999; Todoroki et al. 2005).

Wood quality models may either be used to estimate the volume to quality relation based on inventory data or on future scenario simulation results. Therefore, they need to predict stem structure on the spatial scale of individual boards (Mäkelä et al. 2010). The most central structure of the lower stem (butt log) in radial direction adheres to the juvenile growth phase that is complex and governed by strong competition on the individual tree level (Donato et al. 2012) but has rarely been covered by individual tree models (e.g. Ritchie and Hamann 2007). Hence, one likely approach is a backward projection that is based on a known planting pattern and the current stand structure. This method takes into account the range of diameter growth gained by wood core or stem disk data.

In strength grading the knot size is a decisive indicating property for wood quality. A crucial component of any wood quality simulator that reflects the inner structure of stems and logs to compute board strength thus is the vertical and radial positioning and the number of branches as they have a major impact on strength (Mäkinen et al. 2001). Branch growth depends on assimilation and allocation into branch sapwood and hence on vertical position and local competition (Gort et al. 2010) which is in turn determined by stand age and spacing.

Branch models for wood quality estimation are typically branch distribution models (e.g. Houllier et al. 1995), and only few (e.g. Hein et al. 2007) take into account local stand density as reported by Seifert (2003). However, to capture the effect of management options, local competition has to be taken into account as crowns may reflect aboveground competition by crown position (Muth and Bazzaz 2003), crown dimensions (Thorpe et al. 2010) or details of the hull shape (Rouvinen and Kuuluvainen 1997). Hence, branch growth and dimension need to be modelled based on the situation of the immediate aboveground environment of a tree either on the level of individual branch growth (Seifert 2003) or by means of a competition dependent growth of the crown's convex hull as proposed e.g. by Pretzsch et al. (2002).

Crown and branch architecture and the influence of annual stem growth on the inner structure of logs and boards have been modelled in high detail by considering the description of tree growth and resulting stem architecture on a mechanistic level (Kellomäki 1999; Mäkelä et al. 2000). As an approach to describe structure forming processes even on the microscopic scale, Lang and Kaliske (2013) used the finite elements method to show the influence of bending on fibre direction.

Modelling frameworks for wood quality often package modules of high theoretical detail (Mitchell 1988; Maguire et al. 1991; Meredieu et al. 1999). In contrast, the modelling framework of this study is marked by a generally lean approach for a module chain that spans from reconstructed early growth via individual tree inventory through to future prognosis of board strength and grading. Its basic concept is an actinomorphic perception of the tree with a radially symmetrical convex crown hull. This work in particular aimed to identify the minimum set of features of a distance dependent individual tree model that were necessary to capture the effect of planting density on board strength. It finally evaluated the module set based on the effect of planting density on board strength of Douglas fir (*Pseudotsuga menziesii* [Mirb.] Franco) over a whole rotation period.

The investigation was based on the combination and interdisciplinary evaluation of related tree dimension, stem disk and board strength data from two long term observation sites of pure Douglas fir stands in south-eastern Germany with one representing rather dry and the other indicating favourable soil climatic conditions. We simulated the development of tree architecture on scales ranging from stem and crown shape to branch position and size and even into higher detail via the inner structure of the stem to the knottiness and annual ring width of individual boards. Based on the final result we derived the bending strength on board level. The current model version was evaluated with respect to its quality of reconstruction to age 20 and prognosis to age 40 as compared to an earlier approach (basic model version) that was marked by more simplistic assumptions regarding both wood structure and height to diameter influence on board strength. Eventually, the simulated effect of planting density on board strength over a presumed rotation period of 70 years was studied through comparison of current and basic version as well.

2 Material and methods

2.1 General architecture of the model

The simulation model covers the major relevant linkages reaching from stand management and site influence via individual tree competition and growth to crown shape and branch dimension and further down to knottiness, wood density and strength of the individual board. The functionality of the model may be readily modified by adding or replacement of plug-in computation objects. Parameter values are provided by a data object and given by site and species. Supplementary file 1 (available at http://dx.doi.org/10.14214/sf.1393) provides basic technical documentation.

Predicted growth is driven by diameter increase as dependent on individual tree size and position. It starts at the earliest state of the stand that had been recorded on the individual tree level. Previous growth is reconstructed from first inventory of the tree individual and collective annual ring data. It covers the early phase of stand development when structure has not been recorded by inventory of individual trees. All variable values that refer to the starting conditions of prediction will be marked by the adjective setup in the following. Hence, the inventory that had defined the corresponding stand structure is named setup inventory and any registered diameter at breast height (1.3 m) setup DBH. Fig. 1 gives an outline of simulated individual tree growth finalised by logging and sawing.

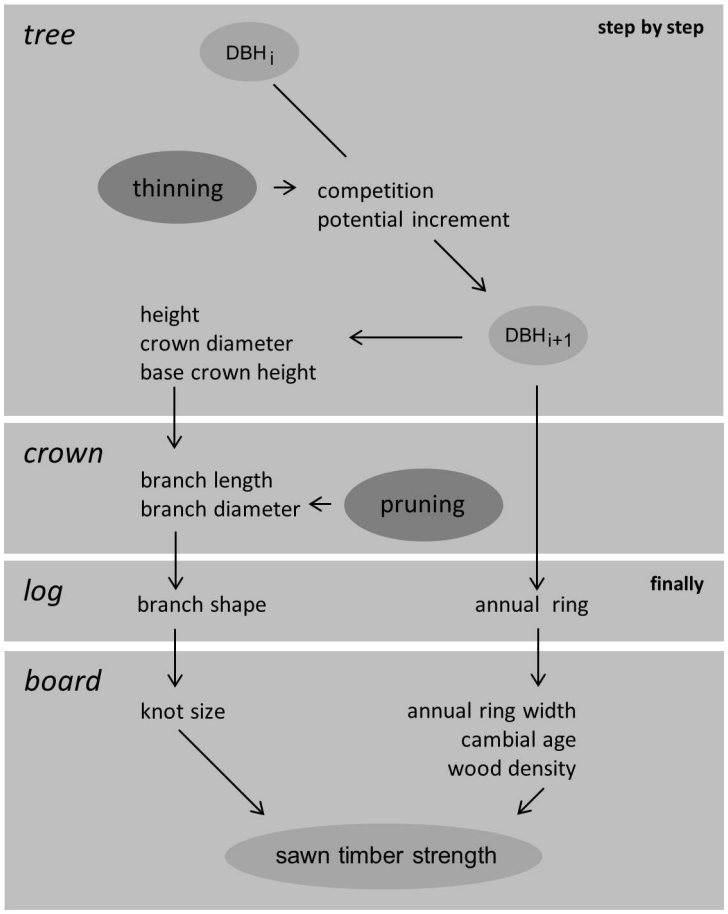

Fig. 1. Simulation of individual tree growth, finalised by logging and sawing; tree and crown components are computed within each time step; thinning and pruning are optional and occasional.

2.2 DBH growth

Potential DBH growth depends on DBH through a unimodal function. Each annual step of growth prediction multiplies potential growth by competition as based on local density, local DBH dominance and local mean neighbour distance. Local density is expressed through stand density index (SDI) (Reineke 1933; Pretzsch and Biber 2010). While potential growth was taken from a quantile regression over stem disk data, the parameters for competition were calibrated using individual tree plot inventory data. Therefore, growth initially was computed based on local SDI within 2.5 fold crown radius alone. In a second step, a regression was applied to both, mean neighbour distance and central tree dominance within 10 m radius as expressed by relation of DBH to the quadratic mean stem diameter of the nearest neighbour trees. When predicted growth was computed during simulation the remaining residuals were randomly drawn from a normal distribution and added after competition had been taken into account. Growth reconstruction guides DBH growth within quantiles of the DBH growth to DBH distribution based on stem disk data.

2.3 Height, crown and branch growth

Predicted tree height depends on tree DBH as controlled by stand biological age. Within the current model the relation was separately parameterised for each planting density. In the basic

version it was considered as independent on early stand density. Reconstructed height is most simply the setup height divided by setup age. Crown shape is built of convex hulls of circular cross-section (cylindric shadow crown and paraboloid light crown). Crown size and base height are computed via allometric relation from stem size. A whorl is generated and appended to the top of stem each time tree height was computed. It has six equal sized branches at regular radial position that originate from the stem vertical axis at identical height and vertical angle. The angle of the branch to the stem axis is close to 90 degrees within the part of the stem that is sawn to logs. Branch diameter is determined by distance of branch origin to crown mantle and an empirical regression between diameter and length. It is computed as long as the whorl is surrounded by the crown and is kept constant at its last computed value if the whorl position is below crown base. Hence, all branches of a whorl are equal in length and diameter and the size of each is inferred from the same idealised circular crown cross section based on a regression through measured data. While the process of branch mortality within the live crown part is not explicitly described, it is represented by its effect on the average branch size at a vertical position. Below the allometrically calculated crown base any branch is assumed to be dead. The following sections explain the algorithms in detail. Table 1 and Table 2 associate parameter values and parameterisation sample sizes to each equation.

2.4 DBH growth details

The equation used for potential growth is the Hugershoff growth function (Hugershoff 1936) that is commonly used to describe the relation between diameter and growth in annual ring data analysis. It is given by Eq. 1:

$$p_q = a_{10} \times d^{a_{11}} \times e^{(-a_{12} \times d)} \quad (1)$$

where p_q is a q-quantile (%) at a given diameter d (equation by Hugershoff 1936), and a_{10} to a_{12} are parameters (a_0 to a_2 in Table 1). Within the scope of this work it was adapted to DBH growth by DBH pairs from stem disks via a 95% quantile regression. Growth prediction is based on the 95% quantile that is reduced by a competition coefficient of local density, neighbour distance and dominance as shown in Eq. 2:

$$\Delta d(d) = p_{95}(d) \times e^{a_{20} + a_{21} \times S} \times \left(a_{22} + a_{23} \times \overline{D} + a_{24} \times \left(d - \overline{d}\right)\right) \quad (2)$$

where $\Delta d(d)$ is growth at diameter d, S is SDI (Pretzsch and Biber 2010; Reineke 1933), $\overline{D}$ is mean distance of nearest neighbours, $\overline{d}$ is the quadratic mean stem diameter of nearest neighbours [cm] and a_{20} to a_{24} are parameters (a_0 to a_4 in Table 1). Nearest neighbour range is within a radius of 10 m around the central tree.

During reconstruction the model uses a reduced set of equations, as outlined in the following. Crown closure marks the onset of competition in the early phase of stand development. It is defined as mechanical contact between crown bases and is based on planting pattern as well as an assumed crown diameter to DBH ratio. As the course of competition in the past is not known, even competition determined DBH growth is immediately based on the Hugershoff equation and computed from additional quantiles defined by the same parameterisation data set as potential growth in prediction. Before crown closure it follows a quantile regression of level 50%. After crown closure it proceeds between quantiles of growth (p_q, Eq. 1), as illustrated by Fig. 2. In detail it is based on coarse diameter approximations summing up p_q over the number of time steps from 1 to n, where n corresponds to the start year of growth prediction (t_0). The resulting diameter approximations

Table 1. Equations of DBH growth given with parameterisation sample size and parameter values.

algorithm		equation	number	specification	sample size	a_0	a_1	a_2	a_3	a_4
growth quantile	[cm yr^{-1}]	$p_q = a_0 \times d^{a_1} \times e^{(-a_2 \times d)}$.	1	q=95	2,080	1.02	0.324	0.028		
				q=50	2,080	0.693	0.328	0.04		
				q=5	2,080	0.382	0.301	0.049		
predicted DBH growth	[cm yr^{-1}]	$\Delta d(d) = p_{95}(d) \times e^{a_0 + a_1 \times S}\left(a_2 + a_3 \bar{D} + a_4 \left(d - \bar{d}\right)\right)$.	2	any	5,713	–0.348	–0.0004	–0.038	0.181	0.032
reconstructed DBH growth at given DBH (d)	[cm yr^{-1}]	$\Delta d(d) = p_1(d) \times \alpha + p_0(d) \times (1 - \alpha)$.	3							
growth corridor (lower)		$p_0 = p_5$ and $p_1 = p_{50}$ if $P_{5,n} \le d_{t0} < P_{50,n}$.	4							
growth corridor (higher)		$p_0 = p_{50}$ and $p_1 = p_{95}$ if $P_{50,n} \le d_{t0} < P_{95,n}$.	5							
weight		$\alpha = \frac{d(t_0) - L_0}{L_1 - L_0}$ where $L_0 = \sum_{i=1}^{n} p_{0,i}$ and $L_1 = \sum_{i=1}^{n} p_{1,i}$.	6							

d = diameter at breast height (DBH, 1.3 m) [cm]

$\bar{D}$ = mean distance of nearest neighbours [m]

Nearest neighbour range is within a radius of 10 m around the central tree.

S = local stand density index within 2.5 × crown radius

$\bar{d}$ = quadratic mean stem diameter of nearest neighbours [cm]

p = growth quantile

α = weight

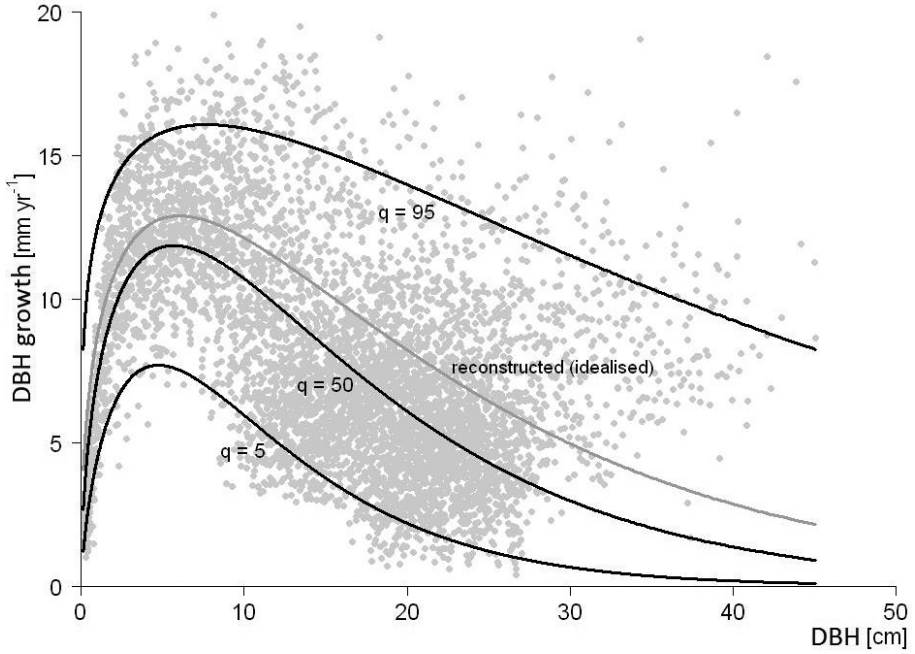

Fig. 2. Exemplary DBH growth reconstruction inferred from a first inventory DBH larger than the one resulting from the corresponding time integral over the 50% quantile; reconstructed growth is drawn in grey (idealised as 75% quantile); guiding quantiles q are drawn in black (5%, 50% and 95%).

will be named $P_{q,n}$ in the following, e.g. $P_{50,n}$ for estimation from the 50% quantile. The estimated *Δd(d)* is controlled by a weight α as shown in Eq. 3:

$$\Delta d(d) = p_1(d) \times \alpha + p_0(d) \times (1 - \alpha) \tag{3}$$

where p_0 and p_1 define a growth corridor as either

$$p_0 = p_5 \text{ and } p_1 = p_{50} \text{ if } P_{5,n} \le d_{t0} < P_{50,n} \tag{4}$$

or

$$p_0 = p_{50} \text{ and } p_1 = p_{95} \text{ if } P_{50,n} \le d_{t0} < P_{95,n} \tag{5}$$

and weight α is defined as

$$\alpha = \frac{d(t_0) - L_0}{L_1 - L_0} \text{ and } L_0 = \sum_{i=1}^{n} p_{0,i} \text{ and } L_1 = \sum_{i=1}^{n} p_{1,i} \; . \tag{6}$$

Thus, Fig. 2 would correspond to a case where Eq. 5 was applied and α was at around 0.2. A final reconstruction step stretches or shrinks each DBH increment by identical factor, i.e. the ratio of measured diameter at simulation start to diameter resulting from the reconstructed increments of Eq. 3.

2.5 Height, crown and branch growth details

Tree height in prediction was computed from DBH via the Michailov stand height curve (Michailoff 1943). To describe the relation of height to DBH as dependent on stand biological age, both parameters of the Michailov curve were controlled by stand quadratic mean stem diameter (QMD) via linear regression functions as given by Eq. 7:

$$h = h_0 + \left(a_{30} + a_{31} \times d_g\right) \times e^{\frac{a_{32} + a_{33} \times d_g}{d}} \quad (7)$$

where h is tree height, h_0 is breast height (const = 1.3 m), d_g is QMD, d is diameter at breast height, and a_{30} to a_{33} are parameters (a_0 to a_3 in Table 2). Crown allometry (Eq. 8, 9) was implemented as in the SILVA individual tree simulator (Pretzsch et al. 2002). Crown base height is defined as

$$\mathcal{B} = h \times (1 - e^{a_{40} + a_{41} \times \frac{h}{d} + a_{42} \times d}) \quad (8)$$

where h is tree height, d is diameter at breast height, and a_{40} to a_{42} are parameters (a_0 to a_2 in Table 2). Crown diameter is given as

$$\mathcal{C} = a_{54} \times e^{a_{50} + a_{51} \times \ln(d) + a_{52} \times h + a_{53} \times \ln\frac{h}{d}} \quad (9)$$

with variable definitions h, d as in Eq. 8 and parameters a_{50} to a_{54} (a_0 to a_4 in Table 2). Branch diameter is coupled to crown diameter through a linear relationship:

$$\mathcal{d} = a_{62} \left(a_{60} + a_{61} \times \mathcal{l}\right). \quad (10)$$

In Eq. 10 $\mathcal{d}$ and $\mathcal{l}$ are branch diameter and length and a_{60} to a_{62} are parameters (a_0 to a_2 in Table 2). Time of crown closure is based on a crown diameter and estimated age at DBH = 5 cm as well as the planting pattern that determines the tree size when crowns touch. Crown base height is at zero before canopy closure. It is interpolated between canopy closure and start of the prognosis part of simulation along DBH via a curve that is initially linear and gradually transitions into the crown base height equation of SILVA (Pretzsch et al. 2002) that implies a strong and positive influence of the height to diameter ratio.

2.6 Computation of board strength from board internal structure

Within the current model version board strength computation uses cambial age to distinguish between juvenile and mature timber. Moreover it is based on two criteria for knot impact of the biggest branch in board, i.e. (1) the ratio of knot to board cross-sectional area (total knot area ratio, tKAR) of British Standard BS 4978 (2007) and (2) the DEK value from German standard DIN 4074-1 (2012) that is defined as the largest ratio among all knots of the minimal surface knot diameter to the side width of the board on which the knot is visible. Parameterisation depends on whether cambial age is more or less than 20 years. Wood density computation at board level uses Eq. 11:

$$\rho = a_{70} \times e^{\frac{-a_{71}}{\mathcal{A}}} + a_{72} + a_{73} \times \mathcal{W} \quad (11)$$

where $\mathcal{A}$ is the mean cambial age and $\mathcal{W}$ is mean ring width of the board. The parameter set a_{70} to a_{73} is named a_0 to a_3 in Table 2. Board strength is coupled to Eq. 11 as given by Eq. 12:

Table 2. Equations of tree height, crown shape, branch size and board strength given with parameterisation sample size and parameter values.

algorithm		equation	number	specification	sample size	a_0	a_1	a_2	a_3	a_4
height	[m]	$h = h_0 + \left(a_0 + a_1 \times d_g\right) \times e^{\frac{a_2 + a_3 \times d_g}{d}}$	7	P = 1,000	866	–4.33	1.27	–4.21	–0.155	
				P = 2,000	1,579	–0.27	1.29	–2.80	–0.20	
				P = 4,000	865	2.65	1.34	–2.00	–0.24	
crown base height	[m]	$\mathcal{B} = h \times (1 - e^{a_0 + a_1 \times \frac{h}{d} + a_2 \times d})$	8	any	3,599	0.630	–0.944	–0.0122		
crown diameter	[m]	$\mathcal{C} = a_4 \times e^{a_0 + a_1 \times \ln(d) + a_2 \times h + a_3 \times \ln\frac{h}{d}}$	9	any	594	0.597	0.0845	0.0340	–0.887	1.25
branch diameter	[mm]	$\mathcal{d} = a_2 \left(a_0 + a_1 \times \ell\right)$	10	any	991	4.78	8.68	1.2		
wood density	[kg m^{-3}]	$\rho = a_0 \times e^{\frac{-a_1}{\mathcal{A}}} + a_2 + a_3 \times \mathcal{W}$	11	any	802	162	39.9	494	–7.11	
bending strength	[N mm^{-2}]	$s = a_0 + a_1 \times \rho + a_2 \times \mathcal{E} + a_3 \times \mathcal{A} + a_4 \times \mathcal{K}$	12	$\mathcal{A} \leq 20$	606	–32.0	0.150	–18.3	0.504	–21.3
				$\mathcal{A} > 20$	103	–45.0	0.175	–5.43	0	–3.64
wood density [1]	[kg m^{-3}]	$\rho = a_0 + a_1 \times \mathcal{W} + a_2 \times \mathcal{D}$	13	any	802	515	–10.7	2.28		
bending strength [1]	[N mm^{-2}]	$s = a_0 + a_1 \times \rho + a_2 \times \mathcal{E} + a_3 \times \mathcal{D} + a_4 \times \mathcal{T}$	14	any	709	–45.22	0.18	–10.69	0.53	–25.81

[1] basic Version

h_0 = breast height, const = 1.3 m

d = diameter at breast height (DBH) [cm]

d_g = quadratic mean stem diameter (QMD) [cm]

ℓ = branch length

P = planting density

$\mathcal{A}$ = mean cambial age of board

$\mathcal{W}$ = mean ring width of board

$\mathcal{E}$ = DEK of biggest branch in board (DIN 4074-1, DIN 2012)

$\mathcal{K}$ = tKAR (BS 4978, 2007)

$\mathcal{D}$ = distance from pith of board cross-sectional centre

$\mathcal{T}$ = top diameter of log

$$s = a_{80} + a_{81} \times \rho + a_{82} \times \mathcal{E} + a_{83} \times \mathcal{A} + a_{84} \times \mathcal{K} \quad (12)$$

where $\mathcal{E}$, $\mathcal{A}$, $\mathcal{K}$ are DEK, mean cambial age and tKAR and a_{80} to a_{84} are parameters (a_0 to a_4 in Table 2). In the basic model version board strength merely relies on distance from pith and DEK as inner structural properties and outer grading criteria, i.e. trunk diameter:

$$\rho = a_{90} + a_{91} \times \mathcal{W} + a_{92} \times \mathcal{D} \quad (13)$$

$$s = a_{100} + a_{101} \times \rho + a_{102} \times \mathcal{E} + a_{103} \times \mathcal{D} + a_{104} \times \mathcal{T} \; . \quad (14)$$

Variables $\mathcal{W}$ and $\mathcal{E}$ are defined as in Eq. 11 and 12 and according conventions apply to parameters a_n in Table 2. $\mathcal{D}$ is distance from pith at the board cross-sectional centre and $\mathcal{T}$ is the top diameter of the enclosing log. Individual board strength is computed by the structural properties of the board cross sectional area within the stem disk taken at median vertical position of the log under consideration. The annual rings and the branch projections from the whorl of biggest branch diameter within the log are intersected with a diameter dependent sawing pattern. While the horizontal angle between neighbouring branches within a whorl is fixed to 60°, the rotational position of each whorl is set by random drawing from an equal distribution between 0° and 360° when the inner structure of the log is constructed. A typical stem cross section from simulation of a pruned future crop tree with board positions and resulting knot interference is illustrated in Fig. 3. The crucial difference between the current model and the basic model is summarised in Table 3.

2.7 Site properties

Two sites were investigated. One is named Heigenbrücken and is located in the Spessart region southeast of Frankfurt. It is marked by a deep root horizon and rather moist climatic conditions. The other is near Ansbach west of Nuremberg. It is marked by a comparatively shallow root zone

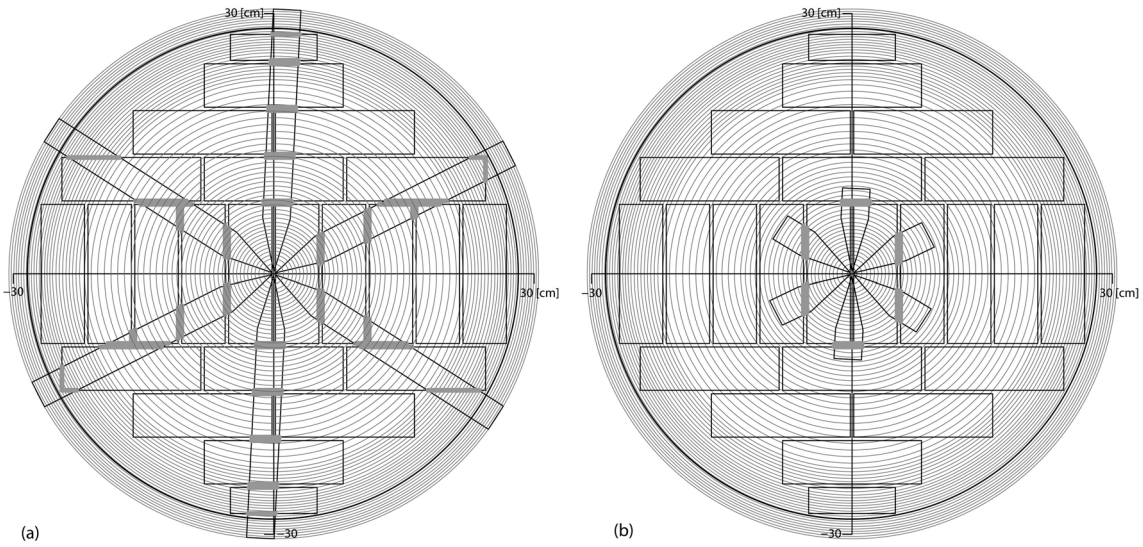

Fig. 3. Inner structure of boards resulting from application of a sawing pattern to simulated branches and annual rings from a stem 60 cm in diameter; if branches not pruned (a) and if pruned (b).

Table 3. Crucial algorithm alternatives implemented in basic (B) and current (C) version.

category of algorithm	focus of algorithm	presumed impact on board strength through	alternatives	version	
				B	C
evaluation of timber strength	structure to board strength	board strength	distance from pith, DEK[1]	x	
			juvenile and mature by cambial age, tKAR[2]		x
calibration of allometry	measured tree heights to parameters of height curve	dynamics of H/D ratio crown base height branch growth	generalist	x	
			planting density specific		x

[1] knot value from DIN 4074-1 (2012)
[2] total knot area ratio from BS 4978 (2007)

due to a clay barrier layer. While to a stand age of 20 it was better in productivity, to an age of 30 it was equal and to an age of 40 it was markedly weaker. Site conditions as taken from Rais et al. (2014b) are presented in Table 4. Both sites are subject to systematic long term observation backed by regular data collection and permanent data maintenance. The individual tree inventory on all plots had started in 1989 at age 19 (setup inventory) and had been repeated at five year time step. Within the scope of this paper the sites will comprehensively be referred to as Favourable and Dry respectively.

Silvicultural treatment aimed to select trees from the mature stand and preserve them for future production of high quality sawn timber. The future crop tree system (1) initially marks individuals for future preservation minimising mutual competition between them and (2) in the neighbourhood of each future crop tree removes the strongest competitors that are non-future crop trees. On the experimental sites of this work an exponentially falling guide curve defined the minimum count of live trees to maintain per unit stand area as dependent on dominant tree height (Kenk and Hradetzky 1984; Klädtke et al. 2012). Stand density was guided through control and thinning at each 3 m step along the curve that started from 2000 ha^{-1} at a height of 12 m, via 700 ha^{-1} at 21 m and 250 ha^{-1} at 36 m, reaching close to the asymptote of 160 ha^{-1} at 48 m.

Table 4. Soil and climate properties of the experimental sites.

property		Ansbach shallow, dry, poor (Dry)	Heigenbrücken moist, fertile (Favourable)
location	AMSL (m)	460	415
	coordinates	49°13′N, 10°33′E	49°59′N, 09°22′E
climate in growing season 1st of May to 30th of September	temperature (°C) [1)]	15.6±0.4	15.3±0.5
	precipitation (mm) [1)]	346±106	379±41
soil	type	sand (SI)	loamy sand (IS)
	depth (cm)	30	> 200

[1] values based on the climate between the years 1998 and 2008

2.8 Parameterisation data

Stem disk data from the site of higher and more general growth potential were preferred for parameterisation while the sample from the dryer site was still investigated for representation of dominant trees (sampling restricted to non-future crop trees). For the main focus of the analysis, exclusively growth parameters of site Favourable were used based on 60 individuals that had been felled in winter 2011 to sample stem disks and detailed data of crown size, branch length and diameter. The same trees were used for the calibration of competition and growth residuals based on the individual tree inventory data. Growth parameters of 100 trees sampled on site Dry were exclusively used for a preceding sensitivity analysis of tree growth prediction. Computation of board strength from internal board structure was parameterised including the tree samples from both sites. Measured strength had been taken from 998 centre boards and 936 side boards. Details are given in Rais et al. (2014a).

2.9 Model setup data

Simulation and evaluation then focused on the rather poor site Dry. The current model version and the basic version both were run on the same set of plots. Setup DBH was taken from the setup inventory, while tree height, crown diameter and crown base height were based on DBH via the relations found on the parameterisation site. Given by planting density per ha (in parentheses), the number of undisturbed selected plots, each 30m by 30m in size, was 6 (1000 ha^{-1}), 5 (2000 ha^{-1}), 3 (4000 ha^{-1}). Table 5 presents the corresponding stand properties at simulation start.

2.10 Model evaluation on measured board strength

To evaluate the quality of prognosis, bending strength of boards was the criterion used. A sample of non-future crop trees of DBH > 25 cm had been taken in winter 2010/2011 (Rais et al. 2014a), i.e. given by planting density in parentheses 50 (1000 ha^{-1}), 38 (2000 ha^{-1}) and 16 (4000 ha^{-1}) at site Favourable and 14 (1000 ha^{-1}), 30 (2000 ha^{-1}) and 16 (4000 ha^{-1}) at site Dry. Accordingly, simulations were run from an age of 19 at setup inventory (referred to as an age of 20 for convenience) to an age of 40 (2010). As virtual sawing was time expensive, the result set of simulated felled trees was reduced to a random sample of 20 to 30 at maximum per plot, stratified by DBH after preselection by DBH > 25 cm. Simulated plots where thinned exactly as it had been recorded within the long term observation database on the individual tree level. Simulation ended with a

Table 5. Stand properties in simulation setup for the evaluation of model versions; stand characteristics from survey 1989.

stand property	planting density (ha^{-1})					
	Heigenbrücken (Favourable)			Ansbach (Dry)		
	1000	2000	4000	1000	2000	4000
QMD (cm)	15	14	12	17	14	13
absolute number of trees	373	1286	1094	497	829	579
absolute number of future crop trees	86	155	108	84	70	44
total area (ha)	0.45	0.81	0.45	0.54	0.45	0.27
number of stems (ha^{-1})	829	1588	2431	920	1842	2144
corresponding number of future crop trees (ha^{-1})	191	191	240	156	156	163
basal area (m^2 ha^{-1})	15	24	25	20	27	26

clearcut but exclusively non future crop trees were selected for virtual sawing. Thus, the number of simulated sawn trees was reduced to around 20 in all plots. Eventually, the number of trees per planting density by site Dry and Favourable respectively was 66 of 108, 72 of 128 (1000 ha^{-1}), 112 of 173, 85 of 105 (2000 ha^{-1}) and 78 of 85, 50 of 52 (4000 ha^{-1}) co-dominant and dominant non future crop trees. As no future crop trees were included, pruning had neither been applied to the real nor to the simulated trees. All simulations applied the same crosscutting to stems as it was used for the sampled trees, starting at breast height (1.3 m) with each log of length 4.1 m (Rais et al. 2014a).

2.11 Model evaluation on long term prognosis

In order to assess the long term effect of the modifications within a whole rotation period, both current version and basic version were run to a stand age of 70 and final clearcut. Thinning in that case was simulated in accordance to the guide curve. Pruning was simulated as it had occurred in the real plot at a top height of 15 m up to a maximum height of 6 m and comprised only branches below crown base and the first whorl above the base of the crown. For virtual sawing, all result trees were pooled by planting density. A sample of 20 trees at maximum, stratified by DBH, was taken from all felled trees per decade, resulting in a total of around 100 per planting density taken from roughly 600.

2.12 Result analysis

To evaluate precision and transferability of individual tree growth prediction, simulated and observed time course of quadratic mean stem diameter (QMD) and total tree volume on the 2000 ha^{-1} planting density plots were compared. Total volume was calculated as sum of all individual tree volumes. Individual tree volume was approximated by the Denzin formula (Graves 2013) given in Eq. 15.

$$v = \frac{d^2}{1000} \times \left[1 + 0.03 \times (h - 30)\right] \tag{15}$$

where v [m^3] is tree volume d [cm] is diameter at breast height (1.3 m) and h [m] is tree height. When simulation results were compared to measured data, statistical analyses of board strength by planting density were confined to boards of a cross sectional area larger or equal 50 cm^2 in accordance to the sampling method that had concentrated on strong boards. They were conducted using the statistical software R (R core team 2014). Probability distributions were compared (1) visually through box plots, (2) by confidence interval of estimated median (3) the post-hoc Tukey HSD test (Miller 1981) based on the results of a preceding analysis of variance (Chambers et al. 1992). In the result section, (1), (2) and (3) will be denoted as VIS, CIM and HSD. The functions used were boxplot {graphics} with default options for the ranges shown (box marks interquartile range, IRQ), boxplot.stats {grDevices} and TukeyHSD with aov {stats}. In addition mean bias (MBE) and mean absolute bias (MABE) of board strength statistics where given and constructed by bootstrapping (Efron 1979; Davison and Hinkley 1997) to extrapolate on iteration of the whole model test. Both were computed from 1000 resamplings with laying back and their confidence intervals estimated nonparametrically by 100 resamplings of the resulting bias collection using boot {boot} from R (Davidson and Hinkley 1997; Canty and Ripley 2014). MBE and MABE were expressed as difference between simulated and measured data statistics. Criterion of significance in general was an α level of 5%. For better comparability to 40 year results, the box plot evaluations of board strength from 70 year simulations used the same restriction to minimum board cross sectional area ($\geq$ 50 cm^2).

3 Results

QMD as well as total tree volume of the 2000 ha^{-1} planting density plots were plausibly reproduced by the model over time of test prognosis from age 20 to 40 (Fig. 4). Moreover, the 2.5% and 97.5% quantiles of simulated DBH were close to the observed range (large dots). Similarity was high in particular if site specific parameters of potential growth had been used at site Favourable (Fig. 4 A). Diameter and volume growth over the last ten years were overestimated if the parameter set of site Favourable was applied to site Dry (Fig. 4 C).

Centre board bending strength at age 40 and grouped by planting density had median values in the range from 20 to 35 Nmm^{-2} (Fig. 5, Fig. 6). Interquartile ranges of measured board strength reached from 12 to 20 Nmm^{-2} while the ranges computed from real board structure or simulated by the model were smaller and lay between 6 and 10 Nmm^{-2}. At the parameterisation site (Favourable), as Fig. 5 A illustrates, measured bending strength significantly increased with initial planting density (HSD). Median strength computed on measured board structure (Fig. 5 B and Table 6, MBE) also was dependent on planting density with a significant increase (HSD). At 2000 ha^{-1} it deviated from the measured board bending strength by –6% to +4% and at 4000 ha^{-1} by –25% to –2% (CIM). Median bending strength as simulated by the current model version (Fig. 5 C and Table 6) was somewhat lower than measured (–21% to –5%) at planting densities of 1000 and 2000 ha^{-1} and underestimated by –28% to –12% (CIM), at a planting density of 4000 ha^{-1}. It was similar (VIS) in the interquartile ranges to the strength data computed on real board structure. The increase of both computed and simulated board strength median with planting density was significant (HSD).

At the test site (Dry) real board strength (Fig. 6 A) showed a considerable and significant shift from 1000 to 2000 ha^{-1} (CIM) but only a trend of increase between 2000 and 4000 ha^{-1} as indicated by a difference in distribution skewness (VIS). The median of simulated bending strength was close to the measured one at 1000 and 4000 ha^{-1} (Fig. 6 B) but underestimated the one at 2000 ha^{-1} planting density (VIS, Table 7). As compared to median measured bending strength it had a more linear relation to the early stand density (VIS, CIM), similar to the measured and simulated strength median at the site of parameterisation. In contrast, the basic model version (Fig. 6 C, Basic Version) significantly underestimated board strength at 2000 and 4000 ha^{-1}. Its median board bending strength showed no significant increase with initial planting density (VIS). Moreover, it was marked by a notably more underestimated variability.

Cambial age that is a predictor of bending strength in the current model increased in simulated as well as in measured boards and by a similar amount along planting density (CIM). Distance from pith that had originally been used to differentiate between juvenile and mature wood underestimated the age of boards from the 4000 ha^{-1} plots by more than 14 ± 4% both in measured and simulated data. Radial board position did only to a part reflect the variability of board cambial age as could be shown by its unprecise prediction of age with a relative residual standard deviation as large as 20%. While in the current model crown base height at simulation start in line with height to diameter ratio significantly and realistically increased along planting density from 3 m (1000 ha^{-1}) to 6 m (4000 ha^{-1}), in the earlier model approach it markedly decreased in median from 7 m to 3.5 m (site Dry, representative plots 9, 8, 3). If height to diameter allometry had been calibrated as dependent on planting density, the main underlying variable that is mean tree height like in reality was around 12 m and suggested a slight increase of around 1 m from the lowest to the highest planting density. In the basic model it ranged from 17 m down to 12 m. Concomitantly, the mean biggest branch diameter from each of the two bottom logs (height to 9.5 m) decreased along planting density in the current model (41.6 ± 0.3 mm down to 31 ± 0.6 mm) as well as in reality (36.8 ± 0.9 mm down to (27.9 ± 1.5 mm), while in the earlier basic approach the slope of the relation was slightly positive (31.9 ± 0.4 mm to 34 ± 0.6 mm). Hence, the realistic dependence

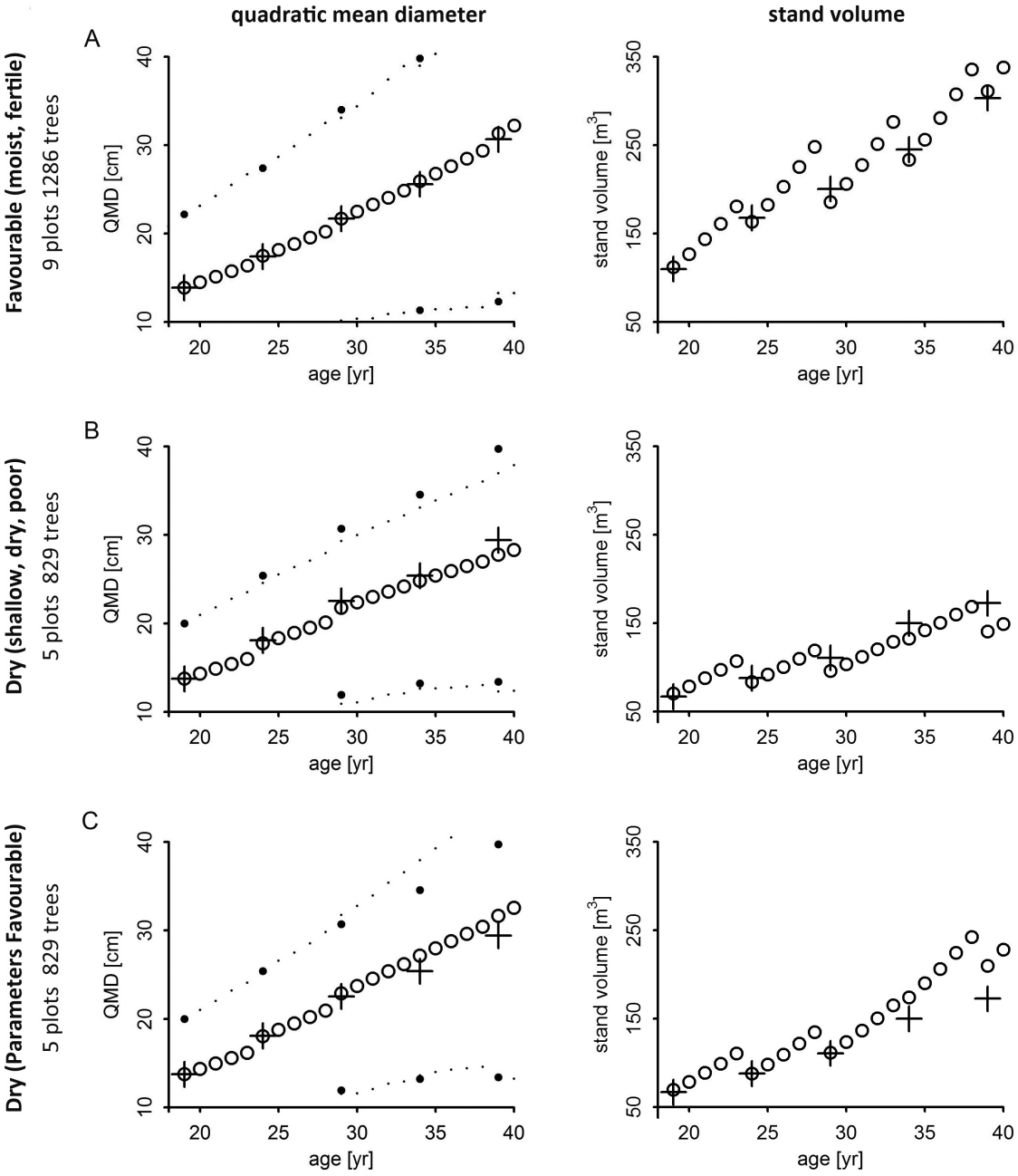

Fig. 4. QMD, DBH quantiles (2.5% and 97.5%) and total tree volume by site using site related parameterisation (rows A, B) and parameters from site Favourable on site Dry (row C); measured data mean given as +.

of board bending strength on planting density in the current model was related to a corresponding sensitivity of underlying board, stem and crown structure key properties.

Over a whole rotation period, the board strength distribution of all trees removed, including the final clearcut, still differed in median and width between current version and basic version if compared at equal planting density (VIS, CIM, Fig. 7). The positive trend from smallest to highest initial density in the result of the current model version was retained (CIM). Board strength resulting from the basic model version is similarly unaffected by the planting density at plot foundation as at age 40 and has a remarkably smaller interquartile range (VIS).

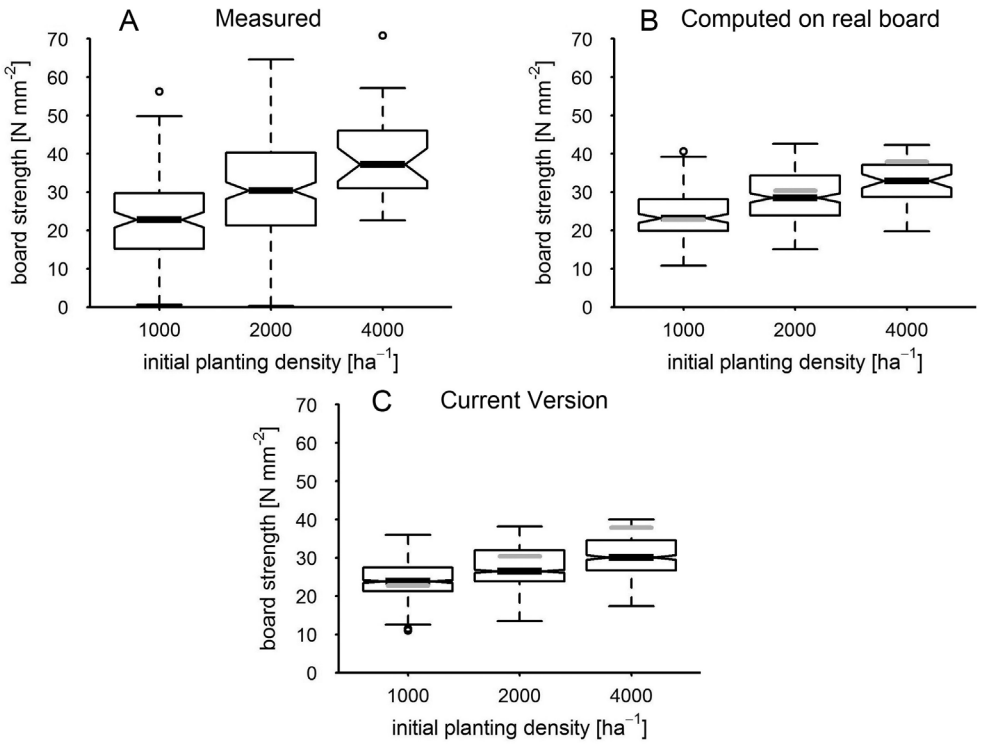

Fig. 5. Board strength at parameterisation site by planting density after 40 years as measured (A), as computed based on sample board structure (B) and as simulated by the current version; the boxplot notches correspond to the 95% confidence interval (CI) of the median; grey horizontal lines mark the median of measured data in diagrams of simulated result distributions.

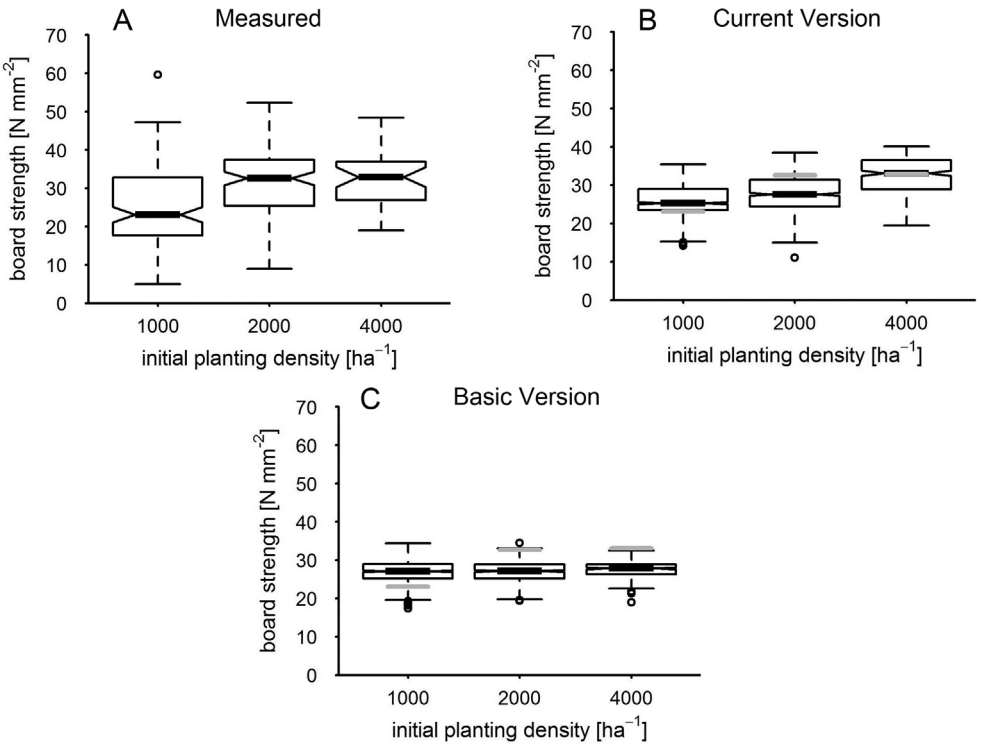

Fig. 6. Board strength by planting density at site Dry after 40 years as measured and as simulated by current and basic version. Grey lines mark the median of measured data; the boxplot notches correspond to the 95% confidence interval (CI) of the median; grey horizontal lines mark the median of measured data in diagrams of simulated result distributions.

Table 6. Bias of real board at parameterisation site Favourable (Fav) given as CI range of bias (Nmm^{-1}) by planting density (ha^{-1}), top row as computed from real board (com), bottom row as simulated (sim).

set	variable	mean			median			Q_1			Q_3		
		1000	2000	4000	1000	2000	4000	1000	2000	4000	1000	2000	4000
Fav com	MBE	1.13	–1.55	–6.96	–0.03	–1.63	–4.55	5.08	2.93	–3.94	–1.79	–6.12	–8.43
		0.99	–1.71	–1.71	–0.25	–1.80	–4.82	4.91	2.67	–4.26	–2.05	–6.35	–8.78
	MABE	1.30	1.74	6.94	1.34	1.89	4.81	5.06	2.95	4.34	2.22	6.32	8.80
		1.18	1.62	6.73	1.20	1.74	4.62	4.92	2.73	4.06	2.01	6.12	8.46
Fav sim	MBE	1.33	–3.15	–8.92	0.61	–3.69	–7.72	6.23	2.8	–5.91	–2.23	–8.42	–10.9
		1.22	–3.27	–9.1	0.39	–3.86	–7.95	6.06	2.57	–6.24	–2.36	–8.59	–11.2
	MABE	1.43	3.27	9.11	1.50	3.83	7.96	6.20	2.83	6.23	2.38	8.58	11.2
		1.30	3.15	8.92	1.38	3.69	7.76	6.08	2.61	5.91	2.22	8.41	10.9

Table 7. Bias of modelled board strength as CI range of bias (Nmm^{-1}) by planting density (ha^{-1}) at site Dry.

set	variable	mean			median			Q_1			Q_3		
		1000	2000	4000	1000	2000	4000	1000	2000	4000	1000	2000	4000
Dry sim	MBE	1.45	–4.77	–0.35	2.21	–4.84	0.43	6.1	–1.56	1.55	–3.9	–6.23	–0.51
		1.34	–4.89	–0.51	1.95	–5	0.23	6	–1.7	1.35	–4.05	–6.4	–0.78
	MABE	1.54	4.89	1.08	2.53	4.99	1.3	6.1	1.86	1.98	4.03	6.39	1.3
		1.41	4.74	0.98	2.31	4.85	1.16	6	1.69	1.83	3.9	6.25	1.44

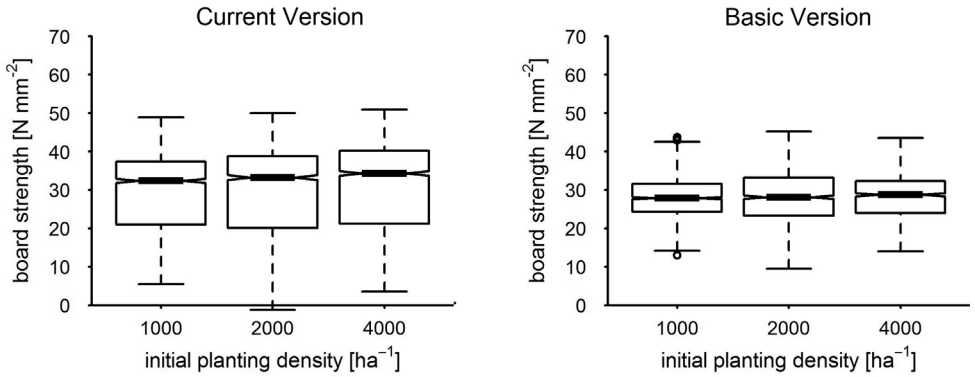

Fig. 7. Board strength by planting density of the current version versus basic version at age 70; the boxplot notches correspond to the 95% confidence interval (CI) of the median.

4 Discussion

As demonstrated by detailed model comparison, sensitivity of centre board bending strength to planting density was based on selective and plausible refinement of crucial model aspects. The final drop and bias of simulated growth in the course of test prognosis at site Dry was likely due to some underestimation of potential QMD increase and determined by an underrepresentation of dominant trees within the stem disk sample. If site dependence of potential growth is accounted for, the model toolbox may be applied as an extensible streamlined simulator to support the expert in estimating the trend of management effects. Variability as currently predicted by the model was lower as compared to measured data. Hence, at the current state of development it is recommendable (1) to discuss the sensitivity of scenario evaluations to an estimated bias of variability or (2) to parameterise a random generator for residual deviation and to add its result to strength on the individual board level.

At the site of parameterisation, measured board strength significantly increased with initial planting density, an effect that could be reproduced by the model due to a refined sensitivity to cambial age and crown structure. The lower real growth potential and a resulting higher cambial age of sample boards at site Dry were a likely determinant of underestimated strength at intermediate planting density and overemphasis of the linearity within the strength to density relation. As potential growth data at the dryer site were still to be verified, the effect has yet to be proven.

The improvement of board structure to bending strength computation had a major influence on board strength median and variability even after a whole rotation period. There is considerable potential in further refinement of structure to strength translation that lead to a markedly similar and underestimated data spread when it was both applied to real and simulated boards.

4.1 Extension of the structure to board strength computation had a strong effect

The importance of a board specific strength calculation is likely due to the fact that for softwood species the majority of the total variation of strength is attributed to differences between boards within a log (Moore et al. 2013). In detail, a significant positive effect on the quality of strength prediction from stem and board structure may certainly be attributed to the consideration of cambial age that is a major determinant of board strength in conifers (e.g. DeBell et al. 2004; Torquato et al. 2014). This likely holds also true for deciduous tree species, due to a general effect of wind on bending and fibre direction within the stems of young trees.

However, one likely improvement within the current version as compared to the basic one also was to take into account the relative area covered by the branch within the cross sectional area of the board. The used knot value tKAR ("total knot area ratio") is defined by the British Standard BS 4978 (2007) and is one of the most important visual knot parameters in sawn timber strength grading (Stapel and Van de Kuilen 2014). An analysis of the individual factors which are most relevant for strength prediction quality might be interesting within the scope of a separate study.

The approaches tried within this work were restricted to macroscopical wood and board properties. They did not include effects on the microscopic scale, e.g. the impact of wind pressure on fibre direction. Forest management controls stand density through planting pattern or thinning. Hence, it will likely take influence on the aerodynamic regime, on stem bending and fibre direction and eventually on bending strength of sawn timber. An interesting question of further model analysis could be, whether there is significant improvement, if bending effects are taken into account, e.g. by including results from fibre direction modelling (Lang and Kaliske 2013).

4.2 Density related H/D allometry is an important indicator of early juvenile competition

Control of tree height parameterisation through planting density strongly improved the prediction of board bending strength. It still had a remarkable influence over a whole rotation period, even if some of the effect of generalised height parameterisation in the basic model was attenuated due to the convergence of relative crown base height in the long term. Reconstruction of early tree development exclusively based on the planting pattern and the state of the already established stand is an essential component of wood quality simulation: As exemplarily measured tree heights and crown base heights at the age of prognosis start indicate, stand density during the early phase of stand development has slightly promoted tree height and considerably suppressed diameter growth as also found by Saha et al. (2012). When a common stand height curve calibration was used for all plots without taking into account initial planting density as a grouping criterion, trees on plots of smaller planting density and larger QMD were falsely assigned a larger height than on plots of higher initial density. The height to diameter ratio is an obvious criterion of preceding early neighbour competition, especially in the juvenile phase of stands (Pretzsch and Rais, submitted), and also was applied to crown dimensions within the scope of this study. Hence, decreasing stand density in the basic model promoted crown base height, reduced branch diameters and raised board strength to an unrealistic level. When stand height curve parameterisation was grouped by planting density, the clearly furthering effect of planting density on crown base height was correctly reflected, as the crown model taken from Pretzsch et al. (2002) is sensitive to early competition via the H to D ratio. The crown dimension model goes in line with e.g. results given by Mäkinen et al. (1999) that the H to D ratio is among the best indicators for branch increment. It stands to reason that the resulting model improvement to a large part was due to the concomitant effect on branch diameter development during the juvenile phase.

4.3 Crown gross shape is generally crucial, age dependence recommendable

Within the scope of this study the conifer crown had the shape of an elliptical paraboloid above the height of maximum crown diameter. While Pretzsch et al. (2002) recommend a reverse truncated cone for the shadow part of the crown, the authors had favoured the concept of a cylindrical crown base, as it had represented the measured branch length at age 40 somewhat more realistically. In addition, the simulation with a truncated conical crown base had not produced a more realistic branch diameter profile during simulation. Hann (1999) presents a model for the crown hull shape that reflects the social status within a stand not only by crown height and diameter but also

by curvature of the light crown longitudinal section. For dominant trees it confirms the concept of a paraboloid light crown and a cylindrical shadow crown whereas suppressed trees are rather represented by a cone. The approach could be applied to further improve the simulation of crown development during the juvenile phase. Within this work a cone crown shape was used in early model prototypes for mature trees as well as it is a convenient gross estimator of branch length. The simple cone is infeasible to represent crown volume (Rautiainen et al. 2008). Consequently it had entailed a notably incorrect prognosis of branch diameter at a given vertical position along the stem and should be strictly avoided for mature stands.

4.4 Additional approaches to branch diameter computation are likely candidates for analysis

Ellsworth and Reich (1993) prove the steep and negative vertical gradient of photosynthetic capacity within the crown that follows the decrease of canopy transmittance in downward direction. In accordance, crown base height that is an indicator of light attenuation within the canopy was used to infer branch size from vertical position via a convex crown hull. Colin and Houllier (1992) based prediction of whorl and branch characteristics by vertical position on the height of the first living branch as well as the crown base height. Houllier et al. (1995) integrated the alternative approach to crown shape into a growth prediction model. They estimated the required crown base properties from the maximum base diameter that would be possible for cone shaped crowns and an empirical survival time of branches below base height. Moreover, they included variability of branch angle, branch size and branch count per whorl into model prediction. Weiskittel et al. (2006) have shown that maximum branch size is the most responsive variable to silvicultural regime among a range of Douglas fir plantations (5 to 65 years old). Hein et al. (2007) successfully predict the effect of planting density in a Norway spruce stand (*Picea abies* [L.] Karst.) with respect to dead branches within the living crown and branch number as well as branch differentiation on the whorl level. Hence, additional variability of board strength prediction can likely be explained and modelled through a higher differentiation of branch and knot properties. Ikonen et al. (2009) applied a mechanistical description of shoot growth based on light interception (Kellomäki and Strandman 1995; Kellomäki et al. 1999) to predict future board quality. It might also be used to extend our model e.g. to cover the early phase of stand development and to describe the dynamics of more complex deciduous tree crown shapes.

4.5 The early growth phase might be replaced by simulation starting in the juvenile phase

The assumption of this work that inter tree contact at the crown base edge marked the onset of crown shift was taken from a proven concept of early stand development simulation outlined by Valentine et al. (2013) for Loblolly Pine (*Pinus taeda* L.). A more detailed approach to crown and branch reconstruction was presented by Seifert (2003) who constructed crown shape at simulation start based on competition on the level of vertical layers, each 30 cm high and interpolated the crown hull back to an assumed state of symmetrical shape before canopy closure. If prognosis would have to be based on planting pattern and site alone, reconstruction would be omitted. An intriguing challenge would be to simulate stand dynamics at a developmental stage that has rarely been described by observation based algorithms. High emphasis was to be put on self-thinning (review by Reynolds and Ford 2005) and mortality in young stands. Crown shape dynamics as described by Seifert (2003) might possibly be used to create a variety of possible stand and crown evolution paths in the course of crown closure supported by stochasticity.

4.6 The modelling toolbox is open to coupling with physiological biomass growth models

The description of growth dynamics, competition and allometry within this work was based on the external observation of individual trees and is insensitive to driving force variability on an intra-annual time scale. In contrast physiological models are sensitive to weather events and may take into account the coupling of belowground and aboveground competition as controlled by water and nitrogen limitation (originally by Schwinning and Weiner 1998). Mäkinen et al. (2001) have shown the influence of nutrient supply on crown characteristics and branch count. Within environmental change studies, there is a strong requirement for physiological models that predict base variables of log grading (e.g. Deckmyn et al. 2008; 2009). Due to a modular object oriented architecture the experimental system that has been presented in this work may be readily coupled with any physiological model, that exports an interface to transport gross cohort volume growth or lists of individual trees on annual time step (e.g. via SOAP, Mitra and Lafon 2007).

5 Conclusion

The wood quality toolbox provides model extensions for stem structure development and board strength prognosis that may even be coupled to the most abstract individual tree representation with a branchless crown of convex hull shape. It realistically predicted the shift of centre board bending strength between stands of minimum and maximum initial planting density, due to the explanation of bending strength by cambial age and knot area ratio and their relation to indicators of early competition. The toolbox is a comprehensive development and testing platform for generalist and portable board strength algorithms that are compatible to growth simulators with a purely external tree perception as well as more mechanistic approaches.

Height to diameter allometry is retention of early competition. Hence, if branch size computation implies stem height to diameter ratio and prognosis is based on data of a mature stand, it is recommendable to couple allometry to planting density. The bending strength and crown base height algorithms applied both address basic properties of the wood quality model and mark a threshold of usability. The suggested modelling system is based on the commonly used statistical R package and is technically convenient to pass within the research community. In its current state it may be applied to assist the expert in trend prediction of density and pruning related stand management options. High potential lies in a further explanation of board strength variability through additional stem structure properties and branch size variation based on theory of existing related work.

Acknowledgement

We thank the Bavarian State Ministry for Nutrition, Agriculture, and Forestry for permanent support of the project W 07 “Long-term experimental plots for forest growth and yield research” and for funding the project X36 ”Relationship between spacing and wood quality of Douglas-fir in Bavaria“. Thanks are also due to Prof. Dr. Thomas Seifert for critical discussion of the evaluation concept, and Dr. Rüdiger Grote for pre-reviewing the paper.

References

British Standards Institution (2011). BS 4978 2007 + A1: 2011. Visual Strength Grading of Softwood. BSI, London. ISBN 978-0-580-73681-0. 22 p.

Canty A., Ripley B. (2014). boot: Bootstrap R (S-Plus) functions. R package version 1.3-11. https://cran.r-project.org/web/packages/boot/index.html.

Colin F., Houllier F. (1992). Branchiness of Norway spruce in northeastern France: predicting the main crown characteristics from usual tree measurements. Annales des Sciences Forestières 49: 511–538. http://dx.doi.org/10.1051/forest:19910606.

Davison A.C., Hinkley D.V. (1997). Bootstrap methods and their applications. Cambridge University Press, Cambridge. ISBN 0-521-57391-2.

DeBell D.S., Singleton R., Gartner B.L., Marshall D.D. (2004). Wood density of young-growth western hemlock: relation to ring age, radial growth, stand density, and site quality. Canadian Journal of Forest Research 34: 2433–2442. http://dx.doi.org/10.1139/x04-123.

Deckmyn G., Verbeeck H., Op de Beeck M., Vansteenkiste D., Steppe K., Ceulemans R. (2008). ANAFORE: a stand-scale process-based forest model that includes wood tissue development and labile carbon storage in trees. Ecological Modelling 215: 345–368. http://dx.doi.org/10.1139/x04-123.

Deckmyn G., Mali B., Kraigher H. (2009). Using the process-based stand model ANAFORE including Bayesian optimisation to predict wood quality and quantity and their uncertainty in Slovenian beech. Silva Fennica 43(3): 523–534. http://dx.doi.org/10.14214/sf.204.

Di Lucca C.M. (1999). TASS/SYLVER/TIPSY: systems for predicting the impact of silvicultural practices on yield, lumber value, economic return and other benefits. In: Bamsey C.R. (ed.). Stand density management conference: using the planning tools. November 23–24, 1998, Clear Lake Ltd., Edmonton, AB. p. 7–16.

DIN (2012). DIN 4074-1. Sortierung von Holz nach der Tragfähigkeit – Teil 1: Nadelschnittholz. [Strength grading of wood – part 1: coniferous sawn timber]. Beuth Verlag, Berlin. [In German].

Donato D.C., Campbell J.L., Franklin J.F. (2012). Multiple successional pathways and precocity in forest development: can some forests be born complex? In: Palmer M. (ed.). Journal of Vegetation Science 23: 576–584. http://dx.doi.org/10.1111/j.1654-1103.2011.01362.x.

Efron B. (1979). Bootstrap methods: another look at the jackknife. The Annals of Statistics 1979: 1–26. http://dx.doi.org/10.1214/aos/1176344552.

Ellsworth D., Reich P. (1993). Canopy structure and vertical patterns of photosynthesis and related leaf traits in a deciduous forest. Oecologia 96: 169–178. http://dx.doi.org/10.1007/BF00317729.

Gort J., Zubizarreta-Gerendiain A., Peltola H., Kilpeläinen A., Pulkkinen P., Jaatinen R., Kellomäki S. (2010). Differences in branch characteristics of Scots pine (*Pinus sylvestris* L.) genetic entries grown at different spacing. Annals of Forest Science 67(7): 705. http://dx.doi.org/10.1051/forest/2010030.

Graves H.S. (2013). Forest Mensuration. In: Forgotten Books, London (Original work published 1906). p. 154.

Hann D. (1999). An adjustable predictor of crown profile for stand-grown Douglas-fir trees. Forest Science 45: 217–225.

Hann D.W., Hester A.S., Olsen C.L. (1997). ORGANON user's manual, version 6.0. Department of Forest Resources, Oregon State University, Corvalli.

Hein S., Mäkinen H., Yue C., Kohnle U. (2007). Modelling branch characteristics of Norway spruce from wide spacings in Germany. Forest Ecology and Management 242: 155–164. http://dx.doi.org/10.1016/j.foreco.2007.01.014.

Houllier F., Leban J., Colin F. (1995). Linking growth modelling to timber quality assessment for Norway spruce. Forest Ecology and Management 74: 91–102. http://dx.doi.org/10.1016/0378-1127(94)03510-4.

Hugershoff R. (1936). Die mathematischen Hilfsmittel des Kulturingenieurs und Biologen. II. Teil: Herleitung von gesetzmäßigen Zusammenhängen. [The mathematical facilities of the forestry engineer and biologist. II. Part: derivation of regular principles]. Manuskriptdruck, Dresden. [In German].

Ikonen V., Kellomäki S., Peltola H. (2009). Sawn timber properties of Scots pine as affected by initial stand density, thinning and pruning: a simulation based approach. Silva Fennica 43(3): 411–431. http://dx.doi.org/ 10.14214/sf.197.

Kellomäki S., Strandman H. (1995). A model for the structural growth of young Scots pine crowns based on light interception by shoots. Ecological Modelling 80: 237–250. http://dx.doi.org/10.1016/0304-3800(94)00065-P.

Kellomäki S., Ikonen V., Peltola H., Kolström T. (1999). Modelling the structural growth of Scots pine with implications for wood quality. Ecological Modelling 122: 117–134. http://dx.doi.org/10.1016/S0304-3800(99)00086-1.

Kenk G., Hradetzky J. (1984). Behandlung und Wachstum der Douglasien in Baden-Württemberg. [Management and growth of douglas fir in Baden-Württemberg]. Mitteilungen der Forstlichen Versuchs und- Forschungsanstalt Baden-Württemberg 113. 89 p. [In German].

Klädtke J., Kohnle U., Kublin E., Ehring A., Pretzsch H., Uhl E., Spellmann H., Weller A. (2012). Wachstum und Wertleistung der Douglasie in Abhängigkeit von der Standraumgestaltung. [Growth and value production of Douglas-fir under varying stand densities]. Schweizerische Zeitschrift für Forstwesen 163(3): 96–104. [In German]. http://dx.doi.org/10.3188/szf.2012.0096. .

Maguire D., Kershaw J., Hann D. (1991). Predicting the effects of silvicultural regime on branch size and crown wood core in Douglas-fir. Forest Science 37(5): 1409–1428.

Mäkelä A., Landsberg J., Ek A.R., Burk T.E., Ter-Mikaelian M., Agren G.I., Oliver C.D., Puttonen P. (2000). Process-based models for forest ecosystem management: current state of the art and challenges for practical implementation. Tree Physiology 20: 289–298. http://dx.doi.org/10.1093/treephys/20.5-6.289.

Mäkelä A., Grace J., Deckmyn G., Kantola A., Kint V. (2010). Simulating wood quality in forest management models. Forest Systems 19: 48–68. http://dx.doi.org/10.5424/fs/201019S-9314.

Mäkinen H., Saranpää P., Linder S. (2001). Effect of nutrient optimization on branch characteristics in *Picea abies* (L.) Karst. Scandinavian Journal of Forest Research 16: 354–362. http://dx.doi.org/10.1080/02827580120345.

Meredieu C., Dreyfus P., Saint-André L., Leban J.-M. (1999). A chain of models from tree growth to properties of boards for *Pinus nigra* ssp. Laricio Arn.: simulation using CAPSIS and WINEpifn. In: Nepveu G. (ed.). Third Workshop "Connection between Silviculture and Wood Quality through Modelling Approaches and Simulation Software". La Londe-Les-Maures, France, September 5–12. IUFRO WP S5.01-04. Proceedings. p. 505–513.

Michailoff I. (1943). Zahlenmäßiges Verfahren für die Ausführung der Bestandeshöhenkurven. [Numerical algorithm for the implementation of stand height curves]. Forstw. Cbl. u. Thar. Jahrb. 6: 273–279. [In German].

Mitchell K.J. (1988). SYLVER, modelling the impact of silviculture on yield, lumber value, and economic return. Forest Chronicle 64: 127–131. http://dx.doi.org/10.5558/tfc64127b1-2.

Mitra N., Lafon Y. (2007). SOAP version 1.2 Part 0: primer (second edition) – W3C recommendation. http://www.w3.org/TR/2007/REC-soap12-part0-20070427/. [Cited 4 Feb. 2015].

Moore J.R., Lyon A.J., Searles G.J., Lehneke S.A., Ridley-Ellis D.J. (2013). Within- and between-

stand variation in selected properties of Sitka spruce sawn timber in the UK: implications for segregation and grade recovery. Annals of Forest Science 70: 403–415. http://dx.doi.org/10.1007/s13595-013-0275-y.

Muth C.C., Bazzaz F.A. (2003). Tree canopy displacement and neighborhood interactions. Canadian Journal of Forest Research 33: 1323–1330. http://dx.doi.org/10.1139/x03-045.

Pretzsch H., Biber P. (2010). Size-symmetric versus size-asymmetric competition and growth partitioning among trees in forest stands along an ecological gradient in Central Europe. Canadian Journal of Forest Research 40: 370–384. http://dx.doi.org/ 10.1139/X09-195.

Pretzsch H., Rais A. (submitted). Wood quality in complex forests versus even-aged monocultures - review, conclusions, and perspective.

Pretzsch H., Biber P., Ďurský J. (2002). The single tree-based stand simulator SILVA: construction, application and evaluation. Forest Ecology and Management 162, 3–21. http://dx.doi.org/10.1016/S0378-1127(02)00047-6.

Pretzsch H., Grote R., Reineking B., Rötzer T., Seifert S. (2008). Models for forest ecosystem management: a European perspective. Annals of Botany 101: 1065–87. http://dx.doi.org/10.1093/aob/mcm246.

Rais A., Poschenrieder W., Pretzsch H., van de Kuilen J.-W.G. (2014a). Influence of initial plant density on sawn timber properties for Douglas-fir (*Pseudotsuga menziesii* (Mirb.) Franco). Annals of Forest Science 71: 617–626. http://dx.doi.org/10.1007/s13595-014-0362-8.

Rais A., van de Kuilen J.-W.G., Pretzsch H. (2014b). Growth reaction patterns of tree height, diameter, and volume of Douglas-fir (*Pseudotsuga menziesii* [Mirb.] Franco) under acute drought stress in Southern Germany. European Journal of Forest Research 133(6): 1043–1056. http://dx.doi.org/10.1007/s10342-014-0821-7.

Rautiainen M., Mõttus M., Stenberg P., Ervasti S. (2008). Crown envelope shape measurements and models. Silva Fennica 42(1): 19–33. http://dx.doi.org/10.14214/sf.261.

R Core Team (2014). R: a language and environment for statistical computing. R Foundation for Statitstical Computing, Vienna, Austria. http://www.R-project.org/.

Reineke L.H. (1933). Perfecting a stand-density index for even-aged forests. Journal of Agricultural Research 46: 627–638. http://dx.doi.org/10.1111/j.1365-2745.2005.00976.x.

Reynolds J.H., Ford E.D. (2005). Improving competition representation in theoretical models of self-thinning: a critical review. Journal of Ecology 93: 362–372. http://dx.doi.org/10.1111/j.1365-2745.2005.00976.x.

Ritchie M.W., Hamann J.D. (2007). Individual-tree height-, diameter- and crown-width increment equations for young Douglas-fir plantations. New Forests 35: 173–186. http://dx.doi.org/10.1007/s11056-007-9070-7.

Rouvinen S., Kuuluvainen T. 1997: Structure and asymmetry of tree crowns in relation to local competition in a natural mature Scots pine forest. Canadian Journal of Forest Research 27 (6): 890–902. http://dx.doi.org/10.1139/x97-012.

Saha S., Kuehne C., Kohnle U., Brang P., Ehring A., Geisel J., Leder B., Muth M., Petersen R., Peter J., Ruhm W., Bauhus J. (2012). Growth and quality of young oaks (*Quercus robur* and *Quercus petraea*) grown in cluster plantings in central Europe: a weighted meta-analysis. Forest Ecology and Management 283: 106–118. http://dx.doi.org/10.1016/j.foreco.2012.07.021.

Schwinning S., Weiner J. (1998). Mechanisms determining the degree of size asymmetry in competition among plants. Oecologia 113(4): 447–455. http://dx.doi.org/10.1007/s004420050397.

Seifert T. (2003). Integration von Holzqualität und Holzsortierung in behandlungssensitive Waldwachstumsmodelle. [Integration of wood quality and wood grading into management sensitive forest growth models]. Doctoral dissertation, Technische Universität München, Universitätsbibliothek. [In German].

Stapel P., Van De Kuilen J.W.G. (2014). Efficiency of visual strength grading of timber with respect to origin, species, cross section, and grading rules: A critical evaluation of the common standards. Holzforschung 68: 203–216. http://dx.doi.org/10.1515/hf-2013-0042.

Thorpe H.C., Astrup R., Trowbridge A., Coates K.D. (2010). Competition and tree crowns: a neighborhood analysis of three boreal tree species. Forest Ecology and Management 259: 1586–1596. http://dx.doi.org/10.1016/j.foreco.2010.01.035.

Todoroki C.L., Monserud R., Parry, D (2005). Predicting internal lumber grade from log surface knots: actual and simulated results. Forest Products Journal 55: 38–47.

Torquato L.P., Auty D., Hernández R.E., Duchesne I., Pothier D., Achim A. (2014). Black spruce trees from fire-origin stands have higher wood mechanical properties than those from older, irregular stands. Canadian Journal of Forest Research 44: 118–127. http://dx.doi.org/10.1139/cjfr-2013-0164.

Valentine H.T., Amateis R.L., Gove J.H., Mäkelä A. (2013). Crown-rise and crown-length dynamics: application to loblolly pine. Forestry 86: 371–375. http://dx.doi.org/10.1093/forestry/cpt007.

Weiskittel A.R., Maguire D., Monserud R., Rose R., Turnblom E.C. (2006). Intensive management influence on Douglas fir stem form, branch characteristics, and simulated product recovery. New Zealand Journal of Forest Science 36: 293–312.

Weiskittel A.R., Maguire D.A., Monserud R.A., Johnson G.P. (2010). A hybrid model for intensively managed Douglas-fir plantations in the Pacific Northwest, USA. European Journal of Forest Research 129: 325–338. http://dx.doi.org/10.1007/s10342-009-0339-6.

Total of 56 references.

Supplementary files

s1_Technical_Basics.pdf

Silva Fennica vol. 50 no. 1 article id 1393, availabe at http://dx.doi.org/10.14214/sf.1393

Supplementary file

Technical Basics

Name: Wood Quality Toolbox
Developer: Chair of Forest Growth and Yield Science
Contact Address: Hans-Carl-von-Carlowitz-Platz 2, D-85354 Freising, Germany
Year first available: 2015
Software required: R statistical environment (R Core Team, 2013).
Software recommended: RStudio.
Availability: Upon request, introductory support recommended.
Program size: 400 KB.

As explained in the referencing publication, the simulation model covers the major relevant linkages reaching from stand management and site influence via individual tree competition and growth to crown shape and branch dimension and further down to knottiness, wood density and strength of the individual board.

During simulation, the developing stand is a container of variable tree objects. The stand state of each finalised year is stored as an age related collection of invariable quasi frozen tree objects to constitute a growth history. Thinning and mortality remove trees from the current year container and store them into a global container of all felled trees. All variable data of tree dimension and structure are held within the tree object and further objects inside that represent nested levels of tree architecture, such as stem, crown, whorl, log, branch, and board. Currently simulation is organised into (1) growth, thinning, pruning, (2) construction of log objects and (3) construction of inner log and board structure. Each tree object is passed through a chain of computation objects starting with growth and thinning and ending with sawing of logs and boards. To the greatest extent the tree object is modified, extended and diversified by functionality of the modules that handle it, whereas its own interface is kept lean and general. The state of each computation object remains constant once initialized with parameter values, while any state change is stored to the passing tree objects. As each module represents an elementary and common task of simulation, such as competition intensity or potential growth, the functionality of the model is readily modified by adding or replacement of plug-in computation objects. The system also includes a module for strength grading in accordance to European standards EN 338, EN 14081 that had not been applied within the scope of the referencing study.

Fig. AP 1 to Fig. AP 5 illustrate the simulation process using the implemented perception of stand, individual tree, log and board. Prediction starts with the stand structure at setup inventory. Reconstruction is based on the stand state at setup inventory and a reported planting pattern (Fig. AP 1).

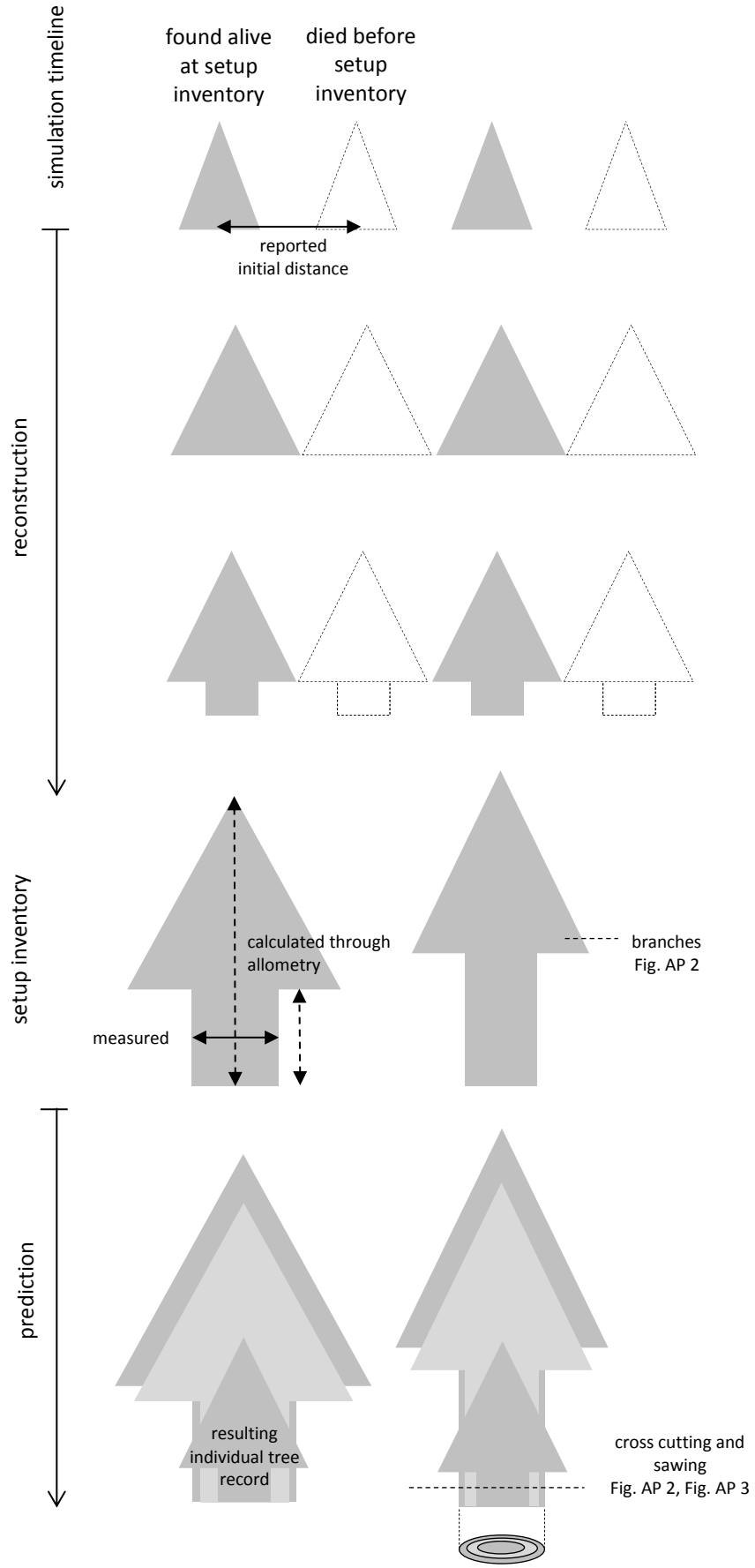

initial phase

DBH growth assumed to follow 50% quantile of DBH growth along DBH (biological age)
height grows linearly towards setup height along time

crown bases touch

onset of crown shift
crown diameter as constant × DBH

early competition

individual DBH growth guided within corridor between 50% quantile and one of the 5% or 95% quantiles along DBH

crown shifts towards setup base height along DBH; function initially linear, progressively allometric

setup inventory

trees are known by DBH; initial height and crown computed via stand height curve and allometry

future growth

potential growth depends on DBH and is reduced by individual tree competition

height computed through stand height curve, tree architecture via allometry

regular thinning

felling

time depends on thinning rule

stem structure then is derived from history

Fig. AP 1. Principles of annual growth reconstruction and prediction.

Branch size is constructed from the hull of the crown. The resulting branch length is translated into branch diameter based on data from field measurement. During growth simulation, branch properties are stored within whorl objects. At that stage there is no requirement for a branch object of explicit inner geometry: Branch objects are constructed as needed from the growth record of the individual tree in a separate step (Fig. AP 2).

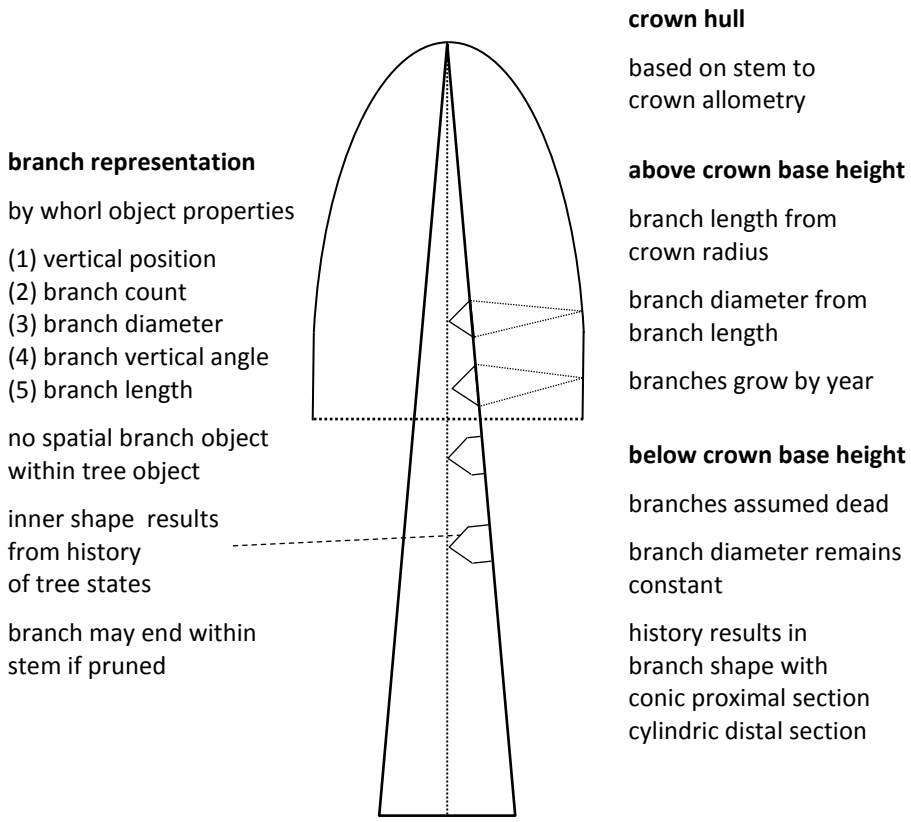

Fig. AP 2. Principle of branch growth reconstruction and prediction.

After reconstruction and prediction, each individual tree object is supplemented with a collection of newly constructed log objects based on the tree history: Log structure is defined by the annual ring radii at median vertical position within the log and the branch properties registered in any whorl object that is enclosed by the vertical log limits (Fig. AP 3). Based on the log objects and the cross sectional sawing pattern that applies to the log radius at top position, the structure of each individual board is computed as explained by Fig. AP 4.

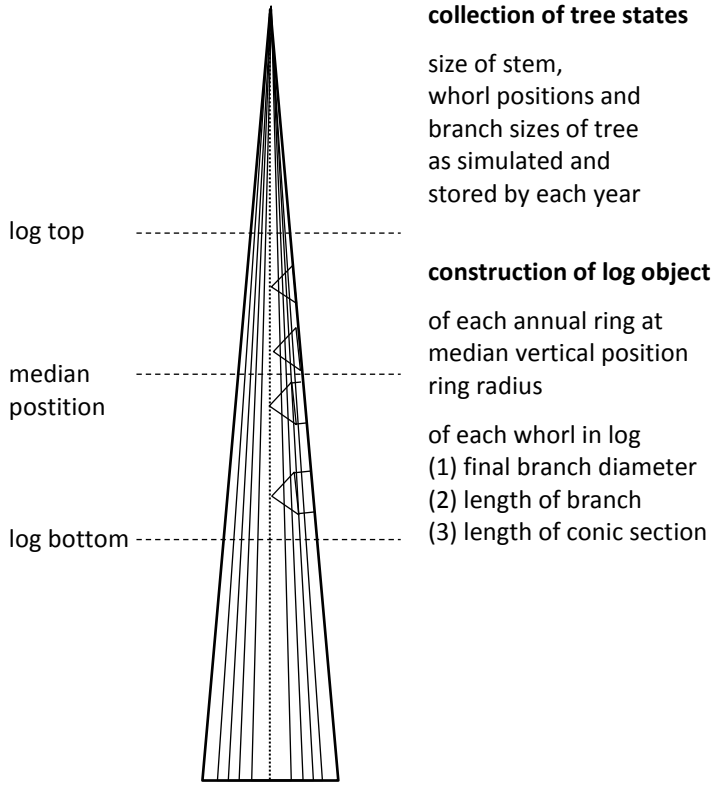

Fig. AP 3. Principle of tree history to log structure translation.

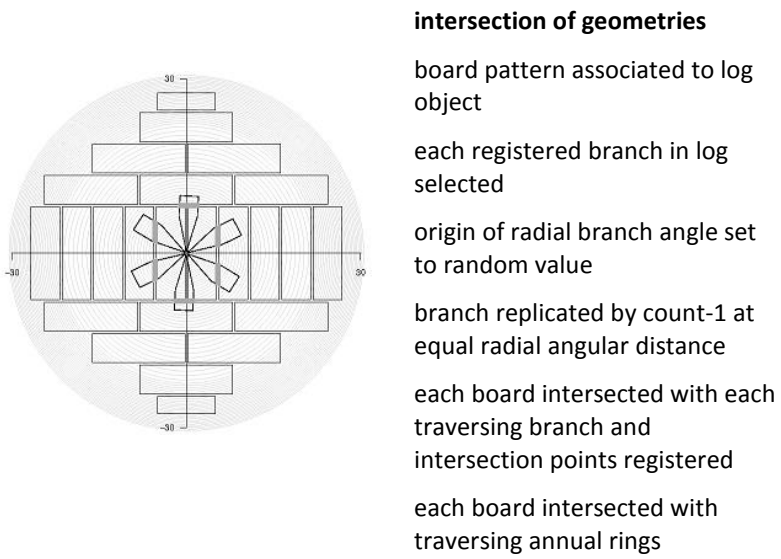

Fig. AP 4. Principle of log to board structure translation.

Board strength is calculated by individual board, based on stored tree objects with associated log objects and board collections. The process may be run at a different time and with any algorithm selected for computation of strength.

Fig. AP 5 finally illustrates the plugin architecture using a snippet of growth computation (whorl and branch geometry): Each current year tree of class Tree is handled by an object of class TreeHandBranchGeometry that is a TreeHandler. Any TreeHandler inherits a list of Growth objects and its function *runallon* applies method *runon* of each list member to the tree that is processed (diagram left top). TreeHandBranchGeometry holds two specialisations of Growth in its list: WhorlDiameter for computation of whorl diameter and BranchGeometry for branch size and vertical angle. Each Tree object is passed to all TreeHandler objects. TreeHandler objects exists for all main tasks of the system, such as growth, stem structure and thinning. Growth algorithms may be readily modified by creating new Growth objects through extension of the base class and inserting them into the appropriate tree handler.

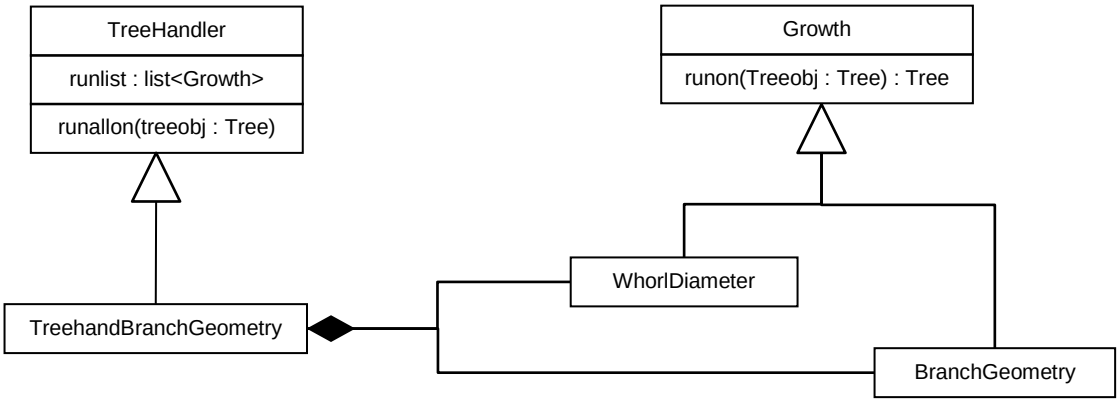

Fig. AP 5. Principle of the plugin architecture as a class diagram (UML).

Betreff:
FW: Request for permission of reprint
Von:
Luke Silva Fennica <silva.fennica@luke.fi>
Datum:
22.12.2016 06:58
An:
Werner Poschenrieder <Werner.Poschenrieder@lrz.tu-muenchen.de>

From: "Korpilahti Eeva (Luke)" <eeva.korpilahti@luke.fi>
Date: Thursday, December 22, 2016 7:56 AM
To: Luke Silva Fennica <silva.fennica@luke.fi>
Subject: RE: Request for permission of reprint

Dear Mr. Werner Poschenrieder,

We permit for you to reprint the below mentioned article of Silva Fennica in your PhD thesis under the condition that all bibliographic information are given to the original publication.

Sincerely yours,

Eeva Korpilahti

Editor-in-chief

Silva Fennica

From: Luke Silva Fennica
Sent: 22. joulukuuta 2016 7:32
To: Korpilahti Eeva (Luke); Nygren Pekka (Luke)
Subject: FW: Request for permission of reprint

From: Werner Poschenrieder <Werner.Poschenrieder@lrz.tu-muenchen.de>
Date: Wednesday, December 21, 2016 11:12 AM
To: Luke Silva Fennica <silva.fennica@luke.fi>
Subject: Request for permission of reprint

Dear Sirs,

is there general permission to reprint publications at Silva Fennica within a p.Hd. thesis,

or is permission to be requested on a per publication basis?

My request concerns

Poschenrieder, W., Rais, A., van de Kuilen, J.-W. G., & Pretzsch, H. (2016). Modelling sawn timber volume and strength development at the individual tree level – essential model features by the example of Douglas fir. Silva Fennica, 50(1), 1–25. http://doi.org/10.14214/sf.1393.

Best regards

Werner Poschenrieder

--

Werner Poschenrieder

Scientific Worker

Wissenschaftlicher Mitarbeiter

Technische Universität München

Wissenschaftszentrum Weihenstephan

Chair of Forest Growth and Yield Science

Lehrstuhl für Waldwachstumskunde

Hans-Carl-von-Carlowitz-Platz 2

85354 Freising

Tel. +49 8161 71 4714

Fax +49 8161 71 4721

Werner.Poschenrieder@lrz.tum.de

waldwachstum.wzw.tum.de

forests

MDPI

Article

An Inventory-Based Regeneration Biomass Model to Initialize Landscape Scale Simulation Scenarios

Werner Poschenrieder *, Peter Biber and Hans Pretzsch

Chair of Forest Growth and Yield Science, Technical University of Munich, Hans-Carl-von-Carlowitz-Platz 2, 85354 Freising, Germany; Peter.Biber@lrz.tum.de (P.B.); Hans.Pretzsch@lrz.tum.de (H.P.)

* Correspondence: Werner.Poschenrieder@lrz.tum.de; Tel.: +49-8161-71-4711

Received: 18 March 2018; Accepted: 12 April 2018; Published: 17 April 2018

Abstract: Dynamic landscape simulation of the forest requires an initial regeneration stock specific to the characteristics of each simulated stand. Forest inventories, however, are sparse with regard to regeneration. Moreover, statistical regeneration models are rare. We introduce an inventory-based statistical model type that (1) quantifies regeneration biomass as a fundamental regeneration attribute and (2) uses the overstory's quadratic mean diameter (*Dq*) together with several other structure attributes and the Site Index as predictors. We form two such models from plots dominated by European beech (*Fagus sylvatica* L.), one from national forest inventory data and the other from spatially denser federal state forest inventory data. We evaluate the first one for capturing the predictors specific to the larger scale level and the latter one to infer the degree of landscape discretization above which the model bias becomes critical due to yet unquantified determinants of regeneration. The most relevant predictors were *Dq*, stand density, and maximum height (significance level $p < 0.0001$). If plot data sets for evaluation differed by the forest management unit in addition to the average diameter, the bias range among them increased from 0.1-fold of predicted biomass to 0.3-fold.

Keywords: regeneration modelling; landscape scale modelling; stand structure; inventory data; *Fagus sylvatica*

1. Introduction

The dynamic simulation of forest growth and structure development is an essential prerequisite to future scenarios that consider ecosystem service provision on a landscape level [1]. In order to start from a realistic representation of the forest in its current state, scenarios require data of the stand structures present within the landscape considered. Sample plots are the primary inventory unit in modern grid-based forest inventories. They provide detailed structure data for modelling and are widely available. However, they have a distance of up to several kilometers from each other.

A proven method that approximately represents the forest stand structures within a landscape groups all available inventory plots into strata [2,3]. Such a stratification classifies plots by stand structure attributes, as well as site quality. Typically, it then uses the data of all inventory plots from a given stratum to construct a virtual forest stand. That virtual stand serves to simulate the stratum's development within a representative subunit [4] (p. 502 ff.). The stratification method yields a good representation of the overstory per stratum, here defined as all trees with a minimum diameter at breast height (DBH) of 7 cm. However, this is much less the case for the understory: it consists of the young trees with a DBH of less than 7 cm that form the basis of the next stand generation. Typical inventories [5,6] sample regeneration in very small sub-areas within an inventory plot, while, conversely, the stand intrinsic variability of regeneration is large [7]. Thus, within a stratum considered, there might often not be enough inventory plots to provide a statistically stable estimation of its

regeneration stock. Moreover, remote sensing will likely support terrestrial inventories in the near future and might even substitute them in some areas or cover regions where forest inventories are completely missing so far [8–10]. Except under very sparse main stands, regeneration trees will almost be undetectable by remote sensors. Therefore, simulation scenarios on the forest landscape level will benefit from a statistical method that, based on overstory structure and site [11–13], contributes a quantitative estimation of regeneration stock to each stratum. That estimation is an essential starting condition for dynamically simulating the ingrowth of regeneration trees into the main stand. Ingrowth, in turn, is the crucial process for the change of forest stand generations and, thus, a key process for adaptation to climate change.

The density of regeneration trees within a stand typically varies on a spatial scale of only a few square meters [7,14,15]. A notable part of that variation will be due to stochastic effects, such as felling damages and small-scale game browsing within small understory sectors. Statistical models of regeneration, thus, will not precisely predict the understory stock within such a small-scale stand sector, even if they would account for any relevant structure attribute of the sector's local overstory. Still, such a model might infer the probability distribution of the stand sector's regeneration stock from the sector's local overstory structure. A realistic case of model application, thus, is to derive a representative collection of such sector-related regeneration stock distributions within a whole stratum from a known set of structure types within the stratum's overstory. That distribution set, through random sampling from each local distribution, could then provide a realistic initial pattern of regeneration within a virtual stand.

Scenarios of forest growth and structure development are typically based on dynamic simulation models. To represent growth within the regeneration layer, or even within the overstory, such models often discretize a given virtual stand into a regular pattern of quadratic tiles with an edge length of 2.5 to 20 m. That way, they take into account the variability of regeneration stock at the horizontal resolution of small-scale effects. Prominent examples are the regeneration module of SILVA [16] and modern patch models [17,18].

National forest inventory (NFI) data are ideal to calibrate a statistical model for regeneration stock. Such a model would cover a wide range of overstory structures and site quality. It would yield the specific distribution of plot-wise regeneration stock at a given overstory structure and given site properties, obtained from a large data set. A straightforward approach for initializing tiles within a stratum-based virtual stand might assume that such a predictor-related distribution is applicable to represent the distribution within any plot-sized stand subsector of corresponding predictor values. Based on a sample of stratum-related overstory attributes, it would first evaluate the overstory surrounding the tile of interest. The result is then related to a specific distribution of regeneration stock. Conveniently, subplots where regeneration is sampled and model tiles are of a similar size. Thus, the algorithm would take a random sample of the tile's regeneration stock directly from the tile-related distribution.

However, any structure-related distribution of regeneration stock from an NFI-based model results from a convolution of many distributions: due to the model's comprehensive data basis, each of them is specific to one of numerous distinct sub regions. On a large national scale level, due to a landscape-related browsing intensity and other regional factors [19], strata of a similar structure and similar site properties might notably differ in their relation between overstory structure and regeneration stock. Model design may counteract such variation by striving for predictors that correlate as closely as possible with biological processes and silvicultural practices. Still, the model's realism will strongly depend on the level of stratum differentiation and discretization that the model user intends.

The study at hand conceptualizes an inventory-based model type that aims to predict the regeneration stock distribution per stratum based on the stratum-intrinsic overstory pattern and the stratum's site properties. In order to obtain the distribution per stratum, the model estimates the distribution of regeneration stock per plot-sized sub-area of the stratum's virtual stand and samples

one value per sub-area related distribution. Within that scope, the study follows two fundamental objectives. The first one is to identify important predictors of regeneration biomass within the large spatial scope of the German state territory (36 million ha with 11 million ha of forest).

More detailed stratification criteria will result in more appropriate management strategies per stratum during simulation. However, using highly detailed criteria is also related to high level of forest landscape discretization. More profound stratification, thus, might lead to smaller strata that differ in their average regeneration stock due to stochastic variation among them. Hence, such stratification might impair the precision of a statistical regeneration model. The second fundamental objective, therefore, is to estimate the degree of stratum differentiation, beyond which the model produces a critical bias of the per-stratum average. To meet both fundamental objectives of the study, we design two closely related model versions: one uses data from the German National Forest Inventory (referred to as NFI in the following). That inventory covers the total German forest area. However, due to its spatial resolution (4 km $\times$ 4 km), it is not ideal for analyzing the model performance on the spatial level of landscape-related simulation scenarios (about 50,000 ha of forest). Therefore, the study uses a second model version that is based on the exceptionally dense Bavarian State Forest Inventory (BSFI, 200 m $\times$ 200 m). That inventory covers a state forest area of almost 1 million ha. In order to determine the limit of spatial resolution that our modelling approach currently has, we evaluated the bias of the BSFI-based model as dependent on the differentiation of strata formed from BSFI plots on two different discretization levels.

Both models use the aboveground regeneration biomass within each plot as a dependent variable that is closely linked to net primary production [20]. As the height of regeneration on the plot scale may be highly heterogeneous [11], regeneration biomass represents resource supply more directly than the total number of regeneration trees per plot.

At the current state of model development, our study focuses on plots dominated by European beech (*Fagus sylvatica* L.) within the overstory. European beech is by far the most important broadleaved species in Central Europe. As it is shade tolerant, it occurs along a broad range of stand structures and sites. Moreover, it primarily regenerates through natural seed dispersion.

2. Materials and Methods

2.1. Data

On the national scale level, the study at hand used the German National Forest Inventory (NFI, 4 km grid) that covers the whole forest area of Germany. The version of these data was the third and most recent survey conducted in 2011 and 2012 [6] with reference date 1 October 2012 [21]. For evaluating the bias of the BSFI-based model as related to the resolution of strata, the study applied plot data from the Bavarian State Forest Inventory that covers the forest area managed by the Federal State of Bavaria (BSFI in the further text, 200 m grid). The BSFI surveys 41 forest management units with an average size of about 20,000 ha, each at a repeat cycle of 10 years. Per each forest management unit, it applies individual due dates.

2.1.1. German National Forest Inventory (NFI)

The German National Forest Inventory (description mostly taken from [6]) is based on a regular 4 km $\times$ 4 km quadrangle grid that covers the entire national forest area (~11,400,000 ha, 59,858 plots). It is denser inside some federal states where it has a 2.83 km $\times$ 2.83 km or 2 km $\times$ 2 km grid. Each grid point represents a north-to-south oriented square with an edge length of 150 m. At the corners of each square, there is exactly one inventory plot, so that the square represents an inventory cluster. On all plots, the NFI measures the overstory (trees of DBH $\geq$ 7) around each plot center as an angle count sample with a standard basal area factor (BAF) of 4. In addition, it takes the DBH of each sampled tree. Based on the BAF and measured DBH, overstory stem densities per ha are calculated. Within most

plots, height measurements are collected on a subset. In continuous cover forests, however, the heights of all sampled trees are measured.

Regeneration trees (DBH < 7 cm) are surveyed within two concentric circles that are situated 5 m north of the plot center. To that end, small saplings with a height of at least 0.2 m and less than 0.5 m are counted on the inner circle of a 1 m radius. Understory trees with a height of at least 0.5 m are counted on the outer circle that has a 2 m radius. Within that circle, the counted trees are attributed to different size classes. The first class comprises trees with a height of less than 1.3 m (and at least 0.5 m). Higher trees are attributed to the DBH classes 0 to 5 cm, 5 to 6 cm, and 6 to 7 cm (upper limits excluded). The radius of the inner circle is extended to 2 m if it would comprise less than four trees within the default radius of 1 m. The NFI registers the browsing of regeneration by an annotation per tree size class. A total of 46% of all plots with a beech-dominated overstory and regeneration had been marked as being browsed by ungulates in at least one regeneration size class.

Within this regeneration survey, the NFI computes regeneration biomass per tree size class from height if the tree considered is less than 1.3 m high and, furthermore, as based on diameter if the tree is higher [22,23]. The height-based part of the biomass calculation, to that end, uses one standard height per class, one of 0.35 m (for height class 0.2 to 0.5 m) and one of 0.9 m (>0.5 m to 1.3 m). It applies one generalist biomass to height relation for either coniferous or broadleaved species. On the contrary, the diameter-based biomass estimation interpolates between the height-based biomass at a height of 1.3 m and a species-specific biomass value at a DBH of 10 cm calculated with a modified Marklund model [24]. For model calibration and evaluation, we selected a subset of 7823 inventory plots with a basal area (BA) share of beech that was more than 55% within the overstory. That data set will be denoted as "NFI data" in the following (Table 1).

Table 1. Value characteristics of the base data set from the German national forest inventory NFI (n = 7823) used to analyze the influence of the overstory on the biomass of the regeneration fraction. Columns q 2.5 and q 97.5 show the 2.5% and 97.5% quantile, respectively. Column n denotes the number of data records used to calculate that range, as well as the mean of the variable considered. Column Ori. (origin) indicates whether the data were native (N) or derived by own computation (D). Further abbreviations are Lr. (layer), BAF (basal area factor), ER (ecoregion), and EL (elevation).

Lr.	Variable	Symbol	Basis	Level	Ori.	n	Mean	q 2.5	q 97.5	Unit
Overstory	tree diameter	D_t	–	tree	N	52,404	42	10	80	cm
	tree height	H_t	–	tree	N	52,404	28	11	40	m
	tree number/ha	N_t	D_t BAF	tree	N	52,404	76	7	520	ha^{-1}
	Stand Density Idx.	*SDI*	N_t, D_t	plot	D	7784	516	90	1 099	–
	Spec. Profile Idx.	*SPI*	H_t	plot	D	7784	0.49	0	1.26	–
	H-D Characteristic	*HD*	H_t, D_t	plot	D	7784	0.58	0.05	0.97	–
	Top height	*Hmax*	H_t	plot	D	7784	30	13	42	m
	Site Index	*SI*	ER, EL	plot	D	7784	36.58	35.37	37.33	m
	Quad. Mean Dia.	*Dq*	N_t, D_t	plot	D	7784	36	11	67	cm
Regeneration	tree height	–	–	tree	N	22,808	3.69	0	9	m
	tree diameter	–	–	tree	N	22,808	0.7	0	5.5	cm
	tree biomass	b_c	–	tree	N	22,808	0.74	0	8.5	kg
	tree number/ha	n_c	–	tree	N	22,808	5253	0	31,831	ha^{-1}
	biomass/ha	–	b_c, n_c	plot	D	7784	6.0	0	46	$t\ ha^{-1}$
	tree number/ha	–	n_c	plot	D	7784	15,392	0	98,218	ha^{-1}

The total BA shares within that set were 84% for beech and 93% for deciduous species in general. We classified 48% of all selected plots as beech monoculture (BA share > 90%). Within the set of beech-dominated plots, the share of regeneration biomass was 74% for beech and 92% for deciduous. Furthermore, 30% of the plots had a regeneration biomass of zero.

2.1.2. Bavarian State Forest Inventory (BSFI)

In contrast to the NFI, which has mainly monitoring purposes, the BSFI is designed to support forest management planning on the level of forest management units (20,000 ha). Therefore, it uses

a much higher spatial sampling density on a square grid of a 200 m grid width on average. Each inventory unit is a circular plot with an area of 400 to 500 m^2 that encloses several smaller concentric inventory circles. Only trees above a certain threshold DBH (typically 30 cm) are recorded on the whole plot area. Trees with a DBH < 30 cm and ≥ 11 cm are measured within an 80 to 125 m^2 circle. The smallest class of trees with a DBH < 11 cm, including regeneration trees, is surveyed on a 25 m^2 circle [25]. The minimum height of regeneration trees to be sampled in the BSFI is 0.2 m, the same as in the NFI. Trees up to a height of 1.3 m are recorded at a higher-class width, i.e., 0.1 m. Trees of a DBH > 0 and < 7 cm are recorded per DBH levels 1.5, 2.5, 3.5, 4.5, 5.5, and 6.5 cm. The beech-dominated BSFI data set used for model calibration and evaluation was selected by the same criteria as the NFI data. That set of plots with beech-dominated overstory will be named "BSFI data" in the following (Table 2).

Table 2. Value characteristics of the base data set from the Bavarian State Forest inventory BSFI (n = 11,954) used to analyze the influence of the overstory on the biomass of the regeneration fraction. Columns q 2.5 and q 97.5 show the 2.5% and 97.5% quantile, respectively. Column n denotes the number of data records used to calculate that range, as well as the mean of the variable considered. Column Ori. (origin) indicates whether the data were native (N) or derived by own computation (D). Further abbreviations are Lr. (layer), BAF (basal area factor), ER (ecoregion), and EL (elevation).

Lr.	Variable	Symbol	Basis	Level	Ori.	n	Mean	q 2.5	q 97.5	Unit
Overstory	tree diameter	D_t	–	tree	N	96,429	34	8.5	65	cm
	tree height	H_t	–	tree	N	96,429	25	9.3	37	m
	tree number/ha	N_t	D_t BAF	tree	N	96,429	73	15	404	ha^{-1}
	Stand Density Idx.	*SDI*	N_t, D_t	plot	D	11,954	519	74	1080	–
	Spec. Profile Idx.	*SPI*	H_t	plot	D	11,954	0.6	0	1.4	–
	H-D Characteristic	*HD*	H_t, D_t	plot	D	11,954	0.54	0.03	0.95	–
	Top height	*Hmax*	H_t	plot	D	11,954	29	10	40	m
	Site Index	*SI*	ER, EL	plot	D	11,954	35.4	36.25	37.33	m
	Quad. Mean Dia.	*Dq*	N_t, D_t	plot	D	11,954	32	9.7	59	cm
Regeneration	tree height	–	–	tree	N	42,342	2.18	0.2	9.2	m
	tree diameter	–	–	tree	N	42,342	1.4	0	6.5	cm
	tree biomass	b_c	–	tree	N	42,342	1.4	0	12	kg
	tree number/ha	n_c	–	tree	N	42,342	2503	321	16,040	ha^{-1}
	biomass/ha	–	b_c, n_c	plot	D	11,954	4.3	0	30	t ha^{-1}
	tree number/ha	–	n_c	plot	D	11,954	7667	0	47,705	ha^{-1}

The study comprised 11,954 plots from 26 spatially independent inventories over the federal state of Bavaria that had been taken within different years for the period from 2003 to 2012. The basal area shares within the BSFI data were 84% for beech and 91% for deciduous. A total of 41% of all plots were beech monoculture. In order to maintain consistency between NFI and BSFI data, we calculated the regeneration biomass per BSFI plot with the biomass algorithm of the NFI. The share of regeneration biomass then was 76% for beech and 89% for deciduous. Within the BSFI data, 29% of the plots had a regeneration biomass of zero. BSFI plot data, in difference to NFI data, have two topological keys: one that refers to the enclosing forest stand and one that is unique to the enclosing forest management unit. A total of 6073 of the 11,954 plots were spared from model calibration to form strata of a sufficient size for evaluation. Thus, half of all, i.e., 5881 plots remained to parameterize the BSFI-based model.

2.2. Data Preparation

The BSFI surveys regeneration trees within a larger collective of DBH < 11 cm. Again, to keep regeneration tree data from NFI and BSFI consistent with each other, we confined regeneration trees from both inventories to the group with a DBH < 7 cm.

Based on an ecophysiological perception of the regeneration process [26,27], we derived a set of overstory characteristics from the inventory plot data that likely determine regeneration biomass. These properties represent above and belowground competition, growth potential, and stand maturity. Both the NFI- and the BSFI-based model use the same set of predictors. In order to parameterize

each model, we computed one independent set of plot-related predictor values per each inventory. For quantifying the overstory stand density, we used the Stand Density Index (SDI) [28] which enables a comparison of stand densities at very different development stages. This structure indicator has been shown to be an effective predictor of regeneration in previous work on experimental plots [29]. It is defined through Equation (1):

$$SDI = N \left(\frac{Dq}{25} \right)^{1.605}, \quad (1)$$

where N is the number of trees per ha and Dq is the quadratic mean diameter in cm. The SDI may be considered to represent the spatial concentration of tree biomass [4] (p. 399 ff.). Thus, it is a comprehensive indicator of the degree of competition for above- and belowground resources.

While the SDI expresses the current stand density at the time of measurement, we also required a variable that indicates whether a stand has been kept at higher or lower densities in the long run, because a low density could also result from heavy thinning in a previously dense stand. Therefore, we developed a method for quantifying whether an overstory tree is slender or stout, or has a normal height for its DBH. As a benchmark for normal heights at a given DBH, we fitted an allometric height-diameter model to overstory tree height and diameter (equation with parameters in Appendix A). Based on the residuals of that model, we estimated a DBH-related probability distribution to standardize the deviation between actual height and normal, i.e., expected height. That distribution enables us to introduce the Height Diameter Characteristic, HD. HD is defined as the probability (P) that any tree of the same diameter might be equally or less high (Equation (2)):

$$HD = P(h \leq h_0 \mid d = d_0), \quad (2)$$

where h is height as a random variable, d is DBH as a predictor, and h_0 and d_0 are tree height and DBH as measured, respectively. Thus, HD can obtain any value between 0 and 1. For a tree of any diameter, $HD = 0.5$ indicates an average, i.e., normal height to diameter ratio. $HD > 0.5$ marks an above average tall tree and $HD < 0.5$ a stout one. That characteristic, hence, aims to indicate the extent to which a tree had been inhibited in diameter growth through neighbor competition in the past.

The Species Profile Index SPI [4] (p. 281 ff.) is a proxy for a forest stand's richness in species and vertical structure simultaneously. High values indicate structurally rich stands and values of 0 indicate homogenous monospecific stands (Equation (3)):

$$SPI = -\sum_{i=1}^{S} \sum_{j=1}^{Z} p_{ij} \, ln p_{ij}, \quad (3)$$

where S is the number of species, Z is the number of height layers, and p is the relative frequency of species i in stand height layer j (exclusively species with $p_{ij} > 0$ considered). The Species Profile Index in its standard form is based on three stand height layers whose upper borders are $H_{max} \times 1$, $H_{max} \times 0.8$, and $H_{max} \times 0.5$, where H_{max} is the maximum tree height in the stand of interest. SPI, thus, might indicate whether biomass is concentrated into exactly one tree class or shared among several ones within the stand being considered.

For quantifying the NFI and BSFI plots' growth potential, we used a Site Index (SI), defined as the site dependent predominant tree height at age 100. It was computed by the site-productivity algorithm as implemented in the forest growth model SILVA [16]. That computation was based on the spatial position of the inventory plots and the German map of forest ecological regions [30]. Moreover, we included the Quadratic Mean Diameter (Dq) as a predictor that indicates the developmental state of the stand with respect to tree maturity for harvest. Stands with high Dq are in a phase where regeneration is promoted through felling. German forestry is marked by a large variety of treatment. Within one third of the forest, area transformation to uneven-aged stands and the maintenance of such stands is common. As an indicator of the stand's development stage, thus, we used the maximum height per

plot (*Hmax*) that is not limited to even-aged stands. Comparing both inventories by mean and range of corresponding native and derived variables, it can be seen that both are similar (Tables 1 and 2).

2.3. Models

Both models, the NFI- and the BSFI-based version, have the same structure. With the key objective to estimate the local probability distribution of regeneration biomass within an inventory plot, each model comprised a deterministic part as well as a stochastic one. The deterministic module aims to predict the distribution's expectancy value. As a complement, the stochastic part serves to estimate the variation around that predicted average. At the current stage of development, we aimed to restrict the presumptions for the deterministic module to a minimum. Accordingly, to predict regeneration biomass per ha B, we used a generalized additive mixed model (GAMM) for both the NFI-based model (Equation (4a)) and the BSFI-based one (Equation (4b)):

$$B_{ij} = \beta_0 + \beta_1 \cdot SDI_{ij} + \beta_2 \cdot SPI_{ij} + \beta_3 \cdot HD_{ij} + \beta_4 \cdot Hmax_{ij} + \beta_5 \cdot SI_{ij} + s(Dq_{ij}) + r_{ij}. \quad (4a)$$

$$B_{ijk} = \beta_0 + \beta_1 \cdot SDI_{ijk} + \beta_2 \cdot SPI_{ijk} + \beta_3 \cdot HD_{ijk} + \beta_4 \cdot Hmax_{ijk} + \beta_5 \cdot SI_{ijk} + s(Dq_{ijk}) + r_{ijk}. \quad (4b)$$

The fixed effects in this model are the Stand Density Index (*SDI*), the Species Profile Index (*SPI*), the Height Diameter Characteristic (*HD*), the stand maturity indicator (*Hmax*), the Site Index (*SI*), and the quadratic diameter (*Dq*). Except for *Dq*, all fixed effects in the model are linear (i.e., they are multiplied by one of the regression parameters $\beta_1, \ldots, \beta_5$). In contrast, the effect of *Dq* is modeled with a nonlinear spline-based smoother [31], which is indicated by the symbol $s(Dq)$. It accounts for a hypothesized nonlinear relation between *Dq* and regeneration stock due to a likely minimum of light transmission between the phase of adolescence and intense harvest.

In the model's NFI-based version, the indices j and i associate any plot j to the corresponding four-plot cluster i. The BSFI-based version uses a further index k to represent the embedding of any plot k into the associated forest stand j and the enclosing forest management unit i. Variable r represents the deterministic part's residuals, which deserve special attention. Due to the clustered data structure, r contains random effects on different levels. Within the NFI-based model, it comprises one single group effect that is due to the organization of plots within the inventory clusters (Equation (5)):

$$r_{ij} = b_i + \varepsilon_{ij}, \quad (5)$$

where b_i is a cluster specific random effect and ε_{ij} represents i.i.d. errors. The BSFI-based model comprises two group effects (Equation (6)):

$$r_{ijk} = b_i + b_{ij} + \varepsilon_{ijk}, \quad (6)$$

where b_i is the random effect related to the forest management unit and b_{ij} is the stand-related one. ε_{ijk} represents the i.i.d. errors.

For fitting each model's deterministic part (Equations (4a) resp. (4b)), we took into account that its absolute residuals (r in Equation (4)) might become larger as regeneration biomass (B) increases. In order to compensate for such heteroscedasticity, we applied a standard method [32] (p. 188).

Therefore, the deterministic part of the model (Equations (4a) resp. (4b)) was first calibrated to unweighted data to obtain the corresponding set of absolute residuals, i.e., the values of r. Then, a specific variance function (Equation (7)) was fitted to the squared residuals:

$$r^2 = e^{u\hat{B}+v}, \quad (7)$$

where r is the absolute residual, $\hat{B}$ is the predicted biomass, and u and v are parameters to be estimated. Finally, the deterministic model part was fitted again with each observation weighted by the inverse of the residual variance as estimated through Equation (7). For fitting the deterministic part, we used

the statistical software R [33] and the function gamm4 from package gamm4 [34]. The distribution assumption implied by the fitting procedure for Equation (4a) is $b_i \sim N(0, {\sigma_1}^2)$ and $\varepsilon_{ij} \sim N(0, {\sigma_2}^2)$. For fitting Equation (4b), we correspondingly assumed $b_i \sim N(0, {\sigma_3}^2)$, $b_{ij} \sim N(0, {\sigma_4}^2)$, and $\varepsilon_{ijk} \sim N(0, {\sigma_5}^2)$. In order to facilitate the reproduction and application of the deterministic model part, we complemented both Equations (4a) and (4b) with an approximation that refrained from the smoothing spline $s(Dq)$. To that end, we replaced $s(Dq)$ with a small set of polynomials. Therefore, we predicted regeneration biomass based on the observed Dq values and the mean of each remainder predictor. Then, we fit one polynomial to the data of predicted biomass over Dq within each of several Dq intervals.

The stochastic model part again uses an identical set of equations within the NFI- and the BSFI-based model. It aims to represent the typical spread of regeneration biomass values around an average value as predicted by Equations (4a) resp. (4b). Therefore, it describes the distribution of the deterministic part's residuals. As these residuals turned out to be heteroscedastic, they were standardized through division by the corresponding predicted mean biomass to obtain relative residuals. For approximating the variability among such relative residuals, the stochastic model part applies the gamma probability density function that is a flexible function confined to positive values. It uses one parameter for shape and one for steepness (rate), as given by Equation (8):

$$W(R) = \frac{\beta^{\alpha}}{\Gamma(\alpha)} R^{\alpha-1} e^{-\beta x}, \tag{8}$$

for $R > 0$, where R is the randomly distributed relative residual. Both α (shape) and β (rate) are parameters (>0). Γ denotes the Gamma function. To obtain parameter values for Equation (8) and to account for remaining heteroscedasticity, we estimated the function's characteristics from the biomass predicted by the deterministic part. Therefore, the stochastic part uses linear trends of the distribution's parameters shape α and rate β over predicted biomass (Equations (9a) and (9b)):

$$\alpha_l = u_{1l} + v_{1l}\hat{B}_l + \varepsilon_{1l}, \tag{9a}$$

$$\beta_l = u_{2l} + v_{2l}\hat{B}_l + \varepsilon_{2l}, \tag{9b}$$

where $\hat{B}$ is a biomass value predicted by Equations (4a) resp. (4b); u_1, u_2, v_1, and v_2 are regression parameters; and index l stands for an observation. Both $\varepsilon_1 \sim N(0, {\sigma_6}^2)$ and $\varepsilon_2 \sim N(0, {\sigma_7}^2)$ are the i.i.d. errors. In order to describe both trends, we divided the range of predicted biomass values into 40 intervals, each representing a quantile width of 2.5%. Within each of them, we fitted one gamma probability density function to the enclosed relative residuals. That way, we obtained a set of 40 distribution functions and, concomitantly, a data set of 40 estimated values for both parameters, shape and rate. For describing the biomass-related trend of a parameter considered—i.e., either shape or rate—we associated each parameter value to the corresponding interval's predicted biomass median and applied a linear regression (Equations (9a) and (9b)) to the resulting point set. Thus, for any predicted biomass and its accompanying residual distribution, we estimated the corresponding parameters, shape and rate. For fitting the density functions, we used the statistical software R and the function fitdist from package fitdistrplus with moment matching estimation [35].

2.4. Evaluation

We considered the deterministic model part (Equations (4a) resp. (4b)) as a prototype that might include non-relevant predictors. In order to present each model in a refined form that was exclusively based on relevant fixed effects, we applied two selection criteria to its predictors: one was the significance as obtained from the fitting of Equations (4a) resp. (4b). The other was the Akaike Information Criterion (AIC) [36]. We used that criterion to identify the model nested into Equations (4a) resp. (4b) that had the minimum tradeoff between goodness of fit and simplicity, i.e., the one with the minimum AIC. Moreover, we assessed the importance of each individual predictor variable using that method (Appendix B).

For evaluating the stochastic model part, we first tested whether the theoretical density distribution function it uses is a feasible model for the true distribution of the relative residuals obtained from the deterministic module. Although we had expressed each residual of the deterministic part as a relative deviation from the predicted value, we could not eliminate the dependence of the residual distribution on the deterministic part's predictors. For analyzing the residual distribution, we thus had to use a subrange of the plot data—including observed and predicted biomasses—with an acceptable homogeneity of the residual distribution therein. To that end, we considered a predictor space that was enclosed by a restricted quantile range of the three most influential predictors but still included enough data (quantile 25 to 75%). We then selected all data with predictor values inside that center range, and fitted the gamma density distribution function to the relative residuals obtained from these data. For evaluating that function, we tested it against the subset's observed relative residuals using the Kolmogorow-Smirnow test of the statistical software R (function ks.test from package stats, [37]). Moreover, we applied a QQ-plot to plausibilize the function's fit (R function qqplot from package stats, [38]).

For evaluating the results generated by the stochastic model part, we simulated relative residuals based on that module. To that end, we predicted the shape and rate of the stochastic part's gamma distribution function based on each predicted biomass from the deterministic model part (Equations (9a) and (9b)). We then sampled one simulated random residual per biomass value from the resulting set of distribution functions. Finally, we compared the simulated residuals to the observed ones within a QQ-plot.

In order to evaluate the bias of our modelling approach as dependent on the level of stratum differentiation, we applied the BSFI-based model to exemplary strata. We formed these strata from the set of BSFI plots that had been spared from model calibration. On the lower one of two discretization levels considered, the strata exclusively differed in the average tree size as a fundamental stratification criterion. On that level, we formed exactly one stratum per tree size class. Concomitantly, each stratum summarized plots from a number of spatially separate forest management units (each typically 20,000 ha). On the second level of discretization, we further subdivided the strata of the lower discretization level by the forest management unit, to obtain the additional model bias related to such higher spatial differentiation. In order to form the tree size classes, we used a basal area weighted average tree diameter that comprises both understory and overstory. It has routinely been applied to classify strata for SILVA-based simulation scenarios on the landscape scale level (Table 3). The set of BSFI plots for exemplary stratification was formed through random sampling of at least 140 plots per diameter class and forest management unit.

Table 3. Classification levels of the average diameter used for stratification with pct of plots in the BSFI (Bavarian State Forest Inventory) data (see Section 2.1.2).

Class	Diameter [cm] [1]	Pct of Plots
4	0 to 8	3
12	8 to 15	6
20	15 to 25	15
30	25 to 35	28
40	35 to 45	28
50	45 to 55	15
60	55 and more	5

[1] Lower limit excluded.

The study at hand used two evaluation criteria for comparing the modelled distribution of regeneration biomass to the observed one per stratum. One criterion is the mean value. The other is the mean value's cumulative frequency within the stratum, i.e., the approximate probability of a below average vs. an above-average regeneration biomass. That probability was used to assess whether the stochastic part of the model leads to a realistic frequency of dense vs. sparse regeneration stock within the stratum being considered. For generating the modelled data, we predicted the regeneration biomass per plot based on Equation (4b). Then, we constructed the according residual distribution

per plot (Equation (8)) using Equations (9a) and (9b) to estimate the parameters shape and rate in Equation (8) from the plot's predicted biomass. Finally, we calculated a modelled biomass value per plot as the product of the plot's predicted biomass and one relative residual value sampled from the estimated distribution. Then, we aggregated the modelled per-plot values on a per-stratum basis to obtain the modelled evaluation criteria. In order to corroborate our per stratum evaluation, we stabilized the value of each evaluation criterion through bootstrapping [39] with 100 replicates per stratum.

3. Results

Most fixed effects of the deterministic model part, i.e., *Dq*, *Hmax*, Stand Density Index *SDI*, Species Profile Index *SPI* and Height-Diameter Characteristic *HD* had a significant influence on regeneration biomass within both models (NFI-based Table 4, BSFI-based Table 5). The remainder predictor, *SI*, was exclusively relevant for the NFI-based model. Thus, the deterministic part of the NFI-based model with minimum AIC (see Section 2.4) was Equation (4a), while the corresponding part of the BSFI model with the smallest AIC was a version of Equation (4b) without Site Index *SI*.

The typical biomass-trend associated with each fixed effect indicates an outstanding relevance of *Dq*, *Hmax*, and *SDI* (NFI: Figure 1a–f, BSFI: Figure 2a–e). Within both the NFI- and the BSFI-based model, the fitted nonlinear effect of *Dq* revealed a strong influence of that predictor on regeneration biomass. That relation had a marked minimum of 3 t ha^{-1} at a *Dq* of 30 cm vs. a value of 5 t ha^{-1} at *Dq* values larger than 40 cm (Figures 1a and 2a).

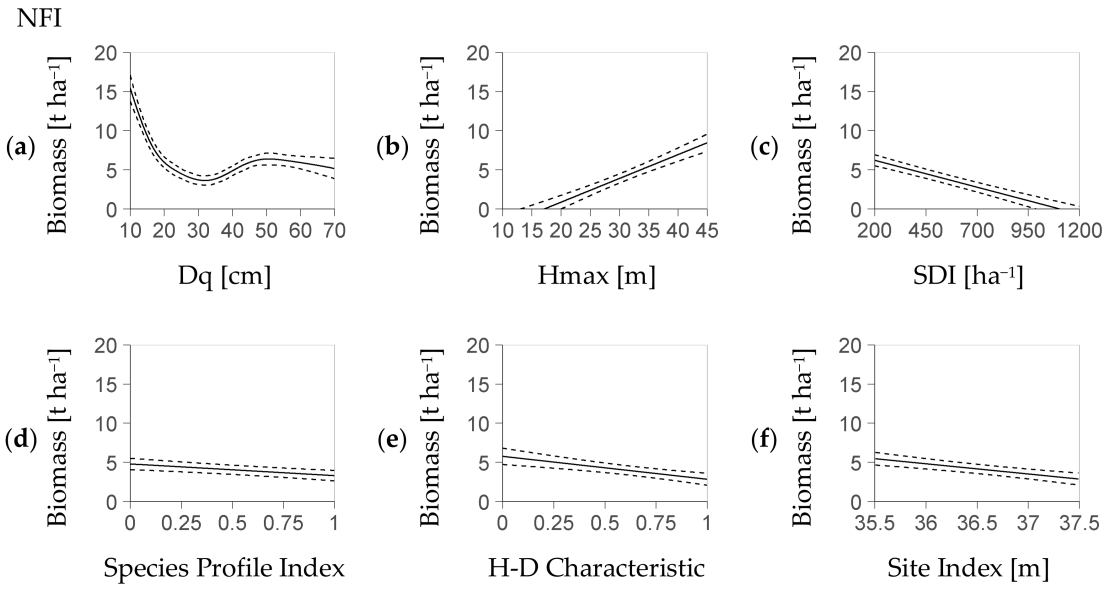

Figure 1. Profiles of regeneration biomass as predicted by the deterministic model part based on the NFI (German National Forest Inventory, Equation (4a)). Each profile is presented over one predictor with, at the same time, the remainder predictors at their mean value (abbreviation H-D: Height-Diameter); profiles ordered by the relevance of the referring predictor based on the AIC criterion ((**a**–**f**), see Section 2.4); dotted lines refer to the confidence interval; each predictor shown within its 95% interval; the stochastic part (Figure 3a,b) covers the residual distribution.

The increase of the AIC related to each predictor when it was removed as the only one from Equation (4a) and Equation (4b) (without *SI*) underpins the predictors' rank in importance (Table 6). In both models, the most important predictor was *Dq*, followed by *Hmax* and *SDI*. However, the NFI-based model and the BSFI-based model differed in the importance of their remainder common predictors: Species Profile Index *SPI* was more relevant than Height-Diameter Characteristic *HD* in the NFI-based model. The approximation to the deterministic part that substitutes the term *s*(*Dq*) (see

Section 2.3) deviated by less than 0.3 t (NFI) and 0.6 t (BSFI) if it used two polynomials (maximum deviation as quantile 95%, parameters in Appendix C, Table A2 resp. Table A3). The mean deviations were at 0.1 t (NFI) and 0.2 t (BSFI).

Table 4. Coefficients of the regeneration biomass model based on the NFI (German National Forest Inventory, Equations (4a) and (5)). The variables are denoted as in Equations (4a) and (5), i.e., *SDI* (Stand Density Index), *SPI* (Species Profile Index), *SI* (Site Index), *Hmax* (maximum height), *HD* (Height Diameter Characteristic), *Dq* (Quadratic Mean Diameter); β_1 to β_5 are corresponding fixed effect coefficients; *s*(*Dq*) is a univariate penalized cubic regression spline [31] over *Dq* (Figure 1a); *b* is the NFI cluster specific random effect, and s_1 is its standard deviation; ε represents the i.i.d. errors and s_2 represents their standard deviation.

	Intercept	**Fixed Effect of**						**Random Effect**	
		SDI	***SPI***	***SI***	***Hmax***	***HD***	***s*(*Dq*)**	b_i	ε_{ij}
Symbol [1]	β_0	β_1	β_2	β_3	β_4	β_5	–	s_1	s_2
Value	74,344	−6.87	−1498	−1304	304	−2927	–	5536	11,750
SE	143	0.60	380	265	32	692	–		
p-value	<0.0001	<0.0001	<0.0001	<0.0001	<0.0001	<0.0001	<0.0001		

[1] In Equation (4a).

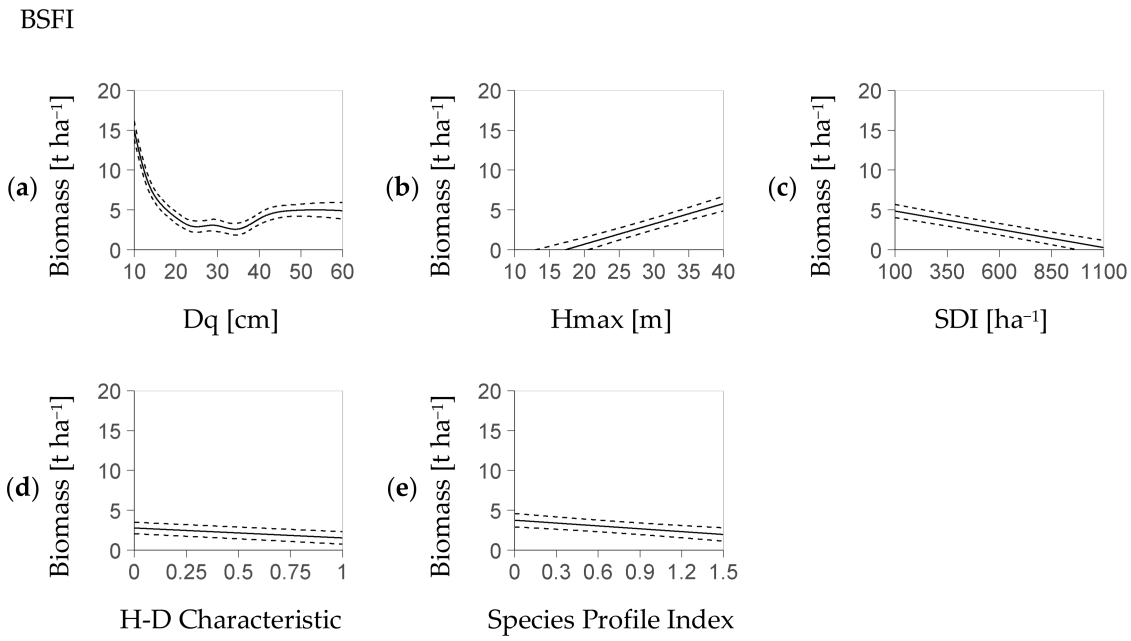

Figure 2. Profiles of regeneration biomass as predicted by the deterministic model part based on the BSFI (Bavarian State Forest Inventory, Equation (4b)). Each profile is presented over one predictor with, at the same time, the remainder predictors at their mean value (abbreviation H-D: Height-Diameter); profiles ordered by the relevance of the referring predictor based on the AIC criterion ((**a**–**e**), see Section 2.4); dotted lines refer to the confidence interval; each predictor shown within its 95% interval; the stochastic part (Figure 3c,d) covers the residual distribution (profiles based on 5881 BSFI plots used for model calibration).

Table 5. Coefficients of the regeneration biomass model based on the BSFI (Bavarian State Forest inventory, Equations (4b) and (6)). Site Index (*SI*) was not significant as a predictor and removed from Equation (4b) (see Section 2.4); the variables are denoted as in Equations (4b) and (6), i.e., *SDI* (Stand Density Index), *SPI* (Species Profile Index), *Hmax* (maximum height), *HD* (Height Diameter Characteristic), *Dq* (Quadratic Mean Diameter); β_1 to β_5 are corresponding fixed effect coefficients; $s(Dq)$ is a univariate penalized cubic regression spline [31] over *Dq* (Figure 2a); b_i is the random effect specific for the forest management unit, and s_3 is its standard deviation; b_{ij} is the stand specific random effect, and s_4 is its standard deviation; ε_{ij} represents the i.i.d errors and s_5 represents their standard deviations.

	Intercept	Fixed Effect of						Random Effect		
		SDI	***SPI***	***SI***	***Hmax***	***HD***	***s(Dq)***	b_i	b_{ij}	ε_{ijk}
Symbol [1]	β_0	β_1	β_2	–	β_4	β_5	–	s_3	s_4	s_5
Value	40,074	−4.59	−1194	–	255	−4610	–	1150	3667	7684
SE	251	0.48	289	–	26	571	–			
p-value	<0.0001	<0.0001	<0.0001	–	<0.0001	<0.0001	<0.0001			

[1] In Equation (4b).

Table 6. The increase of the AIC related to each predictor when it was removed as the only one from Equation (4a) and the nested model of Equation (4b) with minimum AIC (see Section 2.4). Abbreviations are NFI (German National Forest Inventory) and BSFI (Bavarian State Forest Inventory).

Model	Increase in AIC Related to Predictor					
	SDI	***SPI***	***SI***	***Hmax***	***HD***	***s(Dq)***
NFI (Equation (4a))	96	14	10	127	10	229
BSFI (Equation (4b))	388	67	–	406	253	2682

Within the predictors' center range considered for distribution analysis (see Section 2.4), given now by intervals of *Dq*, *Hmax*, and *SDI*, the KS-test rejected the strict hypothesis that the gamma probability density function was a precise theoretical model of the residuals' distribution. A QQ-plot, however, indicates (Figure 3b,d) that this density function is a feasible approximation to the empirical density distribution of the residuals (Figure 3a,c). If estimated from the deterministic part of the NFI-based model and its residuals, the relation between the predicted biomass and each parameter of the gamma density function, shape and rate, is close to a linear one (Figure 4a,b). A linear trend also sufficiently approximates both relations if they are based on the BSFI data and the deterministic part of the BSFI-based model (Figure 4d,e). Sampling from the stochastic parts of both models (as described in Section 2.4), within at least 95% of the data, yielded a distribution that had similar quantiles as the one computed from observed residuals (QQ-plot, Figure 4c,f).

Further results consider the evaluation of the BSFI-based model as dependent on the level of stratum differentiation, i.e., on the degree of landscape discretization. The basic stratification that only used the criterion of diameter class (Table 3) formed a set of seven strata. Among these strata, the ratio of measured to modelled regeneration biomass had a mean of one-fold (Figure 5a). It ranged from 0.8 to 1.2-fold. Among the diameter classes 30, 40, and 50 that represent 71% of all 11,954 BSFI plots used, the bias range was notably smaller, i.e., from 0.8 to 1.0-fold. Cumulative frequency values (%) based on measured data deviated from the predicted ones by absolute values ranging from −7.4 to 2.6 (Figure 5c). Among strata of classes 30, 40, and 50 (Table 3), again, the absolute deviation of measured from modelled cumulative frequency (%) was small at a maximum of ±0.6.

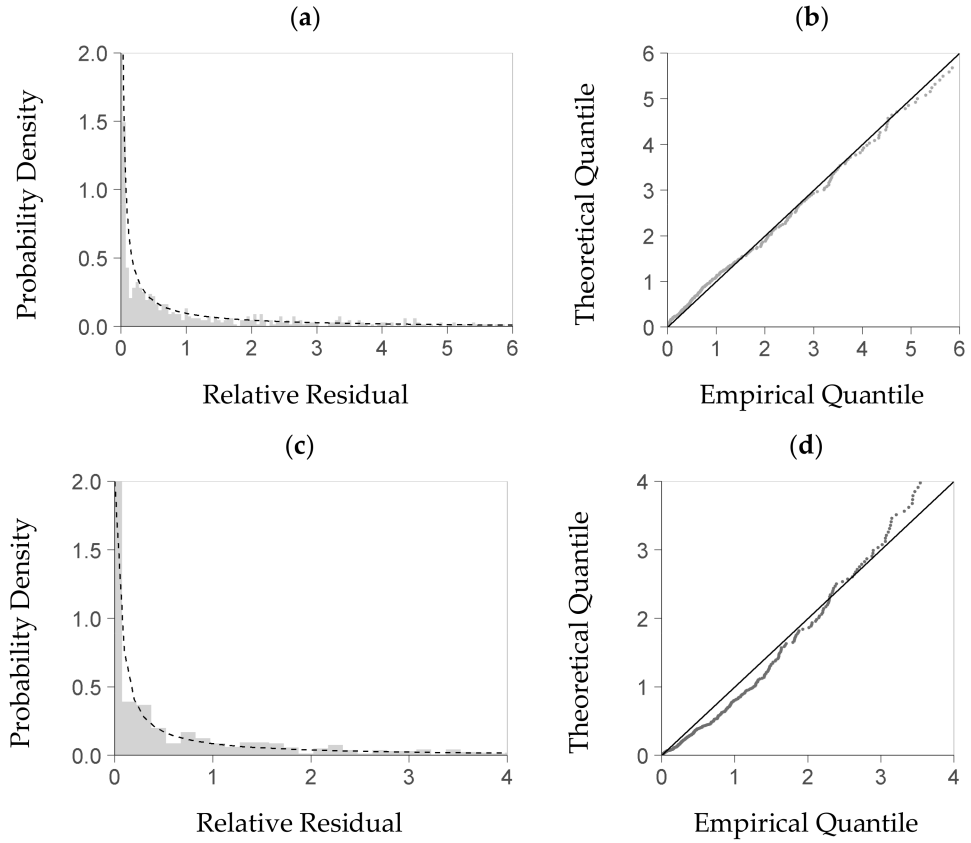

Figure 3. Plausibility test of the theoretical probability distribution that provides the basis for the stochastic part of the model (Equation (8)); diagrams (**a**,**b**) are based on the NFI, i.e., German National Forest Inventory; (**c**,**d**) are based on the BSFI, i.e., Bavarian State Forest Inventory. That distribution of relative residuals (*R* in Equation (8), per-plot regeneration biomass to predicted regeneration biomass) is presented here from within a center range of the data (see Section 2.4) where the three main predictors of the deterministic model part (Figure 1), *Dq*, *SDI*, and Top Height, lie within their interquartile range each; both (**a**) (resp. (**c**)) and (**b**) (resp. (**d**)) compare the theoretical distribution to the empirical one; diagrams (**a**) and (**c**): probability density of the relative residual; the bars refer to the empirical density, and the line refers to the density obtained from a fitted gamma probability density function; diagrams (**b**) and (**d**): the QQ-plot of the quantile based on the fitted probability density function (Theoretical Quantile) over the quantile based on the measured data (Empirical Quantile); all shown within the 95% quantile of the relative residual ((**a**), (**b**) based on 1353 NFI plots, (**c**), (**d**) based on 1069 BSFI plots used for model calibration).

The stratification resulted in a notably smaller plot number per stratum, if it was based on the forest management unit in addition to the diameter class. Then, exclusively strata of diameter classes 30, 40, and 50 provided the minimum sample size postulated by the study at hand (140 plots). Only such strata will be considered by the following analysis. Still, they comprise 71% of all plots from the BSFI data set. The range of bias between measured and predicted per-stratum mean biomass among strata of that group was notably higher than the typical one among such strata that were based on the diameter class only. Their bias range was from 0.6 to 1.2-fold vs. 0.8 to 1.0-fold. The bias had a mean of 0.9-fold (Figure 5b vs. a). Thus, there was an additional bias of predicted stratum biomass within ±0.2-fold, if the strata formation used the forest management unit as a further criterion. That additional data spread was due to the scatter of the observed per-stratum values around their diameter-class average (±0.15-fold).

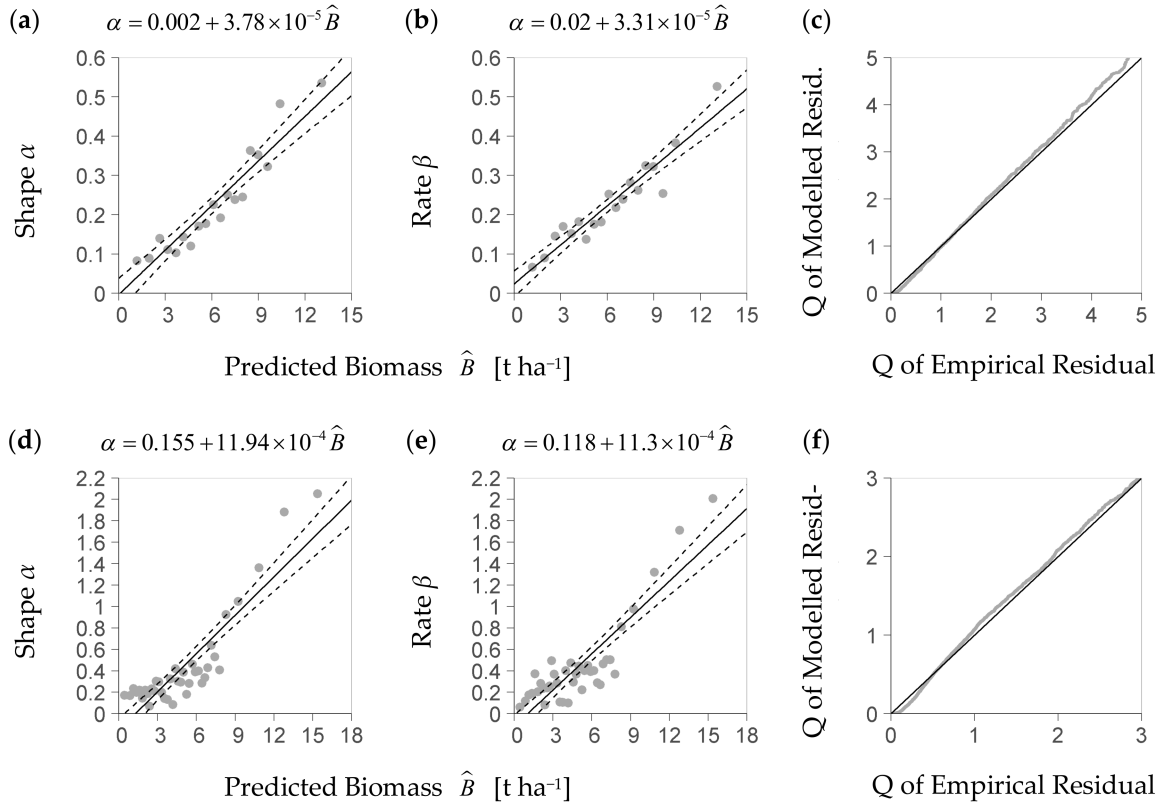

Figure 4. Diagrams (**a**,**b**) show the parameters α and β of the stochastic model part (Equation (8)) based on the NFI (German National Forest Inventory), as represented by the trend line of shape α (diagram (**a**)) and rate β (diagram (**b**)) over the predicted regeneration biomass (Equations (9a) and (9b), parameterized equation shown above corresponding figure); the stochastic model part considers the scattering of the relative residuals of the deterministic part (Figure 1); diagram (**c**) is the result of the corresponding plausibility test of the stochastic model part with a QQ-Plot that compares 7784 quantiles Q of the modelled relative residual vs. the empirical one up to Q = 95% (relative residual is *R* in Equation (8), per-plot regeneration biomass to predicted regeneration biomass); diagrams (**d**–**f**) present the corresponding results based on the data of the BSFI (Bavarian State Forest Inventory, (**d**,**e**) based on 5881 plots used for model calibration; (**f**) based on 6073 points spared from calibration for evaluation).

Moreover, there was also an increase of the absolute deviation in the mean's cumulative frequency (%), related to the forest management unit level, which was at ±6. Hence, there was a notable stochastic effect on the forest management unit-level that reduced the precision of the model, if strata were formed by both diameter class and forest management unit. All stratum-related values that we presented here are stable: the uncertainty of any observed average value per stratum due to per plot variation of regeneration biomass was commonly below 0.05-fold of the observed value.

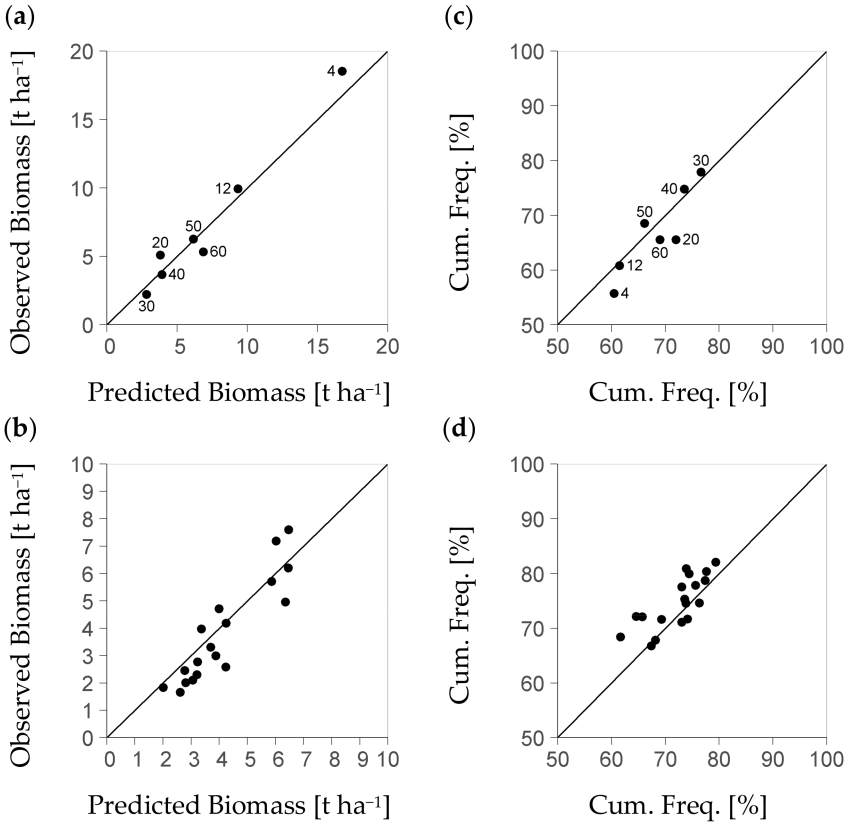

Figure 5. Diagrams (**a**,**b**): Mean of measured regeneration biomass over mean of predicted regeneration biomass per stratum obtained from the BSFI (Bavarian State Forest Inventory); (**a**) if strata have been formed based on the diameter class (Table 3); (**b**) if strata have both been formed based on diameter class and Forest Management Unit: the higher data spread on that scale level points to an as yet stochastic factor to be captured; in diagram (**a**), the numbers 4 to 60 denote diameter classes [cm] of 4 $\pm$ 4, 12 $\pm$ 3, 20 $\pm$ 5, 30 $\pm$ 5, 40 $\pm$ 5, 50 $\pm$ 5, and 55 to 80; in diagram (**b**), due to the sample size required per stratum the data focus on diameter classes 30, 40, and 50 (71% of all 11,954 BSFI plots); diagrams (**c**), (**d**) show the according result of the cumulative frequency (Cum. Freq.) of mean biomass; the cumulative frequency serves to indicate the quality of the modelled distribution characteristics (all based on 6073 inventory plots spared from model calibration for evaluation).

4. Discussion

4.1. The Study Responds to a Common Requirement for Model Initialization

Regeneration constitutes a key process within the development of forest structure and stock [40]. Its initial state is thus a pivotal condition for the result of forest management scenarios that exemplify the development of ecosystem services on the landscape scale level (e.g., [1]). In order to estimate regeneration within the northern Rocky Mountains, Ferguson et al. [41] predicted the probability per tree density class and the maximum tree height among regeneration trees with a statistical model obtained from stand management lists. Schweiger and Sterba [11], as well as Tremer et al. [12], extended that approach in order to represent the tree density per species and height class. Kolo et al. [13], based on the German national forest inventory, presented a model that estimates the probability of regeneration to occur based on German national forest inventory data. They underpin the relevance of structure and site as model predictors.

Biomass growth is closely linked to the stand intrinsic fluxes of radiation, heat, and water. These fluxes, in turn, depend on resistances that originate from canopy and soil properties [42].

Regeneration biomass thus represents a fundamental outcome of the regeneration process. On the experimental plot level, that key variable has enabled researchers to survey the quantitative relation of regeneration stock and structural indicators [29]. The study at hand considers a continuative approach in order to represent regeneration stock on the landscape scale level. It aims to supplement virtual stands from simulation strata with a realistic amount of regeneration biomass. The rationale for using biomass as a predicted variable is to split up the modelling of regeneration stock into two consecutive steps. The first step is the estimation of regeneration biomass involving an essential stochastic component that accounts for previous and unrecorded disturbances. The second one is yet to be implemented. It distributes the biomass estimated per tile of a dynamic regeneration model among tree size classes. In order to initialize dynamic models, we will complement our approach by an algorithm that derives the species-specific proportion of regeneration biomass. Therefore, a logistic model (e.g., as used by Tremer et al. [12]) based on overstory species shares is a likely candidate. Moreover, our model type will translate regeneration biomass into a realistic height profile of tree density. That profile will likely be based on a biomass-related maximum height per plot and a tree biomass to height relation from empirical data.

4.2. The Study Conceptualizes and Evaluates a Novel Biomass-Based Approach

The statistical model from the study at hand comprised a deterministic part and a stochastic one. Both parts complement each other in order to predict the characteristic distribution of regeneration biomass within plot-sized stratum subsectors. Within the deterministic module, we aimed to reduce the number of presumptions on the one hand and the degrees of freedom on the other. Therefore, we applied a linear relationship between the biomass and most of the predictors considered. In order to represent the dependence of regeneration biomass on the *Dq*, however, we presumed a nonlinear partial regression. The results confirmed that nonlinear relationship and showed that *Dq* is a highly relevant predictor. Kolo et al. [13] underpinned that relevance and reported an increase of probability with *Dq*. However, they pointed to the converse trend within previous work. The study at hand demonstrated that both tendencies exist and depend on stand maturity. Moreover, the deterministic part of the NFI-based model points to a local maximum of biomass at a *Dq* of 50 cm. The strong increase of regeneration stock with lower *Dq* values starting from 35 cm is likely due to target diameter felling and the removal of competitors within the overstory. An indicated drop of the biomass at *Dq* values beyond the local maximum is well justified by a decreasing abundance of mature beech [43].

An observed value of regeneration biomass, beyond resource supply to the understory, may imply both intensity and point in time of a disturbance. Disturbance incidents are rarely reported within inventory data. However, they influence the residual distribution of regeneration biomass at given predictor values. Therefore, we complemented the deterministic model part with a stochastic one that describes the distribution of relative residuals. That stochastic model part used the gamma probability density function. After parameterization, that variable shape function strictly monotonically decreased with pole zero and asymptote zero. Previous work [44,45] has reported a distribution of canopy gap size that resembles a falling exponential function. It underpins that the gamma density distribution function is a suitable approximation to the regeneration biomass distribution at given overstory structure attributes. Although the model type of the study at hand is suitable for both of the inventories considered, the NFI-based model, as it has the more general geographical scope, is the actual candidate of further development.

4.3. The Modelling Approach Exemplified Provides a Basis of Future Development

We exemplarily evaluated the predictive quality of the model type presented as dependent on the stratum resolution. Therefore, we applied the BSFI-based model, in a first step, to strata that exclusively differ in the average diameter of their inventory plots. That application test underpinned that a regeneration biomass model of the type considered may sufficiently approximate the regeneration biomass of such generalist strata. Moreover, the model met the observed cumulative frequency of the

average biomass per stratum. The stochastic part of the model thus generated a realistic heterogeneity of the stratum-intrinsic regeneration biomass. However, a test with strata of a higher discretization level that also included the forest management unit was linked to a notable increase of model bias. That additional bias was certainly due to processes that, on the one hand, vary among strata with size of a forest management unit but, on the other, have no equivalents in the model as fixed effects.

4.4. Browsing Is a Likely Missing Indicator

Kupferschmid et al. [19] pointed out that browsing intensity considerably varies among Swiss federal states (Kanton), many of which have a total area of about 150,000 ha. That area size corresponds to the average size of the total landscape around a typical German state forest management unit. Browsing in general has been reported to be a severe inhibitor of regeneration [46–48]. Kolo et al. [13] accordingly assumed that browsing is a major cause of leeway within their prediction of regeneration probability.

4.5. Most of the Random Effect Is Due to Within-Stand Variability

Kolo et al. [13] reported that their model predicts the occurrence of regeneration at a notably high rate of 72%. The remaining leeway of 28% corresponds to the wide probability distribution within the stochastic part of both our models. The variation among forest management unit-based strata, in contrast to that among plots, was notably smaller. That finding indicates that even at the highest discretization level considered, the largest part of variability is intrinsic to each stratum. Thus, the stochastic model part, as given by the residual distribution of the deterministic part, mostly represented a typical stand-intrinsic variation. Hence, one may consider its distribution characteristics as mainly governed by small-scale effects.

4.6. Application of Such Model Has to Account for General Limitations of Any Inventory

A study on inventory plots cannot guarantee that the overstory recorded within a plot is equivalent to the one that takes influence on the plot's regeneration (light from aside [49]). Within the NFI data, an error due to side light effects is less critical, as the small inventory circle for regeneration is situated five meters north of the plot center. Moreover, the radius of angle count sampling increases with DBH and hence canopy height (e.g., at DBH 40 cm to 20 m). Thus, the overstory fraction that controls the influence of direct solar irradiance is likely covered by the inventory method of the NFI to the largest part.

4.7. The Most Relevant Predictors Will Be Accessible through Remote Sensing

The ongoing development of airborne laser scanning (ALS) contributes novel methods for the collection and analysis of 3D point clouds. Such methods permit researchers to access crown diameters and to classify tree species below the top-most layer of a stand, as exemplified by Lindberg and Holmgren [50]. Jucker et al. [51] presented allometric equations that infer the tree diameter from airborne crown dimensions. The most relevant indicators of our model, *Dq*, *Hmax*, and *SDI*, will thus be a regular future outcome of remote sensing-based inventories. ALS, moreover, may gain support through combination with further airborne and terrestrial methods, such as Terrestrial Laser Scanning (TLS) [52].

4.8. Future Work Has to Explain Random Effects and Might Extend the Focus of Model Application

The most relevant task of future development is to identify the processes that explain the model bias on the level of a forest management unit. A possible one is browsing that is strongly related to the local hunting regime [53]. Further research has to quantify the intensity of such processes by predictor variables that are available from local forest management, e.g., as class variables. If one applies the model to inventories that cover multiple tenure types, the model quality will certainly benefit from

including the type of the forest owner [13]. Statistical regeneration models might further be used to support the plausibility of spin-up runs. Such dynamic initializations are well established for defining the initial regeneration status within succession models, e.g., in [54]. A statistical regeneration model, moreover, might be applied to correct values of regeneration stock after several time steps of a simulation have passed.

5. Conclusions

The study's type of regeneration model significantly relates regeneration biomass to indicators of structure and site. Within large subunits of forest landscape classified by dominating species and average diameter, such a model represents regeneration stock at an acceptable precision. For initializing dynamic management scenarios on the landscape scale level, the approach is thus promising. However, this type of model requires additional indicators, if the landscape subunits also differ by the forest management unit. One possible candidate for such a predictor is browsing.

The Quadratic Mean Diameter (*Dq*) is a strong indicator of stand development and, moreover, of regeneration biomass. An average tree diameter is thus a well-reasoned stratification criterion. *Dq*, *Hmax*, and *SDI* are the most relevant predictors. This finding is promising for a remote detection of key stand attributes. Future development of the statistical regeneration model will consider browsing as an additional predictor. Therefore, a quantitative relation between browsing intensity and regeneration stock within inventory data will be advantageous. The modelling approach, as a future benefit, may help to estimate the potential of natural forest recovery after severe overstory loss.

Acknowledgments: The authors wish to express their gratitude to the Bayerische Staatsforsten AÖR, Regensburg (BaySF) for providing valuable data from their regular inventories. Special thanks are also due to the Thünen Institut Eberswalde for supplying national forest inventory data. In particular, we would like to thank Thomas Riedel (Thünen Institut) for consultancy in biomass computation, biomass extraction, and overstory structure extraction from the public database. The authors wish to thank Rüdiger Grote, Michael Heym, Torben Hilmers, Ralf Moshammer, Leonhard Steinacker, and Enno Uhl for inspiration and discussion. Special thanks are due to the European Union for support of this study through funding of (1) project ALTERFOR within the Horizon 2020 research and innovation programme under grant agreement No 676754 and of (2) project ClusterWIS within the European Regional Development fund under grant aggreement EFRE-080003 (EFRE.NRW 2014-2020). Online publication of his work was supported by the German Research Foundation (DFG) and the Technical University of Munich within the funding programme Open Access Publishing.

Author Contributions: Werner Poschenrieder conceptualized the model, the data preparation, the model calibration, the model evaluation, and the article's structure. Werner Poschenrieder conducted all practical work of modelling and data handling and wrote the paper. Peter Biber gave specialist advice in statistical modelling and evaluation. Peter Biber reviewed the paper and contributed to all sections through editing. Hans Pretzsch supervised and reviewed the study and gave profound expert advice in regeneration dynamics.

Conflicts of Interest: The authors declare no conflict of interest.

Appendix A

An allometric height-diameter model was fitted to to overstory tree height and diameter. That model followed Equation (A1):

$$h = A \cdot d^B, \tag{A1}$$

where h and d are individual tree height and diameter, respectively, and A and B are parameters. That model was fitted to individual tree overstory data from the deciduous fraction of the NFI to meet the conditional (1) mean value; (2) 2.5% quantile; and (3) 97.5% quantile of height h as dependent on diamteter d. Thus, we obtained three representations of Equation (A1) with defined parameter values (Table A1) that enabled us to represent a conditional gaussian distribution of h at any given diamteter d. That conditional gaussian distribution enabled us to calculate the Height Diameter Characteristic given by Equation (A2) as a conditional probability P:

$$HDC = P(h \leq h_0 \mid d = d_0), \tag{A2}$$

where h is height as a random variable, d is DBH as a predictor, and h_0 and d_0 are tree height and DBH as measured, respectively.

Table A1. Parameter values that result from fitting of Equation (A1) to the distribution of individual tree height–diameter data.

Distribution Characteristic Equation (A1) Was Fitted to	Parameter Value	
	A	***B***
Mean	5.142	0.437
2.5% quantile	1.803	0.580
97.5% quantile	7.563	0.420

Appendix B

In order to assess the importance of each individual predictor, we removed each predictor variable exclusively from the model of minimum AIC to obtain one nested model per predictor removed. We then compared the AIC value of that nested sub model to the AIC value of the optimal one. That variable whose exclusion caused the greatest AIC difference was considered the most important one.

Appendix C

Two polynomials were applied in order to approximate the spline $s(Dq)$ within the deterministic part of both the NFI-based model (Equation (4a)) and the BSFI-based model (Equation (4b)). They enable the application of each model independently of the original data and of the statistical software R. Each polynomial conforms to the following Equation (A3):

$$\Delta B = d_1 \cdot Dq + d_2 \cdot Dq^2 + d_3 \cdot Dq^3, \quad \text{(A3)}$$

where ΔB is the change in regeneration biomass related to Dq. That approximation may be applied in order to predict biomass from Dq and each remainder predictor (see Equations (4a) resp. (4b)). To that end, first the corresponding row in Table A2(NFI) and Table A3 (BSFI) is to be selected. The row to be considered is the one with the Dq interval that encloses the given value of Dq. The approximate value of predicted regeneration biomass B is then:

$$B = I + S + \Delta B, \quad \text{(A4)}$$

where I is the value in the column Intercept of the table considered; S is the sum of each of the predictors except Dq multiplied by the slope given with its name; and ΔB is the value that results from applying Equation (A3) to Dq and the parameters from columns d_1, d_2, and d_3. Each of these approximations is exclusively valid within the corresponding interval of Dq (hence, the intercepts may notably differ).

Table A2. The parameters of the approximation to the deterministic part of the NFI-based model (see Section 2.3 and Equation (A3)) that substitutes $s(Dq)$ by two polynomials; the intercept implies that of the polynomial approximation and thus depends on the interval of Dq.

***Dq* Interval**	**Intercept**	**Slope of**							
		SDI	***SPI***	***SI***	***Hmax***	***HD***	d_1	d_2	d_3
≤56.6	79,000	−6.87	−1498	−1304	304	−2927	−2543	66.88	−0.54
>56.6	52,630	−6.87	−1498	−1304	304	−2927	−2.06	−0.58	0

Table A3. The parameters of the approximation to the deterministic part of the BSFI-based model (see Section 2.3 and Equation (A3)) that substitutes $s(Dq)$ by two polynomials; the intercept implies that of the polynomial approximation and thus depends on the interval of Dq.

Dq Interval	Intercept	Slope of							
		SDI	*SPI*	*SI*	*Hmax*	*HD*	d_1	d_2	d_3
≤35	50,530	40,074	−4.59	−1194	–	255	1338	−19.06	0.082
>35	−25,973	40,074	−4.59	−1194	–	255	−5522	206	−2.55

References

1. Biber, P.; Borges, J.; Moshammer, R.; Barreiro, S.; Botequim, B.; Brodrechtová, Y.; Brukas, V.; Chirici, G.; Cordero-Debets, R.; Corrigan, E.; et al. How Sensitive Are Ecosystem Services in European Forest Landscapes to Silvicultural Treatment? *Forests* **2015**, *6*, 1666–1695. [CrossRef]
2. Jonsson, B.; Jacobsson, J.; Kallur, H. The Forest Management Planning Package Theory and Application. *Stud. For. Suec.* **1993**, *189*, 1–56.
3. Pott, M.; Fabrika, M. An Information System for the Evaluation and Spatial Analysis of Forest Inventory Data. *Forstwiss. Cent.* **2002**, *121* (Suppl. 1), 80–88.
4. Pretzsch, H. *Forest Dynamics, Growth and Yield*; Springer: Berlin/Heidelberg, Germany, 2009; ISBN 978-3-540-88306-7.
5. Canadian Forest Inventory Committee. *Canada's National Forest Inventory Ground Sampling Guidelines: Specifications for Ongoing Measurement*; Natural Resources Canada, Canadian Forest Service, Pacific Forestry Centre: Victoria, BC, Canada, 2008.
6. Polley, H. *Survey Instructions for the 3rd National Forest Inventory (2011–2012) 2nd Revised Version, May 2011 with 4. Corrigendum (21.03.2014)*; Bundesministerium für Ernährung, Landwirtschaft und Verbraucherschutz Ref. 535; Federal Ministry of Food, Agriculture, and Consumer Protection: Bonn, Germany, 2011.
7. Hunziker, U.; Brang, P. Microsite Patterns of Conifer Seedling Establishment and Growth in a Mixed Stand in the Southern Alps. *For. Ecol. Manag.* **2005**, *210*, 67–79. [CrossRef]
8. Abdullahi, S.; Kugler, F.; Pretzsch, H. Prediction of stem volume in complex temperate forest stands using TanDEM-X SAR data. *Remote Sens. Environ.* **2016**, *174*, 197–211. [CrossRef]
9. Abdullahi, S.; Schardt, M.; Pretzsch, H. An unsupervised two-stage clustering approach for forest structure classification based on X-band InSAR data. A case study in complex temperate forest stands. *Int. J. Appl. Earth Obs. Geoinf.* **2017**, *57*, 36–48. [CrossRef]
10. Kayitakire, F.; Hamel, C.; Defourny, P. Retrieving forest structure variables based on image texture analysis and IKONOS-2 imagery. *Remote Sens. Environ.* **2006**, *102*, 390–401. [CrossRef]
11. Schweiger, J.; Sterba, H. A Model Describing Natural Regeneration Recruitment of Norway Spruce (*Picea abies* (L.) Karst.) in Austria. *For. Ecol. Manag.* **1997**, *97*, 107–118. [CrossRef]
12. Tremer, N.; Schmidt, M.; Hansen, J. Estimating the Structure of Natural Regeneration Based on Inventory Data. *Allg. Forst Jagdztg.* **2005**, *176*, 1–13.
13. Kolo, H.; Ankerst, D.; Knoke, T. Predicting Natural Forest Regeneration: A Statistical Model Based on Inventory Data. *Eur. J. For. Res.* **2017**, *136*, 923–938. [CrossRef]
14. Lutze, M.; Ades, P.; Campbell, R. Spatial Distribution of Regeneration in Mixed-Species Forests of Victoria. *Aust. For.* **2004**, *67*, 172–183. [CrossRef]
15. Gravel, D.; Beaudet, M.; Messier, C. Partitioning the Factors of Spatial Variation in Regeneration Density of Shade-Tolerant Tree Species. *Ecology* **2008**, *89*, 2879–2888. [CrossRef] [PubMed]
16. Pretzsch, H.; Biber, P.; Ďurský, J. The Single Tree-Based Stand Simulator SILVA: Construction, Application and Evaluation. *For. Ecol. Manag.* **2002**, *162*, 3–21. [CrossRef]
17. Seidl, R.; Lexer, M.J.; Jager, D.; Honninger, K. Evaluating the Accuracy and Generality of a Hybrid Patch Model. *Tree Physiol.* **2005**, *25*, 939–951. [CrossRef] [PubMed]
18. Fischer, R.; Bohn, F.; Dantas de Paula, M.; Dislich, C.; Groeneveld, J.; Gutiérrez, A.G.; Kazmierczak, M.; Knapp, N.; Lehmann, S.; Paulick, S.; et al. Lessons Learned from Applying a Forest Gap Model to Understand Ecosystem and Carbon Dynamics of Complex Tropical Forests. *Ecol. Model.* **2016**, *326*, 124–133. [CrossRef]

19. Kupferschmid, A.D.; Heiri, C.; Huber, M.; Fehr, M.; Frei, M.; Gmür, P.; Imesch, N.; Zinggeler, J.; Brang, P.; Clivaz, J.C.; et al. Einfluss Wildlebender Huftiere Auf Die Waldverjüngung: Ein Überblick Für Die Schweiz. *Schweiz. Z. Forst.* **2015**, *166*, 420–431. [CrossRef]
20. Clark, D.A.; Brown, S.; Kicklighter, D.W.; Chambers, J.Q.; Thomlinson, J.R.; Ni, J. Measuring Net Primary Production in Forest Concepts and Field Methods. *Ecol. Appl.* **2001**, *11*, 356–370. [CrossRef]
21. Thünen Institute, Germany. German National Forest Inventory (BWI) Results Database. Available online: https://bwi.info (accessed on 1 September 2015).
22. Kändler, G.; Bösch, B. *Überprüfung und Neukonzeption einer Biomassefunktion. Abschlussbericht 2b*; Abt. Biometrie und Informatik Wonnhaldestraße 4 79100; Forstliche Versuchs- und Forschungsanstalt Baden-Württemberg: Freiburg, Germany, 2013.
23. Röhling, S.; Dunger, K.; Kändler, G.; Klatt, S.; Riedel, T.; Stümer, W.; Brötz, J. Comparison of Calculation Methods for Estimating Annual Carbon Stock Change in German Forests under Forest Management in the German Greenhouse Gas Inventory. *Carbon Balance Manag.* **2016**, *11*, 12. [CrossRef] [PubMed]
24. Marklund, L.G. *Biomass Functions for Norway Spruce (Picea abies (L.) Karst) in Sweden*; SLU, Swedish University of Agricultural Sciences, Department of Forest Survey: Uppsala, Sweden, 1987.
25. Neufanger, M.; Faltl, W.; Schelhaas, C. *Anleitung zur Durchführung von Betriebsinventuren in den Bayerischen Staatsforsten. FE AA 010 Durchführung von Betriebsinventuren*; Bayerische Staatsforsten AöR: Munich, Germany, 2012.
26. Kozlowski, T.T. Physiological Ecology of Natural Regeneration of Harvested and Disturbed Forest Stands: Implications for Forest Management. *For. Ecol. Manag.* **2002**, *158*, 195–221. [CrossRef]
27. Pardos, M.; Montero, G.; Cañellas, I.; Ruiz del Castillo, J. Ecophysiology of Natural Regeneration of Forest Stands in Spain. *For. Syst.* **2005**, *14*, 434–445. [CrossRef]
28. Reineke, L.H. Perfecting a stand-density index for even-aged forests. *J. Agric. Res.* **1933**, *46*, 627–638.
29. Pretzsch, H.; Biber, P.; Uhl, E.; Dauber, E. Long-Term Stand Dynamics of Managed Spruce-Fir-Beech Mountain Forests in Central Europe: Structure, Productivity and Regeneration Success. *Forestry* **2015**, *88*, 407–428. [CrossRef]
30. Thünen Institute, Germany. Digital Map of Forest Ecological Regions (Wuchsgebiete/Wuchsbezirke). Available online: https://gdi.thuenen.de/wo/wgwb/ (accessed on 1 September 2015).
31. Wood, S.N. *Generalized Additive Models: An Introduction with R*, 2nd ed.; Chapman and Hall/CRC Press; Taylor Francis Inc.: New York, NY, USA, 2017; ISBN 978-1-49-872833-1.
32. Fahrmeir, L.; Kneib, T.; Lang, S.; Marx, B. Extensions of the Classical Linear Model. In *Regression*; Springer: Berlin/Heidelberg, Germany, 2013; pp. 177–267, ISBN 978-3-642-34332-2.
33. R Core Team. *R: A Language and Environment for Statistical Computing*; R Foundation for Statistical Computing: Vienna, Austria, 2016; Available online: https://www.R-project.org/ (accessed on 24 April 2016).
34. Wood, S.; Scheipl, F. Gamm4: Generalized Additive Mixed Models Using 'mgcv' and 'lme4'. R Package Version 0.2-5. Available online: https://CRAN.R-project.org/package=gamm4 (accessed on 25 November 2017).
35. Delignette-Muller, M.L.; Dutang, C. fitdistrplus: An R Package for Fitting Distributions. *J. Stat. Softw.* **2015**, *64*, 1–34. Available online: http://www.jstatsoft.org/v64/i04/ (accessed on 24 April 2016). [CrossRef]
36. Akaike, H. Prediction and Entropy. In *A Celebration of Statistics*; Atkinson, A.C., Fienberg, S.E., Eds.; Springer: New York, NY, USA, 1985; pp. 1–24.
37. Marsaglia, G.; Tsang, W.W.; Wang, J. Evaluating Kolmogorov's distribution. *J. Stat. Softw.* **2003**, *8*. Available online: http://www.jstatsoft.org/v08/i18/ (accessed on 24 April 2016). [CrossRef]
38. Becker, R.A.; Chambers, J.M.; Wilks, A.R. *The New S Language*; Chapman & Hall/CRC: London, UK, 1988; ISBN 978-0-534-09192-7.
39. Efron, B. Bootstrap Methods: Another Look at the Jackknife. *Ann. Stat.* **1979**, *7*, 1–26. [CrossRef]
40. Price, D.T.; Zimmermann, N.E.; van der Meer, P.J.; Lexer, M.J.; Leadley, P.; Jorritsma, I.T.M.; Schaber, J.; Clark, D.F.; Lasch, P.; McNulty, S.; et al. Regeneration in Gap Models: Priority Issues for Studying Forest Responses To Climate Change. *Clim. Chang.* **2001**, *51*, 475–508. [CrossRef]
41. Ferguson, D.E.; Carlson, C.E. *Predicting Regeneration Establishment with the Prognosis Model*; No. 467, 1-U54; Forest Service: Ogden, UT, USA, 1993.
42. Landsberg, J.J.; Waring, R.H. A Generalised Model of Forest Productivity Using Simplified Concepts of Radiation-Use Efficiency, Carbon Balance and Partitioning. *For. Ecol. Manag.* **1997**, *95*, 209–228. [CrossRef]

43. Barna, M. The Effects of Cutting Regimes on Natural Regeneration in Submountain Beech Forests: Species Diversity and Abundance. *J. For. Sci.* **2008**, *54*, 533–544. [CrossRef]
44. Foster, J.R.; Reiners, W.A. Size Distribution and Expansion of Canopy Gaps in a Northern Appalachian Spruce-Fir Forest. *Vegetatio* **1986**, *68*, 109–114.
45. Asner, G.P.; Kellner, J.R.; Kennedy-Bowdoin, T.; Knapp, D.E.; Anderson, C.; Martin, R.E. Forest Canopy Gap Distributions in the Southern Peruvian Amazon. *PLoS ONE* **2013**, *8*, e60875. [CrossRef] [PubMed]
46. Ammer, C. Impact of Ungulates on Structure and Dynamics of Natural Regeneration of Mixed Mountain Forests in the Bavarian Alps. *For. Ecol. Manag.* **1996**, *88*, 43–53. [CrossRef]
47. Motta, R. Impact of Wild Ungulates on Forest Regeneration and Tree Composition of Mountain Forests in the Western Italian Alps. *For. Ecol. Manag.* **1996**, *88*, 93–98. [CrossRef]
48. Boulanger, V.; Baltzinger, C.; Saïd, S.; Ballon, P.; Picard, J.F.; Dupouey, J.L. Ranking Temperate Woody Species along a Gradient of Browsing by Deer. *For. Ecol. Manag.* **2009**, *258*, 1397–1406. [CrossRef]
49. Golser, M.; Hasenauer, H. Predicting Juvenile Tree Height Growth in Uneven-Aged Mixed Species Stands in Austria. *For. Ecol. Manag.* **1997**, *97*, 133–146. [CrossRef]
50. Lindberg, E.; Holmgren, J. Individual Tree Crown Methods for 3D Data from Remote Sensing. *Curr. For. Rep.* **2017**, *3*, 19–31. [CrossRef]
51. Jucker, T.; Caspersen, J.; Chave, J.; Antin, C.; Barbier, N.; Bongers, F.; Dalponte, M.; van Ewijk, K.Y.; Forrester, D.I.; Haeni, M.; et al. Allometric Equations for Integrating Remote Sensing Imagery into Forest Monitoring Programmes. *Glob. Chang. Biol.* **2017**, *23*, 177–190. [CrossRef] [PubMed]
52. Hyyppä, J.; Hyyppä, H.; Leckie, D.; Gougeon, F.; Yu, X.; Maltamo, M. Review of Methods of Small-footprint Airborne Laser Scanning for Extracting Forest Inventory Data in Boreal Forests. *Int. J. Remote Sens.* **2008**, *29*, 1339–1366. [CrossRef]
53. Hothorn, T.; Müller, J. Large-Scale Reduction of Ungulate Browsing by Managed Sport Hunting. *For. Ecol. Manag.* **2010**, *260*, 1416–1423. [CrossRef]
54. Didion, M.; Kupferschmid, A.D.; Bugmann, H. Long-Term Effects of Ungulate Browsing on Forest Composition and Structure. *For. Ecol. Manag.* **2009**, *258*, 44–55. [CrossRef]